Evaluating the Impact of Land Use Changes, Drivers of TMDL Development, and Green Infrastructure on Stream Impairments

Charitha Jayasri Gunawardana
Marquette University

EVALUATING THE IMPACT OF LAND USE CHANGES, DRIVERS OF TMDL DEVELOPMENT, AND GREEN INFRASTRUCTURE ON STREAM IMPAIRMENTS

by

Charitha Jayasri Gunawardana

A Dissertation submitted to the Faculty of the Graduate School,
Marquette University,
in Partial Fulfillment of the Requirements
for the Degree of Doctor of Philosophy

Milwaukee, Wisconsin

May 2023

ABSTRACT
EVALUATING THE IMPACT OF LAND USE CHANGES, DRIVERS OF TMDL DEVELOPMENT, AND GREEN INFRASTRUCTURE ON STREAM IMPAIRMENTS

Charitha Jayasri Gunawardana

Marquette University, 2023

Despite the water quality improvements and regulatory advancements over the last 50 years since the enactment of the Clean Water Act, water bodies within the United States are still impaired for a broad range of contaminants from non-point source pollution. Improving watershed management approaches to meet this challenge will require a greater understanding of (1) how changes within a watershed, such as changing land use, impact stream water quality, (2) what influence socioeconomic, spatial and political factors may have on the progress towards meeting water quality goals, such as those set within Total Maximum Daily Loads (TMDLs), and (3) how specific best management practices can be designed to address water body impairments. First, land use within a watershed is known to have a direct impact on downstream water quality; however, temporal dynamics of these relationships are ill-defined. This is an important gap as management approaches are largely compartmentalized among land use types. Additionally, while management plans can span several decades, the impact of land use changes on water quality is often overlooked. Therefore, this dissertation evaluates land-use changes and their relationship to discharge and water quality trends at stream gages across the U.S. Second, the TMDL program is the primary regulatory lever in the U.S. for addressing non-point source pollution, but its implementation has been uneven across states. This could be due to the diverse socioeconomic, spatial, and political factors of each state. This dissertation therefore seeks to define the influence of these factors on indicators of TMDL progress. Finally, at the site level, management actions to meet regulatory permits include the use of green stormwater infrastructure to capture, treat, and infiltrate runoff at the source. One of the largest sources of impairments in the TMDL program is temperature; however, it is unclear the degree to which green stormwater infrastructure in series mitigates runoff temperatures during summer storms. To address this gap, this dissertation analyzes the temperature mitigation potential of interconnected green infrastructure practices through field observations. Altogether, the outcomes of this dissertation help to advance our understanding of how watershed planning, regulatory, and engineering actions affect downstream water quality.

ACKNOWLEDGMENTS

Charitha Jayasri Gunawardana

I would like to express my sincere gratitude to all those who have contributed to the completion of this doctoral dissertation. First and foremost, I would like to thank my advisor Dr. Walter McDonald for his guidance, support, and invaluable insights throughout my doctoral studies. His dedication to my research and his unwavering belief and patience in my abilities has been a constant source of inspiration and motivation for me.

I would also like to extend my gratitude to the members of my PhD committee, Dr. Parolari, Dr. McNamara, and Professor Strifling, for their valuable feedback, constructive criticism, and invaluable suggestions throughout the process. Their insights and suggestions have helped me to refine my research and improve the quality of my work.

I acknowledge the Milwaukee Metropolitan Sewerage District (MMSD) for providing financial support for my research through a grant awarded to Dr. McDonald. Further, I'm grateful for the Joseph A. and Dorothy C. Rutkauskas Fellowship. Their generous support has made it possible for me to conduct my research and I am truly grateful for their investment and belief in my academic pursuits.

Furthermore, I would like to thank the Department of Civil and Environmental Engineering for providing me with a stimulating academic environment and resources that have enabled me to pursue my research interests. I'd specially like to thank Mr. Thomas Silman and his excellent staff at the Discovery Learning Laboratory for all the help and education they provided me for my projects. Thank you to all the graduate and undergraduate student friends, life was made easier with all of you around.

I am most deeply grateful to my parents Dr. Asoka Gunawardana and Mrs. Neetha Illeperumaarachchi for their unwavering love and support throughout my whole life. Their encouragement and support have been instrumental in helping me to achieve my goals and to be the person who I am.

Finally, I would like to express my deepest appreciation to my wife Dr. Maneesha Jayasuriya for her unwavering support, patience, and understanding throughout my graduate life. Her love, encouragement, and belief in me have been a constant source of motivation and inspiration throughout my doctoral studies. Without her love and support, I would not have been able to complete this important milestone in my life.

TABLE OF CONTENTS

LIST OF TABLES

LIST OF FIGURES

1. INTRODUCTION

Protecting the quality of our surface waters such that they are fishable, swimmable, and drinkable has been a key environmental priority, as demonstrated by legislation in the U.S. from the 1948 Water Pollution Control act to the 1972 Clean Water Act (CWA) and its many addendums (Hines, 2013). Since the time of these acts, focus on protecting the water quality of the nation's water bodies has led to increased expenditures on pollution control, reductions of pollutants from point and non-point sources, and a subsequent decrease in pollution levels in surface water bodies (Adler et al., 1993). However, despite the successes in pollution mitigation, a growing number of our nations water bodies are still impaired for a broad range of pollutants, demonstrating a need for continued improvements in watershed management efforts.

Poor water quality has staggering ramifications on humans, plants, and animal life. While water quality related outbreaks in the United States has drastically reduced since the enactment of the CWA, more than 7 million people are estimated to get sick in the U.S. every year due to waterborne diseases caused by exposure to environmental sources, recreational activities, and drinking water (Collier et al., 2021). In addition, 70% of the nation's rivers and streams in 2022 are impaired based on the ability to sustain their biological diversity (*ATTAINS | Water Data and Tools | US EPA*, 2022). For example, from 2008 to 2014, the percentage of streams impaired by excessive phosphorous has increased by 11% (*ATTAINS | Water Data and Tools | US EPA*, 2022). In addition, for many states temperature is the single largest impairment due to increasing stream temperatures that threaten many ecosystem functions that rely on unique

temperature thresholds. Temperature in major rivers and streams across United States was found to be rising at a rate of 0.08 Celsius per year, largely due to increases in air temperatures and urbanization (Kaushal et al., 2010). This rise in stream temperatures can have adverse effects on organisms, such as Chinook salmon, whose pre-spawn mortality rate increase with increasing stream temperatures (Bowerman et al., 2021). Finally, concentrations of emerging contaminants such as PFAS, antibiotics, microplastics, pharmaceuticals, and hormones have been rising over the last decade and have been shown to have adverse impacts such as cancer and hormonal imbalances in humans, fatalities in environmental organisms, and the increase of antibiotic resistant genes depending on contaminant concentrations (Baquero et al., 2008; Cole et al., 2011; Domingo & Nadal, 2019; Richardson & Ternes, 2018). Solutions to these challenges require a greater understanding of the impact planning, management, and best management practices have on the water quality of the nation's water bodies.

Planning and management are critical steps for improving the water quality of the nation's water bodies. While water quality implementation (management) is usually done in watershed scales, planning can span across multiple spatial extents since water quality is a global concern. In the United States, the protection of water quality is enforced through the CWA section 208 and 303(e) which instructs states to develop and maintain continuing planning processes for water quality management. Two of the most impactful programs from the CWA are the National Pollution Discharge Elimination System (NPDES) and the Total Maximum Daily Loads (TMDL) programs. The NPDES program is a permit system that regulates point source pollution, which includes municipal separate storm sewer systems (MS4s) that discharge stormwater at outfalls. The TMDL

program requires states to assess their water bodies based on designated uses and whether the waters meet numerical criteria to enable those uses, list those that are impaired, and for those that are impaired, develop a pollutant reduction target and load allocation to all sources (point and non-point sources) of the pollutant within the watershed. While these programs allow states to plan and manage watersheds based on current water quality conditions, they do not incorporate future projections of changes that could affect water quality such as land use or climate. An analysis of 124 water quality management plans across the nation found that they lack innovative planning methods that consider future watershed conditions such as population growth, climate change, and land use changes (Mika et al., 2019). Yet considering changes in these conditions within water quality management plans can make them more resilient to changes in climate, land use, or socioeconomics, by incorporating future projections of watershed conditions within the planning process (Hung et al., 2020; Mashaly & Fernald, 2020; Phan et al., 2021; G. Wang et al., 2016). Therefore, it is important to understand how temporal changes in watersheds affect water quality for better planning that incorporates future scenarios as well as how socioeconomics impact water quality management processes.

The difficulty of attributing watershed changes to changes in downstream water quality is a crucial challenge for watershed planners and managers. Two methods to do so include capturing the impact of changes through water quality monitoring and predicting the impact of changes through modelling. The largest monitor of water quality in streams and rivers is the USGS, which has more than 11,000 continuous in-situ monitoring gages. However, despite these gages and others, only about 10% of all the water bodies in the nation are monitored in-situ (Sridharan et al., 2022), and this data alone can only help to

understand the impact that current and past actions and changes have on water quality. In addition, modelling methods can be applied to predict the impact of watershed changes on stream water quality. However, modeling approaches vary and a review of 14 different models used for TMDL studies identified several common limitations including large data requirements, spatial limitations, limited water quality parameters, and an ability to run limited storm intensities (Borah et al., 2018). Recent advances in artificial intelligence applied to modeling complex water quality dynamics within watersheds could overcome some, but not all, of these limitations such as limited data availability (Tiyasha et al., 2020). An alternative approach to understand the impact of watershed changes to stream water quality is to use empirical models and relationships that describe water quality behavior based upon characteristics of the watershed. Advantages of applying empirical models are their straightforward application and limited computational or data needs. They therefore have the potential to provide planning-level assessments that watershed planners can utilize to develop resilient and wholistic management strategies.

Development of wholistic watershed management strategies is also impeded by resource availability, politics, and socioeconomics. Funding for water resource management in the U.S. comes mainly from the federal government and its organizations, while states and NGOs also provide limited resources (*Effective Funding Frameworks for Water Infrastructure | US EPA*, 2023). Due to funding limitations, local governments have formed collaborative watershed management bodies that together leverage external funding opportunities, but have avoided binding water quality goals in their planning due to political tensions (Koontz & Newig, 2014; Yoder et al., 2021). Integrated regional

water management in California has also shown that funding for water management is limited and competitive and decisions are impacted by the political climate (Blomquist & Schlager, 2006; Lubell & Lippert, 2011). In addition, socioeconomics can impact watershed management due to the role that the public has in the development of watershed management plans. The Clean Water Act has clear provisions for public involvement in all processes of watershed management that can include assessing water quality by citizen scientists, directing agencies to impaired water bodies as within a community, commenting on water quality planning drafts (*Public Participation in Listing Impaired Waters and the TMDL Process | US EPA*, 2022) and influencing policy development through political activism. To this end, education level and socioeconomic status of these participants have shown to be significant factors in influencing watershed planning and management (Larson & Lach, 2008; Stanford et al., 2018).

Finally, nearly every watershed management plan incorporates best management practices for reducing pollution, and therefore it is important for planners and managers to understand the efficiency of all the tools at their disposal. Green infrastructure is one such tool that can mitigate adverse effects of storm water runoff including reduced runoff volumes and pollutants (J. Wang & Banzhaf, 2018). However, the potential for temperature mitigation is less understood, which may pose a challenge for watershed management plans as temperature is one of the leading impairments through the TMDL program. As storm water management plans incorporate green infrastructure to meet water quality goals, it is important that their impact for addressing a broad range of pollutants is understood.

Given the above understanding, the overall objective of this thesis is to evaluate and improve our understanding of the engineering, regulatory, and socioeconomic principles influencing stormwater management actions which affect downstream water quality and quantity. To that extent, the following sections discuss three research gaps that were identified for further scrutiny: (1) land use changes in watershed and their relationship to water quality, (2) impact of spatial and socioeconomic factors on Total Maximum Daily Load progress, and (3) temperature mitigation of green infrastructure systems.

1.1. Land Use Changes in Watersheds and Their Relationships to Water Quality.

Land-use patterns change over time due to social, economic, political, and geographical conditions of populations. This includes increasing populations and expanding economies that grow the demand for developed land (Creutzig et al., 2019). An escalating number of people are moving to cities, and it is projected that 68% (7 billion) of the global population will live in cities in 2050 compared to the 55% (4 billion) living in 2018 (Ritchie & Roser, 2018). To meet the increased demand for housing, commercial space, infrastructure, industries, and transportation, these cities must modify previously undeveloped space for their economic growth. Furthermore, due to socio-economic changes, agriculture land and other natural land such as forests compositions have and will continue to undergo dramatic changes (Winkler et al., 2021).

Land use has a complex relationship to water quality in streams (A. Baker, 2006). Specifically, anthropogenically modified land adds numerous pollutants to watersheds that get transported to downstream waterbodies through stormwater runoff. For example, agriculture land releases both natural and manmade nutrients, antibiotics, pesticides,

heavy metals, and sediments to downstream waterbodies, which can lead to water quality impairments (Giri & Qiu, 2016; Paudel & Crago, 2021); however, the empirical relationship between agricultural land use and downstream pollution is variable. In many studies, the presence of agricultural land use enhances the sediment and nutrient concentrations within receiving water bodies (Delia et al., 2021; Delkash et al., 2018; Mello et al., 2020); however this is not always the case. In the United States, it was found that flow normalized concentrations of NH_4, suspended solids, and total nitrogen actually decreased overall in receiving waters from agricultural land from 1982-2012 (Stets et al., 2020). In Jordan Lake watershed in North Carolina, over a period of 20 years, the annual total nitrogen loads were found to be negatively correlated to agriculture land percentages (Tasdighi et al., 2017). The variation in the relationship of agricultural land to downstream water quality could be due to several factors including the overall watershed composition (e.g., majority urbanized, forested, or agriculture) (Tu, 2011). For example, the presence of agricultural and natural land uses (wetlands, grasslands, forest, etc.) within the watershed where natural land uses can act as a buffer, mitigating the effects of nutrient export (Fasching et al., 2019).

In addition, runoff from urbanized cities is complex and could contain chemicals such as heavy metals, micro plastics, tire wear particles, and PFAS, as well as other pollutants such as road salts that are applied during winter seasons (Giri & Qiu, 2016; McGrane, 2016). Urban runoff therefore can be the primary cause of impairments to water bodies that no longer meet applicable water quality standards. While over the years nutrient and total suspended solids loading from urban spaces has reduced significantly (Stets et al., 2020), many studies have shown that urban sprawl has strong positive

correlations to nutrient loads to streams and rivers (Ullah et al., 2018; S. Yao et al., 2023). This could contribute to nutrient impairments as in the U.S., 58% of the assessed rivers and streams are impaired due to nutrients while 40% of the assessed lakes, reservoirs, and ponds have excess nutrients (*ATTAINS | Water Data and Tools | US EPA*, 2022). It has also been shown that an increase in imperviousness results in decreased stream baseflow (Shuster et al., 2007), yet imperviousness alone may not be the best indicator of water quality as land cover has been shown to be a better predictor of downstream water quality than imperviousness (Schueler et al., 2009). It is therefore imperative to understand the relationship of land use changes in watersheds to changes in water quality of downstream waterbodies.

To that end, while the spatial relationships between land use patterns and downstream water quality have been widely studied (Wan et al., 2014; F. Zhang et al., 2018), it is less clear how temporal changes in land use impact observed trends in downstream water quality. This is partly because existing empirical studies that do investigate temporal associations between land use change and downstream water quality have limitations that influence the generalization of their findings. For example, many are geographically constrained to either a single watershed or smaller geographic regions (Meneses et al., 2015; Pandey et al., 2023; Risal et al., 2020; J. Smith et al., 2015; L. Wang et al., 2023; Wijesiri et al., 2018). While these geographically limited studies provide valuable insights, their applicability is constrained to their unique geomorphologic, anthropogenic, and climatic contexts. Furthermore, most of these studies use field data to assess how water quality relates to the land use of that watershed at a defined time using a model form similar to *water quality = f (land use)* (Haidary et

al., 2013; S. Li et al., 2009). While these correlations provide valuable information for understanding the impact of land use on stream water quality in ungaged basins, they are not applicable to predicting water quality based on future expected land use changes. This is because they could be biased towards historical land development practices that do not represent the hydrologic impact of contemporary land use changes. For example, contemporary urban land development will have to adhere to stricter stormwater treatment regulations that were not required for historical development. Defining the impact of recent land use changes on water quality is an important gap because this understanding is needed in developing watershed management plans that can reach long-term water quality goals.

In some cases, the impact of land use change on water quality can be estimated through modeling approaches that are able to consider land and its impact on pollutant transport across broad spatial scales (Fan & Shibata, 2015; R. Wang & Kalin, 2018); however, models are constrained by data availability and model assumptions necessary for simulating the complex physiochemical processes involved in pollutant buildup and transport in stormwater runoff. For example, one of the most commonly used physical models for water quality studies is the Soil and Water Assessment tool (SWAT) (Astuti et al., 2019; Hovenga et al., 2016; Risal et al., 2020). However, this model and others require large amounts of data for proper parameterization and model calibration (Akoko et al., 2021), which in most cases are not extensively available for large temporal and spatial scales. An evaluation of SWATs ability to simulate *E. coli* concentrations based on land cover data in a watershed in Georgia, USA, resulted in simulated bacterial concentrations with a low R^2 range of 0.32 – 0.34 (Sowah et al., 2020). This low

predictability is largely due to limitations and assumptions made using current knowledge that resulted in uncertainties in the model outputs. Furthermore, most modelling software relies on assumptions and empirical relationships that are limited by current knowledge. Therefore, modeling approaches have limited value in delineating between diverse and distributed pollutant sources and their subsequent transport and impact on downstream pollution. Given these limitations, it is not surprising that the impact of land use changes on trends in downstream water quality from monitoring and modeling studies is unclear. For example, while some have shown that increases in agricultural and urban land-uses results in a subsequent increase of total suspended solid (TSS) loads in downstream water bodies (Ahearn et al., 2005; Hovenga et al., 2016), others have found the opposite effect, likely due to the impact that best management practices in agricultural and urban land areas have on reducing pollution from runoff (J. C. Murphy, 2020; Stets et al., 2020).

A lack of empirical studies that evaluate the impact that changes within watersheds have on changes in water quality, in addition to modeling limitations, has limited our ability to develop wholistic management plans. To overcome this limitation, generalized models that relate water quality changes to land use changes could be used to project how water quality of a watershed might change based on limited data (current water quality and expected land use percentage). Doing so can improve watershed management and planning efforts by making management actions more resilient and economically efficient. Specifically, watershed actions could be designed and developed to incorporate future needs, thereby reducing risk associated with the impact of land use changes on water quality. This would limit the need to make excessive changes to management plans and solutions due to future land use changes, reducing economic

burdens. Therefore, there is a need to understand the correlations between land use change and water quality of the nation's water bodies at a broad spatial scale.

1.2. Total Maximum Daily Loads for Water Quality Management

Within the United States, the quality of most freshwater bodies is regulated through the Clean Water Act (CWA). Section 303(d) of the CWA requires states to assess their water bodies and establish Total Maximum Daily Loads (TMDLs) for water bodies that are identified as impaired. This program, while imperfect, is the only federal statutory method capable of addressing non-point source pollution in the nation's water bodies and relies on a system of policy implementation where the federal government delegates primary authority to agencies at the state level. The TMDL development process, federally mandated by EPA, has three distinct steps that need to be implemented in sequence: (1) assessment of surface water bodies, (2) listing impaired water bodies, and (3) development of Total Maximum Daily Loads to impaired water bodies. Once TMDLs are developed, these limits can only be reached by reducing both point source and non-point source pollution. Point source pollution is limited through National Pollutant Discharge Elimination System (NPDES) permits which are regulated by section 402 of the CWA. However, no federal regulation or authority exists to enforce pollutant reductions against non-point sources, including the enforcement of implementing TMDLs to achieve these target loads. Rather, the implementation of TMDLs are incentivized. For example, the CWA section 319 grant programs provide funding for non-point source pollution controls when the control of point source pollution through NPDES alone doesn't achieve TMDL goals (S. Jones, 2014).

Achieving water quality goals of a TMDL is a challenge for any watershed. For example, a TMDL was developed for the Neuse River and Estuary in North Carolina in 1999, which has since led to a reduction in nitrate and nitrites but an increase in organic nitrogen (Lebo et al., 2012). Perhaps the largest efforts are towards the TMDLs for Chesapeake Bay that were approved by the EPA in 2010 and required more than 24% reduction of both nitrogen and phosphorus loading. This TMDL is unique in that it spans 5 states – Maryland, Pennsylvania, Virginia, New York, and West Virginia – who were mandated to reduce 60% of the target reductions by 2017, however, only West Virginia has achieved it (Ritter, 2019). In contrary, an analysis of 63 watersheds in Ohio and West Virginia revealed that 65% of them had TMDL implementation projects and 38% of those had observed non-point source pollutant load reductions (Hoornbeek et al., 2013). These examples show that, while the implementation of TMDL within watersheds may vary, if done well it can result in improved water quality.

Though the TMDL is approved by the EPA, TMDL development is the responsibility of state agencies therefore, the extent to which states assess water bodies, identify impairments, and develop TMDLs can vary from state to state. It has been almost 30 years since EPA published regulations establishing TMDL requirements (Houck, 1997) and therefore presents an opportune time to reflect on the progress of the TMDL programs across the U.S.. This reflection is valuable in understanding what factors may contribute to advancing or prohibiting the progress of TMDLs. U.S. states vary in their populations, geography, demographics, and economic output, which may influence both the approach and extent to which they enact water quality programs. To that end, there are a diversity of approaches to assessing and implementing TMDLs through monitoring

and modeling technologies. This includes assessment methods to monitor water quality parameters that range from detailed monitoring requiring scientific expertise to those that can be carried out by volunteer citizens (Loperfido et al., 2010; Nation & Johnson, 2016). For example, stream water quality assessments can be developed using in-situ gages from agencies such as USGS that continually collect multiple discharge and water quality parameters; however, these monitoring networks are not available in every stream, or every location within a stream, that would be needed for robust assessments. Therefore, the CWA allows the use of "all readily available and existing" data, which can include data gathered by diverse sources, such as universities and volunteer organizations (Brett, 2017). For example, in the Chesapeake Bay watershed, citizen scientists have collected data that has been directly used to develop TMDLs and inform management decisions (Webster & Dennison, 2022). If citizen scientists and voluntary groups are properly trained and managed, they can help to improve TMDL development by water bodies (Brett, 2017; Nation & Johnson, 2016).

In addition, due to the scarcity of watershed wide data for every pollutant of concern, a common method to develop TMDLs is using mathematical models. There are a wide array of methods to model TMDLs that require various levels of technical expertise for implementation (Frost et al., 2019; Sridharan et al., 2021). For example, models are developed using dissolved oxygen, turbidity, and chlorophyll distributions to assess habitat quality of streams (Hernandez Cordero et al., 2020). These models allow managers to assess habitat without frequent field visits and standardize habitat quality across multiple watersheds. Analyzing the 14 most current watershed models used in TMDL development shows that they vary in complexity and applicability (Borah et al.,

2018). Most of these models are developed specifically for use in agricultural watersheds, while models such as HEC-HMS and SWMM can model mixed use watersheds. Furthermore, while these 14 models do not readily integrate with GIS software, remote sensing and GIS technologies have been used for watershed modeling successfully (Quinn, Kumar, & Imen, 2019). Using hyperspectral sensing data and spatial and modelling capabilities of GIS software, TMDLs for pollutants such as temperature, suspended sediments and algal biomass (through surrogates) have been developed (Quinn, Kumar, & Imen, 2019). Linking GIS to computational models such as SWMM can improve the TMDL process throughout all modeling, planning, and managing stages. The most recent developments in watershed modelling for TMDL include the use of machine learning techniques. An attempt to use five different machine learning methods to develop predictive models for water quality parameters such as nutrients, DO, and suspended sediments based on limited data that is publicly available have been successfully validated against field data (Adedeji et al., 2022). While machine learning models are being developed to predict water quality for different scenarios (R. Wang et al., 2021), they are yet to be used for TMDL development.

While technical approaches to assessing water bodies and applying models to develop TMDLs are well defined and available for use, it is less clear the extent to which different states have implemented TMDL programs and the factors that contribute to their progress. This is important because understanding the factors that impact the progress of protecting the nations water bodies can help to improve TMDL methods and ultimately reach the designated goal of obtaining fishable, swimmable, and/or drinkable waters. One of the main challenges in developing TMDLs is the lack of data and uncertainties related

to various models used. Therefore, model calibration, verification, and validation steps are crucial components of this process. The ASCE Environmental and Water Resources Institute TMDL Analysis and Modeling Task Committee recently published a review of 14 different models and their calibration and validation methodologies, uncertainty analysis, and future recommendations (Ahmadisharaf et al., 2019). The authors recommend that model selection should be carefully analyzed to fit the needs of the watershed and pollutants, and future research should be done to optimize validation and uncertainty analysis processes. To that end, machine learning has been utilized to quantify uncertainties in water quality index models (Uddin et al., 2023) and utilization of these methods in models such as SWAT and SWMM could be imminent in the near future. Apart from data and modelling challenges, institutional and socioeconomic challenges that impede the TMDL development have not been thoroughly studied. However, it has been shown that funding, public and stakeholder engagement, and agency interest and involvement have a considerable impact on TMDL implementation (Benham et al., 2008; Hoornbeek et al., 2013). Therefore, socioeconomic factors may also impact the process of TMDL development.

However, the extent to which socioeconomics or the geography of a state influences the implementation of TMDLs is underexplored. This is a critical gap as socioeconomics, land use and environmental dynamics have been shown to be important factors in developing effective TMDL plans (Mirchi & WatkinsJr., 2012) and in implementing other aspects of the CWA, such as the National Pollutant Discharge Elimination System (NPDES) program (McDonald & Naughton, 2019). It has also been shown that water quality impairments have a negative impact on housing prices

(Papenfus, 2019). Water quality perception surveys of randomly selected 8,772 people in West Virginia has shown that per capita income has a positive correlation with environmental concerns (Andrew et al., 2019). Since the TMDL process has a public involvement component, the positive correlation between income and environment concerns of the public could mean that per capita income has an impact on TMDL development as well. In 20 urban watersheds in Iowa, USA, conductivity of the stream was positively correlated with population density, which itself was correlated to higher road densities, and phosphorus concentrations were negatively correlated with college degree attainment, which could have been due to lower solid-derived nutrient inputs from watersheds dominated with impervious surfaces (Wu et al., 2015). Finally, education, ethnic composition, age structure, land use, population density, and watershed area were all found to be significantly correlated with the water quality parameters in California streams (Farzin & Grogan, 2013). While these correlation studies do not necessarily reflect causation, these examples demonstrate how water quality may be impacted by the socioeconomic and spatial factors of a watershed; however, no studies have evaluated how they relate to the efforts to improve those impairments through TMDL development. This is important as the social context and economic resources could influence the ability and willingness of a state to pursue TMDL progress.

There may also be regional similarities among states in their approach to managing water quality due to common geomorphologic or climatic similarities, or their presence in similar EPA regions. The US EPA is divided into 10 different regions with a regional office associated with each that is responsible for enforcing implementation of TMDL programs within their states. This regionalization of enforcement offices may

therefore lead to different levels of program development, as these regions have largely developed independently due to different factors such as water body priorities, litigation, and resource availability (Neilson & Stevens, 2002). However, no nationwide studies have evaluated the relationship between socioeconomics, regionalization, and TMDL implementation. Understanding these relationships could allow watershed managers and planners to better allocate resources and guide efforts to improve upon TMDL development programs.

1.3. Runoff Temperature Mitigation by Green Infrastructure

Temperatures in streams and rivers are increasing across the world, especially in streams that are impacted by urbanization (Kaushal et al., 2010). Within the U.S. TMDL program, temperature is second to bacteria as the most frequent number one cause of impairment in a state's streams and rivers. While climate change plays a major role, this is exacerbated by anthropogenic land cover, such as impervious surfaces, that have a greater thermal absorptivity than natural land covers and a direct hydrologic connection to surface water bodies. These impervious surfaces capture solar radiation and transfer that energy to stormwater runoff and subsequent downstream water bodies (Herb et al., 2008; Zeiger & Hubbart, 2015). This creates hydrologic urban heat islands, where urban streams have comparatively higher baseflow temperatures and are subject to greater temperature surges from stormwater runoff (Zahn et al., 2021) . Coupled with rising global air temperatures (Pachauri & Reisinger, 2007) and uncertainty in the hydrologic cycle (Huntington, 2006), this is likely to influence ecological processes and community shifts in freshwater bodies (Nelson & Palmer, 2007). This includes negative impacts to temperature-sensitive species (Caissie, 2006), increased contaminant toxicity (Patra et al.,

2015) and a proliferation of toxic algal blooms (Griffith & Gobler, 2020). It is therefore imperative that stormwater is managed in a way that mitigates the temperature of stormwater runoff to protect human and environmental health.

One potential management approach to increasing urban runoff temperatures is green stormwater infrastructure that captures, treats, and infiltrates stormwater runoff at the source. Green stormwater infrastructure has been shown to be an effective approach to manage stormwater volumes and pollutants in urban and agricultural settings (Clary et al., 2020; Regier & McDonald, 2022). Recently, it has been shown that a combination of green infrastructure (GI) practices at larger scales could achieve runoff reduction goals more effectively (J. Chen et al., 2019; Staccione et al., 2022; Y. Yao et al., 2022; J. Zhang & Peralta, 2019) and that a combination of rain cisterns, porous pavements, and bio retentions are the most cost effective considering space requirements, cost of implementation, and runoff reduction in urban spaces (Boening-Ulman et al., 2022; F. Li et al., 2021). Apart from runoff reductions, green infrastructure has also been proven to reduce runoff pollutants including total suspended sediments, total nitrogen, and total phosphorous (J. Chen et al., 2019; Choi et al., 2021) and improve air pollution (Kumar et al., 2019). In addition, it has been demonstrated as an effective means of reducing the urban heat island effect through lower ambient air temperatures (Balany et al., 2020).

Green infrastructure can also reduce runoff temperatures through heat exchange that occurs when runoff filters through cooler green infrastructure plants and media. In the context of green infrastructure, there are several ways in which energy is transported and transferred including conduction (transfer of thermal energy by direct contact between molecules), advection (transfer of thermal energy by the bulk movement of

fluids), transpiration (process by which water is taken up by plant roots and then released into the atmosphere through leaves of plants), and evaporation (transfer of thermal energy through phase change of a substance). The most direct pathways to cooling stormwater runoff with high temperatures are through conduction, advection, and evapotranspiration (combination of evaporation and transpiration).

When runoff enters a green infrastructure practice during warm summer months, it is filtered through a media that is likely cooler than the surface of surrounding watershed. This is because the media below the surface is not subject to direct thermal radiation; furthermore, the media or soil surface itself could be cooler than the surrounding watershed due to surface material, shading, and soil moisture evaporation. During filtration through the media, heat is primarily transferred through advective and conductive processes. Because of this, the physical parameters of the soil media, such as volumetric heat capacity and thermal conductivity, are important parameters that control the rates of conduction and advection (de Vries, 1975). GI also promotes runoff reduction through exfiltration, further reducing the total thermal energy received by water bodies. In addition, when considering timescales larger than storm events, evaporation acting in the uppermost layer of the soil surface and transpiration from the root uptake of water may contribute to heat exchange of runoff captured by green infrastructure. Temperature itself is also an important component to the hydraulic performance of green infrastructure as temperature of stormwater runoff entering a green infrastructure practice influences the infiltration rate due to temperature-dependent changes in viscosity (Lewellyn et al., 2016). However, despite the potential for green infrastructure to reduce runoff temperatures and its importance in their overall performance, the impact of specific green

stormwater infrastructure types on temperature mitigation of urban stormwater runoff is underexplored.

One type of green stormwater infrastructure that has potential for reducing the temperature of stormwater runoff is permeable pavements. These systems, which capture stormwater runoff through gaps between concrete or brick pavers on the surface and then filter and infiltrate through a trench filled with crushed aggregate, are effective at reducing stormwater runoff volumes and reducing pollutant concentrations (Sambito et al., 2021). Permeable pavements may mitigate runoff temperatures by redirecting stormwater through cooler permeable pavement media and soils. In addition, they have been shown to have lower surface temperatures than other permeable surfaces such as porous asphalt(Cheng et al., 2019); however, the comparative surface temperatures of permeable to impermeable pavers are unclear, with studies finding permeable pavers to be both lower (Cheng et al., 2019) and higher (LeBleu et al., 2019) than impermeable surfaces. This divergence could be due to variations in surface roughness or heat capture within saturated pore spaces that influence temperatures of these surfaces.

Bioretention practices are perhaps the most studied green stormwater infrastructure practice for thermal mitigation; however, the most appropriate way to use them to meet downstream temperature goals is unclear. Bioretention practices have produced statistically significant reductions in both peak and mean temperatures during simulated rainfall events for watersheds that contain streams with temperature-sensitive trout species (Long & Dymond, 2014). Design components that influence temperature reductions in bioretention include the vegetated surface, the soil depth of effluent pipes, as well as the size of the contributing watershed area (M. Jones & Hunt, 2009). However,

bioretention alone may not be enough to reduce runoff temperatures to levels needed for temperature-sensitive species (H. Y. Chen et al., 2021; Ketabchy et al., 2019), and in fact at a watershed scale have been correlated to higher downstream water temperatures due to green infrastructures such as retention ponds with larger surface areas and shallow depths that absorb thermal energy (Jalali & Rabotyagov, 2020).

One potential solution is connecting green infrastructure in series in a treatment train that can effectively reduce pollutants to acceptable levels. Connected green infrastructure in series have been shown to improve volume-based reduction goals (Wadzuk et al., 2017; Woznicki et al., 2018), and improve the removal of pollutants from stormwater runoff (Brodeur-Doucet et al., 2021; Winston et al., 2020). However, the impact of green infrastructure connected in series for reducing thermal pollution in urban stormwater runoff is underexplored. While research has demonstrated the cumulative effect of rain gardens and riparian buffers on receiving stream temperatures (R. M. Martin et al., 2021), there are no studies evaluating the impact of green infrastructure directly connected in series.

Therefore, more research is needed to determine comparative thermal mitigation among practices, the appropriate design of those individual practices for optimizing temperature reductions, and the best placement and configuration for achieving watershed-level outcomes (R. M. Martin et al., 2021; Timm et al., 2020). Doing so can help inform watershed planners, managers, designers, landscape architects, and policy makers as they consider the benefit of using GIs in networks to mitigate the temperature of runoff that is discharged into urban water bodies.

2. RESEARCH GAPS AND OBJECTIVES

The **overall objective** of this dissertation is to evaluate and improve our understanding of the engineering, regulatory, and socioeconomic principles influencing stormwater management actions which affect downstream water quality and quantity. Based on the literature review above, three main knowledge gaps were identified. The objectives of this dissertation to meet these gaps are:

Objective 1. **Analyze land-use changes and their relationship to discharge and water quality trends in the United States.**

In many cases, water management plans lack a wholistic approach that considers the impact of future land use projections. This may partly be due to the difficulty in attributing changes in land use to expected changes in stream water quality as modeling approaches to do so are constrained by data availability and model assumptions necessary for simulating the complex physiochemical processes involved in pollutant buildup and transport in stormwater runoff. Empirical approaches that overcome these limitations are largely constrained to single watersheds or correlation studies based on a single point in time. This objective seeks to fill this gap by defining the relationships between changes in land use and changes in water quality based on USGS stream gage data (discharge, specific conductance, dissolved oxygen, and turbidity) data for multiple watersheds (60) over 9 years.

Objective 2. Define the influence of socioeconomic and spatial variables on TMDL progress in the United States.

The TMDL program is the federal statutory method of addressing non-point source pollution in the nation's water bodies and relies on a system of policy

implementation where the federal government delegates primary authority to agencies at the state level. Therefore, the extent to which states assess water bodies, identify impairments, and develop TMDLs varies from state to state. While it is known that spatial factors, socioeconomics, and politics can influence management decisions and are correlated to water quality impairments, the effect of these indicators on TMDL progress is unknown. This is an important gap in knowledge as future planning for TMDL development would benefit from understanding what factors may contribute to advancing or prohibiting the progress of TMDLs. Therefore, this objective assesses the progress of TMDLs across all U.S. states and defines the relationship between indicators of TMDL progress and socioeconomic, spatial, and political factors.

Objective 3. Monitor and analyze the temperature mitigation potential of interconnected green infrastructure practices.

Temperature is a leading cause of stream impairments through TMDL assessments. This is due in part to runoff from urban watersheds that is heated from anthropogenic surfaces and subsequently increases the temperatures of receiving waters that it flows into. Green infrastructure may be a tool that can reduce runoff temperatures before they reach downstream water bodies. However, no studies have evaluated the ability of green infrastructure connected within a network to mitigate runoff temperatures. This objective meets this gap by monitoring and evaluating the temperature mitigation potential of green infrastructure connected in series.

In addition to these objectives, a study focused on the development of low-cost active controls to improve volume and peak flow mitigation of green infrastructure is

provided in Appendix 4. Green infrastructures are used extensively to aid in managing urban runoff volumes and pollution. While they provide a vital service to our urban ecosystem, their efficiency may be increased by actively controlling the water balance of these systems. Therefore, this study explores the hydrologic performance of a real-time control system through field applications and computer modelling. While this work is not part of the main objective of the dissertation, its results are included in Appendix 4.

3. ANALYZE LAND-USE CHANGES AND THEIR RELATIONSHIPS TO DISCHARGE AND WATER QUALITY TRENDS IN THE UNITED STATES

3.1. Rationale

Watershed management programs enforced by regulations in USA do not mandate a wholistic planning approach based upon future watershed changes. However, studies have proven that a more wholistic approach to watershed management can improve water quality over time and utilize financial resources more efficiently (Stoker et al., 2022). Anthropogenic land use changes over time due to population, economic, cultural, and environmental shifts thus impacting water quality of our water bodies. While many empirical studies investigate how watershed scale land uses impact water quality (Wan et al., 2014; F. Zhang et al., 2018), they have several limitations including their application for predicting future land use changes due to the bias that historical land development may have on the model generation. Most studies that assess the relationship between land use and water quality are model based, which are limited by current knowledge, and are simulated to one point in time. Understanding temporal relationships between land use changes and water quality changes based on measured data can better inform water quality management planning by incorporating future projections in developing solutions to water quality issues. This objective seeks to fill this gap by evaluating the relationship between changes in land use and water quality and quantity parameters at USGS stream gages (Figure 3-3) over the period of 2008 to 2016. To this extent, I (1) analyzed temporal changes of water quality parameters and discharge of selected watersheds, (2) analyzed land use changes over the said period for all

watersheds, and (3) statistically analyzed the relationships between land use and water quality temporal changes.

I *hypothesize* that the changes in land use categories over time can explain the variations in water quality changes over the same period.

3.2. Methodology

3.2.1. Study Area

This study evaluated the watersheds from a candidate list of 72 USGS stream gages across the contiguous United States (Figure 3-1). In selecting gages, they had to meet the criteria of having continuous mean daily discharge and water quality data from 2008 to 2016, corresponding to the date range in which national land-use data is available. While land use data is available up to the year 2001, water quality data for most of the gages are not available beyond the selected period. The final set of selected gages had watersheds that ranged in area between 22 km^2 and 36,927 km^2, had diverse land use characteristics, and covered most geographic regions of the United States, as illustrated in Figure 3-1.

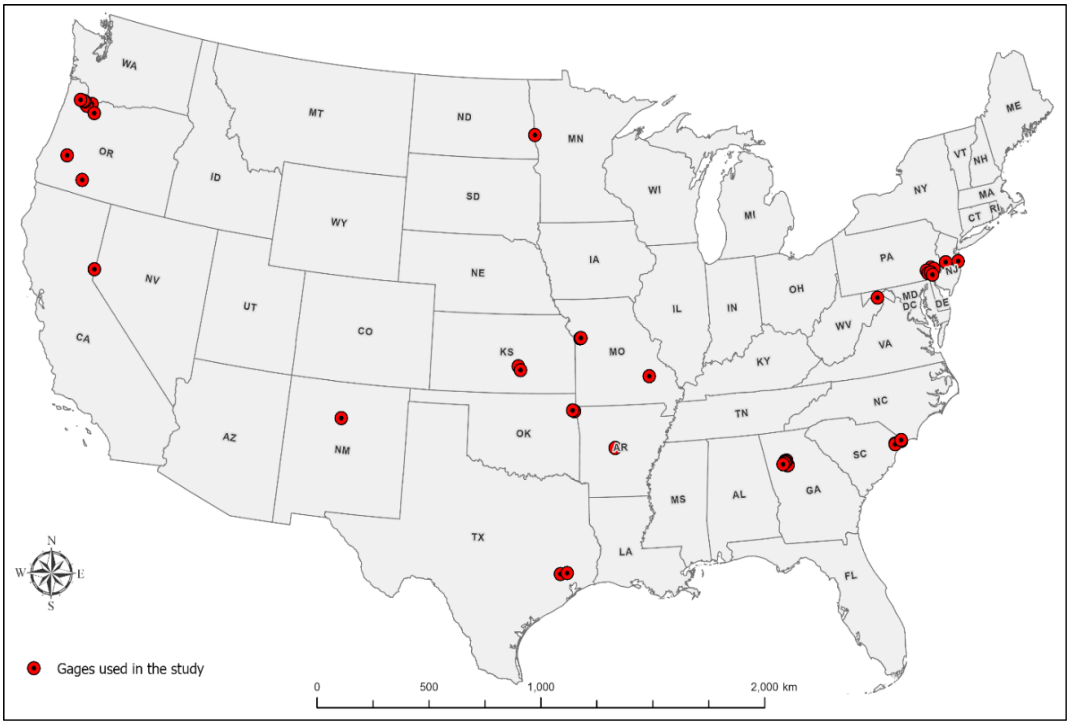

Figure 3-1 Locations of all 60 gages used in the study.

3.2.2. Data Sets

Mean daily discharge and water quality (turbidity, dissolved oxygen, and specific conductance) data were collected over the study period (2008-2016) from each of the selected USGS gages (USGS, 2014). Turbidity, dissolved oxygen, and specific conductance were chosen as parameters based upon their availability across a wide range of USGS gages over the years of the study period. A total of 72 gages were initially selected; however, some were removed due to characteristics of the watershed that influenced their hydrologic response. Four of the gages were removed due to their location less than 3 miles downstream of a regulated dam. This is because gages affected by regulation exhibit varied flows dominated by controlled dam releases, which also affects water quality (de Necker et al., 2019; Zuo et al., 2015). In addition, eight gages

were removed because the watersheds had no land use diversity or changes throughout the study period, or encompassed many of the other watersheds analyzed in the study, resulting in nested watersheds. Streamflow behavior is highly dependent upon watersheds size with markedly different hydrologic response in watersheds with areas that are several orders of magnitude apart (Romshoo et al., 2012). The study incorporates watersheds of different magnitudes thus, allowing to generalize the relationships found in the study to varying watershed characteristics. After removing these gages, there were a total of 60 gages that fit the criteria for the final analysis.

Land use data from the National Land Cover Database (NLCD) were obtained for the contiguous from the U.S. Multi-Resolution Land Characteristics Consortium (https://www.mrlc.gov/data) for the years of 2008 and 2016. This data set contains 16 distinct land use categories in 30 m resolution. In addition, impervious land use data in 1% increments were obtained in the same resolution from MRLC for the years of 2006 and 2016.

3.2.3. Data Preparation

3.2.3.1. Water Quality Data

USGS data sets sometimes have periods of missing data due to environmental interference with the sensors or technical malfunctions of the gage. Therefore, to evaluate trends over a continuous data set, I applied methods to interpolate data (Baddoo et al., 2021; Han et al., 2023) where there were gaps within time series of discharge and water quality. However, data sets from gages with more than 40% missing data in any one category – discharge, turbidity, dissolved oxygen, and specific conductivity – were removed from the analysis. General guidance suggests limiting data imputation up to

40% if the resultant data is used for predictions (Madley-Dowd et al., 2019). Furthermore, it has been shown that even higher missing percentages of more than 50% can be successfully imputed for trend analysis given the use of proper imputation methods (Aguilera et al., 2020; Milleana Shaharudin et al., 2020). Proper imputation methods can reduce biases in datasets with missing percentages larger than 50% (Madley-Dowd et al., 2019). Furthermore, Kalman filtering methods for imputation of hourly evapotranspiration data with 44% missing data, have approximated the original data within acceptable margins (greater than 70% agreement and less than 5% bias) and annual and monthly averages (as is analyzed in this study) calculated by imputed hourly data resulted in even lower errors (85% agreement) (Alavi et al., 2006).

Where data gaps were observed, benchmark tests were performed over the complete data set of each parameter to identify the most appropriate imputation method. Specifically, I used the R package 'imputeTestbench' (Beck et al., 2018) and 'imputeTS', which provides a wide variety of statistical methods to analyze and impute univariate data sets (Moritz & Bartz-Beielstein, 2017). The best imputation method for a specific data set depends on the characteristics of the missing data such as percentage of missing data and gap size. Therefore, the distribution of missing data, average gap size, and percentage of missing data were computed for each data set. This information for each gage was then summarized and the overall average gap sizes for each water quality parameter were used in testing imputation methods.

Several imputation methods were then applied to the data, including linear interpolation, spline interpolation, structural model & Kalman smoothing, simple moving average, imputation by mean, and exponential moving average, among others. To do so,

first a data set with no missing data was used to generate 30 random testing samples for each parameter (discharge, turbidity, dissolved oxygen, and specific conductivity). These samples were then imputed using each method and the methods were compared using the Mean Absolute Error (MAE). The imputation method with the lowest MAE was then selected to impute data for the specific parameter. While data imputation adds a certain error to the data set, it allows me to include much of the available USGS data in our analysis. Imputation results are shown in Appendix 1. After imputation, daily data were used to compute the monthly averages, further reducing the influence of imputation error, which were then applied to evaluate trends. Limitations of this method are acknowledged in Section 3.4.4.

Water quality data is available in a daily frequency; however, land use data for the entire USA is temporally limited to every 2-4 years and land use over the last decade has changed at a slow pace (Homer et al., 2020). In this study, the land use change between the years of 2008 and 2016 is calculated as a percentage and assumed to have changed at a constant rate over the study period. Given the temporal resolution of available land use data, it is only possible to perform trend analysis that spans several years (2008-2016). While the water quality and discharge data is available as a daily dataset, reducing the temporal frequency to monthly data is better suited for long term trend analysis (Mcleod et al., 1991). This is because serial correlation of daily data increases the chance of type II error by Mann-Kendall test (von Storch, 1999). Furthermore, since this study looks at long term impact of land use change, monthly data allows removing seasonality effects from the data as land use have varying impacts through seasons. Influence of land use during wet and dry periods on water quality was studied in the Dan River basin in China

showing that total suspended solids were significantly higher in wet periods while dissolved oxygen was much higher on dry periods (P. Shi et al., 2017). Furthermore, agriculture land plays a key role in seasonal changes of water quality depending on agricultural crops. For example, seasonal crops and perennial crops require different patterns of irrigation and fertilization, which can impact the seasonal water balance and pollutant loads within a watershed (Schilling et al., 2008).

3.2.3.2. Land-use data

Watersheds for each of the 60 stream gages were delineated using ESRI's ArcGIS online and validated using watershed areas listed on the USGS stream gage site (https://waterwatch.usgs.gov/). The NLCD provides land use data in 16 categories; however, these were condensed to 7 categories for ease of analysis and included open water, developed (developed, open space; developed, low intensity; developed, medium intensity; and developed, high intensity), barren land, forest (deciduous forest, evergreen forest, and mixed forest), shrub/grassland (shrub/scrub, herbaceous, and hay/pasture), cultivated, and wetland (woody wetlands and emergent herbaceous wetlands). Using these land use categories and the delineated watersheds, land-use data for each year (2008, and 2016) were extracted from each respective watershed.

3.2.4. Statistical Methods

3.2.4.1. Water Quality and Land Use Trends

Simple descriptive statistics were performed to visualize and evaluate the central tendency and distribution of land use, flow rate and water quality data. Land use changes for each watershed were computed as the percent change in each land use category from 2008 to 2016 for each watershed. In addition, two methods were used to identify and

quantify temporal trends within the water quality and quantity data: Seasonal Mann Kendall tests and Theil-Sen slope. The Seasonal Mann Kendall test was selected to quantify temporal trends in water quality and quantity parameters over time due to seasonal autocorrelation and non-normality of residuals in the USGS gage data. This test is a nonparametric method commonly used to quantify and analyze the significance of a timeseries trend (Helsel et al., 2020). Using this test, correction for serial-correlation due to seasonality is done by removing the seasonal trend from the data by statistical methods introduced by Hirsch (Hirsch & Slack, 1984). While the Mann-Kendall test determines the existence or significance of a monotonic trend, the Theil-Sen slope can provide a robust estimate of the slope or magnitude of this trend (Helsel et al., 2020). Theil-Sen slope is frequently used to compute the magnitude of trends in environmental studies (He et al., 2015; Mahmoodi et al., 2021; Rozemeijer et al., 2014; Ryberg & Chanat, 2022) and represents the change in discharge or water quality parameters over time as shown in the following equation:

$$Theil - Sen\ Slope = Median\ \frac{X_i - X_j}{t_i - t_j}\ where, j > i \qquad \text{Equation 1}$$

where X_i and X_j are gage data at times t_i and t_j, respectively. Gages with significant trends based on a p-statistic of less than 0.1 ($\alpha = 10\%$) were selected for further analysis.

3.2.4.2. Relationship between water quality and land use changes

Robust regression was carried out to analyze how change in water quality and quantity over time (represented by the Theil-Sen slopes) are related to the change in land-use over the same period. Robust regression is a non-parametric technique that reduces the influence of extreme outliers, which are common in streamflow and other

environmental data, and therefore results in better representative slope coefficients (Helsel et al., 2020).

To do so, first single variable regressions were developed to observe the direct relationships between the explanatory variables and the change in discharge and water quality. This relationship is represented by the following equation:

$$y = b_0 + b_1 x \qquad \text{Equation 2}$$

where y is the dependent variable (discharge and water quality changes), x is the explanatory variable (land use change), b_0 is the intercept, and b_1 is the slope coefficient.

Second, multiple robust regressions were carried out to determine if multiple variables (i.e., land use changes) could provide better predictions of discharge and water quality trends. Due to correlations between some explanatory variables, a backwards elimination method coupled with variance inflation factor (VIF) was used to generate final multiple regression models. These relationships generated by robust regression are represented by the following equation:

$$y = b_0 + b_1 x_1 + b_2 x_2 + \cdots + b_n x_n \qquad \text{Equation 3}$$

where, y represents the change in water quality parameter, b_0 represents the intercept, and b_n represents the regression coefficient for n land use changes represented by x_n . The final results include explanatory variables with a VIF value less than 10.

Once regression models for monthly data vs. land use percentage changes over 9 years are developed, the resulting *b* coefficients are converted (multiplied by 12*9) to represent relationships between yearly water quality data vs. yearly land use percentage changes.

Lastly, the slopes of water quality and quantity parameters were categorized as increasing, decreasing, or no trend for each gage based upon the Mann-Kendall test. Then the Kruskal-Wallis (one-way ANOVA on ranks) test was performed to identify whether the categorical increasing or decreasing trends were due to specific land use changes. The hypothesis of the Kruskal-Wallis test is that there is a significant difference between the medians of the groups being compared.

3.3. Results

3.3.1. Land Use Characteristics of the Watersheds

The land use characteristics across all 60 of the watersheds used in this study are summarized in Table 3-1 and their overall distribution is illustrated in Figure 3-2. From the table, forested land use is the most common with an average coverage of 38% that ranges between 3.5% - 93.9% of the total watershed area. This is followed by developed and cultivated land uses, with no other land use making up more than 10% of the watershed coverage on average. The variation in land uses across watersheds in this study is further illustrated in Figure 3-2, which shows the distribution of land cover for each individual watershed. As illustrated, there is a wide distribution in the dominant land use across each watershed, with many land uses – forest, agriculture, developed, and shrub – making up over 50% of an individual watersheds' composition. Examples of this diversity in land use composition is further illustrated in Figure 3-3, which provides four examples of watersheds characterized by a diversity of land cover that dominate the watershed areas.

Table 3-1. Overall land use characteristics of 60 watersheds selected for analysis for the year 2016.

Land Use type	*Mean %*	*Median %*	*Standard Deviation*	*Minimum %*	*Maximum %*
Open Water	1.21	0.39	3.00	0.02	21.89
Developed	28.36	12.05	30.49	0.68	90.40
Barren Land	0.21	0.12	0.26	0.00	1.13
Forest	38.38	33.33	26.02	3.51	93.88
Shrub/Grass Land	8.96	2.44	13.76	0.13	62.91
Cultivated	18.08	11.07	20.96	0.00	71.80
Wetland	4.80	0.70	10.25	0.00	42.84
Imperviousness	9.65	3.03	12.45	0.07	41.03

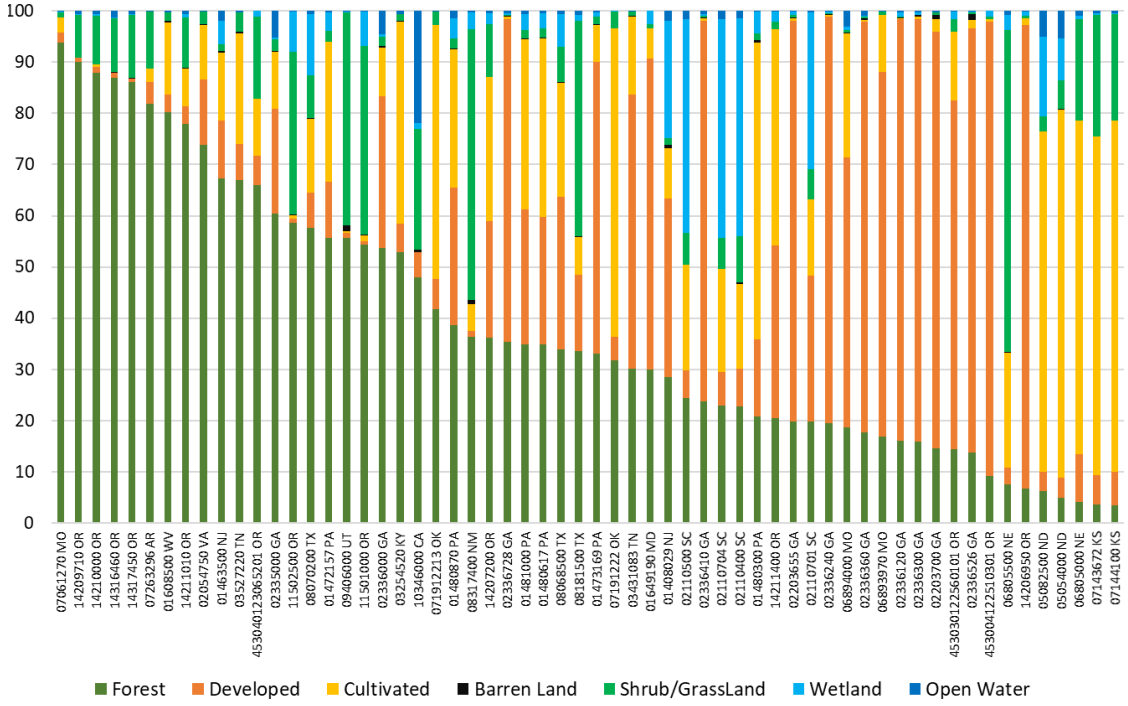

Figure 3-2. Land use composition of the 60 watersheds used for analysis for the year of 2016. Vertical axis is the percentage of the land use category within the watershed while horizontal axis is the list of gages.

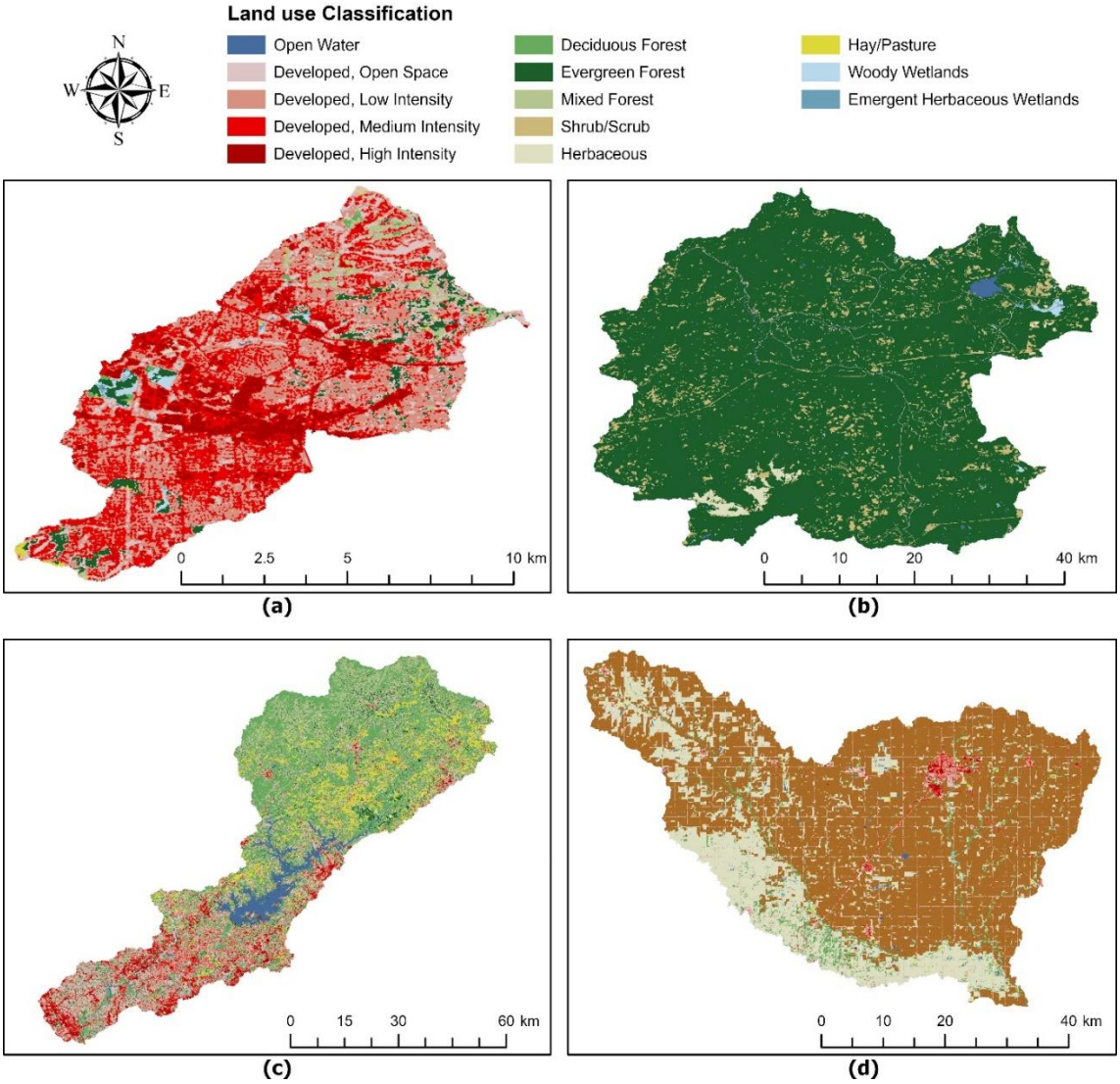

Figure 3-3. Example of the land use distribution within watersheds for four USGS stream gages ((a) 453004122510301 OR, (b) 14209710 OR, (c) 02336000 GA, (d) 07143672 KS) used within this study for year 2008.

3.3.2. Land-Use Changes

A summary of the land-use changes from 2006 to 2016 across all watersheds in this study is shown in Figure 3-4. This figure shows box and whisker plots that represent the distribution of the land cover change in each watershed as a percentage of the overall watershed area. As illustrated, impervious land area and developed land area increased in

every watershed in the study with a mean increase of 0.41% (impervious) and 0.73% (developed) between 2008 and 2016. Mean changes to open water, barren land and wetlands are all under 0.03%, while shrubland declined by the largest amount of 0.62%. Forest land percentages increased on average across all watersheds; however, the median value is negative, indicating a skewed distribution.

This is further elucidated by Figure 3-5, which summarizes the overall change in land use across all watersheds in this study, as well as the overall change across the U.S. As illustrated, the total area of forest land both across the case study watersheds and the U.S. as a whole have reduced. Therefore, the mean increase in forest as a percent of watershed area is likely due to the varying size of the watersheds, with positive changes in smaller watersheds skewing the distribution. The same pattern can be seen in cultivated land with a mean decrease of -0.17% (Figure 3-4), yet an increase in the overall cultivated land cover of over 3% (Figure 3-5).

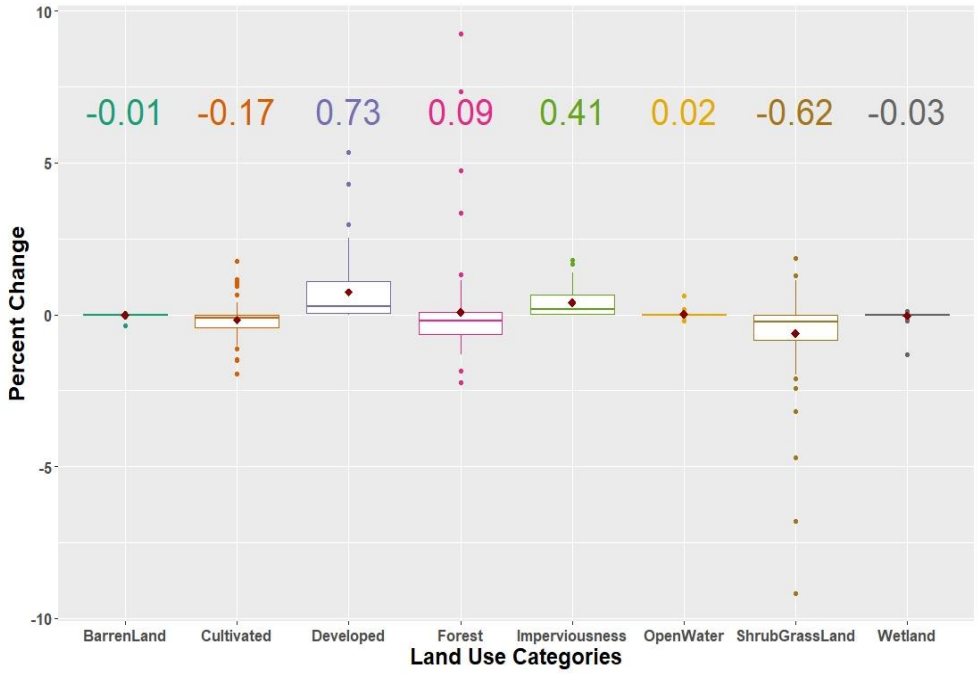

Figure 3-4. Percent land-use change distribution in boxplots within watersheds over the period of 2006-2016 (the highlighted value is the mean of each distribution)

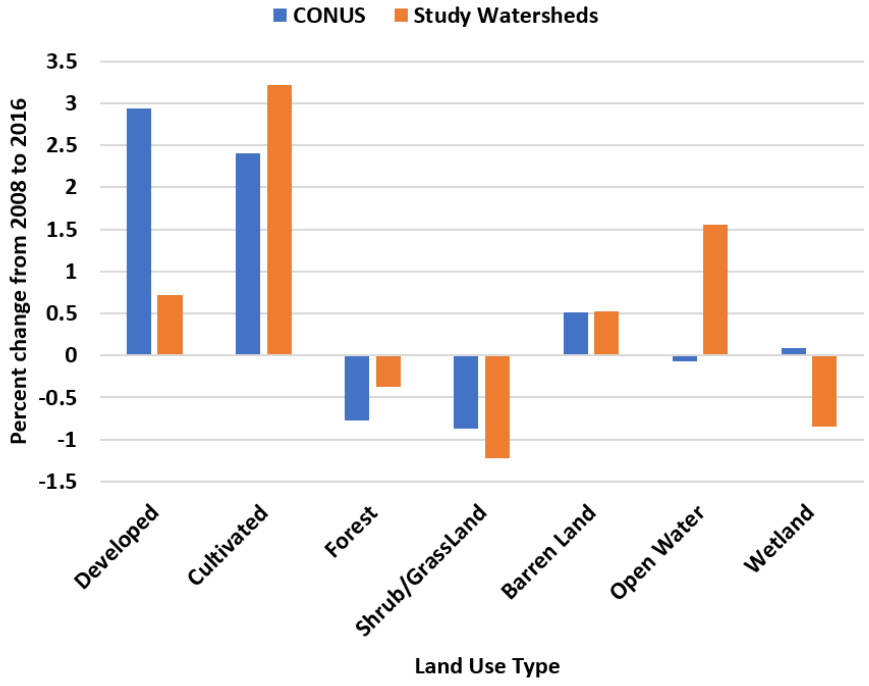

Figure 3-5. Percent land-use change comparison between the 60 watersheds in this study and the contiguous USA.

Figure 3-5 also compares the overall changes in land cover composition from the watersheds in this study to that of the entire contiguous U.S. As illustrated, except for wetland and open water, all other land use changes follow the same increasing or decreasing pattern. Therefore, the land use changes (positive or negative) captured within this study are largely reflective of what has happened across the contiguous U.S.. While wetlands and open water are not reflective of the changes in the country as a whole, they are both under 5% of the total watershed areas on average.

3.3.3. Trends in Water Quality

Theil-Sen slope was generated for all the gage data sets and those with statistically significant trends ($p < 0.10$) were selected for further analysis. The number of gages with significant trends included 23 gages for discharge (40%), 18 gages for dissolved oxygen (35%), 24 gages for specific conductance (44%), and 28 gages for turbidity (44%). The distribution of the Theil-Sen slope for each water quality parameter across all gages used in this study is shown in Figure 3-6. As illustrated, the change in discharge and specific conductance are normally distributed and while discharge is spread equally among positive and negative trends with both mean and median values near zero, specific conductance has a positive average and median trend. For dissolved oxygen, the majority of trends were negative, with the exception of three gages. In addition, for turbidity all gages except for one indicated a decrease in turbidity.

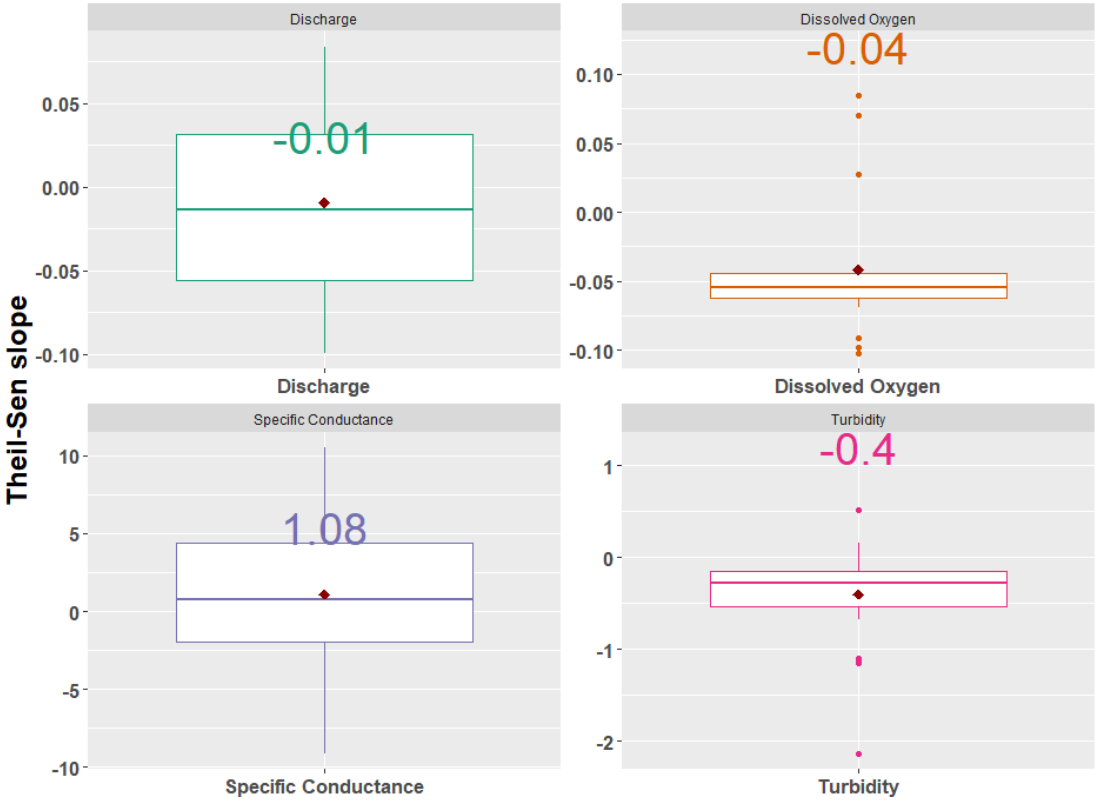

Figure 3-6. Theil-Sen slope distribution of parameters over the period of 2006-2016 with highlighted mean values (Discharge: cfs/miles^2, DO: mg/l, Specific Conductance: µS/cm^{-1} at 25 Celsius, and Turbidity: FNU).

3.3.4. Relationships Between Land-Use and Water Quality Changes

Robust regression was performed to relate the Theil-Sen slopes of the water quality parameter (dependent variable) to the change in land use (independent variable). The significant relationships ($p<0.05$) generated by robust regression are shown in Table 3-2. For all models, the change in land use type explains between 12% and 25% of the variance in discharge and water quality changes. All discharge and water quality variables were linearly related to a change in land use except for dissolved oxygen. Discharge is inversely related to shrub/grass land changes while directly related to changes in cultivated land area. Specific conductance on the other hand is inversely

related to changes in cultivated land and open water while directly related to changes in developed land area. Turbidity is directly related to changes in developed land and impervious area while inversely related to changes in cultivated and wetlands.

Table 3-2. Simple robust regression coefficients with a p statistic less than 0.05 for **yearly** water parameters as dependent variables and **yearly land use percentage changes** as independent variables (discharge n = 24, specific conductance n = 24, turbidity n = 28).

Water Quality Parameter	Land Use Type	Slope Coefficient	R^2
Discharge ($ft^3s^{-1}mile^{-2}$)	Shrub/Grass land	-4.55	0.21
Discharge ($ft^3s^{-1}mile^{-2}$)	Cultivated	4.88	0.22
Specific Conductivity ($\mu S\ cm^{-1}$ @ 25 Celsius)	Open water	-7009.8	0.30
Specific Conductivity ($\mu S\ cm^{-1}$ @ 25 Celsius)	Developed	426.68	0.12
Specific Conductivity ($\mu S\ cm^{-1}$ @ 25 Celsius)	Cultivated	-589.38	0.22
Turbidity (FNU)	Developed	-20.25	0.25
Turbidity (FNU)	Cultivated	95.72	0.23
Turbidity (FNU)	Wetland	69.64	0.14
Turbidity (FNU)	Impervious	-56.21	0.23

To explore if a combination of these land use types could further explain the variance in water quality changes, multiple robust regression was performed as summarized in Table 3-3. Both discharge and specific conductivity resulted in multivariable equations that improved the goodness of fit, while also ensuring no multicollinearity among the data. According to these models, 58% of the variance in discharge trends can be explained by changes in barren, shrub/grass, and cultivated land uses. Using the watersheds that had statistically significant changes in discharge, developed land and cultivated land were inversely correlated with a spearman correlation of -0.75 ($p<0.001$). Finally, open water, cultivated and developed land were able to explain 46% of the variance in specific conductance.

Turbidity did not result in a statistically significant multivariable equation, most likely due to multicollinearity among explanatory variables. Each regression analysis was restricted to watersheds for which there were statistically significant Theil-Sen slope slopes in the water quality data. In the case of turbidity, the 28 watersheds had significant positive correlations between developed land impervious land (0.93) and negative correlations cultivated (-0.82) and wetlands (-0.46) land uses.

Table 3-3. Multiple Robust regression parameters. This shows how **yearly water quality** changes relate to **yearly land use percentage changes**.

Water Quality Parameter	Land Use Category	Slope Coefficient ($p < 0.05$)	R^2
Discharge ($ft^3s^{-1}mile^{-2}$)	Cultivated	4.59	0.58
	Barren Land	-35.67	
	Shrub/Grass Land	-4.56	
Specific Conductance (µS cm^{-1} @ 25 Celsius)	Open Water	-5411.0	0.47
	Developed	-216.2	
	Cultivated	-1443.3	
Turbidity (FNU)	Developed	-20.25	0.25

3.3.4.1. Kruskal-Wallis test

The relationship between land cover changes and changes in discharge and water quality were further analyzed using the Kruskal-Wallis test. Figure 3-7 illustrates the distribution in land cover changes, which are categorized based upon whether the stream gage at that watershed had an increasing or decreasing trend in discharge. A Kruskal-Wallis p-statistic of less than 0.05 means that there is a significant difference (with 95% confidence) in land use changes between watersheds with upward and downward discharge trends. Only discharge was found to have statistically significant differences

between gages with increasing and decreasing trends (Figure 3-7). From this figure, watersheds with increasing discharge were likely to have a greater decrease in shrub/grassland (p = 0.002), barren land (p = 0.045) and wetlands (p = 0.04) than those that had a decreasing trend in discharge. This is consistent with the regression results that found a negative correlation between discharge and shrub/grassland and barren land. Although not significant at the 0.05 level (p = 0.2), increases in discharge may correspond to increases in impervious area.

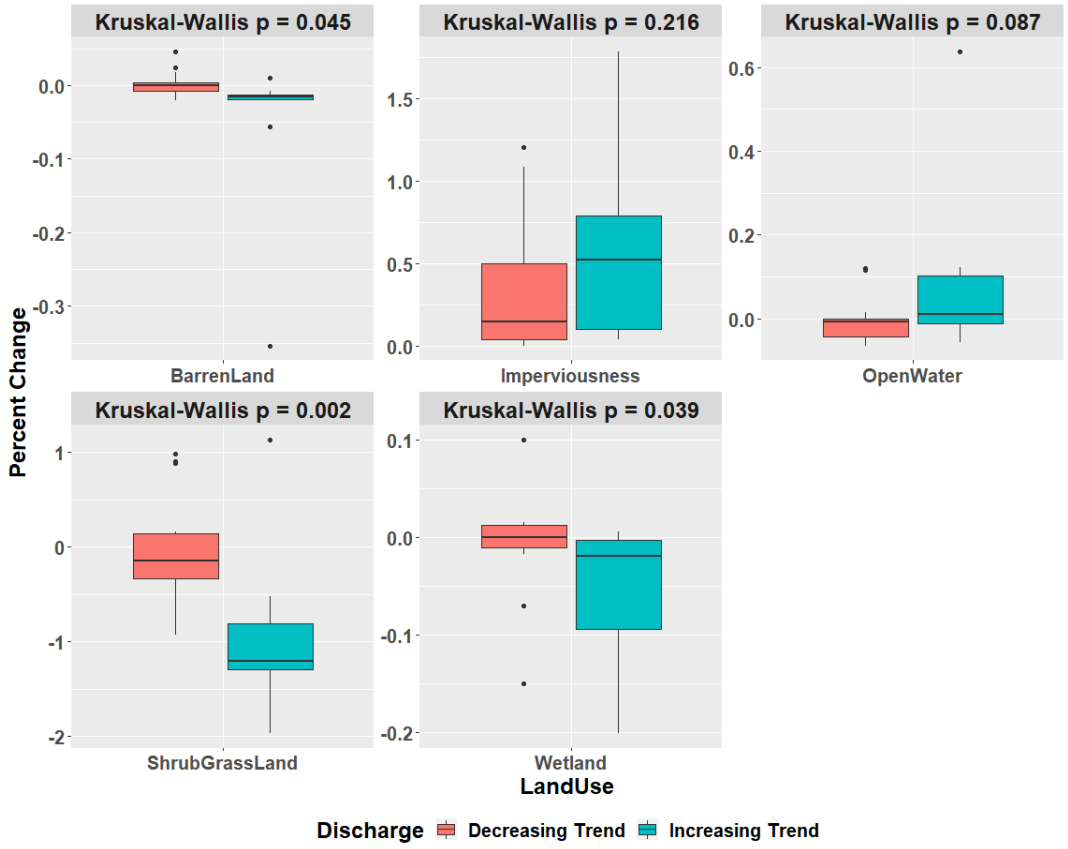

Figure 3-7. Kruskal - Wallis test on water discharge trend direction as the categorical variable and land use types as explanatory variables. Y-axis shows the percentage change in each land use type.

3.4. Discussion

This study evaluated the land use and water quality changes in 60 watersheds over 2008 to 2016. The watersheds used represent a balanced variability in land-use types, with dominant land uses including developed, forest, agriculture, and shrub/grass across all watersheds. In terms of water quality, specific conductance generally increased, and turbidity decreased; while there was little to no overall trend in discharge, there was a large variation in discharge trends across all watersheds. While almost all gages saw negative trends in dissolved oxygen, they were relatively small changes (median of -0.05 %). Furthermore, in evaluating the relationship between land use changes and water quality, it was clear from the Kruskal-Wallis test that changes in barren land, shrub/grasslands and wetlands corresponded to a change in discharge. To that end, there are several implications of these results.

3.4.1. Land Use Changes

In this study, the watersheds on average had increases in imperviousness and cultivated areas, with decreases in shrub/grasslands and forest lands. This is consistent with other studies that found increasing imperviousness and decreasing forest within the United States (Sleeter et al., 2013; Theobald, 2005; Wilson, 2015). Additionally, on average, imperviousness and cultivated areas increased the most over the study period, with shrub/grassland land use having the greatest decrease. The overall changes are relatively small with the highest median percentage change of any land-use type of 0.45% over the 9 year study period (Figure 3-4). This is not surprising as the rate of change of land use has been decreasing since 2005 (Winkler et al., 2021). As a whole, these land

use changes within the watersheds were found to be similar to the changes observed across the U.S. over the same time period.

3.4.2. Water Quality Trends

Specific conductance concentrations increased in a majority of watersheds for which a significant trend was detected. This is consistent with other findings that have found mean increases in the specific conductance in rivers and streams within human dominated landscapes across the U.S. (M. E. Baker et al., 2019; Stets et al., 2020). Specific conductance is representative of the amount of dissolved ions in water, and in streams is largely impacted by dissolved salts. This can come from point source pollution from industrial and residential discharges, but it is largely comprised of non-point source pollution from agricultural land use and activities such as tilling, deforestation, and fertilizer/pesticide application (Stets et al., 2020), as well as urban land uses and activities such as road de-icing (Shoda et al., 2019).

Dissolved oxygen decreased in a majority of watersheds for which a significant trend was detected. This could partly be due to the observed increase in specific conductance, as higher ionic strengths reduce oxygen solubility (Heddam, 2014). In addition, low dissolved oxygen in streams can be caused by other factors such as increases in nutrients, oxygen demand, temperature, ionic strength, and sediments, as well as reductions in aeration (Allan et al., 2021). Nutrients have reduced in urban streams in United States, with no change in agricultural streams over a 30 year time period from 1982 – 2012 (Stets et al., 2020); therefore, oxygen demand caused by increasing nutrient loads might not be the cause of reducing dissolved oxygen across watersheds. However, most streams are impounded by dams and other flow controlling

infrastructure that reduce dissolved oxygen within the structures, which could impact downstream oxygen levels absent of aeration at the outlet of the structures (Zaidel, 2018). Furthermore, temperature in streams in US has been rising (Kaushal et al., 2010) and increase in stream temperature reduces oxygen solubility.

Turbidity decreased in more than 85% of the watersheds with significant trends. Reduction in turbidity could be due to management of surface runoff, as stormwater regulations in the U.S. largely focus on reductions in total suspended solids as the primary regulatory criteria (Naughton et al., 2021). For example, the watershed of USGS gage 01480870 is located in Chester County, PA which has a county specific comprehensive stormwater management ordinance (*2022 County-Wide Act 167 Stormwater Management Model Ordinance | Chester County, PA - Official Website*, 2022) and a plan that requires best management practices to control storm water pollutants, especially total suspended solids. In my analysis, this gage saw a monthly decreasing rate of 0.33 FNU/month (p value of 0.006) for turbidity. This suggests total suspended solids concentrations in streams and rivers may have reduced due to the implementation of best management practices, even if there is an increase in anthropogenic disturbances (J. C. Murphy, 2020; Stets et al., 2020).

Discharge had both positive and negative trends throughout the study period. The lack of an overall trend could be due to a few reasons, including varying precipitation patterns across the dispersed watersheds in this study. For example, precipitation trends in the United States vary with some regions experiences increasing trends and others decreasing trends in precipitation (Easterling et al., 2017). The reasons for this are complex but could be due to climate change, which has been shown to have a

considerable impact on discharge both negatively and positively (Croitoru & Minea, 2015; Leppi et al., 2012). However, it has been further shown that increase in extreme precipitation due to climate change does not necessarily correlate with increases in stream discharges due to the complex nature of factors impacting stream volumes such as antecedent moisture conditions based on climate regions (Ivancic & Shaw, 2015). Regional variations in stream/river discharge has been seen in other parts of the world such as Canada and South American countries as well and they can be attributed to climatic variations and anthropogenic activities such as flow diversions (Déry et al., 2016; Pasquini & Depetris, 2007). Therefore, due to the dispersed nature of the gages across regions where precipitation and other factors vary, there may not be a consistent pattern in discharge trends.

3.4.3. Impact of Land Use Change on Discharge and Water Quality Trends

Changes in discharge were negatively correlated to changes in shrub/grassland and barren land uses and positively correlated to changes in cultivated land use. Loss of vegetated ground cover due to an increase in agricultural land has generally been found to increase ground water recharge and reduce evapotranspiration, which leads to increases in stream baseflows (Ahiablame et al., 2017; Astuti et al., 2019; Y. K. Zhang & Schilling, 2006). Artificial irrigation of agriculture land contributes to a considerable increase in the water budget of the watershed. Evapotranspiration is generally lower on agriculture land as compared to compared to shrub/grass lands due to the use of seasonal crops in the USA (Schilling et al., 2008); however, a study in India, where most crops are perennial, has found that agriculture land increases ET considerably while also increasing the base stream flows caused by artificial irrigation (Shah et al., 2019). Similar increases in

baseflows may explain the observed trends in this study, as I used average monthly area adjusted flow, encompassing both baseflow and stormflow. Increases in discharge were also moderately correlated with reductions in wetlands using the Kruskal-Wallis test ($p < 0.1$). This could be due to the higher water retention capacity of wetlands compared to the other land use types (Procházka et al., 2019).

Trends in discharge were not correlated to developed land use changes. While it is established that developed land increases peak discharge and runoff (P. J. Shi et al., 2007), this might not be seen in monthly averaged data which also encompasses baseflow. The annual temporal scale these models represent, and monthly data used for trend generation, do not capture discharge differences caused by urban runoff which happens at a much smaller time scale (hours, days). While increase in imperviousness and urban land cover has shown to increase stream discharge variation at hourly and daily time scales (Simmons & Reynolds, 1982), this might not be seeing in annual and monthly scales. Furthermore, many studies have found that groundwater infiltration is reduced due to imperviousness of developed land thus reducing base flow in streams (Aboelnour et al., 2020; Chithra et al., 2015; Kauffman et al., 2009). For example, in Long Island, New York an increase in imperviousness over 30 years reduced base flow to 20% of total annual stream flow compared to 95% before urbanization and a continuous reduction of average base flow with high fluctuations in stream flow (Simmons & Reynolds, 1982). Contradicting these observations, 5 watersheds in the Delaware river basin has not seen a reduction in baseflows despite heavy urbanization and increase of imperviousness (Brandes et al., 2005).

Turbidity was found to be positively correlated with cultivated land use changes and negatively correlated to developed land use changes. Cultivated lands often result in runoff of sediments to streams (Mello et al., 2020), which may explain this relationship. In addition, a negative relationship of turbidity with developed land could be due to better pollution control practices within urban landscapes (Stets et al., 2020). This is because new developments and redevelopments in the U.S. are largely now subject to much more stringent stormwater control measures and regulations than those in the past (J. Murphy & Sprague, 2019). Therefore, even if urban land uses produce a greater pollutant runoff than their pre-development conditions, the implementation of best management practices to capture and treat this runoff could lead to downstream pollutant reductions.

Finally, specific conductance was negatively correlated to cultivated and open water land uses and positively correlated to developed land use. Open water variation within selected watersheds is minute, with an average change of 0.008%. Thus, the impact of open water change relative to other land-use change might not be as influential. However, reduction in open water land could mean increase in ionic concentrations due to land alterations and volume reductions. The negative correlation between specific conductance and cultivated land could be due to improved management of agricultural runoff or the conversion of agricultural land to other land uses that increase the runoff of dissolved ions. The latter is supported by the positive correlation between specific conductance and developed land observed in this study. This has also been observed in regional studies (Tu, 2013) and is likely due to the influence of urban land uses and activities on salt and dissolved ions in runoff as discussed previously.

3.4.4. Implications and Limitations of the Study

The main outcomes of this study are the correlations found between land use changes over time and water quality changes at a larger spatial scale. Understanding these relationships has implications for the development and implementation of watershed management plans. This study demonstrates that land use changes that occurred over a decade, however small, are correlated to discharge and water quality. While water quality management plans are developed and updated frequently (e.g. TMDLs need to be done every 2 years and section 303(e) of the Clean Water Act requires a continuing planning process), implementation of best management practices to reduce pollution through non-point source runoff takes decades; however, in most cases, water management plans do not project land use changes and their future impacts on water quality. For example, none of the 2017 water management plans for Wisconsin watersheds certified by the EPA and the approved 2020 TMDL report for Upper Fox and Wolf Basins have future land use projections and their impacts on water quality (Wisconsin Department of Natural Resources, 2017). However, the handbook for developing watershed plans by EPA does suggest the use of future land use projections. But doing so is largely constrained to loading estimations from models that may be resource-intensive to develop and limited to prior knowledge. Incorporating predictions of land use change and their subsequent impact on the water quality changes through an empirical model, such as the one developed in this study, could improve the planning process which currently is relied upon margins of safety and current or older water quality and land use data.

One advantage of the approach presented is in the form of the model and therefore what the data represents and how it can be applied. The empirical model developed in

this study takes the form of *water quality change = f (land use change)*. However, the majority of empirical studies evaluating the relationship between stream water quality and land use develop a model in the form of *water quality = f (land use)*, which represents a relationship at one point in time and therefore does not capture the degree to which changes in land use might influence changes in water quality. This could make the models biased towards the composition of historical land uses that may not have the same impact on discharge or water quality as contemporary land development. For example, a model that captures the impact of urban land use on water quality at one point in time might be biased by historical development within that watershed that did not have to adhere to water quality requirements derived from programs after the Clean Water Act. However, the model in this study only looks at recent changes where the implementation of BMPs and modern drainage designs are captured. Furthermore, while the form of the model *water quality = f (land use)* may be good for estimating water quality in ungaged basins, for applications where water quality is known, such as streams that are already listed as impaired in the TMDL program, there is no way to calibrate the model to current conditions. However, the model proposed in this study can be applied to data representing current water quality or discharge, to estimate what the subsequent change in water quality or discharge might be due to land use changes. In addition, the model proposed in this study is independent of current land use conditions and therefore can be applied based only on expected land use changes (as a percentage of the overall watershed) without having to define the existing land use composition.

While the models in this study were able to explain 11% to 57% of the variance in water quality and discharge trends, there are several unobserved factors that also

influence water quality and discharge in rivers. These include changes to policy, land-use patterns, stormwater control measures, legacy effects, and other human interventions, such as treatment plants, irrigation, and fertilization. For example, changes to watersheds that do not modify a land use category, such as increases in population density, conversions of grazing land into crop agriculture, and improvements to waste management methods have been shown to have a significant effect on water quality (Panthi et al., 2017; Vrebos et al., 2017; Wijesiri et al., 2018; Wilson, 2015). Furthermore, watershed management approaches, such as best management practices installed to address Total Maximum Daily Loads (TMDLs), also can decrease pollutant levels in downstream water bodies by prevention and mitigation of pollutants (J. Murphy & Sprague, 2019; Stets et al., 2020). While this study looks at changes in land use composition, the pattern and scale of that land use (Chiang et al., 2021; Shehab et al., 2021; P. Shi et al., 2017; G. Wang et al., 2014), topography (Lei et al., 2021), and point sources (Pak et al., 2021) may also play a considerable role in affecting stream water quality and quantity.

The temporal scale of land use change impact on water quality and quantity varies due to factors such as the topographical characteristics of the watersheds and pollutant in question. While overland flow reaches streams in a considerably shorter time period (within days) ground water flow contributes to a legacy effect based on the topography (S. L. Martin et al., 2011), anthropogenic environments such as artificial lakes and landfills, and natural environments (Basu et al., 2022). However, it has been shown that current land use explains the current water quality just as well as legacy land use and is mostly dependent on the pollutant in question (S. L. Martin et al., 2017). For example,

conservative pollutants (i.e., those that are less reactive in the environment) such as Cl^-, Na^+, total nitrogen, and NO_3^-, have a higher mobility within watersheds such that current land use patterns describe the variation as well as or even better than legacy land use. But pollutants such as NH_4^- seem to be explained better when legacy land use is incorporated in models since these are much more biogeochemically active. With regards to legacy effect on the parameters used in this study: specific conductance is an indicator of ionic pollutants, and the above study shows that most ionic compounds can be better modeled by current land use patterns. Therefore, specific conductance is not impacted by legacy effects as much. Turbidity is an indicator of total suspended sediments and other visible pollutants such as dyes and colored organic matter. Suspended sediments such as clay and silt has shown complicated transport dynamics therefore, the relationships developed should be interpreted within the temporal scale used in the study (Vercruysse et al., 2017). Temporal studies evaluating the legacy effect on dissolved oxygen are lacking. However, legacy effects of nutrient loadings could impact the effect of land use change on dissolved oxygen since nutrients are correlated to it. Furthermore, temperature and specific conductance are also directly correlated to dissolved oxygen concentration. These complicated interactions of dissolved oxygen might have been the cause for this study to not find any relationships between land use and DO.

Finally, the imputation of daily data using structural timeseries and Kalman smoothing is commonly used with environmental data (Afrifa-Yamoah et al., 2020; Alavi et al., 2006; Hadeed et al., 2020). However, there may be impacts of using imputed data on the statistical significance of a model, depending upon the characteristics of the data and models used. For example, imputed data increases the significance of trend analysis

of the same data if the same regression methods are used for quantifying the trends (Enders, 2022). However, this study is different in two respects. First, the imputation method and the regression models used are different in that the imputations are done using a Kalman smoothing, while the regressions are done using non-parametric linear regression. Secondly, the time scale of the data is different in that the imputations are performed on daily data (with a maximum average data gap of 10 days for all parameters) and linear regression are performed on averaged monthly data. Averaging the daily data helps maintain the variability of monthly data by reducing the bias of imputed data on trend analysis.

3.5. Conclusion

This study quantified and evaluated the relationships between land-use and water quality trends for 60 watersheds across U.S. over a 9-year period from 2006 to 2016. Developed land use had the largest increase across all watersheds with a median of 0.26% (mean of 0.73%) of the total watershed area, while shrub and grass land had the largest decrease with a median of -0.22% (mean of -0.62%). Regarding water quality, specific conductance had an increasing trend in 63% of the watersheds with significant trends, while dissolved oxygen and turbidity had a decreasing trend in 83% and 86% of the watersheds with significant trends. Discharge trends varied among watersheds and observed changes were comparatively small (less than ± 0.1%). In terms of relationships between land use change and trends in hydrologic data, discharge was found to be positively corelated with cultivated land and negatively corelated with shrub/grass and barren land. Surprisingly, discharge was not correlated with developed land use changes at a statistically significant level ($p < 0.05$), which could be because the daily discharge

data is influenced by stream baseflow. Turbidity trends were positively correlated with changes in cultivated land and negatively correlated with changes in developed land. This perhaps suggests that current stormwater management regulations that focus on solids removal have a positive impact on downstream water quality. Finally, specific conductance trends were negatively correlated to cultivated land, perhaps due to the conversion of agricultural land to other land uses that increase the runoff of dissolved ions rather than improved management of runoff. As a whole, this case study provides broad analysis trends in land use and water quality, providing an improved understanding of the complex relationships between human land development activity and its subsequent effect on downstream hydrology and water quality which can be used for water management planning and decision making.

4. DEFINE THE INFLUENCE OF SOCIOECONOMIC AND SPATIAL VARIABLES ON TMDL PROGRESS IN THE UNITED STATES

4.1. Rationale

The Total Maximum Daily Load (TMDL) program is the federal statutory method of addressing non-point source pollution in the nation's water bodies, where states in the U.S. are required to assess their water bodies and establish TMDLs for water bodies that are identified as impaired. This program relies on a system of policy implementation known as cooperative federalism where the federal government delegates primary authority to agencies at the state level and therefore the extent to which states assess water bodies, identify impairments, and develop TMDLs can vary from state to state. Therefore, socioeconomic, political, and spatial variations between states could potentially impact how TMDLs are developed. Furthermore, socioeconomic factors within water management regions have shown to have correlations to its water quality. While technical aspects of the TMDL program are well researched, the socioeconomic, political, and regional impact on the TMDL development process is unknown. Understanding this impact will allow water managers and planners to utilize the relationships between socioeconomics and TMDL progress to inform the development of TMDLs. This objective seeks to fill this gap through a nation-wide analysis of the relationships between TMDL progress and socioeconomic, political, and regional variables.

I hypothesize that socioeconomic, political, and spatial factors are correlated to the progress of the TMDL process.

4.2. Methodology

4.2.1. Data Collection

TMDL assessment data were extracted from EPA Assessment and Total Maximum Daily Load Tracking and Implementation System (ATTAINS) archived data (*ATTAINS | Water Data and Tools | US EPA*, 2022). For each State, ATTAINS includes data on the status of TMDL for surface water bodies including the miles of water body that are assessed, miles unassessed, specific impairment, miles impaired, and miles with a completed TMDL. In addition, U.S. Census data was obtained for each state including the population, gross domestic product, percentage without high school diplomas, bachelor's degree percentage, and per capita earnings (*Census Bureau Data*, 2017). Finally, other spatial information, namely state land area, elevation gain, average slope, average annual rainfall, and remote land percentage was derived using various sources which are all listed in Table Appendix 2-1.

Elevation gain and average geographical slopes were used with the intent of generating relationships between TMDL progress, such as percent of streams that are impaired, and dominant geographical nature of the states, and they have been used successfully in water quality studies where slope has been shown to be a significant factor impacting stream water quality (Connolly et al., 2018). Annual rainfall is used as a parameter because it is directly related to water quality of surface water bodies (Coulliette & Noble, 2008; Prathumratana et al., 2008). Remote land percentage (Frontier and remote land area) developed by Economic Research Service (Cromartie & Nulph, 2019), is a remoteness index developed based on frontier communities, defined by population, and travel times from those communities. This index has been used for

comparative studies of socioeconomic patterns such as health care services in remote populations (Mueller et al., 2016), and in this study it will be used to generate remote land area percentages within each state. Disparities between rural and urban water quality and air quality has been found in the United States over the last decade (Strosnider et al., 2017). In the case of assessing streams, it may be that the more remote areas the state has, the more effort and resources it takes to travel to and assess stream quality. Furthermore, remoteness may also provide an indication of the level of interest in better water quality among citizens, as water quality perceptions have been linked to income level and location (Andrew et al., 2019).

4.2.2. Data Preparation

Once data was obtained from ATTAINS, it was processed to ensure consistency across each state. Because TMDLs are implemented at the state-level, each state operates independently and may have different ways in which they classify pollutants, perform monitoring and testing, and report their results. This can make it challenging to summarize data across all states due to differences in methodology and reporting. For example, in evaluating the suspended matter in water, states may list this as Total Suspended Solids (TSS) or turbidity. Therefore, to enable comparisons among states, the data was aggregated into common categories as shown in Table 4-1.

Table 4-1. Summarized stream and river impairment causes.

Cause	Included causes
Ammonia	Ammonia, Ammonia (Un-ionized), Ammonia Total
Arsenic	Arsenic
Bacteria	Bacteria, E. Coli, Enterococcus Bacteria, Fecal Coliform, Total Coliform, Pathogens
Chloride	Chloride
Dissolved Oxygen (DO)	Dissolved Oxygen, Organic Enrichment / Low Dissolved Oxygen, Dissolved Oxygen Saturation, Organic Enrichment
Flow Alterations	Flow Alterations, Other Flow Regime Alterations, Low Flow Alterations, Instream Flow, Water/Flow Variability, Changes in Stream Depth and Velocity Patterns, Change in Flow Patterns
Habitat Alterations	Alteration in Streamside or Littoral Vegetation, Direct Habitat Alterations, Other Habitat Alterations, Physical Substrate Habitat Alterations, Alteration in Stream-Side or Littoral Vegetative Covers, Physical Substrate Habitat Alterations, Other Anthropogenic Habitat Alterations, Loss of Instream Cover, Habitat Assessment (Streams) Alterations in Wetland Habitats, Fish Habitat, Other Anthropogenic Substrate Alterations, Direct Habitat Alterations
Impaired Biota	Biological Impairment, Fish Bioassessments, Cause Unknown-Biological Integrity, Ecological/Biological Integrity Benthos, Benthic Macroinvertebrates Bioassessments, Fish Bio Assessments, Fish Bioassessments (Streams), Combination Benthic/Fishes Bioassessment, Unknown Biologic Stressor, Aquatic Macroinvertebrate Bioassessments, Combined Biota/Habitat Assessments, Biology, Impaired Fish Community, Impaired Microbenthos Community
Lead	Lead
Mercury	Mercury
Metals	Metals, Copper, Iron, Zinc, Aluminum, Manganese, Nickel
Nutrients	Nutrients, Phosphorus, Total Phosphorus, Nutrient Eutrophication, Nitrogen, Total Nitrogen, Total Kjehldahl Nitrogen, Nitrate/Nitrites, Biostimulatory Conditions
PCBs	PCBs, PCB in Water Column, PCBs in Fish Tissue
pH	pH
Sediments	Sedimentation/Siltation, Siltation, Sedimentation
Selenium	Selenium
Temperature	Temperature, Water Temperature
Turbidity	Turbidity, Total Suspended Solids

4.2.3. Data Analysis

To analyze the data, I performed three types of analysis: summary statistics, clustering, and linear regression. To summarize data across all states, descriptive statistics (mean, median, and standard deviation) were performed on the TMDL and socioeconomic data. Two types of clustering were used to evaluate the TMDL progress and socioeconomic data and how they spatially aggregate. Clustering is a common method to allocate objects (e.g., States) with multiple data sets (e.g., water quality parameters of each state) into groups that have similar attributes across datasets (Javadi et al., 2017). For TMDL progress, k-means clustering (Hartigan & Wong, 1979) was used to identify if states had any common groupings considering the percent of streams that were assessed, those that were impaired, and those in which a TMDL was completed. K-means clustering is one of the most commonly used clustering method and it can be used to generate an optimally defined number of clusters (Ali & Kadhum, 2017). The hypothesis for k-means cluster analysis was that, given an optimal k-value (number of clusters), the data set will reveal meaningful groupings that could represent the progress of the TMDL process. In other words, I assume that clustering will allow to group states based on the performance of TMDL process in to high, mid, and low (when $k = 3$ is used).

For socioeconomic data, a hierarchical clustering (Murtagh & Contreras, 2012) based on Euclidean distance and complete linkage method was used to determine different levels of clustering among socioeconomic variables. Unlike k-means method, hierarchical method does not require prior knowledge of the number of clusters. It is a stepwise clustering method that merges the most similar data points together into groups

at each level and depending on the number of steps analyzed, several different groupings will result in this method and can be used for making observations regarding the relationships between states based on socioeconomic data. Hierarchical clustering is the most used clustering method in analyzing socioeconomic data. For example, this method has been applied to identify differences in the socioeconomical status of immigrants and domestic populations in Chile (Cabieses et al., 2015). Furthermore, hierarchical cluster analysis has been used to assess the socioeconomics of sustainable development among European Union countries and the cluster analysis has shown that based on the selected factors, Germany has the most sustainable socioeconomic development within the region (Skvarciany et al., 2020). The objective of using this method to analyze socioeconomic data between states is to generate spatial information to compare with TMDL progress and EPA region information. I hypothesis that hierarchical clustering will generate groupings of states based on similarities among socioeconomic data that will emulate EPA groupings, TMDL performance groupings, or similar.

Once clustering was done, I observed that, spatially, the clusters appeared to mirror the boundaries of the EPA regions or a collection of them. Therefore, rather than evaluate the data based upon clusters, they were evaluated based upon the EPA regions that they fell within. Use of EPA regions in the analysis is important since the EPA regional offices have developed independently (Neilson & Stevens, 2002) and have the potential to influence the TMDL process. It is the EPA's responsibility to guide and enforce the development of TMDLs by the states, and I therefore hypothesized that TMDL process differs significantly based on EPA regions. Descriptive statistics were performed on subsets of the data including those within certain clusters described below

or within specific EPA regions. ANOVA tests were performed between these multiple subsets of data to test the above hypothesis.

In addition, linear regressions, both multiple and simple, were performed to find statistical relationships between dependent (percentage of TMDL completed, percentage of assessed streams, etc.) and independent variables (socioeconomic variables and regional clusters). The relationship generated by the regression can be represented as:

$$y = b_0 + b_1 x_1 + \cdots + b_n x_n + e \qquad \text{Equation 1}$$

where y represents the dependent variable, b_0 represents the intercept, and $b_{(1-n)}$ represents the independent variables represented by $x_{(1-n)}$. All regression models were checked for assumptions of linear regression including normality of the residuals, multicollinearity among independent variables, and homoscedasticity and normality of the residuals. Stepwise model selection using bidirectional elimination was carried out for multiple linear regression based on a significance level to entry of 0.10 and a significance level to stay of 0.05. Stepwise method allows me to analyze all possible regression models and was carried out using SAS software. The parameters used for regression analysis are given in Table 4-2. The hypothesis of the regression analysis is that the socioeconomic parameters have a significant relationship to the TMDL progress parameters.

Table 4-2. Parameters used in regression analysis of the TMDL study

Dependent Variable	Independent Variable
Assessed percent	Total stream miles
Impaired percent	Stream Density
TMDL Complete percent	State Land Area (Miles)
Assessed miles	Average Area Rainfall
Impaired miles	Elevation Gain feet
TMDL complete miles	Average Slope
	Population
	Population Density
	GDP (Billion USD)
	No High School Diploma percentage
	Bachelor's Degree or higher percentage
	Per-Capita Earnings
	Remote area percentage

Finally, to assess the influence of politics, the average representation of the party that holds the legislative chambers and governorship was calculated for the last decade (NCSL, 2020). If both the legislative chambers and the governorship are held by a single party for the particular year, the state is considered controlled by that political party, otherwise it was considered as neutral. Once the average composition is computed, TMDL parameters were categorized, and non-parametric Wilcoxon Rank-Sum test was carried out to test the hypothesis that TMDL progress significantly different between state legislative biases (Republican Vs. Democrat). Wilcoxon Rank-Sum test is used to compare samples when the data used is not normally distributed (Mann & Whitney, 1947).

4.3. Results and Discussion

4.3.1. TMDL Assessment

Within the ATTAINS database, summary data is reported as (1) the percent of streams and rivers that have been assessed, (2) the percentage of the assessed rivers that are listed as impaired, and (3) the percentage of impaired rivers for which a TMDL has been completed. The distribution of these statistics across all states is illustrated in Figure 4-1. The wide range of the whiskers for all three of these parameters highlights the extent of the variation in the progress of states in implementing the TMDL program. For example, the mean percent of streams with assessments complete is 43% with a standard deviation of 33.1%, illustrating a vast range in the percentage of streams that have been assessed. Of those assessed water bodies, on average 61% were impaired and of those impaired, on average 25% had a TMDL completed. Similar statistics for miles are in Figure 4-1 and they state that on average 22,165 miles are assessed, 13,256 miles are impaired, and 3,348 miles have TMDLs developed in each state.

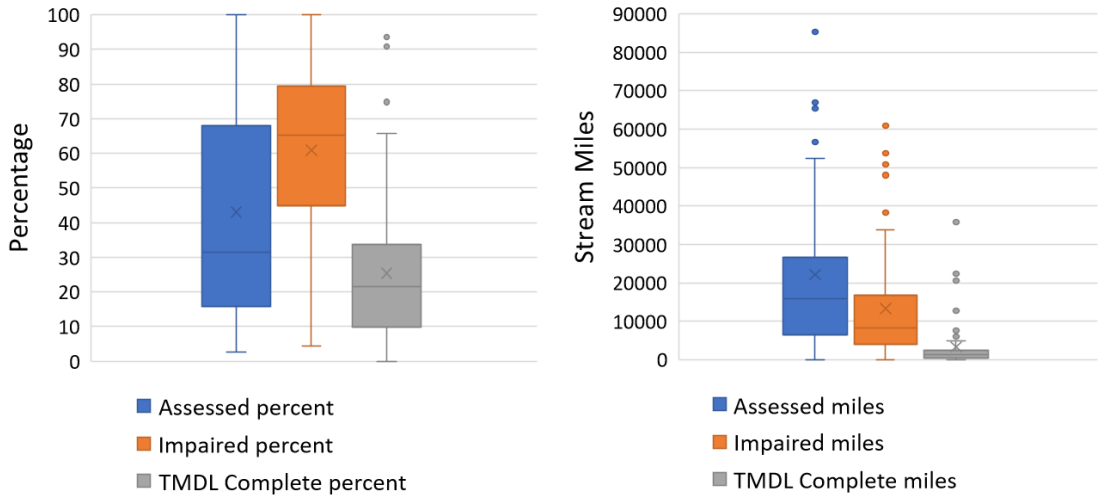

Figure 4-1. Distribution of the percent of streams (left) and total stream miles (right) within a state that have been assessed, listed as impaired, and have had a completed TMDL.

To determine if there were any groupings in the progress of TMDLs among states, I performed K-means clustering, considering the three variables in Figure 4-1, and three distinct groups were identified. Figure 4-2 (left) illustrates how each cluster behaves in terms of each TMDL percentage parameter. As illustrated, there appear to be three distinct groups of states, with cluster 1 (blue) which has the lowest percentage of assessments done. Even though most of these assessed streams are impaired, these states have the least amount of completed TMDLs as well. Cluster 2 (red) comparatively performs the best as they have performed the most assessments and have completed the most TMDLs. Though states in cluster 3 (green) have not completed many TMDLs, they have assessed almost the same amount of streams as cluster 2 yet, their streams are the least impaired.

North Carolina stands out as the only state that has done 100% of the assessments (32,000 miles) and has completed 93.5% of the TMDL preparation. It is also notable that 99.99% of the assessed streams in North Carolina were listed as impaired. New

Hampshire also stands out as an outlier, which with 16,962 miles of streams assessed has assessed 100% of their streams, found 100% of them to be impaired, and completed TMDLs on 75% of their streams. The lowest point in the bottom left is Alaska, which has assessed 4,409 miles of streams representing only 1.2 % of their total streams, finding 9.4% to be impaired and completing a TMDL on none of their streams. The spatial distribution of these clusters is illustrated in Figure 4-2 (right), which demonstrates that there are some states, especially within the northeast, that appear to cluster together. These northeastern states that cluster together are mostly from EPA regions 1, 2, and 3. The performance comparison between states is shown in Figure 4-3 where each state is color coded based on groupings of EPA regions.

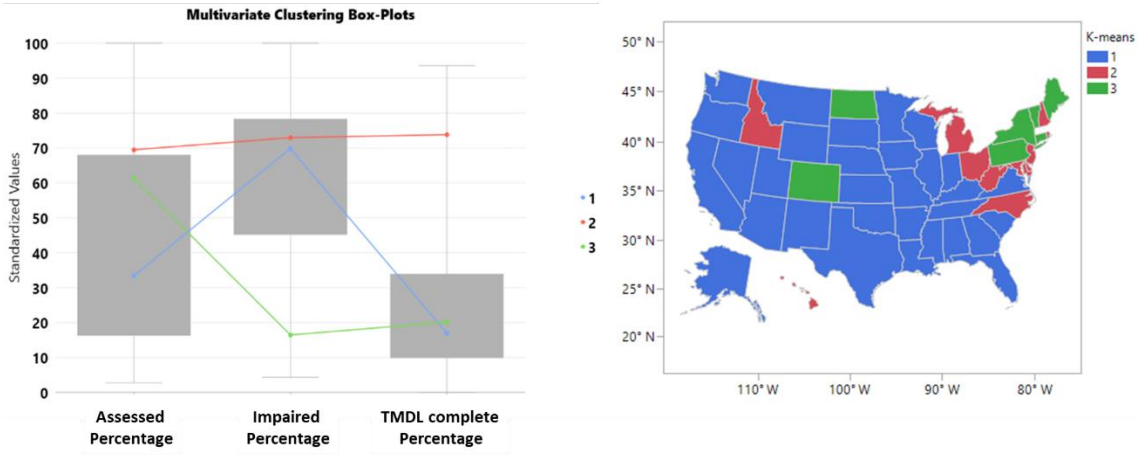

Figure 4-2. K-means clustering of assessed, impaired, and TMDL complete percentages. Groups 1 (blue), 2 (red), and 3 (green) represent clusters of states that behave similarly in terms of TMDL progress.

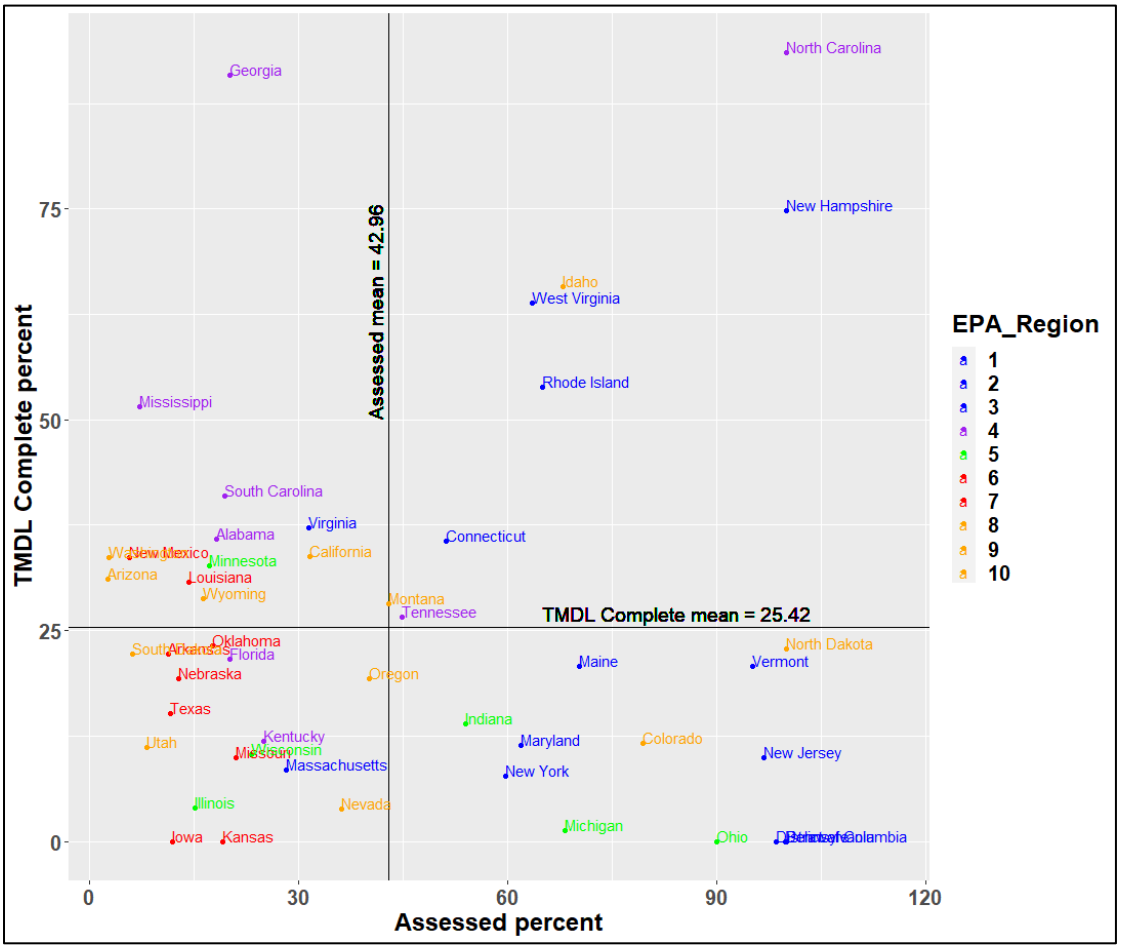

Figure 4-3. Performance comparison of the states measured by assessed water body percentage and percent TMDL completions.

Once it was identified that the states cluster together in terms of TMDL progress and some clusters fall under specific EPA regions, it was hypothesized that indicators of TMDL progress will differ between EPA regions. Therefore, to further explore this potential spatial relationship, the data was categorized into EPA regions (Figure 4-4 d) to identify any common trends in TMDL progress among these regions. Figure 4-4 illustrates the distribution of the percentage of streams assessed, streams impaired, and those streams with a TMDL complete. As illustrated, there is noticeable variance among all categories within EPA regions; therefore, a grouped analysis of variance (ANOVA)

was applied and it found a p-value of 0.005 for assessed streams, suggesting some EPA regions are significantly different than others based upon the percent of streams they have assessed. Furthermore, using paired ANOVA, it was observed that Region 6 is significantly different from Regions 1 and 3 ($p < 0.05$) and Region 7 is significantly different from Region 3 ($p < 0.05$). This may be because both Region 6 and 7 have assessed less than 25% of their streams.

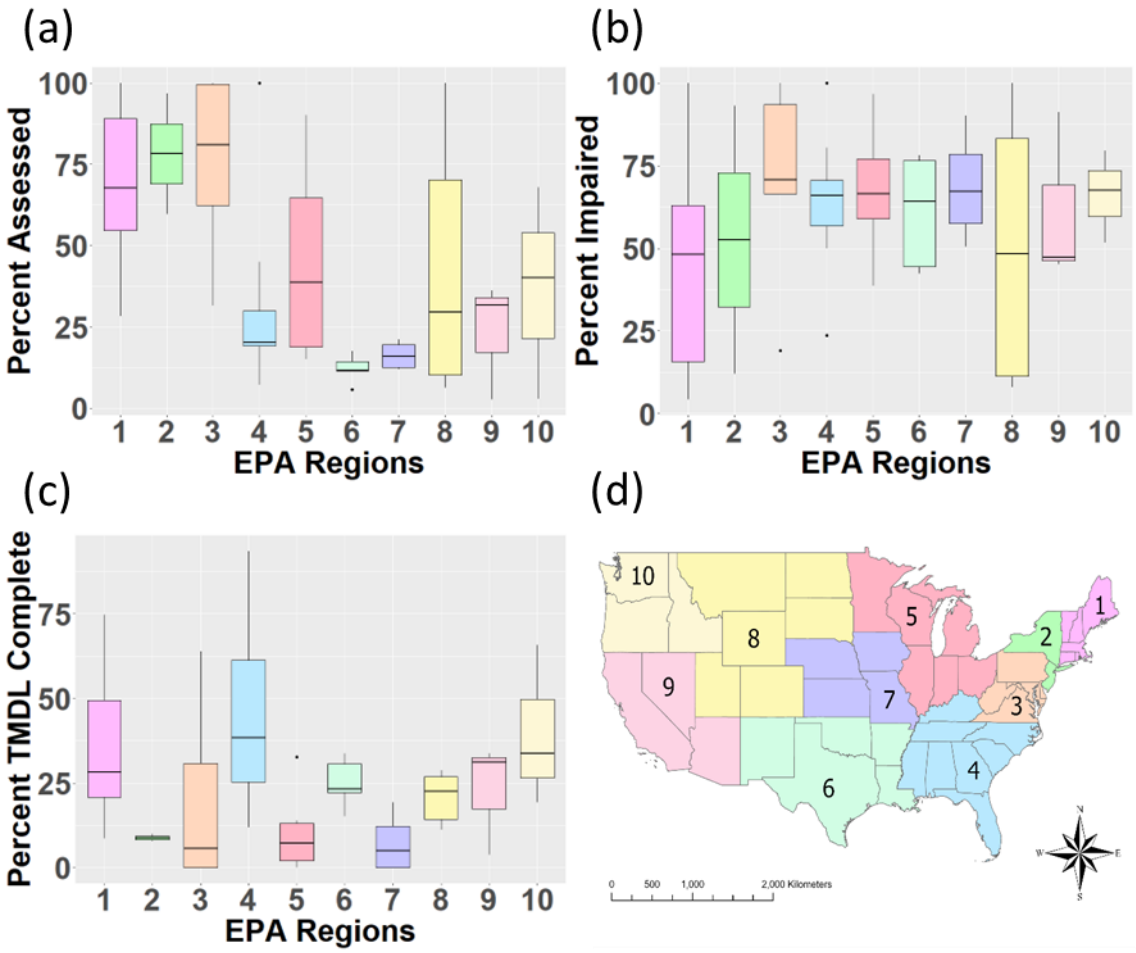

Figure 4-4. Assessed percentage (a), impaired percentage (b) and TMDL completed percentage (c) for streams by EPA region. EPA regions are shown in (d).

Disparities between EPA regions have been observed in other studies as well. For example, it has been found that in EPA region 6 and 7, the racial inequality in industrial toxic air exposure is significantly higher compared to other EPA regions (Zwickl et al., 2014). A study of exposure to polychlorinated biphenyls (PCBs) in EPA regions 1, 2, 4, and 5 has found significant differences of sampling and monitoring methodologies, and guidelines and their basis between these regions. EPA regions have different levels of resources (e.g., laboratories) due to historic political fluctuations and differences, funding limitations, and different organizational philosophies (Williams, 1993). Though no studies can be found regarding internal funding differences between EPA regions, the financial report of the EPA for year 2022 shows that funding allocations are based on the interests of regional offices and they perform differently from one another (*Fiscal Year 2022 Agency Financial Report*, 2022). Finally, newspaper articles based on EPA personnel interviews have alluded to funding and resources disparities between EPA regional units (A. Smith, 2018) which could potentially result in performance differences.

4.3.2. Impairment Types

The ATTAINS database ranks the top impairments within each state and lists the total miles of streams impaired for each pollutant or impairment cause. The categorization of the top four impairments across all states is illustrated in Figure 4-5. In this figure, a first-level impairment is the largest impairment cause in terms of miles of rivers and streams that are impaired within an individual state. As illustrated, bacteria are the most frequent first-level and second-level impairment across the nation and is followed as the top impairment by temperature, sediments, and nutrients.

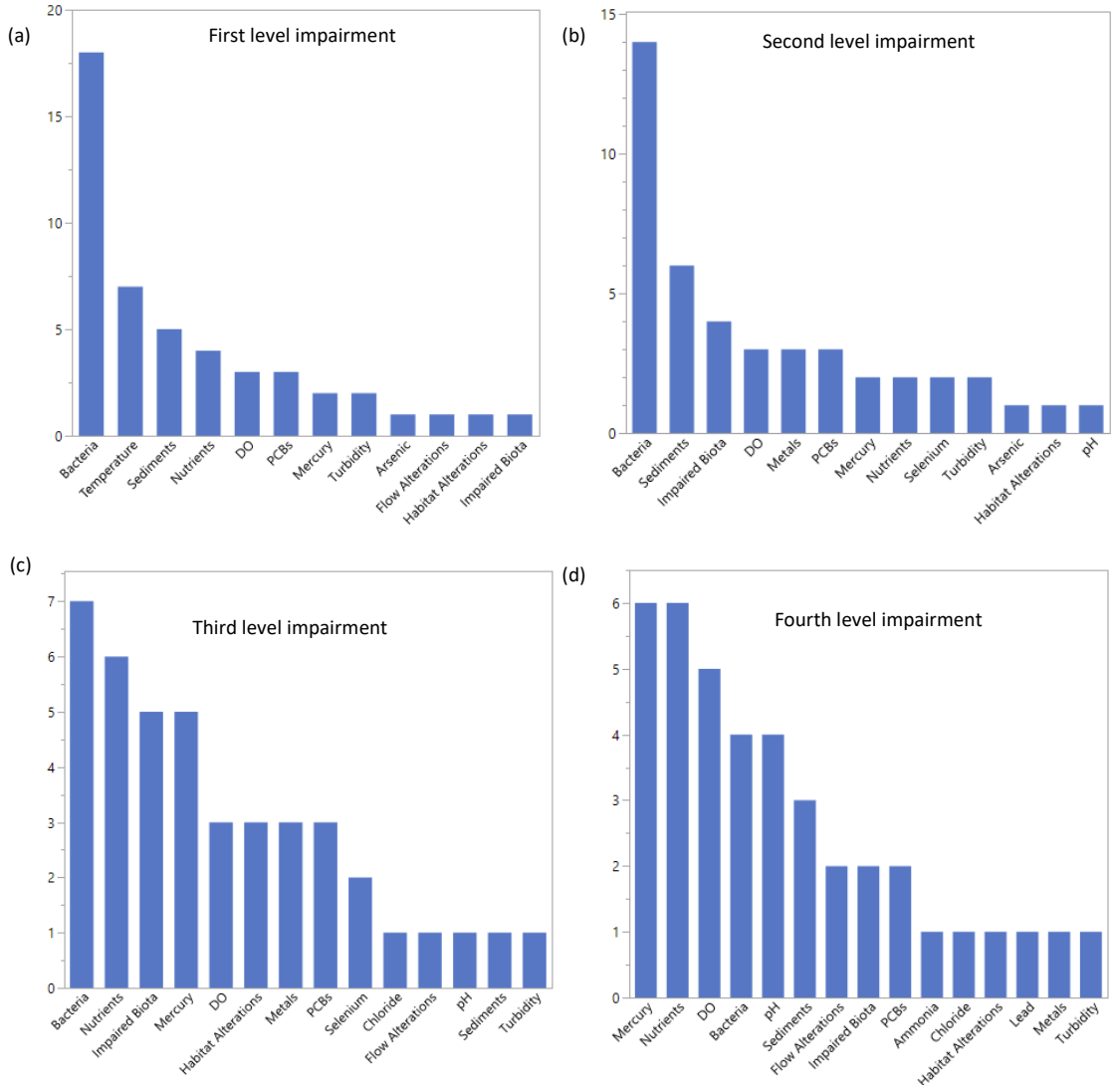

Figure 4-5. Summary of the top four impairments across each state with the number of states on the y-axis.

Figure 4-6a further illustrates the top impairments across the U.S. and represents the number of states for which an impairment appears at any level. As illustrated, bacteria, which was the most frequent level-one impairment, is also the most frequent impairment overall at any level. Interestingly, while temperature is a level-one impairment in 14.3% (7 out of 49) states, it only shows up in 15 states in total as an impairment. Finally, Figure 4-6b represents the distribution of the percentage of assessed

streams that are listed as impaired for each individual pollutant. As illustrated, bacteria are the largest impairment with a median of 20% of assessed streams having a bacteria impairment cause.

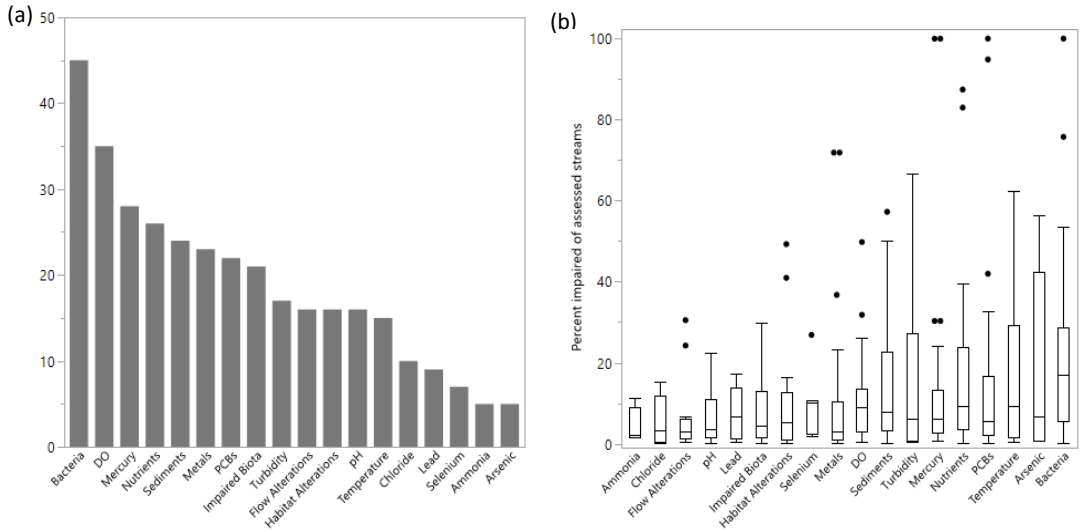

Figure 4-6. Total number of states with each impairment cause (a); Distribution of the percent of assessed streams that are listed as impaired within each state for each impairment cause (b).

4.3.3. Socioeconomics

Socioeconomic data was collected from the U.S. Census for each state and the distribution of some selected variables is illustrated within Figure 4-7. This figure demonstrates the variation within the land area, population, gross domestic product (GDP), percent with no high school diploma, percent of population with a bachelor's degree or higher, and per capita earnings. As illustrated, there is a large degree of variation in socioeconomic variables with a few large outliers for several of the parameters.

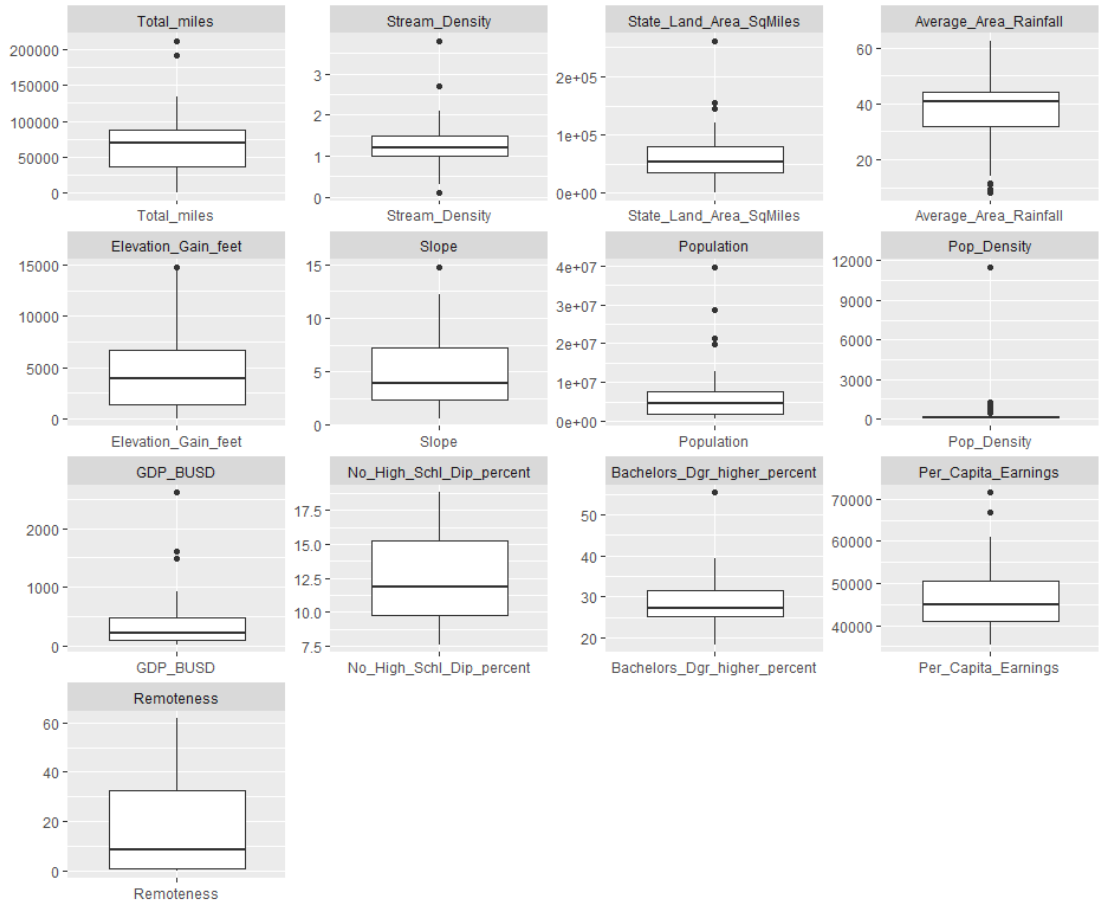

Figure 4-7. Boxplot distribution of the socioeconomic data used in the study across all U.S. states (rainfall in mm, slope as a percentage, GDP in Billions of USD, and remoteness as a percentage).

To determine if there were any groupings among states with common socioeconomic variables, I performed hierarchical clustering as illustrated in Figure 4-8. This figure represents various levels of clusters, with the states color coded based upon their EPA region. For simplicity, the most northeast EPA regions (1, 2, and 3), west EPA regions (8, 9, and 10), and southwest / great plains regions (6,7) are coded the same color. As illustrated, Texas and California are grouped together as a single cluster, as they have the largest land areas, population, GDP, and percent population without high school diplomas. The District of Columbia is the smallest region considered and has the highest

population with bachelor's degrees or higher (55.4%); therefore, it stands apart as its own second-level cluster. Finally, notably most of the northeastern states are also clustered together.

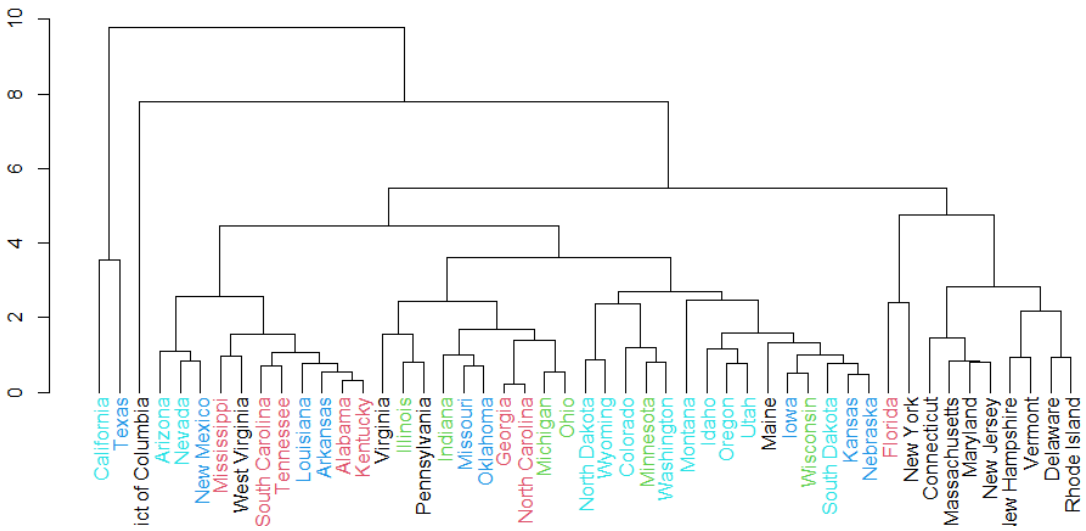

Figure 4-8. Cluster analysis of socioeconomic data color coded by EPA regions: Black – 1, 2, 3. Red – 4. Green – 5. Blue – 6, 7. Light blue – 8, 9, 10.

4.3.4. Relationship between TMDLs and Socioeconomics

Response screening was performed to determine if there are any correlations among TMDL progress and socioeconomic variables. The results in Table 4-3 and Figures A2-1 – A2-2 indicate that the percent of streams that are assessed are negatively correlated to state land area, total stream miles, and percentage of population without high school diplomas while positively correlated to percent of population with a bachelor's degree or higher, and per capita earnings ($p < 0.05$). This suggests that the larger the land area and length of streams to assess, the lower the percentage of streams that are actually assessed, likely due to the sheer size and length of streams and rivers

within the state. In addition, the positive correlations with per capita earnings and bachelor's degree or higher suggests that the economic output of a state has an influence on the percentage of streams that are assessed. This implies that state economic resources are a contributing factor to TMDL progress. Funding for the development of TMDLs mainly comes from state taxes and to a certain degree from nonprofit organizations directly involved with the water quality concerns of the regions. Therefore, per capita earnings have a direct relationship to these processes.

CWA mandates and highlights the need for community involvement in all stages of the TMDL. A more educated community will be more aware of environmental issues and the available options to mitigate them. They will be more inclined to participate in water quality monitoring programs and commenting on impairment lists and draft TMDL reports which are mandatory stages in the TMDL development process. Furthermore, the collective correlation of economic and education parameters may also suggest that a more educated population could devote more resources and effort to addressing environmental issues. This could be a result of the Maslow's Hierarchy of Needs, where more educated and financially stable populations strive for self-esteem and self-actualization (Maslow & Lewis, 1987). This observation has been seen in regional water quality studies (Farzin & Grogan, 2013; Stanford et al., 2018), where educated communities are more aware and have the means to address water quality issues within their localities.

Finally, the percent of TMDLs that are complete has a low positive correlation ($p < 0.1$) to percentage of population without high school diplomas and negative correlation to per capita earnings, and despite having a moderate significance of the slope also have the lowest model fits ($R^2 < 0.7$) These trends are opposite to what is observed with the

percent that are assessed and is unclear how these variables would act in such a way to influence the completion of TMDLs. Finally, there were no correlations between any socioeconomic variables or the percentage of streams that are impaired or to specific impairments themselves.

Table 4-3. Single variable regression (n = 50 states) analysis for all relationships with a $p < 0.1$

Dependent (y)	Independent (x)	Equation	P-value	R^2
Assessed (%)	Total stream length (mi)	y = 66.6 - 0.00035 * x	0.0006	0.22
Assessed (%)	State land area (km2)	y = 61.3 - 0.0003*x	0.0019	0.19
Assessed (%)	Bachelor or higher degree (%)	y = -12.5 + 1.94 * x	0.01	0.13
Assessed (%)	Per capita earnings ($)	y = -27.3 + 0.0015 * x	0.0116	0.13
Assessed (%)	No high school diploma (%)	y = 77.4 - 2.75 * x	0.0001	0.07
TMDL complete (%)	No high school diploma (%)	y = 3 + 1.80 * x	0.08	0.07
TMDL complete (%)	Per capita earnings ($)	y = 59 - 0.0007 * x	0.08	0.06

To understand how multiple variables might better predict TMDL progress I performed multivariable linear regression using a stepwise bidirectional elimination approach. Results demonstrated that the prediction of the percentage of assessed streams could be improved by combining the total stream length and per capita earnings, with an adjusted R^2 of 0.26 (Table 4-4). No multivariable equations were statistically significant for the percent of impairments or TMDLs completed. Furthermore, un-normalized dependent variables did not improve on the regression's effort.

Table 4-4. Multiple linear regression model output for percentage of streams that are assessed. Estimate is the slope coefficient for each independent variable.

Variables	Estimate	P value
Intercept	11.07	0.7
Per capita earnings ($)	0.0011	0.04
Total stream length (mi)	-0.003	0.002

I also sought to evaluate how these particular variables might be influenced by the EPA region. To do so, I plotted the mean TMDL progress variables (assessed, impaired, and TMDL complete percentages) against the mean socioeconomic variables for each EPA region. In doing so, only one statistically significant relationship was found: the mean percent of assessed streams and per capita earnings of each EPA region as illustrated in Figure 4-9c. Mean per capita earnings of each EPA region can explain the variation of mean assessed stream/river percentage of each EPA region. Figure 4-9b is plotted in descending order based upon the mean per capita earnings, and as illustrated in Figure 4-9a, the percentage of assessed streams follows a similar trend. This indicates that the resources available within each region may have an influence on the progress of TMDL implementation within the states. This could be due to the distribution of resources at the regional level, as federal funding is dispersed to regions for implementation of TMDL programs and is dependent upon revenue from point-source discharges within the region, among other sources (Neilson & Stevens, 2002).

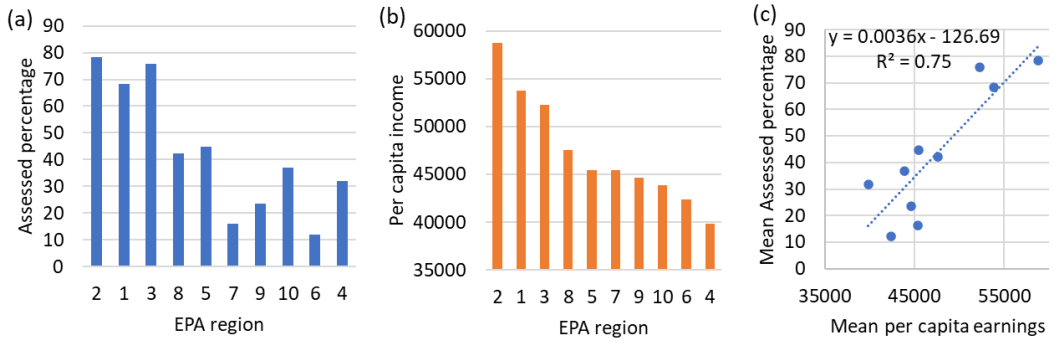

Figure 4-9. Comparison of (a) mean assessed miles and (b) per capita earnings (plotted in descending order) in each EPA region and their correlation (c).

4.3.5. Relationship between TMDLs and Politics

Figure 4-10 represents the historic (10 years) political inclination of each state for reference, and the categorical distribution of TMDL parameters based on political inclination. Both impaired stream and completed TMDL percentages are distributed similarly and therefore their differences are not statistically significant; however, the Wilcoxon Rank-Sum test which test whether two populations are equal in median, found that the difference in percentage of assessed streams are moderately significant (p value of 0.09). However, the states that seem to have a higher number of streams assessed and a higher number of TMDLs completed include the east coast states (Figure 4-2) that have older cities that historically were heavily industrialized, which resulted in heavy environmental pollution from point sources (Tarr, 1996). Most of these states have very high impairment levels. For example, streams in New Hampshire, District of Columbia, Delaware, New Jersey, and North Carolina are all more than 90% impaired, Due to this reason, their concern might be driven by the level of historical and current pollution, and less by the party that controls state-level politics. More analysis on how political influence impact funding, public involvement and consensus, and state regulations and policies would be needed to draw further conclusions and is discussed in future research section.

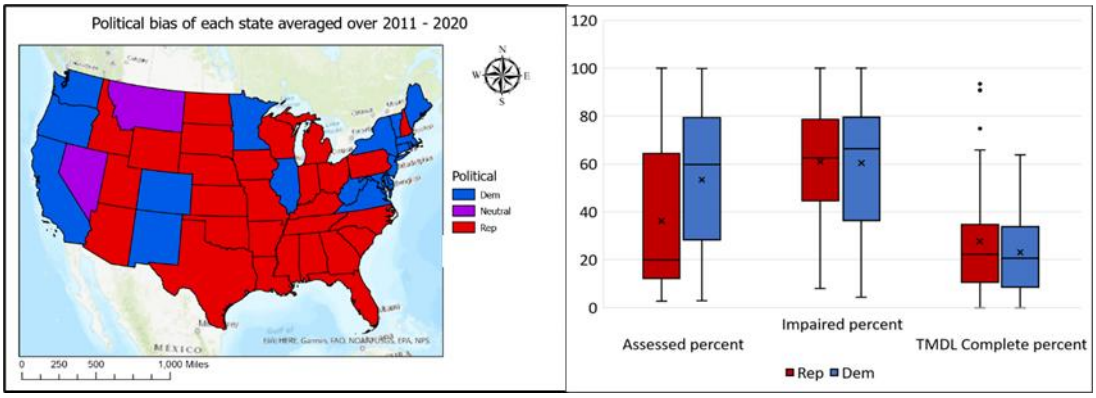

Figure 4-10. Political inclination of each state for averaged over the last decade (left). Categorical distribution for TMDL performance parameters (right): Red – Republican, Blue – Democratic.

4.4. Implications of Results

This study presents TMDL progress across the country and the influence that spatial and socioeconomic factors have on the percent of streams that are assessed, those that are impaired, and those for which a TMDL is complete. The outcomes of this work demonstrate that not all states have implemented their TMDL programs to the same degree. While some of this can be attributed to the difference in state land areas and stream miles that must be assessed, there are other socioeconomic factors that have a similar degree of explanatory power.

To that end, per capita earnings had a significant relationship with the percentage of streams that are assessed within a state. Without financial resources, states may not have the necessary personnel to collect the data that is needed for assessing streams. Arguments have been made that this lack of funding inhibits progress and should be addressed by permitting states to calculate TMDLs with alternative and less costly assessment methods, such as using proxies (e.g., impervious cover or stormwater volume) that are correlated with water quality (DeGioia, 2019). Other policy changes to

advance TMDL progress could include more direct obligations to limit pollution with discretion and flexibility on how to do so, rather than whether and how much to do so (Stephenson et al., 2022). In addition, there may be an economic case that there are returns to investments to improve water quality. These returns can be quantified by economic models to determine the cost and benefits of water quality improvements; however, uncertainties in these models regarding pollution damages and economic benefits make them difficult to apply (D. J. Bosch et al., 2006).

Public participation is an important part in the TMDL development process as they can provide information regarding impairments, collect water quality data, and review and comment on impairment lists and TMDL drafts. Public participation is mandated through the CWA. This study shows that education, both population with college degrees and population without high school diplomas, have a considerable impact on the assessment of streams and rivers. Efforts to improve public awareness of water quality issues and their implications could improve their participation in various stages of the TMDL process. Furthermore, it has been shown that citizen scientist programs not only allow states to collect water quality data but also to educate socioeconomically underprivileged communities through information dissemination (Webster & Dennison, 2022).

One limitation in this study is that I was unable to evaluate the methodology for which streams are assessed, which could also vary depending upon what resources are available. For example, a robust assessment would have large amounts of data that demonstrate an impairment, while others could have a “drive by” assessment (Neilson & Stevens, 2002). Furthermore, some states may list a large number of impairments due to a

large amount of data, while others could have impaired streams that are not listed due to a lack of assessment data. As a matter of practical implementation, states with more streams have a greater workload and therefore the results indicate that these states have not assessed as many streams as a percentage of their overall stream lengths.

It is also clear that EPA regions themselves tend to have a similar level of TMDL progress. Some of this can be attributed to spatial similarities as demonstrated in the clustering analysis; however, as Figure 4-8 indicates, there could be economic factors common to certain regions that influence TMDL progress. The fact that EPA regions have a significant influence on the implementation of programs is not surprising as they are the office charged with enforcing and overseeing state adherence to the Clean Water Act. The findings suggest that progress towards assessing streams and completing TMDLs varies depending upon the EPA region, with those with higher amounts of per capita earnings having a larger percentage of their streams assessed. This is aligned with other studies that have found similar differences among EPA regions in implementing elements of the Clean Water Act, including the NPDES program (Woods, 2021).

This study demonstrates the variability in TMDL progress across states and what factors may contribute to it; however, how to bridge the gap between states is unclear. As the TMDL programs continue to mature, modeling approaches and technologies may accelerate assessment and TMDL development for waters of the United States. For example, modeling approaches have evolved over time and different impairment types may require different modeling tools (Quinn, Kumar, La Plante, et al., 2019), which can be selected based upon the unique technical criteria and management constraints of a watershed (Sridharan et al., 2021). Furthermore, advancements in remote sensing and

geospatial analysis can be used to support TMDL assessment and modeling (Quinn, Kumar, & Imen, 2019; Sridharan et al., 2022). In addition, there may be ways to further improve the process of developing TMDLs with modelers, stakeholders, and regulatory entities. This is important as in many cases, the TMDL serves as the framework for contextualizing watershed science and regulatory policies towards stakeholders and the general public through collaboration and coordination of watershed management (Slota, 2021).

4.5. Conclusions

This study evaluated the relationship that socioeconomics and regionalization have on TMDL progress and implementation. Outcomes indicate that TMDL progress and impairments had a large degree of variation, some of which could be explained by EPA region, spatial clustering, and socioeconomic variables. To that end, results suggest that the size of a state, the length of total streams, education, and the economic output are related to the percentage of streams that are assessed within a state. In addition, states largely followed similar patterns based upon the EPA region that they were within, indicating that regions play a large role in TMDL progress. Overall, this study highlights the diversity in implementation of TMDLs across states and highlights some of the factors that may explain variation in TMDL approaches to date. The outcomes of this study can be used to inform water resource decision makers to better strategize their approach and increase efficiencies of the TMDL development process mandated by the federal government. For example, for states or regions with higher economic capacities but low education levels, it might be efficient to reallocate resources to educate communities about the need for public participation in the TMDL process. Furthermore,

while the TMDL is a federally mandated national requirement, this study demonstrates progress towards meeting TMDL requirements differ among EPA regions. Therefore, it may be beneficial to investigate how to reallocate resources to EPA regions such that these discrepancies could be alleviated. To that extent, the use of new federal funding methods and regulations could be explored.

5. MONITOR AND ANALYZE THE TEMPERATURE MITIGATION POTENTIAL OF INTERCONNECTED GREEN INFRASTRUCTURE PRACTICES

5.1. Rationale

Green infrastructures are increasingly being used as a more resilient storm water management option. The watershed wide use of these structures has resulted in interconnected networks that increase their runoff mitigation potential (Dong et al., 2022; Ferreira et al., 2021; Staccione et al., 2022). To develop wholistic water management plans, the many other benefits of green infrastructure should also be considered, such as the potential to mitigate the temperature of urban runoff (R. M. Martin et al., 2021). This is because urban runoff can increase the temperature of their receiving water bodies (Zahn et al., 2021) and across the national TMDL program, temperature is second to bacteria as the most frequent number one cause of impairment in a state's streams and rivers. Green infrastructure's potential to be utilized to reduce the impact of urban runoff on downstream temperatures in networks of structures, especially those connected in series, is unknown. Understanding the cumulative benefits of GIs ability to mitigate runoff temperature will allow water managers and planners to better utilize these structures in achieving downstream water quality goals. This study seeks to fill this gap by monitoring a green infrastructure system in Milwaukee, WI – a bioswale and permeable pavement that both discharge into a second bioswale – to evaluate its temperature mitigation potential.

I ***hypothesize*** that green infrastructure in series will improve stormwater runoff temperature mitigation.

5.2. Materials and Methods

5.2.1. Site Description

The Milwaukee War Memorial parking lot was constructed in the spring of 2021 and has a surface composed of a mix of asphalt and permeable pavement surfaced with concrete pavers. The runoff from the parking lot is managed using a combination of bioswales and permeable paver systems that discharge at various points into a rip-rap lined swale. For this project, the outlets of three green infrastructure practices were monitored for flow and temperature including: (1) a permeable paver system collecting parking lot runoff, (2) a bioswale collecting parking lot runoff, and (3) a downstream bioswale that collects parking lot runoff and runoff from the underdrain of 1 and 2, and then discharges to a rip-rap lined swale (Figure 5-1).

The permeable paver system is approximately 465 m^2 in size and collects runoff from an overall area of 1,580 m^2. The paver system is unlined and is drained by a 6-inch (0.15 m) diameter 35.7 m long perforated PVC pipe (0.001% slope) and then is discharged through a 6-inch (0.15 m) diameter 20.1 m long PVC underdrain (1.5 % slope) that outfalls to the surface of Bioswale 2.

Bioswale 1 has an area that is approximately 222 m^2 and drains a total area of 2,062 m^2. It is planted with a mix of native grasses and shrubs. It is unlined and has a 6-inch (0.15 m) perforated PVC pipe running underneath the bioswale for 40.2 m (0.001 % slope) and connects to an 8-inch (0.20 m) overflow grate where effluent is discharged through a 6-inch (0.15 m) diameter 19 m long (0.5 % slope) underdrain that outfalls to the surface of Bioswale 2.

Bioswale 2 is approximately 270 m^2 and collects runoff from the underdrain of the permeable paver system, Bioswale 1, as well as a drainage area of 1,775 m^2. The bioswale is planted with a mix of native grasses and shrubs. It is unlined and has a 6-inch (0.15 m) perforated PVC pipe that runs 63.7 m along the bioswale (0.5 % slope). This underdrain is connected to an 8-inch (0.20 m) overflow pipe and effluent is discharged through an 8-inch (0.20 m) diameter 17.5 m long underdrain (0.5 % slope) that outfalls to a rip-rap lined swale.

Figure 5-1. Photo of green infrastructure facing north, with monitored infrastructure outlined in bright green (1: permeable pavers; 2: bioswale 1; 3: bioswale 2) and connectivity of the underdrains in blue (left); photo of green infrastructure facing west, along with gravel rip rap channel that system discharges into (right).

5.2.2. Monitoring Methods and Equipment

To continuously measure water level and temperature, Onset HOBO U20 water level sensors were placed within the outlet of each structure and a v-notch weir was placed at the end of each outlet pipe in order to estimate flow rates. The water level sensors collected both water level and temperature at 2-minute intervals over the study period. Additionally, an Onset HOBO tipping bucket rain gauge was installed at the site to collect rainfall data that was applied to estimate overland flow volumes into the green

infrastructure practices. All sensors were connected to one of two data collection hubs that were solar powered and broadcasted data through a cellular connection (Figure 5-2).

Figure 5-2. Bioswale 2 outfall into riprap channel, rain gage, and data logger (left); data logger in bioswale 2 that measures the discharge from the permeable paver and bioswale 1 underdrains (right).

5.2.3. Volumetric Flow Computations

Influent runoff into each green infrastructure practice entered as overland flow; therefore, influent flow rates were estimated using rainfall data collected at the site. The curve number method was used to estimate inflow surface runoff volumes to each green infrastructure.

$$Q = ((P - I_a)^2)/((P - I_a) + S) \quad \text{[Equation 1]}$$

$$I_a = 0.2S \quad \text{[Equation 2]}$$

$$S = (1000/CN) - 10 \quad \text{[Equation 3]}$$

where Q is the runoff in inches, P is the accumulated rainfall depth (inches), I_a is the initial abstraction calculated by Equation 2, and S is the potential maximum retention after runoff begins which is calculated using Equation 3. Curve number, CN, for each

surface was derived using the TR-55 manual provided by USDA (*WinTR-55 User Manual*, 2002): CN for parking and paved spaces is 98. Once runoff is estimated, inflow volume was calculated by multiplying runoff height with respective watershed areas and converted to SI. Curve number method is the most widely used runoff model (Hawkins et al., 2008). As the complexity of the watersheds increase, the accuracy of the curve number diminishes and the hydraulic complexities of land use types such as forests are not well represented (Bartlett et al., 2016). However, it has been shown that CN method can be applied to urbanized watersheds with acceptable accuracy (Reilly & Piechota, 2005). Due to the small-scale nature of the study's watershed, having only one directly connected land use type (paved parking lot), and the homogeneous nature of the newly built parking lot, CN method will produce adequate results for this study.

Flow in the effluent of the underdrains were calculated using a standard equation for a 90-degree v-notch weir (Hwang et al., 1996):

$$Q = 2.49h^{2.48} \quad \text{[Equation 4]}$$

where h is the height of the water behind the weir as measured by the water level sensors. The volume reduction within each infrastructure was calculated as the difference between the estimated inflow into each watershed and outflow through each underdrain. The rainfall data was applied to the rational method for estimating peak flow into the green infrastructure practices using Equation 5.

$$Q = ciA \quad \text{[Equation 5]}$$

where Q is the peak flow, c is the runoff coefficient, i is the rainfall depth over the specified time period and A is the drainage area. The catchments of each practice contained asphalt parking lots and therefore a runoff coefficient of 0.9 was used. Rational

method is widely used in designing stormwater infrastructure (C. Li et al., 2019). Similar to curve number method, the rational method is applicable to the monitored site due to its simplistic nature of land use type and small scale (Yazdanfar & Sharma, 2015). Furthermore, rational method is still widely used in recent published research work in watersheds with similar characteristics to this study (Winston et al., 2019) as well as in watersheds that are more complex with multiple surfaces and as three times as larger than this study (Purvis et al., 2019). Peak flow reduction (PFR) was calculated using the estimated peak inflow computed using Equation 5 and observed peak out flows from each infrastructure for each rain event.

5.2.4. Temperature Computation

The temperature at each outlet location was evaluated using both the peak temperature observed during a storm event, as well as the event mean temperatures (EMTs) (Picksley & Deletic, 1999). The event mean temperature represents a volume-weighted average of the temperature in the runoff during a storm event and is calculated by the following equation:

$$EMT = (\Sigma(V_i * T_i))/(\Sigma(V_i)) \quad \text{[Equation 3]}$$

where V_i and T_i are the runoff volume and temperature at time step i.

In addition to peak temperature and EMT, the slopes of the increase and the decay in temperature were evaluated using the following equation for each rain event:

$$T = \beta_0 + \ln(t) * \beta_1 \quad \text{[Equation 4]}$$

where T is the temperature, t is the time after the start of the event (mins) and β_0 and β_1 are regression coefficients. This log transformed equation better fits the characteristics of the temperature increase and decay by satisfying the assumptions of linear regression.

The regression coefficient β_1 represents the slope of the increase and decay and was determined for each individual runoff event with summary statistics calculated across all observed events. The slope of this relationship explains the speed at which temperature changes within each infrastructure during runoff events, which is an indication of their temperature mitigation performance. The runoff events were delineated based upon rainfall that was separated by at least 24 hours. Peak temperature, mean temperature, rate of temperature increase, and rate of temperature decay were used to define the temperature behavior for each rain event observed from start to finish.

Peak temperature and EMT distributions for each infrastructure were analyzed using ANOVA (Analysis of Variance) test. The hypothesis for the test is that there is a significant difference between the mean temperature performance of each infrastructure.

Finally, ambient air temperature and solar radiation was measured during the study period. To determine how these parameters independently influenced the effluent temperatures in the green infrastructure, simple linear regression was performed to estimate the EMT computed above with air temperature and solar radiation as the independent variables. I hypothesize that the variation in EMT can be separately explained by the air temperature and hourly solar radiation preceding each rain event. This allows me to determine the impact that air temperature and solar radiation had on the ultimate EMT of each due to the observed impact of season and air temperature on effluent temperatures.

5.3. Results and discussion

5.3.1. Hydrological Performance

A total of 21 runoff events were captured at the site over a period from June 29, 2021 to October 29, 2021. During these events, the three green infrastructure practices were estimated to reduce 91% of the stormwater runoff volume on average as indicated in Figure 5-3. The volume reduction through individual structures was similar in magnitude, with the permeable pavers, bioswale 1, and bioswale 2 producing average volume reductions of 77%, 84% and 85%, respectively. The observed higher overall volume reduction (91%) is due to the placement of the green infrastructure in series, where the overflow of the permeable pavers and bioswale 1 is further reduced through bioswale 2.

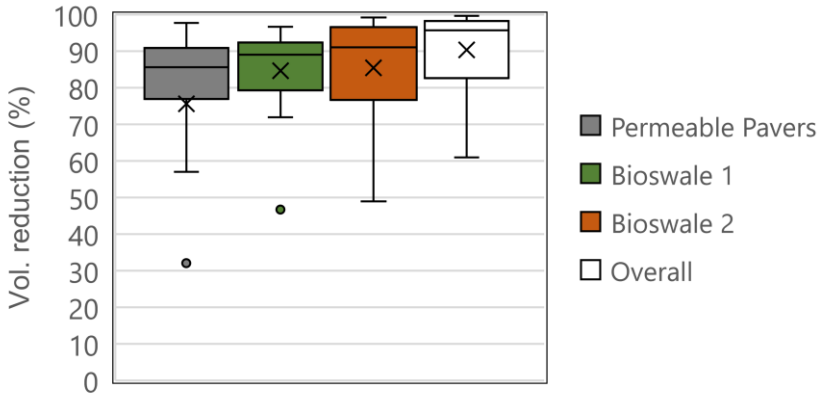

Figure 5-3. Distribution of the percent of stormwater runoff volume per rain event that is reduced by the three green infrastructure practices and the overall system.

To evaluate how volume removal was influenced by storm characteristics, I plotted the volume reduction percent as a function of the log of the rainfall depth (Figure 5-4). Log transformation to the rainfall depth was carried out to ensure that the regression analysis satisfies the linearity assumptions, including normality and homoscedasticity of

the residuals. As illustrated, the permeable pavers, bioswale 2, and the overall system had a statistically significant relationship ($p < 0.05$ of the slope coefficient) between the percent of the volume captured and the rainfall depth, suggesting that the volume reduction capacity of the green stormwater infrastructure decreases as it becomes more saturated during larger rainfall events. However, the impact of rainfall depth on volume reduction for bioswale 1 was less clear with an R^2 of only 6% and a p value higher than 0.05. This is caused by the 114mm rainfall event, which is nearly a 24 hour, 25-year rain event (116mm for Milwaukee) that has high influence and leverage in the model with a cook's D value higher than 1.

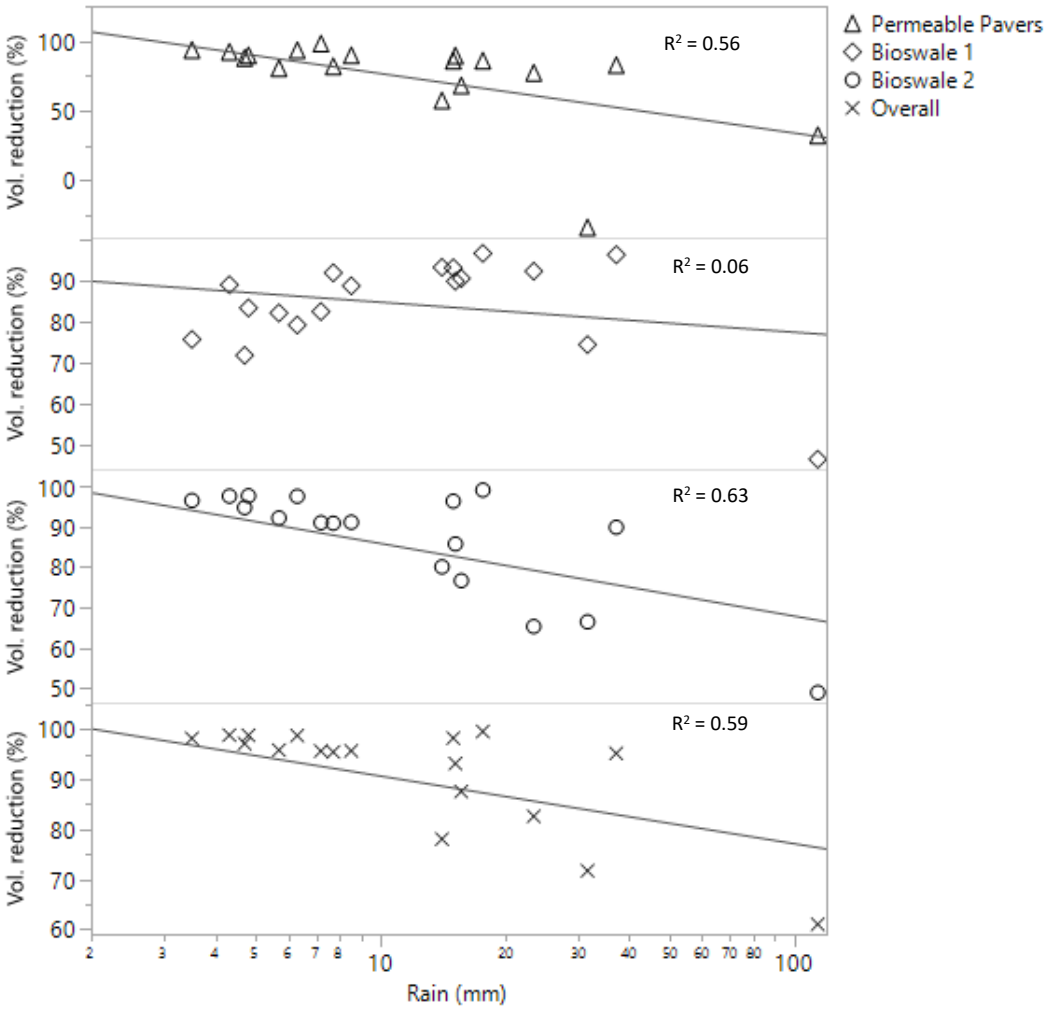

Figure 5-4. The percentage of stormwater runoff that is infiltrated as a function of rainfall depth.

Overall, the green infrastructure system reduced peak flow rates by over 98% on average, with slightly less reduction in the permeable pavers (90%) than the bioswales (both 95%) (Figure 5-5). Similar to volumetric performance, the peak flow reductions were impacted by the size of the rainfall event with less peak flow reduction for larger rainfall events (Figure 5-6). While there is an observable outlier at the far end for a storm with above a 100 mm depth, it does not have significant influence on the linear regression model with a Cook's D value less than 1.0 for all models (Helsel et al., 2020).

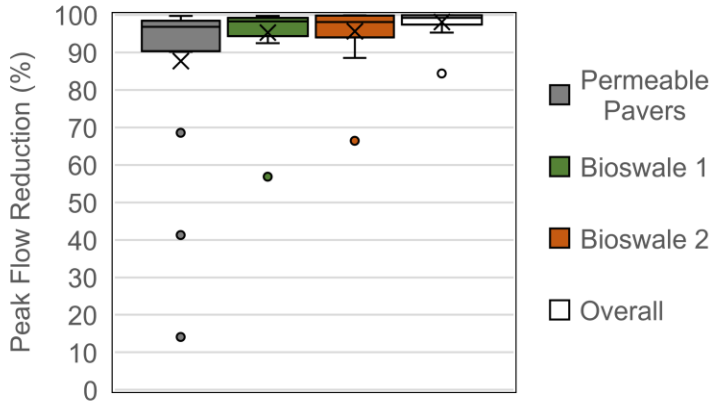

Figure 5-5. Distribution of the peak flow reduction in each green infrastructure practice and the overall system.

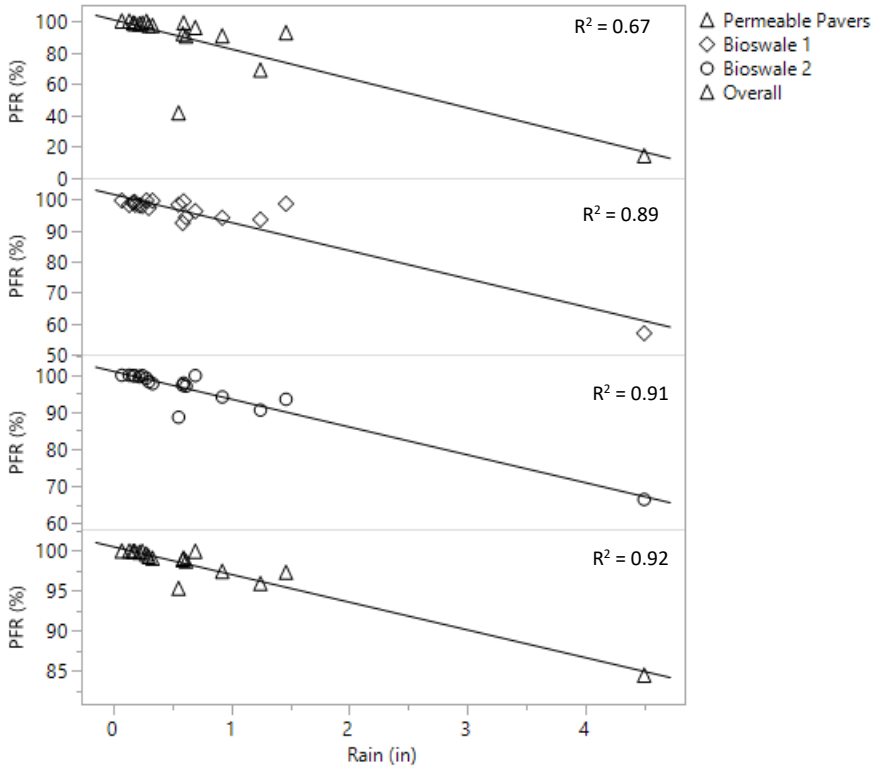

Figure 5-6. Peak flow reduction (PFR) as a function of the rainfall depth.

5.3.2. Temperature Performance

For the two green infrastructure practices in parallel – permeable paver and bioswale 1 – the bioswale had lower EMT across all storms and lower peak temperatures across all but 3 events (Figure 5-7). Further EMT reductions were observed in bioswale 2, which on average was 4.2 °C cooler than the flow from permeable pavers and 2.4 °C cooler than the flow from bioswale 1. This is within the range of other studies that have found median temperature differences between the influent and effluent of green infrastructure between 0.8 and 8.8 °C (M. Jones & Hunt, 2009; Long & Dymond, 2014). The reduction in EMT was similar in magnitude for the peak temperature with the bioswale 2 on average 4.3 °C cooler than the permeable pavers and 3.4 °C cooler than bioswale 1. On an ANOVA test, peak temperature for bioswale 2 was significantly ($p < 0.05$) lower than the infrastructure feeding into it while permeable paver had a significantly higher EMT than the bioswales. The reductions in both EMT and peak temperatures highlight the potential for green infrastructure in series as a way to further mitigate runoff temperatures. In fact, by further treating the stormwater runoff, this system reduced the EMT to 22 °C on average, below the upper temperature tolerated by trout for 1-14 days of 22.5 °C in the upper Midwest of the U.S. (Wehrly et al., 2011).

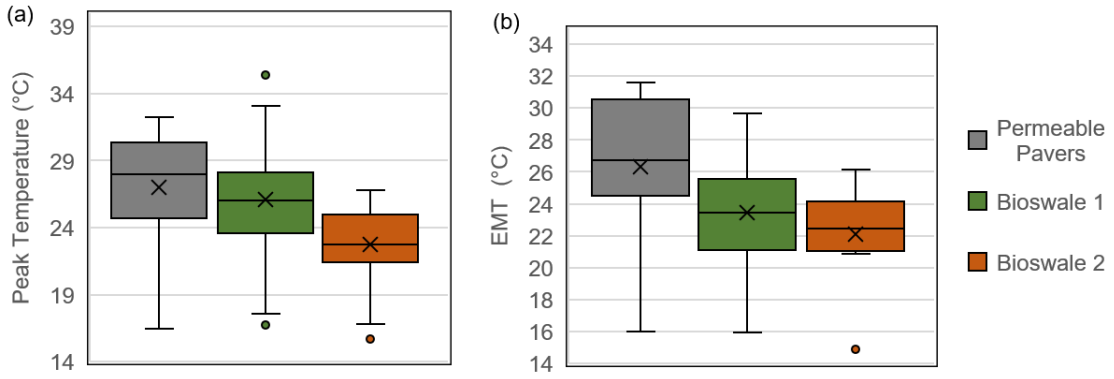

Figure 5-7. Distribution of the peak temperature (a) and the event mean temperature (b) for stormwater runoff events captured at the underdrain of each green infrastructure practice.

To evaluate the impact that ambient air temperature has on the peak and event mean temperature, I plotted all outflow water temperatures as a function of the date of the runoff event and colored by ambient air temperature (Figure 5-8). In this figure the peak and event mean temperature points are fit with spline interpolation to illustrate the trends over time. As illustrated, the air temperature is cooler towards the beginning and end of the study period and appears to peak during sometime in August. Not surprisingly, this appears to have a substantial impact on the peak and event mean water temperature, as these follow a similar trend.

An important observation is the peak temperature of the permeable pavement exceeding that of the bioswale 1 for three rain events during the hottest period of the study, end of August. This could be due to differences in the contributing area of each watershed. The asphalt parking area contributing to the runoff collected by the bioswale is 65% larger than the area contributing to the porous pavement but, the bioswale is half the size of the pavement. Furthermore, the time of concentration for the bioswale is longer due to the inlet placements. Therefore, during much warmer events, the runoff

temperature difference resulting from these surfaces could potentially reduce the cooling effect of the bioswale compared to the pavement which result in the observed performance. Even though porous pavements get hotter than bioswale surfaces, it has been shown that they can be 14 ^{o}C colder than regular asphalt pavement during dry days and 6.6 ^{o}C colder during rain events (Cheng et al., 2019). However, the EMT of the bioswale 1 effluent is consistently lower than the effluent from the porous pavement due to its better temperature mitigation performance resulting from shading and potential material differences of each infrastructure.

Bioswale 2 consistently shows lower effluent EMT and peak temperatures. This is due to cooler effluent from the connected GIs mixing with runoff captured by the bioswale 2 itself. Bioswale 2 is 20% larger than bioswale 1 however, has a contributing parking lot area which is 14% smaller. These size differences result in the perceived better performance of the Bioswale 2. During these events at the height of the summer, the temperature of the water leaving bioswale 2 are above the threshold for freshwater species of 22.5 °C (as indicated by the horizontal line) (Wehrly et al., 2011), suggesting that despite further reductions in temperature, the green infrastructure in series may not be enough to meet that threshold. However even so, it may be further diluted by the lower temperature of receiving streams.

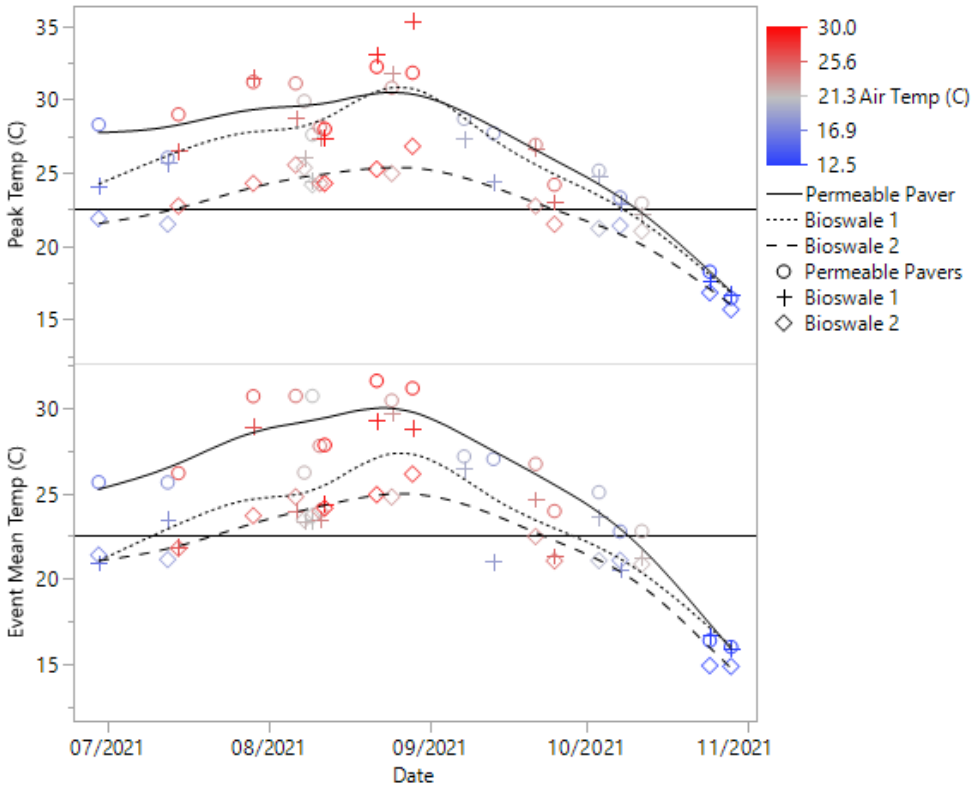

Figure 5-8. Peak temperature and event mean temperature as a function of the date. The ambient air temperature for each event is represented by the color bar and the horizontal line represents the minimum mean temperature threshold for freshwater species (22.5 °C).

To further understand the impact of ambient conditions, I separately evaluated the correlation between air temperature and hourly solar radiation immediately preceding the storm event on the EMT and peak temperatures of the green infrastructure system using simple linear regression. The relationship between air temperature and solar radiation on the EMT of each structure is illustrated in Figure 5-9. As illustrated, there is a positive correlation between both air temperature and solar radiation, with periods of zero solar radiation during nighttime storms. Solar radiation and air temperature are moderately correlated to each other with a Pearson correlation of 0.59 (p value < 0.05) for the rain events that happen during the day. This may indicate that when both the ambient air is

warmer and incident solar radiation is higher, the runoff into the green infrastructure is hotter due to higher warming of the pavers within the catchment of each practice. The simple linear regression shows that air temperature at the start of the rain event can explain 28% to 40% of the variation in EMT and solar radiation at the start of the rain event can explain 24% to 37% of the variation. Other explanatory factors that affect the complex energy balance taking place within the system include wind speeds, soil moisture content (Purdy et al., 2016), infiltration rates, and subsoil temperature (Krayenhoff & Voogt, 2007). It has been shown that wind speeds have a positive correlation with thermal energy transfer between urban surfaces and the atmosphere (Ahmed et al., 2015) thus, higher wind speeds prior to rain events will reduce the surface temperature and vice versa. Soil moisture content determines the overall thermal capacity and the thermal conductance of the subsoil composite therefore, the moisture content within the GI during the rain event has an impact on the temperature performance. Infiltration rates within GI can change based on soil moisture content as well. The more soil moisture there is, the slower the rate of infiltration will be. Slower infiltration rates will increase the time of contact between soil particles and storm water allowing for more thermal energy to transfer between them. Furthermore, environmental variables such as energy are continuous variables which are autocorrelated (Di Cecco & Gouhier, 2018; Parolari et al., 2021). Therefore, inclusion of antecedent weather conditions could also improve predicting power of EMT.

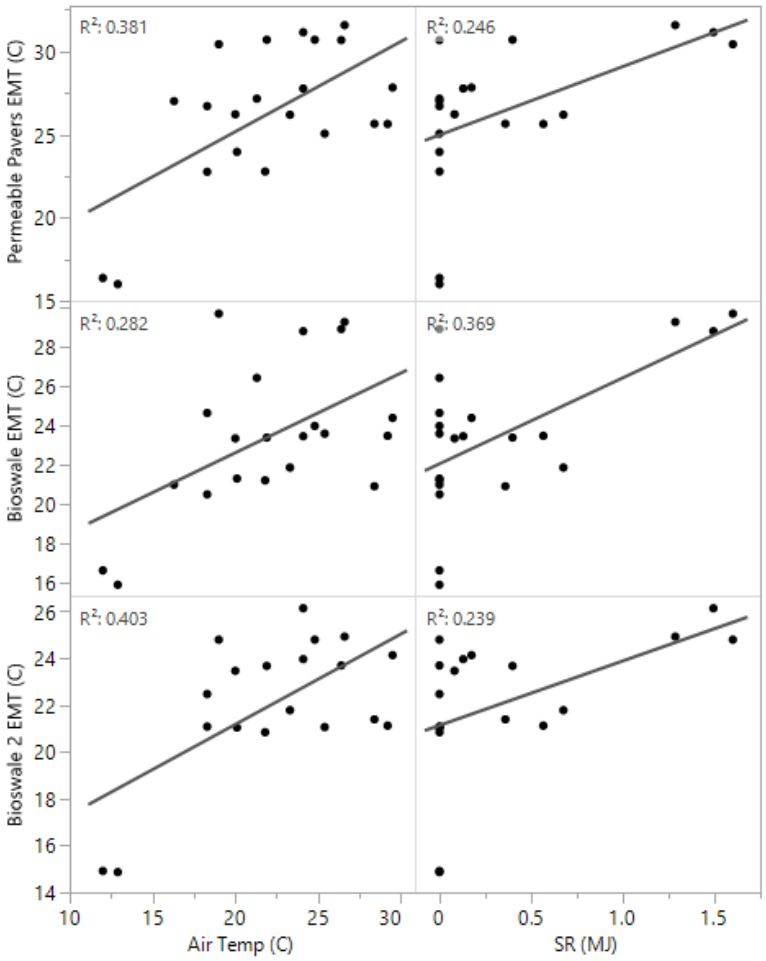

Figure 5-9. Relationship between EMT and air temperature and solar radiation. Air temperature is measured immediately before rain event and solar radiation is the cumulative radiation for the hour preceding the rain event.

An example of the change in temperature over the course of a runoff event is illustrated in Figure 5-10 for a storm on August 21, 2021. During this runoff event, temperatures at the outlets initially decrease, likely due to the flushing of cooler water from the green infrastructure (within the underdrain pipe or subsurface of the green infrastructure itself) than the ambient air temperature or temperature of the standing water behind each weir. However, after the initial decrease, the temperature immediately spikes. This is particularly pronounced for bioswale 1 and the permeable pavers that

collect direct surface runoff from the asphalt parking lot. Additionally, the falling limb of the temperature appear to vary among the bioswales and permeable pavers with bioswale 1 having a sharp drop in temperature while the permeable pavers and bioswale 2 had a more gradual reduction.

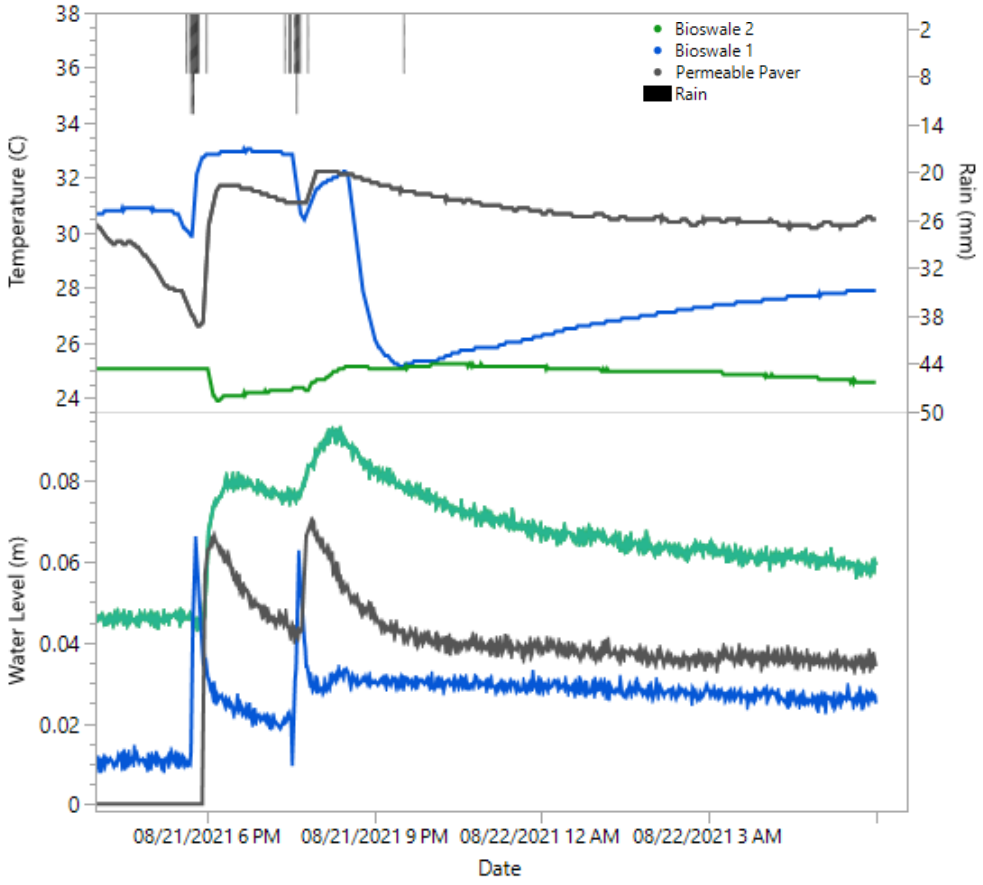

Figure 5-10. Example of temperature fluctuations over the course of a runoff event.

To further evaluate the temporal dynamics of effluent temperature during runoff events, I quantified the rate of change in the rising and falling slopes of the temperature. This rate of change is represented as β_1 from Equation 4 and the distributions of β_1 across all observed storms is illustrated in Figure 5-11. As illustrated, the permeable

paver has the slowest rate of increase in comparison to the bioswales, with bioswale 1 having the greatest rate of increase overall; however, none of these were statistically different using the students t-test ($p < 0.05$). In evaluating the rate of decay, the permeable paver and bioswale 2 had a similar decay; however, bioswale 1 had a significantly steeper decay ($p < 0.05$) than the other green infrastructure practices. This could be due to several factors. In comparison to the permeable pavers, bioswale 1 could have a greater cooling capacity than permeable pavers, which is also evident in the lower peak and event mean temperatures. For bioswale 2, it could be that it is receiving effluent from the other bioswale and permeable pavers; therefore, there is a lower rate of heat exchange due to a lower temperature of its influent. Other possible mechanisms driving these differences are discussed in the following section.

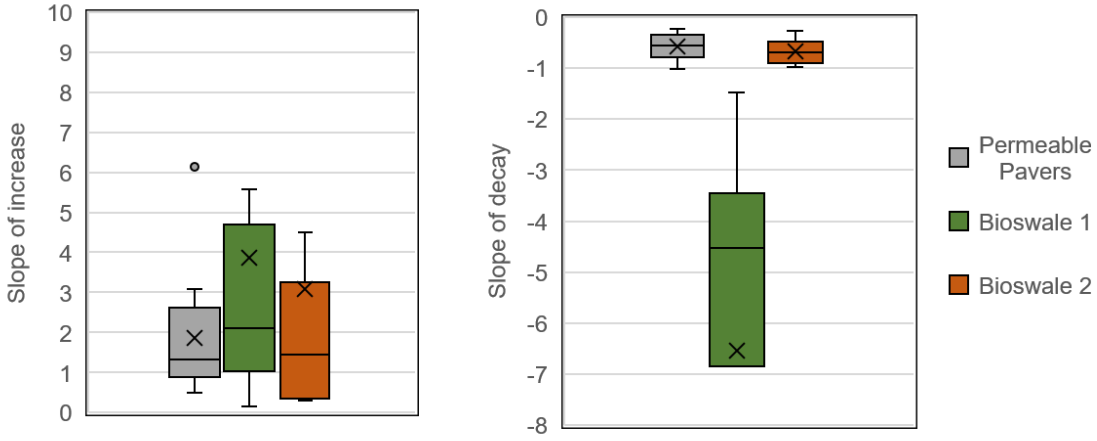

Figure 5-11. Slope coefficients of the increase and decay of the effluent temperatures.

5.4. Implication of Results and Limitations

The green infrastructure connected in series reduced both the EMT and peak temperatures on average to levels that are below the threshold for freshwater fish species

in the Midwest United States of 22.5 °C (Wehrly et al., 2011); however, this was not the case in the hottest summer month, as the EMT and peak temperatures were strongly influenced by ambient temperatures. The bioretention installed in parallel to the permeable pavers had lower event mean and peak temperatures and had a significantly higher rate of temperature decay. Though inflow temperatures were not measured, since the contributing parking lot area has identical thermal characteristics to one another and the contributing parking area for the bioswale 1 is 16% larger than the contributing area for the porous pavement, it can be assumed that the incoming runoff temperature to the bioswale 1 is similar to the pavement. If this assumption is true, then this would suggest that the bioswale in parallel to the pavement performs better overall. The higher rate of temperature decay could be due to several factors including an increased residence time within the bioswale to facilitate energy transfer, cooler soil and plant temperatures on the surface of the bioswale than the surface of the permeable pavers, or thermal conductivity and capacity differences between soil media in the bioretention and crushed aggregate media in the permeable pavers. Bioretention, consisting of soils and plants, are known to have a lower surface temperature than permeable pavers, which could be a factor in their performance. This is largely due to the shading from plants within the bioretention itself (Muerdter et al., 2018) and evapotranspiration from plants and surfaces. Shading acts as the primary method in reducing surface temperatures through vegetation that can block more than 60 – 90% of incoming radiation (Rahman et al., 2019; Winbourne et al., 2020). Evaporation of water on the surface reduces surface temperature through a combination of conduction and material phase changes, while plant transpiration reduces the near

surface air temperature, which in turn reduces the surface temperature through conduction and convection (C. Wang et al., 2018).

In addition, the primary mechanism for which runoff temperatures are reduced during events is heat dissipation through conduction with the media when runoff is filtered through the green infrastructure practice (H. Y. Chen et al., 2021; Long & Dymond, 2014). While not quantified in this study, the thermal capacity of the media may be something that plays a considerable role in temperature mitigation as soils generally have a greater thermal capacity than permeable pavers. In addition to reductions of event mean and peak temperature, the significant overall volume reduction (91%) further reduces the impact of elevated stormwater runoff temperatures on downstream waters. This indicates that volume reduction through capture, infiltration, and evapotranspiration, in as much as temperature reduction, is an important component to consider for thermal mitigation.

While the results demonstrate the overall outcome of green infrastructure in series, there are several limitations to the monitoring approach that limit the interpretation of the data. Because the runoff entered the system as overland flow, there is no data on the temperature of the runoff as it enters the green infrastructure practices. While this does not significantly affect the comparative analysis between practices, it does limit our understanding of the overall reduction in runoff temperatures, especially in the green infrastructure practices in the headwater (porous pavement and bioswale 1). An inability to directly measure overland flow also means there will be uncertainties in the computation of incoming peak flows and volumes using a modeling approach based upon rainfall data. Even though it has been shown that these modeling methods are valid in

given watershed conditions (Winston et al., 2019), errors introduced by these empirical models could be exacerbated for smaller storm events. Additionally, there could be uncertainties within the estimations of effluent flow rates using a water level and weir. Based upon this data, I am also unable to define the extent to which thermal cooling of the stormwater runoff occurs within different portions of the system. For example, cooling could occur in the bioretention as it infiltrates through the soil layers, as well as during its transport through the underdrain.

To that end, the outcomes of this work lead to several potential research directions that would be valuable for elucidating the exact design characteristics of green infrastructure for mitigating runoff temperature. First, the specific thermal capacity of the media for effectively reducing runoff temperatures is something that is underexplored and may have competing objectives with the need to adsorb pollutants and infiltrate runoff at a sufficient rate. For example, sand is known to have a greater thermal capacity than clay soils (Ghuman et al., 1985); therefore, the recommended mix of bioretention media may be an important consideration. There may also be design parameters for the depth of the underdrain that could impact the temperature of the effluent that leaves the system, with greater depths to underdrains producing lower effluent temperatures due to the cooler temperature of deeper soils that are buffered from atmospheric temperatures changes and solar radiation (M. Jones & Hunt, 2009). Even so, there may be design and cost considerations that limit the depth to which the underdrain can be installed.

5.5. Conclusion

This study evaluated the impact of green stormwater infrastructure connected in series on the temperature mitigation of stormwater runoff. Results indicate that for the

bioswale and the permeable pavers connected in parallel, the bioswale had a lower event mean temperature than the permeable pavers (2.8 °C cooler); however, neither was able to decrease the event mean temperature below the 22 °C threshold for freshwater trout species. The bioswale that performed secondary treatment did, however, further reduce the temperature of the cumulative effluent across all storms, as the average event mean temperature of bioswale 2 was 4.2 °C cooler than the permeable paver and 2.4 °C cooler than the bioswale 1. These findings have practical implications as increasing global temperatures and land development will further the impact of stormwater runoff on stream temperatures. Therefore, for stormwater managers, the need to reduce the thermal load of stormwater runoff will likely only grow as temperature becomes a driver of water body impairments. This study demonstrates that green infrastructure can be a useful tool in the mitigation of runoff temperatures, especially those installed in series.

6. CONCLUSIONS

Water quality of the nation's water bodies impact health and recreation of humans, plant and animal lives, and the ecosystems that sustain us. Due to its utmost importance, nations around the world have established regulations and policies that protect and rehabilitate the quality of water resources. The overall objective of this dissertation was to evaluate and improve our understanding of the engineering, regulatory, and socioeconomic principles influencing stormwater management actions which affect downstream water quality and quantity.

The minimum requirements for water management and planning mandated by the CWA do not require a wholistic approach that considers future projections of land use; however, doing so is increasingly encouraged by water quality scientists and suggested by the EPA (Stoker et al., 2022; Younos et al., 2019). As this dissertation demonstrates, land use changes can have a significant relationship to changes in stream water quality; therefore, it would be prudent for watershed management plans to assess how projected land use changes might influence trends in stream water quality. The outcomes of this work could be used for developing better TMDLs, by incorporating the predicted influence of land use changes on downstream water quality in margins of safety calculations. Furthermore, these outcomes could be incorporated in water quality management plans to make more resilient decisions based on future land use projections.

The TMDL program is the primary federal mechanism to regulate non-point source pollution in the U.S.; however, since its authorization 25 years ago, no studies have evaluated what factors might influence the variation in its implementation across states. Socioeconomics has been shown to be related to water quality (Andrew et al.,

2019; Wu et al., 2015), yet the relationships between socioeconomics and watershed management actions, especially the TMDL process, is unknown. This dissertation therefore evaluated the progress of TMDLs and defined the relationship between socioeconomic, spatial, and political factors on indicators of TMDL progress. The outcomes can be used to improve the TMDL development process by identifying spatial and socioeconomic obstacles and catalysts to progress.

In several U.S. states, temperature is the leading impairment of stream and rivers and is the 2nd greatest cause for impairments among all states. Green infrastructures are a stormwater best management practice that are primarily used to reduce runoff volumes and pollutant concentrations of regulated pollutants (e.g., TSS); however, they also hold promise for reduce the temperature of stormwater runoff. While previous studies have demonstrated the potential of green infrastructure such as bioswales and permeable pavers for reducing runoff temperatures, none have evaluated how green infrastructure connected in series can improve temperature mitigation. The outcome of this objective demonstrates the extent to which green infrastructure (porous pavement and bioswales) connected in series can reduce outfall runoff temperatures into streams. These outcomes can help inform effective designs of green stormwater infrastructure to address one of the leading causes of stream impairments in the U.S.

6.1. Outcomes and key findings

The following sections summarize the outcomes, key findings, and implications of each dissertation objective.

6.1.1. Analyze Land-Use Changes and their Impact on Discharge and Water Quality Trends in the United States.

The outcomes of this objective include (1) defining the land use changes within case study watersheds, (2) determining the trends in discharge and water quality, and (3) a regression model that relates the change in land use to trends in water quality. The key findings of these outcomes were that (1) imperviousness and developed land increased in every watershed, (2) of the watersheds with statistically significant trends, the majority had increases in specific conductance and decreases in dissolved oxygen and turbidity, (3) between 12% - 58% of the variance in water quality trends could be explained by the land use changes within the watersheds.

Trend analysis revealed that land use changes in the watersheds over the study period largely followed trends within the U.S. at large, with every watershed demonstrating an increase in impervious area, with an average increase of 0.41% and a maximum of 1.78% over the period 2008 to 2016. Trends in discharge and water quality in streams were mixed, with a majority of watersheds demonstrating a decrease in dissolved oxygen and turbidity, both an increase and decrease in discharge, and an increase in specific conductance. A regression analysis revealed that discharge, turbidity, and specific conductance were correlated with changes in individual land use types with an R^2 between 0.12 – 0.25. Combining the influences of multiple land uses in multivariate regression improved the predictions for discharge (R^2 0.58) and specific conductance (R^2 0.47), highlighting the magnitude for which land cover changes may influence trends in water quality. Overall, this study demonstrates the relationship between land use changes and surface water quality at a broad spatial (continental U.S.) and temporal (9 years) scales. These outcomes could be applied in watershed

management plans, where the impact of future land use projections could provide a basis for expected changes in downstream water quality.

6.1.2. Define the Influence of Socioeconomic and Spatial Variables on TMDL Progress in the United States.

The outcomes of this objective were (1) an assessment of the progress of TMDLs within the U.S., and (2) a determination of how socioeconomic or spatial variables influence aspects of TMDL progress. The key findings of this objective were that across all U.S. states (1) the median percentage of streams and rivers assessed within states is 33%, of those streams that are assessed, a median of 27% are listed as impaired, and of those listed as impaired a median of 22% have a TMDL complete, and (2) the spatial and socioeconomic variables that are significantly correlated to indicators of TMDL progress include total stream length, state land area, per capita earnings, percentage of population with bachelor degrees, percentage of population without high school degrees, EPA region, and political inclination .

Results indicate that TMDL progress and impairments had a large degree of variation, some of which could be explained by spatial location including EPA region, as well as socioeconomic variables. To that end, results suggest that the size of a state (R^2 0.19) and the length of total streams (R^2 0.22) are negatively correlated while per capita earnings (R^2 0.13) and percentage with bachelor's degrees or higher (R^2 0.13) are positively correlated to the percentage of streams that are assessed within a state. In addition, states largely followed similar patterns based upon the EPA region that they were within, indicating that EPA regions play a large role in TMDL progress. Finally, the study found a moderately significant relationship between the overall political inclination within state legislature and the percentage of assessed streams, where states historically

controlled by democrats assessed a greater percentage of streams. The major impact of this study is that it contextualizes the progress in TMDL development and can help aid in our understanding of the influence that socioeconomics or regionalization may have on implementation of water quality programs. This understanding of the factors that affect the TMDL development will allow federal, regional, or state-level agencies to modify their watershed management planning approaches in a way that wholistically considers the diverse influences that may affect progress towards meeting water quality goals.

6.1.3. Monitor and Analyze the Temperature Mitigation Potential of Interconnected Green Infrastructure Practices.

The outcome of this objective is a determination of the temperature mitigation in green infrastructure connected in series – a bioswale and permeable pavement that both discharge into a second bioswale – over the course of the summer and fall. The key finding of this objective is that green infrastructure connected in series further reduce stormwater runoff temperatures.

Three GI practices were studied in a parking lot consisting of asphalt, permeable pavements, and sidewalks. Results indicate that for the bioswale and permeable pavers connected in parallel, the bioswale effluent had lower event mean temperatures than the permeable pavers (2.8 °C cooler). In addition, the bioswale that performed secondary treatment further reduced the average event mean temperature across all storms by 4.2 °C from the permeable pavers and 2.4 °C from the bioswale. This study demonstrates the effectiveness of green infrastructure connected in series for reducing effluent temperatures, which is important for addressing a critical threat to environmental and human health. As temperature impairments in urban water bodies increase due to the urban heat island effect and global temperature rises caused by climate change,

mitigation efforts are critical. This study demonstrates that green infrastructure connected in series can improve temperature mitigation compared to stand alone structures. Watershed managers and planners can use this knowledge in designing green infrastructure approaches to addressing the second largest level-1 impairment of streams and rivers in the U.S.

6.2. Future Work Recommendations

The following sections introduce suggested future work based on the results and limitations of each dissertation objective.

6.2.1. Analyze Land-Use Changes and Their Impact on Discharge and Water Quality Trends in the United States.

While this objective was able to find a sizeable number of gages (60) that collected discharge, specific conductance, and turbidity over the time period of interest (2008 - 2016), there are other pollutants of concern that were not available for which land use could have large impact. For example, nutrients, temperature, and total suspended sediments are leading causes of impairments; however, these parameters are not available over a long time period (>9 years) at a large number of USGS sites (>30). As new gages that collect these parameters come online, future empirical studies could attempt to assess how trends in these pollutants are impacted by land use changes. Furthermore, while continuous data might not be available, it is possible that grab samples that are representative of monthly or annual time scales could also be used to evaluate trends in water quality (Wijesiri et al., 2018). While the time frame of this study was limited by the availability of continuous data, data over a much longer period could provide stronger assessment of temporal trends in both land use and stream discharge and water quality. This is especially true if historical data is available prior to the period of this case study

as land use changes in the U.S. were more prominent during the late 90's and early 2000's (Winkler et al., 2021). To that end, historical land use maps may become increasingly available as machine learning approaches have recently been used to develop land use classifications based upon satellite data, aerial imagery, and historic paper maps (D. Liu et al., 2018; Talukdar et al., 2020; J. Wang et al., 2022). Utilizing these new data sources as they become available could improve the observations from this study.

This study identified the relationship between land use change and trends in discharge and water quality; however, there may be other explanatory factors not captured by this study that could further explain the mechanisms within watersheds that impact trends in discharge and water quality. An example of this is given by the observed relationship between changes in turbidity and land use. Turbidity has a negative correlation with urban land increases, and it has decreasing trends in more than 85% of the watersheds. Other studies (J. C. Murphy, 2020; Stets et al., 2020) have observed similar trends in stream discharge and water quality and attribute them to the implementation of best management practice within the watershed. An additional finding was that the relationship between discharge and imperviousness was not statistically significant at $p < 0.1$. This could be related to regulations that require new developments to match post-development volume and peak discharges (Prey et al., 1995). A future study that can also quantify the rate at which best management practices are implemented within a watershed may be able to elucidate the impact to which land use changes are also associated with BMP implementation.

6.2.2. Define the Influence of Socioeconomic and Spatial Variables on TMDL Progress in the United States.

The study revealed linkages between economic (e.g., per capita earnings) and educational (e.g., attainment of a bachelor's degree) indicators and the percentage of streams that were assessed. Future studies could further parse out the exact mechanisms for which these indicators translate to stream assessments. For example, states with higher income tax and higher per capita earnings may have a greater base for which to disperse funds to the state-level agencies that performs assessments. There may also be support from non-profits and advocacy groups such as Sweet Water (Southern Wisconsin Watershed Trust) and Milwaukee Riverkeeper that fund assessments through voluntary groups and that implement educational programs that support watershed management goals. To that end, assessing to what degree and how many community organizations get involved in the TMDL process could shed light on how much the educational background and non-profit organizational efforts support TMDL progress.

In collecting TMDL data from the ATTAINS database, it was observed that states have different methods of categorizing, testing, and reporting pollutants. A future study could identify the reasons for which states, or EPA regions, use specific testing methods and test for specific pollutants. These could be related to finances, availability of expertise, or the specific water quality challenges or polluters (e.g., agriculture) within a state. Similarly, states or EPA regions could also have varying laboratory capabilities to assess and test water quality resulting in varying approaches to TMDL assessments (Williams, 1993). Understanding reasons for which states use specific testing methods or test for specific pollutants could assist the EPA in providing further guidance to states on how to assess their water bodies.

Finally, this study demonstrated the relationships between indicators of TMDL progress and historical political control within a state. An assessment of state regulations, policy, and legal codes addressing water quality issues could reveal more information about how the platform of political parties in control of state-level environmental agencies impact the TMDL process. For example, the approach to TMDL development is often codified by state legislatures, such as chapter NR 212 subchapter 3 of the Wisconsin administrative code, that defines the requirements of TMDL development. Comparing these and other state legislation and regulation that impact water quality and TMDL development could further shed light on the variation in approaches.

6.2.3. Monitor and Analyze the Temperature Mitigation Potential of Interconnected Green Infrastructure Practices.

Future work could build upon the outcomes of this objective to quantify the impact of green infrastructure design on temperature mitigation. First, the specific thermal capacity of the media for effectively reducing runoff temperatures is something that may have competing objectives with the need to adsorb pollutants and infiltrate runoff at a sufficient rate. For example, sand is known to have a greater thermal capacity than clay soils (Ghuman et al., 1985); therefore, future studies could evaluate how the recommended mix of bioretention media impacts its ability to reduce runoff temperature. In addition, soil amendments used for removing other pollutants may have an impact on the conductivity of the soil. For example, artificial soils used for green roofs and green walls have shown varying thermal conductivity with ‘Biochar-coconut coir compost’ showing the least amount of conductivity (Lunt et al., 2023). Investigating GI subsoil thermal properties could help improve the design of these structures to meet both objectives of high infiltration and temperature mitigation.

There may also be specific design parameters of GI, such as the depth of the underdrain, that could impact the temperature of the effluent that leaves the system. For example, greater depths to the underdrain have been found to produces lower effluent temperatures due to the cooler temperature of deeper soils that are buffered from atmospheric temperatures changes and solar radiation (Jones & Hunt, 2009). To that extent, field experiments could test how design parameters, such as the depth to the underdrain, influence the temperature reduction of stormwater runoff. Furthermore, increasing residence time of flow through design alterations in the subsoil trench could improve the temperature reduction of flow through the system. Internal baffles in bioretention's have been used to improve volume capture and pollutant removal by increasing residence time (H. Li et al., 2021). A carefully designed baffle system that increases the residence time while performing adequate runoff capture could allow the storm water to reach thermal equilibrium with the subsoil before being released through the underdrain.

Finally, this study was able to measure the temperature of the effluent of the three practices, but future studies could incorporate a greater number of sensors to measure the runoff temperature within other parts of the watershed and GI. Other sites where flow is concentrated at the inlet of the green infrastructure practice could be used so that influent temperatures could also be captured with a thermocouple. However, doing so with porous pavements would be a challenge since they are aligned with the roadway, but could possibly be done by constructing a temporary blockage around the pavement. In addition, soil moisture content has a profound impact on the thermal dynamics of the system due to its impact on infiltrations rates, thermal capacity, and thermal conduction rates of the

trench media. Therefore, using moisture and temperature sensors in multiple depth profiles within each structure could allow us to capture the thermal dynamics within the green infrastructure media itself.

BIBLIOGRAPHY

2022 County-wide Act 167 Stormwater Management Model Ordinance | Chester County, PA - Official Website. (2022). https://www.chesco.org/5111/Updating-County-Wide-Stormwater-Ordinanc

Aboelnour, M., Gitau, M. W., & Engel, B. A. (2020). A Comparison of Streamflow and Baseflow Responses to Land-Use Change and the Variation in Climate Parameters Using SWAT. *Water 2020, Vol. 12, Page 191*, *12*(1), 191. https://doi.org/10.3390/W12010191

Adedeji, I. C., Ahmadisharaf, E., & Sun, Y. (2022). Predicting in-stream water quality constituents at the watershed scale using machine learning. *Journal of Contaminant Hydrology*, *251*, 104078. https://doi.org/10.1016/J.JCONHYD.2022.104078

Adler, R. W., Landman, J. C., & Cameron, D. M. (1993). The clean water act 20 years later. In *Island Press*. Island Press.

Afrifa-Yamoah, E., Mueller, U. A., Taylor, S. M., & Fisher, A. J. (2020). Missing data imputation of high-resolution temporal climate time series data. *Meteorological Applications*, *27*(1), e1873. https://doi.org/10.1002/MET.1873

Aguilera, H., Guardiola-Albert, C., & Serrano-Hidalgo, C. (2020). Estimating extremely large amounts of missing precipitation data. *Journal of Hydroinformatics*, *22*(3), 578–592. https://doi.org/10.2166/HYDRO.2020.127

Ahearn, D. S., Sheibley, R. W., Dahlgren, R. A., Anderson, M., Johnson, J., & Tate, K. W. (2005). Land use and land cover influence on water quality in the last free-flowing river draining the western Sierra Nevada, California. *Journal of Hydrology*, *313*(3–4), 234–247. https://doi.org/10.1016/J.JHYDROL.2005.02.038

Ahiablame, L., Sheshukov, A. Y., Rahmani, V., & Moriasi, D. (2017). Annual baseflow variations as influenced by climate variability and agricultural land use change in the Missouri River Basin. *Journal of Hydrology*, *551*, 188–202. https://doi.org/10.1016/J.JHYDROL.2017.05.055

Ahmadisharaf, E., Asce, A. M., Camacho, R. A., Asce, M., Zhang, H. X., Hantush, M. M., & Mohamoud, Y. M. (2019). Calibration and Validation of Watershed Models and Advances in Uncertainty Analysis in TMDL Studies. *Journal of Hydrologic Engineering*, *24*(7), 03119001. https://doi.org/10.1061/(ASCE)HE.1943-5584.0001794

Ahmed, A. Q., Ossen, D. R., Jamei, E., Manaf, N. A., Said, I., & Ahmad, M. H. (2015). Urban surface temperature behaviour and heat island effect in a tropical planned city. *Theoretical and Applied Climatology*, *119*(3–4), 493–514. https://doi.org/10.1007/S00704-014-1122-2/FIGURES/15

Akoko, G., Le, T. H., Gomi, T., & Kato, T. (2021). A Review of SWAT Model

Application in Africa. *Water 2021, Vol. 13, Page 1313*, *13*(9), 1313. https://doi.org/10.3390/W13091313

Alavi, N., Warland, J. S., & Berg, A. A. (2006). Filling gaps in evapotranspiration measurements for water budget studies: Evaluation of a Kalman filtering approach. *Agricultural and Forest Meteorology*, *141*(1), 57–66. https://doi.org/10.1016/J.AGRFORMET.2006.09.011

Ali, H. H., & Kadhum, L. E. (2017). *K- Means Clustering Algorithm Applications in Data Mining and Pattern Recognition*.

Allan, J. D., Castillo, M. M., & Capps, K. A. (2021). *Stream ecology: structure and function of running waters*. Springer Nature.

Andrew, R. G., Burns, R. C., & Allen, M. E. (2019). The Influence of Location on Water Quality Perceptions across a Geographic and Socioeconomic Gradient in Appalachia. *Water 2019, Vol. 11, Page 2225*, *11*(11), 2225. https://doi.org/10.3390/W11112225

Astuti, I. S., Sahoo, K., Milewski, A., & Mishra, D. R. (2019). Impact of Land Use Land Cover (LULC) Change on Surface Runoff in an Increasingly Urbanized Tropical Watershed. *Water Resources Management 2019 33:12*, *33*(12), 4087–4103. https://doi.org/10.1007/S11269-019-02320-W

ATTAINS | Water Data and Tools | US EPA. (2022). https://www.epa.gov/waterdata/attains

Avellaneda, P. M., & Jefferson, A. J. (2020). Sensitivity of streamflow metrics to infiltration-based stormwater management networks. *Water Resources Research*, *56*(7), e2019WR026555.

Baddoo, T. D., Li, Z., Odai, S. N., Boni, K. R. C., Nooni, I. K., & Andam-Akorful, S. A. (2021). Comparison of missing data infilling mechanisms for recovering a real-world single station streamflow observation. *International Journal of Environmental Research and Public Health*, *18*(16), 8375. https://doi.org/10.3390/IJERPH18168375/S1

Baker, A. (2006). Land Use and Water Quality. In *Encyclopedia of Hydrological Sciences*. John Wiley & Sons, Ltd. https://doi.org/10.1002/0470848944.hsa195

Baker, M. E., Schley, M. L., & Sexton, J. O. (2019). Impacts of Expanding Impervious Surface on Specific Conductance in Urbanizing Streams. *Water Resources Research*, *55*(8), 6482–6498. https://doi.org/10.1029/2019WR025014

Balany, F., Ng, A. W. M., Muttil, N., Muthukumaran, S., & Wong, M. S. (2020). Green infrastructure as an urban heat island mitigation strategy—a review. *Water (Switzerland)*, *12*(12), 1–22. https://doi.org/10.3390/w12123577

Ballestero, T. P. (2020). *Final Report: Taking it to the Streets: Green Infrastructure for Sustainable Philadelphia Communities*.

Baquero, F., Martínez, J. L., & Cantón, R. (2008). Antibiotics and antibiotic resistance in water environments. *Current Opinion in Biotechnology*, *19*(3), 260–265. https://doi.org/10.1016/J.COPBIO.2008.05.006

Bartlett, M. S., Parolari, A. J., McDonnell, J. J., & Porporato, A. (2016). Beyond the SCS-CN method: A theoretical framework for spatially lumped rainfall-runoff response. *Water Resources Research*, *52*(6), 4608–4627. https://doi.org/10.1002/2015WR018439

Basu, N. B., Van Meter, K. J., Byrnes, D. K., Van Cappellen, P., Brouwer, R., Jacobsen, B. H., Jarsjö, J., Rudolph, D. L., Cunha, M. C., Nelson, N., Bhattacharya, R., Destouni, G., & Olsen, S. B. (2022). Managing nitrogen legacies to accelerate water quality improvement. *Nature Geoscience 2022 15:2*, *15*(2), 97–105. https://doi.org/10.1038/s41561-021-00889-9

Beck, M. W., Bokde, N., Asencio-Cortés, G., & Kulat, K. (2018). R Package imputeTestbench to Compare Imputation Methods for Univariate Time Series. *The R Journal*, *10*(1), 218. /pmc/articles/PMC6309171/

Bell, C. D., Wolfand, J. M., Panos, C. L., Bhaskar, A. S., Gilliom, R. L., Hogue, T. S., Hopkins, K. G., & Jefferson, A. J. (2020). Stormwater control impacts on runoff volume and peak flow: A meta-analysis of watershed modelling studies. *Hydrological Processes*, *November 2019*, 3134–3152. https://doi.org/10.1002/hyp.13784

Benham, B., Zeckoski, R., Pract, G. Y.-W., & 2008, undefined. (2008). Lessons learned from TMDL implementation case studies. *Researchgate.Net*. https://doi.org/10.2175/193317708X281370

Blomquist, W., & Schlager, E. (2006). Political Pitfalls of Integrated Watershed Management. *Http://Dx.Doi.Org/10.1080/08941920590894435*, *18*(2), 101–117. https://doi.org/10.1080/08941920590894435

Boening-Ulman, K. M., Winston, R. J., Wituszynski, D. M., Smith, J. S., Andrew Tirpak, R., & Martin, J. F. (2022). Hydrologic impacts of sewershed-scale green infrastructure retrofits: Outcomes of a four-year paired watershed monitoring study. *Journal of Hydrology*, *611*, 128014. https://doi.org/10.1016/J.JHYDROL.2022.128014

Borah, D. K., Ahmadisharaf, E., Padmanabhan, G., Imen, S., & Mohamoud, Y. M. (2018). Watershed Models for Development and Implementation of Total Maximum Daily Loads. *Journal of Hydrologic Engineering*, *24*(1), 03118001. https://doi.org/10.1061/(ASCE)HE.1943-5584.0001724

Bowerman, T. E., Keefer, M. L., & Caudill, C. C. (2021). Elevated stream temperature, origin, and individual size influence Chinook salmon prespawn mortality across the Columbia River Basin. *Fisheries Research*, *237*, 105874. https://doi.org/10.1016/J.FISHRES.2021.105874

Brandes, D., Cavallo, G. J., & Nilson, M. L. (2005). Base flow trends in urbanizing

watersheds of the Delaware River basin. *Journal of the American Water Resources Association*, *41*(6), 1377–1391. https://doi.org/10.1111/j.1752-1688.2005.tb03806.x

Brett, A. E. (2017). Putting the Public on Trial: Can Citizen Science Data be Used in Litigation and Regulation? *Villanova Environmental Law Journal*, *28*(2), 1–44. https://heinonline.org/hol-cgi-bin/get_pdf.cgi?handle=hein.journals/vilenvlj28&section=12

Brodeur-Doucet, C., Pineau, B., Corrivault-Gascon, J., Arjoon, D., Lessard, P., Pelletier, G., & Duchesne, S. (2021). Seasonal hydrological and water quality performance of individual and in-series stormwater infrastructures as treatment trains in cold climate. *Water Quality Research Journal*, *56*(4), 205–217. https://doi.org/10.2166/wqrj.2021.026

Bryant, S., & Wadzuk, B. M. (2017). *Modeling of a Real-Time Controlled Green Roof*. 567–583.

Cabieses, B., Tunstall, H., & Pickett, K. (2015). Understanding the Socioeconomic Status of International Immigrants in Chile Through Hierarchical Cluster Analysis: a Population-Based Study. *International Migration*, *53*(2), 303–320. https://doi.org/10.1111/IMIG.12077

Caissie, D. (2006). The thermal regime of rivers: a review. *Freshwater Biology*, *51*(8), 1389–1406.

Census Bureau Data. (2017). https://data.census.gov/cedsci/

Chen, H. Y., Hodges, C. C., & Dymond, R. L. (2021). Modeling Watershed-Wide Bioretention Stormwater Retrofits to Achieve Thermal Pollution Mitigation Goals. *JAWRA Journal of the American Water Resources Association*, *57*(1), 109–133.

Chen, J., Liu, Y., Gitau, M. W., Engel, B. A., Flanagan, D. C., & Harbor, J. M. (2019). Evaluation of the effectiveness of green infrastructure on hydrology and water quality in a combined sewer overflow community. *Science of The Total Environment*, *665*, 69–79. https://doi.org/10.1016/J.SCITOTENV.2019.01.416

Cheng, Y. Y., Lo, S. L., Ho, C. C., Lin, J. Y., & Yu, S. L. (2019). Field testing of porous pavement performance on runoff and temperature control in Taipei City. *Water (Switzerland)*, *11*(12). https://doi.org/10.3390/W11122635

Chiang, L. C., Wang, Y. C., Chen, Y. K., & Liao, C. J. (2021). Quantification of land use/land cover impacts on stream water quality across Taiwan. *Journal of Cleaner Production*, *318*, 128443. https://doi.org/10.1016/J.JCLEPRO.2021.128443

Chithra, S. V., Harindranathan Nair, M., Amarnath, A., & Anjana, N. S. (2015). Impacts of Impervious Surfaces on the Environment. *International Journal of Engineering Science Invention*, *4*(5), 27–31. www.ijesi.org%7C%7CVolumewww.ijesi.org

Choi, C., Berry, P., & Smith, A. (2021). The climate benefits, co-benefits, and trade-offs of green infrastructure: A systematic literature review. *Journal of Environmental Management*, *291*, 112583. https://doi.org/10.1016/J.JENVMAN.2021.112583

City of Milwaukee. (2018). Chapter 120 Storm Water Management Regulations. *City of Milwaukee Code of Ordinances*, 1–15.

Clary, J., Jones, J., Leisenring, M., Hobson, P., & Strecker, E. (2020). International Stormwater BMP Database 2020 Summary Statistics. In *WRF* (Issue 4968).

Cole, M., Lindeque, P., Halsband, C., & Galloway, T. S. (2011). Microplastics as contaminants in the marine environment: A review. *Marine Pollution Bulletin*, *62*(12), 2588–2597. https://doi.org/10.1016/J.MARPOLBUL.2011.09.025

Collier, S. A., Deng, L., Adam, E. A., Benedict, K. M., Beshearse, E. M., Blackstock, A. J., Bruce, B. B., Derado, G., Edens, C., Fullerton, K. E., Gargano, J. W., Geissler, A. L., Hall, A. J., Havelaar, A. H., Hill, V. R., Hoekstra, R. M., Reddy, S. C., Scallan, E., Stokes, E. K., … Beach, M. J. (2021). Estimate of Burden and Direct Healthcare Cost of Infectious Waterborne Disease in the United States - Volume 27, Number 1—January 2021 - Emerging Infectious Diseases journal - CDC. *Emerging Infectious Diseases*, *27*(1), 140–149. https://doi.org/10.3201/EID2701.190676

Connolly, C. T., Khosh, M. S., Burkart, G. A., Douglas, T. A., Holmes, R. M., Jacobson, A. D., Tank, S. E., & McClelland, J. W. (2018). Watershed slope as a predictor of fluvial dissolved organic matter and nitrate concentrations across geographical space and catchment size in the Arctic. *Environmental Research Letters*, *13*(10), 104015. https://doi.org/10.1088/1748-9326/AAE35D

Coulliette, A. D., & Noble, R. T. (2008). Impacts of rainfall on the water quality of the Newport River Estuary (Eastern North Carolina, USA). *Journal of Water and Health*, *6*(4), 473–482. https://doi.org/10.2166/WH.2008.136

Creutzig, F., Bren D'Amour, C., Weddige, U., Fuss, S., Beringer, T., Gläser, A., Kalkuhl, M., Steckel, J. C., Radebach, A., & Edenhofer, O. (2019). Assessing human and environmental pressures of global land-use change 2000–2010. *Global Sustainability*, *2*. https://doi.org/10.1017/SUS.2018.15

Croitoru, A. E., & Minea, I. (2015). The impact of climate changes on rivers discharge in Eastern Romania. *Theoretical and Applied Climatology*, *120*(3–4), 563–573. https://doi.org/10.1007/S00704-014-1194-Z/METRICS

Cromartie, J., & Nulph, D. (2019, June 20). *USDA ERS - 2010 Frontier and Remote (FAR) Area Codes Documentation*. https://www.ers.usda.gov/data-products/frontier-and-remote-area-codes/documentation/

D. J. Bosch, C. Ogg, E. Osei, & A. L. Stoecker. (2006). Economic Models for Tmdl Assessment and Implementation. *Transactions of the ASABE*, *49*(4), 1051–1065. https://doi.org/10.13031/2013.21744

Davis, A. P. (2008). Field Performance of Bioretention: Hydrology Impacts. *Journal of Hydrologic Engineering*, *13*(2), 90–95. https://doi.org/10.1061/(ASCE)1084-0699(2008)13:2(90)

de Necker, L., Neswiswi, T., Greenfield, R., van Vuren, J., Brendonck, L., Wepener, V.,

& Smit, N. (2019). Long-Term Water Quality Patterns of a Flow Regulated Tropical Lowland River. *Water 2020, Vol. 12, Page 37*, *12*(1), 37. https://doi.org/10.3390/W12010037

de Vries, D. A. (1975). HEAT TRANSFER IN SOILS. *Semin on Heat and Mass Transfer in the Environ of Veg, Heat and Mass Transfer in the Biosphere, Pt 1*, 5–28.

DeGioia, M. (2019). Overboard: The Complexity of Traditional TMDL Calculations under the Clean Water Act. *Environmental Law Reporter News & Analysis*, *49*.

Delia, K. A., Haney, C. R., Dyer, J. L., & Paul, V. G. (2021). Spatial Analysis of a Chesapeake Bay Sub-Watershed: How Land Use and Precipitation Patterns Impact Water Quality in the James River. *Water 2021, Vol. 13, Page 1592*, *13*(11), 1592. https://doi.org/10.3390/W13111592

Delkash, M., Al-Faraj, F. A. M., & Scholz, M. (2018). Impacts of Anthropogenic Land Use Changes on Nutrient Concentrations in Surface Waterbodies: A Review. *CLEAN – Soil, Air, Water*, *46*(5), 1800051. https://doi.org/10.1002/CLEN.201800051

Déry, S. J., Stadnyk, T. A., MacDonald, M. K., & Gauli-Sharma, B. (2016). Recent trends and variability in river discharge across northern Canada. *Hydrology and Earth System Sciences*, *20*(12), 4801–4818. https://doi.org/10.5194/HESS-20-4801-2016

Di Cecco, G. J., & Gouhier, T. C. (2018). Increased spatial and temporal autocorrelation of temperature under climate change. *Scientific Reports 2018 8:1*, *8*(1), 1–9. https://doi.org/10.1038/s41598-018-33217-0

Domingo, J. L., & Nadal, M. (2019). Human exposure to per- and polyfluoroalkyl substances (PFAS) through drinking water: A review of the recent scientific literature. *Environmental Research*, *177*, 108648. https://doi.org/10.1016/J.ENVRES.2019.108648

Dong, J., Guo, F., Lin, M., Zhang, H., & Zhu, P. (2022). Optimization of green infrastructure networks based on potential green roof integration in a high-density urban area—A case study of Beijing, China. *Science of The Total Environment*, *834*, 155307. https://doi.org/10.1016/J.SCITOTENV.2022.155307

Easterling, D. R., Kunkel, K. E., Arnold, J. R., Knutson, T., Legrande, A. N., Leung, L. R., Vose, R. S., Wal-Iser, D. E., Wehner, M. F., Fahey, D. J. W., Hibbard, K. A., Dokken, D. J., Stewart, B. C., & Maycock, T. K. (2017). Precipitation change in the United States. *Climate Science Special Report: Fourth National Climate Assessment, 1*, 207–230. https://doi.org/10.7930/J0H993CC

Effective Funding Frameworks for Water Infrastructure | US EPA. (2023). EPA. https://www.epa.gov/waterfinancecenter/effective-funding-frameworks-water-infrastructure

Enders, C. K. (2022). *Applied missing data analysis*. Guilford Publications.

Environment Water Federation. (2015). *The Real Cost of Green Infrastructure*. 4366–4378.

Fan, M., & Shibata, H. (2015). Simulation of watershed hydrology and stream water quality under land use and climate change scenarios in Teshio River watershed, northern Japan. *Ecological Indicators*, *50*, 79–89. https://doi.org/10.1016/J.ECOLIND.2014.11.003

Farzin, Y. H., & Grogan, K. A. (2013). Socioeconomic factors and water quality in California. *Environmental Economics and Policy Studies*, *15*(1), 1–37. https://doi.org/10.1007/s10018-012-0040-8

Fasching, C., Wilson, H. F., D'Amario, S. C., & Xenopoulos, M. A. (2019). Natural Land Cover in Agricultural Catchments Alters Flood Effects on DOM Composition and Decreases Nutrient Levels in Streams. *Ecosystems*, *22*(7), 1530–1545. https://doi.org/10.1007/S10021-019-00354-0/TABLES/3

Ferreira, J. C., Monteiro, R., & Silva, V. R. (2021). Planning a Green Infrastructure Network from Theory to Practice: The Case Study of Setúbal, Portugal. *Sustainability 2021, Vol. 13, Page 8432*, *13*(15), 8432. https://doi.org/10.3390/SU13158432

Fiscal Year 2022 Agency Financial Report. (2022). https://www.epa.gov/planandbudget/results

Frost, W., Lott, R. C., LaPlante, R., & Rose, F. (2019). Modeling for TMDL Implementation. *Journal of Hydrologic Engineering*, *24*(6), 05019010. https://doi.org/10.1061/(ASCE)HE.1943-5584.0001786

Ghuman, B., Science, R. L.-S., & 1985, undefined. (1985). Thermal conductivity, thermal diffusivity, and thermal capacity of some Nigerian soils. *Journals.Lww.Com*, *139*(1). https://journals.lww.com/soilsci/Abstract/1985/01000/Thermal_Conductivity,_Thermal_Diffusivity,_and.11.aspx

Giri, S., & Qiu, Z. (2016). Understanding the relationship of land uses and water quality in Twenty First Century: A review. *Journal of Environmental Management*, *173*, 41–48. https://doi.org/10.1016/J.JENVMAN.2016.02.029

Griffith, A. W., & Gobler, C. J. (2020). Harmful algal blooms: a climate change co-stressor in marine and freshwater ecosystems. *Harmful Algae*, *91*, 101590.

Hadeed, S. J., O'Rourke, M. K., Burgess, J. L., Harris, R. B., & Canales, R. A. (2020). Imputation methods for addressing missing data in short-term monitoring of air pollutants. *Science of The Total Environment*, *730*, 139140. https://doi.org/10.1016/J.SCITOTENV.2020.139140

Haidary, A., Amiri, B. J., Adamowski, J., Fohrer, N., & Nakane, K. (2013). Assessing the Impacts of Four Land Use Types on the Water Quality of Wetlands in Japan. *Water*

Resources Management, *27*(7), 2217–2229. https://doi.org/10.1007/S11269-013-0284-5/TABLES/5

Han, H., Sun, M., Han, H., Wu, X., & Qiao, J. (2023). Univariate imputation method for recovering missing data in wastewater treatment process. *Chinese Journal of Chemical Engineering*, *53*, 201–210. https://doi.org/10.1016/J.CJCHE.2022.01.033

Hartigan, J. A., & Wong, M. A. (1979). Algorithm AS 136: A k-means clustering algorithm. *Journal of the Royal Statistical Society. Series c (Applied Statistics)*, *28*(1), 100–108.

Hathaway, J. M., & Hunt, W. F. (2011). Evaluation of first flush for indicator bacteria and total suspended solids in urban stormwater runoff. *Water, Air, and Soil Pollution*, *217*(1–4), 135–147. https://doi.org/10.1007/s11270-010-0574-y

Hawkins, R. H., Ward, T. J., Woodward, D. E., & Van Mullem, J. A. (2008). Curve Number Hydrology: State of the Practice. In *Curve Number Hydrology: State of the Practice*. American Society of Civil Engineers. https://doi.org/10.1061/9780784410042

He, T., Lu, Y., Cui, Y., Luo, Y., Wang, M., Meng, W., Zhang, K., & Zhao, F. (2015). Detecting gradual and abrupt changes in water quality time series in response to regional payment programs for watershed services in an agricultural area. *Journal of Hydrology*, *525*, 457–471. https://doi.org/10.1016/j.jhydrol.2015.04.005

Heddam, S. (2014). Modelling hourly dissolved oxygen concentration (DO) using dynamic evolving neural-fuzzy inference system (DENFIS)-based approach: Case study of Klamath River at Miller Island Boat Ramp, OR, USA. *Environmental Science and Pollution Research*, *21*(15), 9212–9227. https://doi.org/10.1007/S11356-014-2842-7/TABLES/9

Helsel, D. R., Hirsch, R. M., Ryberg, K. R., Archfield, S. A., & Gilroy, E. J. (2020). Statistical methods in water resources. *U.S. Geological Survey Techniques and Methods*, *2020*(4-A3), 1–484. https://doi.org/10.3133/tm4a3

Herb, W. R., Janke, B., Mohseni, O., & Stefan, H. G. (2008). Thermal pollution of streams by runoff from paved surfaces. *Hydrological Processes: An International Journal*, *22*(7), 987–999.

Hernandez Cordero, A. L., Tango, P. J., & Batiuk, R. A. (2020). Development of a multimetric water quality Indicator for tracking progress towards the achievement of Chesapeake Bay water quality standards. *Environmental Monitoring and Assessment*, *192*(2), 1–16. https://doi.org/10.1007/S10661-019-7969-Z/METRICS

Hines, N. W. (2013). History of the 1972 Clean Water Act: The Story behind How the 1972 Act became the Capstone on a Decade of Extraordinary Environmental Reform. *George Washington Journal of Energy and Environmental Law*, *4*. https://heinonline.org/HOL/Page?handle=hein.journals/gwjeel4&id=216&div=17&collection=journals

Hirsch, R. M., & Slack, J. R. (1984). A Nonparametric Trend Test for Seasonal Data With Serial Dependence. *Water Resources Research*, *20*(6), 727–732.

Homer, C., Dewitz, J., Jin, S., Xian, G., Costello, C., Danielson, P., Gass, L., Funk, M., Wickham, J., Stehman, S., Auch, R., & Riitters, K. (2020). Conterminous United States land cover change patterns 2001–2016 from the 2016 National Land Cover Database. *ISPRS Journal of Photogrammetry and Remote Sensing*, *162*, 184–199. https://doi.org/10.1016/J.ISPRSJPRS.2020.02.019

Hoornbeek, J., Hansen, E., Ringquist, E., & Carlson, R. (2013). Implementing Water Pollution Policy in the United States: Total Maximum Daily Loads and Collaborative Watershed Management. *Http://Dx.Doi.Org/10.1080/08941920.2012.700761*, *26*(4), 420–436. https://doi.org/10.1080/08941920.2012.700761

Houck, O. A. (1997). TMDLs: the resurrection of water quality standards-based regulation under the Clean Water Act. *Envtl. L. Rep. News & Analysis*, *27*, 10329.

Hovenga, P. A., Wang, D., Medeiros, S. C., Hagen, S. C., & Alizad, K. (2016). The response of runoff and sediment loading in the Apalachicola River, Florida to climate and land use land cover change. *Earth's Future*, *4*(5), 124–142. https://doi.org/10.1002/2015EF000348

Hung, C. L. J., James, L. A., Carbone, G. J., & Williams, J. M. (2020). Impacts of combined land-use and climate change on streamflow in two nested catchments in the Southeastern United States. *Ecological Engineering*, *143*, 105665. https://doi.org/10.1016/J.ECOLENG.2019.105665

Huntington, T. G. (2006). Evidence for intensification of the global water cycle: review and synthesis. *Journal of Hydrology*, *319*(1–4), 83–95.

Hwang, N. H., Houghtalen, R. J., & Akan, A. O. (1996). *Fundamentals of hydraulic engineering systems*. Prentice Hall. https://www.just.edu.jo/FacultiesandDepartments/FacultyofAgriculture/Departments/NaturalResourcesandEnvironment/Documents/Syllabus_NR340 Principles Of Hydraulics.pdf

Ivancic, T. J., & Shaw, S. B. (2015). Examining why trends in very heavy precipitation should not be mistaken for trends in very high river discharge. *Climatic Change*, *133*(4), 681–693. https://doi.org/10.1007/S10584-015-1476-1/METRICS

Jalali, P., & Rabotyagov, S. (2020). Quantifying cumulative effectiveness of green stormwater infrastructure in improving water quality. *Science of the Total Environment*, *731*, 138953. https://doi.org/10.1016/j.scitotenv.2020.138953

Javadi, S., Hashemy, S. M., Mohammadi, K., Howard, K. W. F., & Neshat, A. (2017). Classification of aquifer vulnerability using K-means cluster analysis. *Journal of Hydrology*, *549*, 27–37. https://doi.org/10.1016/J.JHYDROL.2017.03.060

Jean, M.-È., Morin, C., Duchesne, S., Pelletier, G., & Pleau, M. (2021). Optimization of

Real-Time Control With Green and Gray Infrastructure Design for a Cost-Effective Mitigation of Combined Sewer Overflows. *Water Resources Research*, *57*(12), e2021WR030282. https://doi.org/10.1029/2021WR030282

Jefferson, A. J., Bhaskar, A. S., Hopkins, K. G., Fanelli, R., Avellaneda, P. M., & McMillan, S. K. (2017). Stormwater management network effectiveness and implications for urban watershed function: A critical review. *Hydrological Processes*, *31*(23), 4056–4080. https://doi.org/10.1002/hyp.11347

Jones, M., & Hunt, W. F. (2009). Effect of bioretention on runoff temperature in trout sensitive regions. *Low Impact Development for Urban Ecosystem and Habitat Protection*, *135*(8), 577–585. https://doi.org/10.1061/41009(333)80

Jones, S. (2014). Making Regional and Local TMDLs Work: The Chesapeake Bay TMDL and Lessons from the Lynnhaven River. *William & Mary Environmental Law and Policy Review*, *38*(2). https://scholarship.law.wm.edu/wmelpr/vol38/iss2/2

Kauffman, G. J., Belden, A. C., Vonck, K. J., & Homsey, A. R. (2009). Link between Impervious Cover and Base Flow in the White Clay Creek Wild and Scenic Watershed in Delaware. *Journal of Hydrologic Engineering*, *14*(4), 324–334. https://doi.org/10.1061/(ASCE)1084-0699(2009)14:4(324)

Kaushal, S. S., Likens, G. E., Jaworski, N. A., Pace, M. L., Sides, A. M., Seekell, D., Belt, K. T., Secor, D. H., & Wingate, R. L. (2010). Rising stream and river temperatures in the United States. *Frontiers in Ecology and the Environment*, *8*(9), 461–466. https://doi.org/10.1890/090037

Ketabchy, M., Sample, D. J., Wynn-Thompson, T., & Yazdi, M. N. (2019). Simulation of watershed-scale practices for mitigating stream thermal pollution due to urbanization. *Science of the Total Environment*, *671*, 215–231.

Koontz, T. M., & Newig, J. (2014). From Planning to Implementation: Top-Down and Bottom-Up Approaches for Collaborative Watershed Management. *Policy Studies Journal*, *42*(3), 416–442. https://doi.org/10.1111/PSJ.12067

Krayenhoff, S. E., & Voogt, J. A. (2007). A microscale three-dimensional urban energy balance model for studying surface temperatures. *Boundary-Layer Meteorology*, *123*(3), 433–461. https://doi.org/10.1007/S10546-006-9153-6/METRICS

Kumar, P., Druckman, A., Gallagher, J., Gatersleben, B., Allison, S., Eisenman, T. S., Hoang, U., Hama, S., Tiwari, A., Sharma, A., Abhijith, K. V., Adlakha, D., McNabola, A., Astell-Burt, T., Feng, X., Skeldon, A. C., de Lusignan, S., & Morawska, L. (2019). The nexus between air pollution, green infrastructure and human health. *Environment International*, *133*, 105181. https://doi.org/10.1016/J.ENVINT.2019.105181

Larson, K. L., & Lach, D. (2008). Participants and non-participants of place-based groups: An assessment of attitudes and implications for public participation in water resource management. *Journal of Environmental Management*, *88*(4), 817–830. https://doi.org/10.1016/J.JENVMAN.2007.04.008

LeBleu, C., Dougherty, M., Rahn, K., Wright, A., Bowen, R., Wang, R., Orjuela, J. A., & Britton, K. (2019). Quantifying thermal characteristics of stormwater through low impact development systems. *Hydrology*, *6*(1), 16.

Lebo, M. E., Paerl, H. W., & Peierls, B. L. (2012). Evaluation of progress in achieving TMDL mandated nitrogen reductions in the Neuse river basin, North Carolina. *Environmental Management*, *49*(1), 253–266. https://doi.org/10.1007/S00267-011-9774-5/FIGURES/9

Lee, J. H., Bang, K. W., Ketchum, J. H., Choe, J. S., & Yu, M. J. (2002). First flush analysis of urban storm runoff. *Science of The Total Environment*, *293*(1–3), 163–175. https://doi.org/10.1016/S0048-9697(02)00006-2

Lei, C., Wagner, P. D., & Fohrer, N. (2021). Effects of land cover, topography, and soil on stream water quality at multiple spatial and seasonal scales in a German lowland catchment. *Ecological Indicators*, *120*, 106940. https://doi.org/10.1016/J.ECOLIND.2020.106940

Leppi, J. C., DeLuca, T. H., Harrar, S. W., & Running, S. W. (2012). Impacts of climate change on August stream discharge in the Central-Rocky Mountains. *Climatic Change*, *112*(3–4), 997–1014. https://doi.org/10.1007/S10584-011-0235-1/TABLES/8

Lewellyn, C., Lyons, C. E., Traver, R. G., & Wadzuk, B. M. (2016). Evaluation of Seasonal and Large Storm Runoff Volume Capture of an Infiltration Green Infrastructure System. *Journal of Hydrologic Engineering*, *21*(1), 04015047. https://doi.org/10.1061/(asce)he.1943-5584.0001257

Li, C., Peng, C., Chiang, P. C., Cai, Y., Wang, X., & Yang, Z. (2019). Mechanisms and applications of green infrastructure practices for stormwater control: A review. *Journal of Hydrology*, *568*, 626–637. https://doi.org/10.1016/J.JHYDROL.2018.10.074

Li, F., Chen, J., Engel, B. A., Liu, Y., Wang, S., & Sun, H. (2021). Assessing the effectiveness and cost efficiency of green infrastructure practices on surface runoff reduction at an urban watershed in China. *Water (Switzerland)*, *13*(1). https://doi.org/10.3390/w13010024

Li, H., Asce, A. M., Sansalone, J., & Asce, M. (2021). CFD with Evolutionary Optimization for Stormwater Basin Retrofits. *Journal of Environmental Engineering*, *147*(7), 04021017. https://doi.org/10.1061/(ASCE)EE.1943-7870.0001881

Li, S., Gu, S., Tan, X., & Zhang, Q. (2009). Water quality in the upper Han River basin, China: The impacts of land use/land cover in riparian buffer zone. *Journal of Hazardous Materials*, *165*(1–3), 317–324. https://doi.org/10.1016/J.JHAZMAT.2008.09.123

Liang, R., di Matteo, M., Maier, H. R., & Thyer, M. A. (2019). Real-time, smart rainwater storage systems: Potential solution to mitigate urban flooding. *Water*

(Switzerland), *11*(12). https://doi.org/10.3390/W11122428

Liu, D., Toman, E., Fuller, Z., Chen, G., Londo, A., Zhang, X., & Zhao, K. (2018). Integration of historical map and aerial imagery to characterize long-term land-use change and landscape dynamics: An object-based analysis via Random Forests. *Ecological Indicators*, *95*, 595–605. https://doi.org/10.1016/J.ECOLIND.2018.08.004

Liu, W., Feng, Q., Chen, W., & Deo, R. C. (2020). Stormwater runoff and pollution retention performances of permeable pavements and the effects of structural factors. *Environmental Science and Pollution Research*, *27*(24), 30831–30843. https://doi.org/10.1007/S11356-020-09220-2

Long, D. L., & Dymond, R. L. (2014). Thermal Pollution Mitigation in Cold Water Stream Watersheds. *Journal of the American Water Resources Association*, *50*(4). https://doi.org/10.1111/jawr.12152

Loperfido, J. V., Beyer, P., Just, C. L., & Schnoor, J. L. (2010). Uses and Biases of Volunteer Water Quality Data. *Environmental Science and Technology*, *44*(19), 7193–7199. https://doi.org/10.1021/ES100164C

Lubell, M., & Lippert, L. (2011). Integrated regional water management: a study of collaboration or water politics-as-usual in California, USA. *Http://Dx.Doi.Org/10.1177/0020852310388367*, *77*(1), 76–100. https://doi.org/10.1177/0020852310388367

Lunt, P. H., Fuller, K., Fox, M., Goodhew, S., & Murphy, T. R. (2023). Comparing the thermal conductivity of three artificial soils under differing moisture and density conditions for use in green infrastructure. *Soil Use and Management*, *39*(1), 260–269. https://doi.org/10.1111/SUM.12841

Madley-Dowd, P., Hughes, R., Tilling, K., & Heron, J. (2019). The proportion of missing data should not be used to guide decisions on multiple imputation. *Journal of Clinical Epidemiology*, *110*, 63–73. https://doi.org/10.1016/J.JCLINEPI.2019.02.016

Mahmoodi, N., Osati, K., Salajegheh, A., & Saravi, M. M. (2021). Trend in river water quality: tracking the overall impacts of climate change and human activities on water quality in the Dez River Basin. *Journal of Water and Health*, *19*(1), 159–173. https://doi.org/10.2166/WH.2020.123

Maine DEP. (2012). *Maine stormwater best management practices manual*.

Maiolo, M., Palermo, S. A., Brusco, A. C., Pirouz, B., Turco, M., Vinci, A., Spezzano, G., & Piro, P. (2020). On the use of a real-time control approach for urban stormwater management. *Water (Switzerland)*, *12*(10). https://doi.org/10.3390/w12102842

Mann, H. B., & Whitney, D. R. (1947). On a Test of Whether one of Two Random Variables is Stochastically Larger than the Other. *The Annals of Mathematical*

Statistics, *18*(1), 50–60. https://doi.org/10.1214/aoms/1177730491

Martin, R. M., Carvajal Sanchez, S., Welker, A. L., & Komlos, J. (2021). Thermal Effects of Stormwater Control Measures on a Receiving Headwater Stream. *Journal of Sustainable Water in the Built Environment*, *7*(1), 06020002. https://doi.org/10.1061/jswbay.0000928

Martin, S. L., Hayes, D. B., Kendall, A. D., & Hyndman, D. W. (2017). The land-use legacy effect: Towards a mechanistic understanding of time-lagged water quality responses to land use/cover. *Science of The Total Environment*, *579*, 1794–1803. https://doi.org/10.1016/J.SCITOTENV.2016.11.158

Martin, S. L., Hayes, D. B., Rutledge, D. T., & Hyndman, D. W. (2011). The land-use legacy effect: Adding temporal context to lake chemistry. *Limnology and Oceanography*, *56*(6), 2362–2370. https://doi.org/10.4319/LO.2011.56.6.2362

Mashaly, A. F., & Fernald, A. G. (2020). Identifying Capabilities and Potentials of System Dynamics in Hydrology and Water Resources as a Promising Modeling Approach for Water Management. *Water 2020, Vol. 12, Page 1432*, *12*(5), 1432. https://doi.org/10.3390/W12051432

Maslow, A., & Lewis, K. J. (1987). Maslow's hierarchy of needs. *Salenger Incorporated*, *14*(17), 987–990.

McDonald, W. M., & Naughton, J. B. (2019). Stormwater management actions under regulatory pressure: a case study of southeast Wisconsin. *Journal of Environmental Planning and Management*, *0*(0), 1–22. https://doi.org/10.1080/09640568.2018.1539391

McGrane, S. J. (2016). Impacts of urbanisation on hydrological and water quality dynamics, and urban water management: a review. *Https://Doi.Org/10.1080/02626667.2015.1128084*, *61*(13), 2295–2311. https://doi.org/10.1080/02626667.2015.1128084

Mcleod, A. I., Hipei, K. W., & Bodo, B. A. (1991). Trend analysis methodology for water quality time series. *Environmetrics*, *2*(2), 169–200. https://doi.org/10.1002/ENV.3770020205

Mello, K. de, Taniwaki, R. H., Paula, F. R. de, Valente, R. A., Randhir, T. O., Macedo, D. R., Leal, C. G., Rodrigues, C. B., & Hughes, R. M. (2020). Multiscale land use impacts on water quality: Assessment, planning, and future perspectives in Brazil. *Journal of Environmental Management*, *270*, 110879. https://doi.org/10.1016/J.JENVMAN.2020.110879

Meneses, B. M., Reis, R., Vale, M. J., & Saraiva, R. (2015). Land use and land cover changes in Zêzere watershed (Portugal) — Water quality implications. *Science of The Total Environment*, *527–528*, 439–447. https://doi.org/10.1016/J.SCITOTENV.2015.04.092

Mika, M. L., Dymond, R. L., Aguilar, M. F., & Hodges, C. C. (2019). Evolution and

Application of Urban Watershed Management Planning. *JAWRA Journal of the American Water Resources Association*, *55*(5), 1216–1234. https://doi.org/10.1111/1752-1688.12765

Milleana Shaharudin, S., Andayani, S., Binatari, N., Kurniawan, A., Afdal Ahmad Basri, M., & Hila Zainuddin, N. (2020). Imputation methods for addressing missing data of monthly rainfall in Yogyakarta, Indonesia. *Researchgate.Net*, *9*, 646–651. https://doi.org/10.30534/ijatcse/2020/9091.42020

Miller, A. J., Welty, C., Duncan, J. M., Baeck, M. L., & Smith, J. A. (2021). Assessing urban rainfall-runoff response to stormwater management extent. *Hydrological Processes*, *35*(7), e14287.

Mirchi, A., & WatkinsJr., D. (2012). A Systems Approach to Holistic Total Maximum Daily Load Policy: Case of Lake Allegan, Michigan. *Journal of Water Resources Planning and Management*, *139*(5), 544–553. https://doi.org/10.1061/(ASCE)WR.1943-5452.0000292

Moriasi, D. N., Gitau, M. W., Pai, N., & Daggupati, P. (2015). Hydrologic and water quality models: Performance measures and evaluation criteria. *Transactions of the ASABE*, *58*(6), 1763–1785.

Moritz, S., & Bartz-Beielstein, T. (2017). imputeTS: Time series missing value imputation in R. *R Journal*, *9*(1), 207–218. https://doi.org/10.32614/rj-2017-009

Mueller, L. R., Donnelly, J. P., Jacobson, K. E., Carlson, J. N., Mann, N. C., & Wang, H. E. (2016). National Characteristics of Emergency Medical Services in Frontier and Remote Areas. *Https://Doi.Org/10.3109/10903127.2015.1086846*, *20*(2), 191–199. https://doi.org/10.3109/10903127.2015.1086846

Muerdter, C. P., Wong, C. K., & Lefevre, G. H. (2018). Emerging investigator series: the role of vegetation in bioretention for stormwater treatment in the built environment: pollutant removal, hydrologic function, and ancillary benefits. *Environmental Science: Water Research & Technology*, *4*(5), 592–612. https://doi.org/10.1039/C7EW00511C

Murphy, J. C. (2020). Changing suspended sediment in United States rivers and streams: Linking sediment trends to changes in land use/cover, hydrology and climate. *Hydrology and Earth System Sciences*, *24*(2), 991–1010. https://doi.org/10.5194/HESS-24-991-2020

Murphy, J., & Sprague, L. (2019). Water-quality trends in US rivers: Exploring effects from streamflow trends and changes in watershed management. *Science of the Total Environment*, *656*, 645–658. https://doi.org/10.1016/j.scitotenv.2018.11.255

Murtagh, F., & Contreras, P. (2012). Algorithms for hierarchical clustering: an overview. *Wiley Interdisciplinary Reviews: Data Mining and Knowledge Discovery*, *2*(1), 86–97.

Nation, T. H., & Johnson, L. A. (2016). Use of a Volunteer Monitoring Program to

Assess Water Quality in a TMDL Watershed Utilized for Recreational Use, Pickens County, South Carolina. *Journal of South Carolina Water Resources*, *2*(1), 11. https://doi.org/https://doi.org/10.34068/JSCWR.02.02

Naughton, J., Sharior, S., Parolari, A., Strifling, D., & McDonald, W. (2021). Barriers to Real-Time Control of Stormwater Systems. *Journal of Sustainable Water in the Built Environment*, *7*(4), 1–10. https://doi.org/10.1061/jswbay.0000961

NCSL. (2020). *State partisan composition*. State Partisan Composition. https://www.ncsl.org/research/about-state-legislatures/partisan-composition.aspx#Timelines

Neilson, B. T., & Stevens, D. K. (2002). Issues Related to the Success of the TMDL Program. *Journal of Contemporary Water Research and Education*, *122*(1), 8.

Nelson, K. C., & Palmer, M. A. (2007). Stream temperature surges under urbanization and climate change: Data, models, and responses. *Journal of the American Water Resources Association*, *43*(2), 440–452. https://doi.org/10.1111/j.1752-1688.2007.00034.x

Pachauri, R. K., & Reisinger, A. (2007). IPCC fourth assessment report. *IPCC, Geneva*, *2007*.

Pak, H. Y., Chuah, C. J., Yong, E. L., & Snyder, S. A. (2021). Effects of land use configuration, seasonality and point source on water quality in a tropical watershed: A case study of the Johor River Basin. *Science of The Total Environment*, *780*, 146661. https://doi.org/10.1016/J.SCITOTENV.2021.146661

Pandey, S., Kumari, N., & Al Nawajish, S. (2023). Land Use Land Cover (LULC) and Surface Water Quality Assessment in and around Selected Dams of Jharkhand using Water Quality Index (WQI) and Geographic Information System (GIS). *Journal of the Geological Society of India*, *99*(2), 205–218. https://doi.org/10.1007/S12594-023-2288-Y/METRICS

Panthi, J., Li, F., Wang, H., Aryal, S., Dahal, P., Ghimire, S., & Kabenge, M. (2017). Evaluating climatic and non-climatic stresses for declining surface water quality in Bagmati River of Nepal. *Environmental Monitoring and Assessment*, *189*(6). https://doi.org/10.1007/S10661-017-6000-9

Papenfus, M. (2019). Do housing prices reflect water quality impairments? Evidence from the Puget Sound. *Water Resources and Economics*, *27*, 100133.

Parolari, A. J., Sizemore, J., & Katul, G. G. (2021). Multiscale Legacy Responses of Soil Gas Concentrations to Soil Moisture and Temperature Fluctuations. *Journal of Geophysical Research: Biogeosciences*, *126*(2), e2020JG005865. https://doi.org/10.1029/2020JG005865

Pasquini, A. I., & Depetris, P. J. (2007). Discharge trends and flow dynamics of South American rivers draining the southern Atlantic seaboard: An overview. *Journal of Hydrology*, *333*(2–4), 385–399. https://doi.org/10.1016/J.JHYDROL.2006.09.005

Patra, R. W., Chapman, J. C., Lim, R. P., Gehrke, P. C., & Sunderam, R. M. (2015). Interactions between water temperature and contaminant toxicity to freshwater fish. *Environmental Toxicology and Chemistry*, *34*(8), 1809–1817.

Paudel, J., & Crago, C. L. (2021). Environmental Externalities from Agriculture: Evidence from Water Quality in the United States. *American Journal of Agricultural Economics*, *103*(1), 185–210. https://doi.org/10.1111/AJAE.12130

Persaud, P. P., Hathaway, J. M., Kerkez, B., & Mccarthy, D. T. (2022). *Hydrologic and Water Quality Implications of Real-Time Control Schemes in Bioretention*. https://doi.org/10.1177/088541202400903563

Phan, T. D., Bertone, E., & Stewart, R. A. (2021). Critical review of system dynamics modelling applications for water resources planning and management. *Cleaner Environmental Systems*, *2*, 100031. https://doi.org/10.1016/J.CESYS.2021.100031

Picksley, J., & Deletic, A. (1999). The Thermal Enrichment of Storm Runoff from Paved Areas-a Statistical Analysis. *Article in Journal of Water Management Modeling*, 204–211. https://doi.org/10.14796/JWMM.R204-07

Poresky, A., Bracken, C., Strecker, E., & Clary, J. (2012). *Expanded Analysis of Volume Reduction in Bioretention BMPs*. *January 2011*, 48.

Poresky, A., Clary, J., Strecker, E., & Earles, A. (2011). *International Stormwater Best Management Practices (BMP) Database Technical Summary: Volume Reduction*. *January*, International Stormwater BMP Database.

Prathumratana, L., Sthiannopkao, S., & Kim, K. W. (2008). The relationship of climatic and hydrological parameters to surface water quality in the lower Mekong River. *Environment International*, *34*(6), 860–866. https://doi.org/10.1016/J.ENVINT.2007.10.011

Prey, J., Chern, L., Holaday, S., Johnson, C., Donovan, T., & Mather, P. (1995). *The Wisconsin Stormwater Manual*. https://dnr.wi.gov/topic/stormwater/documents/StormwaterManual1-Overview.pdf

Procházka, J., Pokorný, J., Vácha, A., Novotná, K., & Kobesová, M. (2019). Land cover effect on water discharge, matter losses and surface temperature: Results of 20 years monitoring in the Šumava Mts. *Ecological Engineering*, *127*, 220–234. https://doi.org/10.1016/J.ECOLENG.2018.11.030

Public Participation in Listing Impaired Waters and the TMDL Process | US EPA. (2022). EPA. https://www.epa.gov/tmdl/public-participation-listing-impaired-waters-and-tmdl-process

Purdy, A. J., Fisher, J. B., Goulden, M. L., & Famiglietti, J. S. (2016). Ground heat flux: An analytical review of 6 models evaluated at 88 sites and globally. *Journal of Geophysical Research: Biogeosciences*, *121*(12), 3045–3059. https://doi.org/10.1002/2016JG003591

Purvis, R. A., Winston, R. J., Hunt, W. F., Lipscomb, B., Narayanaswamy, K., McDaniel,

A., Lauffer, M. S., & Libes, S. (2019). Evaluating the Hydrologic Benefits of a Bioswale in Brunswick County, North Carolina (NC), USA. *Water 2019, Vol. 11, Page 1291*, *11*(6), 1291. https://doi.org/10.3390/W11061291

PWD. (2020). *Green stormwater infrastructure monitoring*.

Quigley, M., & Brown, C. (2014). *Transforming Our Cities : High-Performance Green Infrastructure*.

Quinn, N. W. T., Kumar, S., & Imen, S. (2019). Overview of Remote Sensing and GIS Uses in Watershed and TMDL Analyses. *Journal of Hydrologic Engineering*, *24*(4). https://doi.org/10.1061/(asce)he.1943-5584.0001742

Quinn, N. W. T., Kumar, S., La Plante, R., & Cubas, F. (2019). Tool for Searching USEPA's TMDL Reports Repository to Analyze TMDL Modeling State of the Practice. *Journal of Hydrologic Engineering*, *24*(9), 1–11. https://doi.org/10.1061/(asce)he.1943-5584.0001805

Rahman, M. A., Moser, A., Rötzer, T., & Pauleit, S. (2019). Comparing the transpirational and shading effects of two contrasting urban tree species. *Urban Ecosystems*, *22*(4), 683–697. https://doi.org/10.1007/S11252-019-00853-X/METRICS

Regier, E., & McDonald, W. (2022). Hydrologic and Water Quality Performance of Two Bioswales at an Urban Farm. *Journal of Sustainable Water in the Built Environment*, *8*(3), 5022004.

Reilly, J. A., & Piechota, T. C. (2005). Actual Storm Events Outperform Synthetic Design Storms: A Review of SCS Curve Number Applicability. *World Water Congress 2005: Impacts of Global Climate Change - Proceedings of the 2005 World Water and Environmental Resources Congress*, 1–13. https://doi.org/10.1061/40792(173)95

Richardson, S. D., & Ternes, T. A. (2018). Water Analysis: Emerging Contaminants and Current Issues. *Analytical Chemistry*, *90*(1), 398–428. https://doi.org/10.1021/ACS.ANALCHEM.7B04577

Risal, A., Parajuli, P. B., Dash, P., Ouyang, Y., & Linhoss, A. (2020). Sensitivity of hydrology and water quality to variation in land use and land cover data. *Agricultural Water Management*, *241*, 106366. https://doi.org/10.1016/J.AGWAT.2020.106366

Ritchie, H., & Roser, M. (2018). *Urbanization*. OurWorldInData.Org. https://ourworldindata.org/urbanization

Ritter, W. F. (2019). Progress on the Chesapeake Bay TMDL and Challenges in Meeting the 2025 Pollution-Reduction Loads. *World Environmental and Water Resources Congress 2019: Watershed Management, Irrigation and Drainage, and Water Resources Planning and Management - Selected Papers from the World Environmental and Water Resources Congress 2019*, 63–70.

https://doi.org/10.1061/9780784482339.006

Romshoo, S. A., Bhat, S. A., & Rashid, I. (2012). Geoinformatics for assessing the morphometric control on hydrological response at watershed scale in the Upper Indus Basin. *Journal of Earth System Science 2012 121:3*, *121*(3), 659–686. https://doi.org/10.1007/S12040-012-0192-8

Rozemeijer, J. C., Klein, J., Broers, H. P., van Tol-Leenders, T. P., & van der Grift, B. (2014). Water quality status and trends in agriculture-dominated headwaters; a national monitoring network for assessing the effectiveness of national and European manure legislation in The Netherlands. *Environmental Monitoring and Assessment*, *186*(12), 8981–8995. https://doi.org/10.1007/s10661-014-4059-0

Ryberg, K. R., & Chanat, J. G. (2022). Climate extremes as drivers of surface-water-quality trends in the United States. *Science of The Total Environment*, *809*, 152165. https://doi.org/10.1016/J.SCITOTENV.2021.152165

Sambito, M., Severino, A., Freni, G., & Neduzha, L. (2021). A systematic review of the hydrological, environmental and durability performance of permeable pavement systems. *Sustainability (Switzerland)*, *13*(8). https://doi.org/10.3390/su13084509

Schilling, K. E., Jha, M. K., Zhang, Y.-K. Y.-K., Gassman, P. W., Wolter, C. F., Schilling, C. :, Jha, M. K., Zhang, Y.-K. Y.-K., Gassman, P. W., & Wolter, C. F. (2008). Impact of land use and land cover change on the water balance of a large agricultural watershed: Historical effects and future directions. *Water Resources Research*, *44*(7), 0–09. https://doi.org/10.1029/2007WR006644

Schueler, T. R., Fraley-McNeal, L., & Cappiella, K. (2009). Is Impervious Cover Still Important? Review of Recent Research. *Journal of Hydrologic Engineering*, *14*(4), 309–315. https://doi.org/10.1061/(ASCE)1084-0699(2009)14:4(309)

Shah, H. L., Zhou, T., Huang, M., & Mishra, V. (2019). Strong Influence of Irrigation on Water Budget and Land Surface Temperature in Indian Subcontinental River Basins. *Journal of Geophysical Research: Atmospheres*, *124*(3), 1449–1462. https://doi.org/10.1029/2018JD029132

Shehab, Z. N., Jamil, N. R., Aris, A. Z., & Shafie, N. S. (2021). Spatial variation impact of landscape patterns and land use on water quality across an urbanized watershed in Bentong, Malaysia. *Ecological Indicators*, *122*, 107254. https://doi.org/10.1016/J.ECOLIND.2020.107254

Shen, P., Deletic, A., Bratieres, K., & McCarthy, D. T. (2020). Real time control of biofilters delivers stormwater suitable for harvesting and reuse. *Water Research*, *169*, 115257. https://doi.org/10.1016/J.WATRES.2019.115257

Shetty, N. H., Wang, M., & Culligan, P. (2022). *Studying the hydrological performance of a rainwater harvesting cistern with real time control collecting stormwater runoff from a green roof*. www.optirtc.com

Shi, P. J., Yuan, Y., Zheng, J., Wang, J. A., Ge, Y., & Qiu, G. Y. (2007). The effect of

land use/cover change on surface runoff in Shenzhen region, China. *Catena*, *69*(1), 31–35. https://doi.org/10.1016/J.CATENA.2006.04.015

Shi, P., Zhang, Y., Li, Z., Li, P., & Xu, G. (2017). Influence of land use and land cover patterns on seasonal water quality at multi-spatial scales. *CATENA*, *151*, 182–190. https://doi.org/10.1016/J.CATENA.2016.12.017

Shoda, M. E., Sprague, L. A., Murphy, J. C., & Riskin, M. L. (2019). Water-quality trends in U.S. rivers, 2002 to 2012: Relations to levels of concern. *Science of the Total Environment*, *650*, 2314–2324. https://doi.org/10.1016/j.scitotenv.2018.09.377

Shuster, W. D., Bonta, J., Thurston, H., Warnemuende, E., & Smith, D. R. (2007). Impacts of impervious surface on watershed hydrology: A review. *Http://Dx.Doi.Org/10.1080/15730620500386529*, *2*(4), 263–275. https://doi.org/10.1080/15730620500386529

Simmons, D. L., & Reynolds, R. J. (1982). Effects of urbanization on base flow of selected south-shore streams, Long Island, New York. *JAWRA Journal of the American Water Resources Association*, *18*(5), 797–805. https://doi.org/10.1111/J.1752-1688.1982.TB00075.X

Skvarciany, V., Jurevičiene, D., & Volskyte, G. (2020). Assessment of Sustainable Socioeconomic Development in European Union Countries. *Sustainability 2020, Vol. 12, Page 1986*, *12*(5), 1986. https://doi.org/10.3390/SU12051986

Sleeter, B. M., Sohl, T. L., Loveland, T. R., Auch, R. F., Acevedo, W., Drummond, M. A., Sayler, K. L., & Stehman, S. V. (2013). Land-cover change in the conterminous United States from 1973 to 2000. *Global Environmental Change*, *23*(4), 733–748. https://doi.org/10.1016/j.gloenvcha.2013.03.006

Slota, S. C. (2021). Bootstrapping the Boundary between Research and Environmental Management: The TMDL as a Point of Engagement between Science and Governance. *Science Technology and Human Values*, *47*(4), 750–773. https://doi.org/10.1177/01622439211026364

Smith, A. (2018). Trump's EPA Makeover Could Put Regional Offices on Shorter Leash. *Bloomberg Law*. https://news.bloomberglaw.com/environment-and-energy/trumps-epa-makeover-could-put-regional-offices-on-shorter-leash

Smith, J., Welsh, S. A., Anderson, J. T., Fortney, R. H., & Virginia, W. (2015). *Water Quality Trends in the Blackwater River Watershed , West Virginia*. *14*(7), 103–111.

Sowah, R. A., Bradshaw, K., Snyder, B., Spidle, D., & Molina, M. (2020). Evaluation of the soil and water assessment tool (SWAT) for simulating E. coli concentrations at the watershed-scale. *Science of The Total Environment*, *746*, 140669. https://doi.org/10.1016/J.SCITOTENV.2020.140669

Sridharan, V. K., Kumar, S., & Kumar, S. M. (2022). Can Remote Sensing Fill the United States' Monitoring Gap for Watershed Management? *Water (Switzerland)*, *14*(13). https://doi.org/10.3390/w14131985

Sridharan, V. K., Quinn, N. W. T., Kumar, S., McCutcheon, S. C., Ahmadisharaf, E., Fang, X., Zhang, H. X., & Parker, A. (2021). Selecting Reliable Models for Total Maximum Daily Load Development: Holistic Protocol. *Journal of Hydrologic Engineering*, *26*(10), 04021031. https://doi.org/10.1061/(ASCE)HE.1943-5584.0002102

Staccione, A., Candiago, S., & Mysiak, J. (2022). Mapping a Green Infrastructure Network: a framework for spatial connectivity applied in Northern Italy. *Environmental Science & Policy*, *131*, 57–67. https://doi.org/10.1016/J.ENVSCI.2022.01.017

Stanford, B., Zavaleta, E., & Millard-Ball, A. (2018). Where and why does restoration happen? Ecological and sociopolitical influences on stream restoration in coastal California. *Biological Conservation*, *221*, 219–227. https://doi.org/10.1016/J.BIOCON.2018.03.016

Stephenson, K., Shabman, L., Shortle, J., & Easton, Z. (2022). Confronting our Agricultural Nonpoint Source Control Policy Problem. *Journal of the American Water Resources Association*, *58*(4), 496–501. https://doi.org/10.1111/1752-1688.13010

Stets, E. G., Sprague, L. A., Oelsner, G. P., Johnson, H. M., Murphy, J. C., Ryberg, K., Vecchia, A. V., Zuellig, R. E., Falcone, J. A., & Riskin, M. L. (2020). Landscape Drivers of Dynamic Change in Water Quality of U.S. Rivers. *Environmental Science and Technology*, *54*(7), 4336–4343. https://doi.org/10.1021/ACS.EST.9B05344/SUPPL_FILE/ES9B05344_SI_001.PDF

Stoker, P., Albrecht, T., Follingstad, G., & Carlson, E. (2022). Integrating Land Use Planning and Water Management in U.S. Cities: A Literature Review. *Journal of the American Water Resources Association*, *58*(3), 321–335. https://doi.org/10.1111/1752-1688.13022

Strosnider, H., Kennedy, C., Monti, M., & Yip, F. (2017). Rural and Urban Differences in Air Quality, 2008–2012, and Community Drinking Water Quality, 2010–2015 — United States. *MMWR Surveillance Summaries*, *66*(13), 1. https://doi.org/10.15585/MMWR.SS6613A1

Talukdar, S., Singha, P., Mahato, S., Shahfahad, Pal, S., Liou, Y. A., & Rahman, A. (2020). Land-Use Land-Cover Classification by Machine Learning Classifiers for Satellite Observations—A Review. *Remote Sensing 2020, Vol. 12, Page 1135*, *12*(7), 1135. https://doi.org/10.3390/RS12071135

Tarr, J. (1996). *The search for the ultimate sink: urban pollution in historical perspective*. The University of Akron Press. https://muse.jhu.edu/book/4186/

Tasdighi, A., Arabi, M., & Osmond, D. L. (2017). The Relationship between Land Use and Vulnerability to Nitrogen and Phosphorus Pollution in an Urban Watershed. *Journal of Environmental Quality*, *46*(1), 113–122. https://doi.org/10.2134/JEQ2016.06.0239

Theobald, D. M. (2005). Landscape patterns of exurban growth in the USA from 1980 to 2020. *Ecology and Society*, *10*(1). https://doi.org/10.5751/ES-01390-100132

Timm, A., Ouellet, V., & Daniels, M. (2020). Swimming through the urban heat island: Can thermal mitigation practices reduce the stress? *River Research and Applications*, *36*(10), 1973–1984. https://doi.org/10.1002/rra.3732

Tiyasha, Tung, T. M., & Yaseen, Z. M. (2020). A survey on river water quality modelling using artificial intelligence models: 2000–2020. *Journal of Hydrology*, *585*, 124670. https://doi.org/10.1016/J.JHYDROL.2020.124670

Tu, J. (2011). Spatially varying relationships between land use and water quality across an urbanization gradient explored by geographically weighted regression. *Applied Geography*, *31*(1), 376–392.

Tu, J. (2013). Spatial variations in the relationships between land use and water quality across an urbanization gradient in the watersheds of northern Georgia, USA. *Environmental Management*, *51*(1), 1–17. https://doi.org/10.1007/S00267-011-9738-9/FIGURES/5

Uddin, M. G., Nash, S., Rahman, A., & Olbert, A. I. (2023). A novel approach for estimating and predicting uncertainty in water quality index model using machine learning approaches. *Water Research*, *229*, 119422. https://doi.org/10.1016/J.WATRES.2022.119422

Ullah, K. A., Jiang, J., & Wang, P. (2018). Land use impacts on surface water quality by statistical approaches. *Global J. Environ. Sci. Manage*, *4*(2), 231–250. https://doi.org/10.22034/gjesm.2018.04.02.010

Vercruysse, K., Grabowski, R. C., & Rickson, R. J. (2017). Suspended sediment transport dynamics in rivers: Multi-scale drivers of temporal variation. *Earth-Science Reviews*, *166*, 38–52. https://doi.org/10.1016/J.EARSCIREV.2016.12.016

von Storch, H. (1999). Misuses of Statistical Analysis in Climate Research. *Analysis of Climate Variability*, 11–26. https://doi.org/10.1007/978-3-662-03744-7_2

Vrebos, D., Beauchard, O., & Meire, P. (2017). The impact of land use and spatial mediated processes on the water quality in a river system. *Science of The Total Environment*, *601–602*, 365–373. https://doi.org/10.1016/J.SCITOTENV.2017.05.217

Wadzuk, B. M., Lewellyn, C., Lee, R., & Traver, R. G. (2017). Green Infrastructure Recovery: Analysis of the Influence of Back-to-Back Rainfall Events. *Journal of Sustainable Water in the Built Environment*, *3*(1), 04017001. https://doi.org/10.1061/jswbay.0000819

Wan, R., Cai, S., Li, H., Yang, G., Li, Z., & Nie, X. (2014). Inferring land use and land cover impact on stream water quality using a Bayesian hierarchical modeling approach in the Xitiaoxi River Watershed, China. *Journal of Environmental Management*, *133*, 1–11. https://doi.org/10.1016/J.JENVMAN.2013.11.035

Wang, C., Wang, Z. H., & Yang, J. (2018). Cooling Effect of Urban Trees on the Built Environment of Contiguous United States. *Earth's Future*, *6*(8), 1066–1081. https://doi.org/10.1029/2018EF000891

Wang, G., Mang, S., Cai, H., Liu, S., Zhang, Z., Wang, L., & Innes, J. L. (2016). Integrated watershed management: evolution, development and emerging trends. *Journal of Forestry Research*, *27*(5), 967–994. https://doi.org/10.1007/S11676-016-0293-3/FIGURES/4

Wang, G., Yinglan, A., Xu, Z., & Zhang, S. (2014). The influence of land use patterns on water quality at multiple spatial scales in a river system. *Hydrological Processes*, *28*(20), 5259–5272. https://doi.org/10.1002/hyp.10017

Wang, J., & Banzhaf, E. (2018). Towards a better understanding of Green Infrastructure: A critical review. *Ecological Indicators*, *85*, 758–772. https://doi.org/10.1016/J.ECOLIND.2017.09.018

Wang, J., Bretz, M., Dewan, M. A. A., & Delavar, M. A. (2022). Machine learning in modelling land-use and land cover-change (LULCC): Current status, challenges and prospects. *Science of The Total Environment*, *822*, 153559. https://doi.org/10.1016/J.SCITOTENV.2022.153559

Wang, L., Han, X., Zhang, Y., Zhang, Q., Wan, X., Liang, T., Song, H., Bolan, N., Shaheen, S. M., White, J. R., & Rinklebe, J. (2023). Impacts of land uses on spatio-temporal variations of seasonal water quality in a regulated river basin, Huai River, China. *Science of The Total Environment*, *857*, 159584. https://doi.org/10.1016/J.SCITOTENV.2022.159584

Wang, R., & Kalin, L. (2018). Combined and synergistic effects of climate change and urbanization on water quality in the Wolf Bay watershed, southern Alabama. *Journal of Environmental Sciences*, *64*, 107–121. https://doi.org/10.1016/J.JES.2016.11.021

Wang, R., Kim, J. H., & Li, M. H. (2021). Predicting stream water quality under different urban development pattern scenarios with an interpretable machine learning approach. *Science of The Total Environment*, *761*, 144057. https://doi.org/10.1016/J.SCITOTENV.2020.144057

Webster, S. E., & Dennison, W. C. (2022). Stakeholder Perspectives on the Roles of Science and Citizen Science in Chesapeake Bay Environmental Management. *Estuaries and Coasts*, *45*(8), 2310–2326. https://doi.org/10.1007/S12237-022-01106-5/METRICS

Wehrly, K. E., Wang, L., & Mitro, M. (2011). Field-Based Estimates of Thermal Tolerance Limits for Trout: Incorporating Exposure Time and Temperature Fluctuation. *Changed Publisher: Wiley*, *136*(2), 365–374. https://doi.org/10.1577/T06-163.1

Wijesiri, B., Deilami, K., & Goonetilleke, A. (2018). Evaluating the relationship between temporal changes in land use and resulting water quality. *Environmental Pollution*,

234, 480–486. https://doi.org/10.1016/J.ENVPOL.2017.11.096

Williams, D. C. (1993). *Why Are Our Regional Offices and Labs Located Where They Are? A Historical Perspective on Siting | US EPA*. https://www.epa.gov/history/why-are-our-regional-offices-and-labs-located-where-they-are-historical-perspective-siting

Wilson, C. O. (2015). Land use/land cover water quality nexus: quantifying anthropogenic influences on surface water quality. *Environmental Monitoring and Assessment*, *187*(7). https://doi.org/10.1007/S10661-015-4666-4

Winbourne, J. B., Jones, T. S., Garvey, S. M., Harrison, J. L., Wang, L., Li, D., Templer, P. H., & Hutyra, L. R. (2020). Tree Transpiration and Urban Temperatures: Current Understanding, Implications, and Future Research Directions. *BioScience*, *70*(7), 576–588. https://doi.org/10.1093/BIOSCI/BIAA055

Winkler, K., Fuchs, R., Rounsevell, M., & Herold, M. (2021). Global land use changes are four times greater than previously estimated. *Nature Communications 2021 12:1*, *12*(1), 1–10. https://doi.org/10.1038/s41467-021-22702-2

Winston, R. J., Arend, K., Dorsey, J. D., & Hunt, W. F. (2020). Water quality performance of a permeable pavement and stormwater harvesting treatment train stormwater control measure. *Blue-Green Systems*, *2*(1), 91–111. https://doi.org/10.2166/bgs.2020.914

Winston, R. J., Asce, M., Arend, K., Dorsey, J. D., Johnson, J. P., Hunt, W. F., & Wre, D. (2019). Hydrologic Performance of a Permeable Pavement and Stormwater Harvesting Treatment Train Stormwater Control Measure. *Journal of Sustainable Water in the Built Environment*, *6*(1), 04019011. https://doi.org/10.1061/JSWBAY.0000889

WinTR-55 User Manual. (2002). USDA Natural Resource Conservation Service. https://www.hydrocad.net/tr-55.htm

Wisconsin Department of Natural Resources. (2017). *Clean Water Act Water Quality Plans and Reports | Targeted Assessments of Wisconsin Water Resources | Wisconsin DNR*. https://dnr.wisconsin.gov/topic/SurfaceWater/wqmplan

Woods, N. D. (2021). Regulatory competition, administrative discretion, and environmental policy implementation. *Review of Policy Research*, *March*, 486–511. https://doi.org/10.1111/ropr.12461

Woznicki, S. A., Hondula, K. L., & Jarnagin, S. T. (2018). Effectiveness of landscape-based green infrastructure for stormwater management in suburban catchments. *Hydrological Processes*, *32*(15), 2346–2361. https://doi.org/10.1002/hyp.13144

Wu, J., Stewart, T. W., Thompson, J. R., Kolka, R. K., & Franz, K. J. (2015). Watershed features and stream water quality: Gaining insight through path analysis in a Midwest urban landscape, U.S.A. *Landscape and Urban Planning*, *143*, 219–229. https://doi.org/10.1016/J.LANDURBPLAN.2015.08.001

Xu, W. D., Burns, M. J., Cherqui, F., & Fletcher, T. D. (2020). Enhancing stormwater control measures using real-time control technology: a review. Urban Water Journal,. *Urban Water Journal*, *18*(2), 101–114. https://sci-hub.se/10.1080/1573062X.2020.1857797

Yao, S., Chen, C., He, M., Cui, Z., Mo, K., Pang, R., & Chen, Q. (2023). Land use as an important indicator for water quality prediction in a region under rapid urbanization. *Ecological Indicators*, *146*, 109768. https://doi.org/10.1016/J.ECOLIND.2022.109768

Yao, Y., Li, J., lv, P., Li, N., & Jiang, C. (2022). Optimizing the layout of coupled grey-green stormwater infrastructure with multi-objective oriented decision making. *Journal of Cleaner Production*, *367*, 133061. https://doi.org/10.1016/J.JCLEPRO.2022.133061

Yazdanfar, Z., & Sharma, A. (2015). Urban drainage system planning and design – challenges with climate change and urbanization: a review. *Water Science and Technology*, *72*(2), 165–179. https://doi.org/10.2166/WST.2015.207

Yoder, L., Ward, A. S., Spak, S., & Dalrymple, K. E. (2021). Local Government Perspectives on Collaborative Governance: A Comparative Analysis of Iowa's Watershed Management Authorities. *Policy Studies Journal*, *49*(4), 1087–1109. https://doi.org/10.1111/PSJ.12389

Younos, T., Lee, J., & Parece, T. (2019). Twenty-first century urban water management: the imperative for holistic and cross-disciplinary approach. *Journal of Environmental Studies and Sciences*, *9*(1), 90–95. https://doi.org/10.1007/S13412-018-0524-3/METRICS

Zahn, E., Welty, C., Smith, J. A., Kemp, S. J., Baeck, M. L., & Bou-Zeid, E. (2021). The Hydrological Urban Heat Island: Determinants of Acute and Chronic Heat Stress in Urban Streams. *Journal of the American Water Resources Association*, *57*(6), 941–955. https://doi.org/10.1111/1752-1688.12963

Zaidel, P. (2018). Impacts of Small, Surface-Release Dams on Stream Temperature and Dissolved Oxygen in Massachusetts. *Masters Theses*. https://doi.org/https://doi.org/10.7275/11948958

Zeiger, S. J., & Hubbart, J. A. (2015). Urban stormwater temperature surges: A central US watershed study. *Hydrology*, *2*(4), 193–209.

Zhang, F., Wang, J., & Wang, X. (2018). Recognizing the Relationship between Spatial Patterns in Water Quality and Land-Use/Cover Types: A Case Study of the Jinghe Oasis in Xinjiang, China. *Water 2018, Vol. 10, Page 646*, *10*(5), 646. https://doi.org/10.3390/W10050646

Zhang, J., & Peralta, R. C. (2019). Estimating infiltration increase and runoff reduction due to green infrastructure. *Journal of Water and Climate Change*, *10*(2). https://doi.org/10.2166/wcc.2018.354

Zhang, Y. K., & Schilling, K. E. (2006). Increasing streamflow and baseflow in Mississippi River since the 1940 s: Effect of land use change. *Journal of Hydrology*, *324*(1–4), 412–422. https://doi.org/10.1016/J.JHYDROL.2005.09.033

Zuo, Q., Chen, H., Dou, M., Zhang, Y., & Li, D. (2015). Experimental analysis of the impact of sluice regulation on water quality in the highly polluted Huai River Basin, China. *Environmental Monitoring and Assessment 2015 187:7*, *187*(7), 1–15. https://doi.org/10.1007/S10661-015-4642-Z

Zwickl, K., Ash, M., & Boyce, J. K. (2014). Regional variation in environmental inequality: Industrial air toxics exposure in U.S. cities. *Ecological Economics*, *107*, 494–509. https://doi.org/10.1016/J.ECOLECON.2014.09.013

APPENDICES

1. SUPPORTING DOCUMENTS FOR OBJECTIVE 1

Imputation of water quality data:

Imputation methods were applied to fill in missing data gaps in the data sets over the continuous 9-year period of record. However, several data sets were removed from the analysis due to more than 40% missing data over the study period (2008-2016). This resulted in 52, 58, 46, and 51 gages for discharge, turbidity, dissolved oxygen, and specific conductance, respectively. Out of these, 8 (discharge), 56 (turbidity), 44 (dissolved oxygen), and 49 (specific conductance) data sets had at least some missing data that needed to be filled in using imputation methods. This is summarized in Table A 1-1, which illustrates that the average gap size ranged between 4.3 and 9.7 days.

Table A 1-1. Summary of the data gap in days for each stream gage measurement. Discharge – $ft^3s^{-1}mile^{-2}$, Dissolved Oxygen – mg/l, Specific Conductance - $\mu S\ cm^{-1}$ @ 25 Celsius, Turbidity - FNU

STATISTIC	DISCHARGE	TURBIDITY	DO	SPCOND
MEAN	9.7	4.3	8.6	6.3
MEDIAN	2	3	2	2
STD. DEV.	40.9	12.9	36.5	20.6
SKEWNESS	6.9	25.7	20.1	9.1
MINIMUM	1	1	1	1
MAXIMUM	367	509	981	354

These mean gap values in Table A 1-1 were then used to test the different imputations methods on complete data sets. The error associated with each imputation method as a function of the number of missing days percentage is illustrated in Figure A

1-1. This figure shows the Mean Absolute Error (MAE) for the best four imputation methods for Discharge at a gage with complete data. As illustrated, the Kalman Smoothing method produced the lowest error among all four imputation methods. Kalman smoothing method was also found to be the best method for imputation for all water quality and quantity parameters; therefore, it was used to fill in missing data within the gages. This technique is commonly used in hydrological studies as it has been found to give optimum results in time-series data imputation (Afrifa-Yamoah et al., 2020).

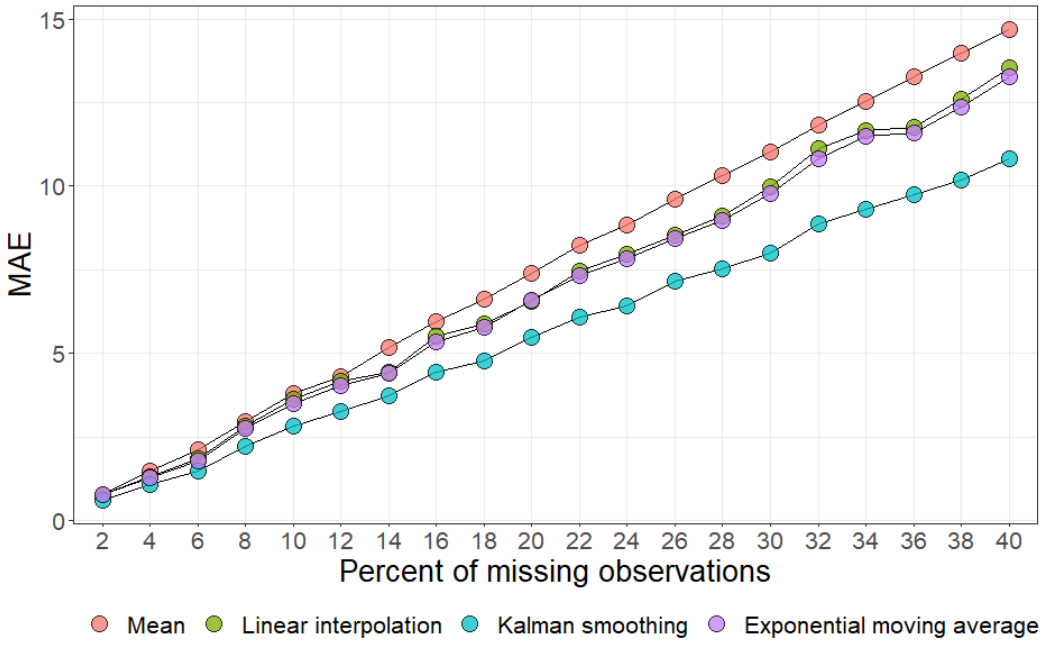

Figure A 1-1. Example of Absolute mean Error values (ft^3s^{-1}) for the four best imputation methods tested on Discharge data of a single gage.

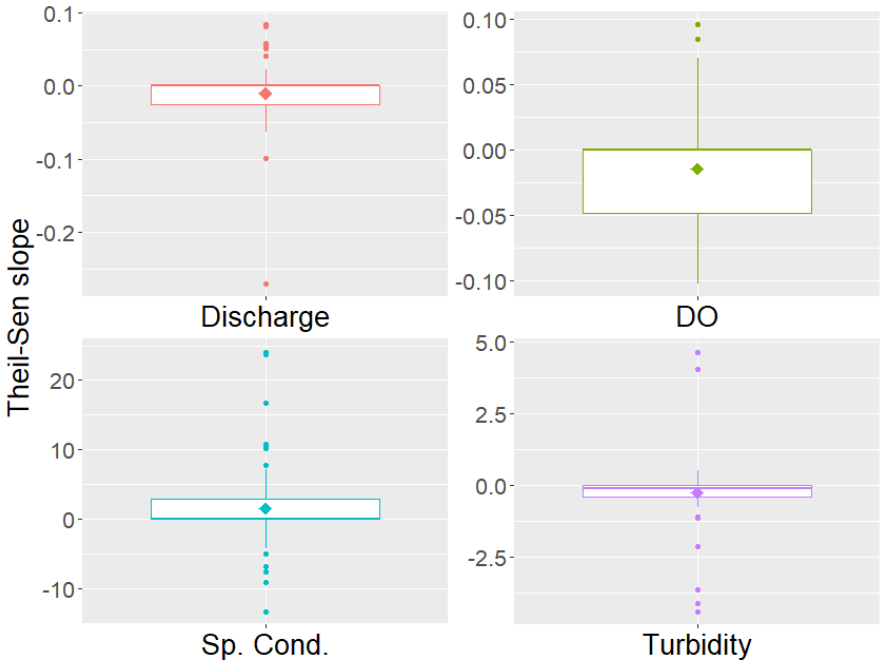

Figure A 1-2. Theil-Sen slope distribution for all gages analyzed. Due to more than 50% of the gages having no significant (at $p<0.1$) water quality changes over time, the distribution is skewed towards zero, yet the same overall observations in the averages are being seen. Discharge – $ft^3s^{-1}mile^{-2}$, Dissolved Oxygen – mg/l, Specific Conductance - $\mu S\ cm^{-1}$ @ 25 Celsius, Turbidity - FNU

Table A 1-2. All Theil Sen slopes (per month) and their p values for each gage and water quality parameters and discharge. Discharge – $ft^3s^{-1}mile^{-2}$, Dissolved Oxygen – mg/l, Specific Conductance - $\mu S\ cm^{-1}$ @ 25 Celsius, Turbidity - FNU

State	Turbidity		Discharge		Dissolved Oxygen		Specific Conductance	
	p	Theil Sen slope	p	Theil Sen slope	p	Theil Sen slope	p	Theil Sen slope
01408029 NJ	0.000	-0.624	0.050	-0.032	NA	NA	0.000	7.150
01463500 NJ	0.000	-0.435	0.001	-0.099	0.125	-0.029	0.001	4.500
01472157 PA	0.020	-0.253	0.000	-0.064	NA	NA	NA	NA
01473169 PA	0.003	-0.388	0.044	-0.032	NA	NA	NA	NA
01480300 PA	0.000	-1.154	0.004	-0.061	NA	NA	NA	NA
01480617 PA	0.001	-0.489	0.076	-0.033	0.000	0.085	0.000	10.536
01480870 PA	0.006	-0.327	0.012	-0.056	0.786	0.007	0.000	10.188
01481000 PA	0.086	-0.273	0.003	-0.056	0.833	-0.012	0.000	7.819
01569460 PA	0.000	0.242	0.000	-0.271	NA	NA	NA	NA
01608500 WV	0.833	0.016	0.786	-0.003	0.002	-0.048	0.527	0.614
01649190 MD	0.741	-0.081	0.609	0.014	0.252	-0.012	0.000	16.788
02110400 SC	0.292	0.190	0.000	0.041	0.416	-0.043	0.321	-3.479
02110500 SC	0.265	-0.108	0.000	0.084	0.012	-0.091	0.000	-5.027
02110701 SC	0.000	-1.095	0.489	-0.051	0.050	-0.098	0.002	-4.288
02110704 SC	0.001	-0.164	0.000	0.082	0.028	-0.053	0.000	-6.798
02203603 GA	0.125	-0.281	0.976	-0.001	0.786	-0.005	0.652	-0.475
02203655 GA	0.880	-0.037	0.086	0.051	0.434	-0.017	0.567	0.397
02203700 GA	0.489	-0.172	0.265	0.025	0.058	-0.048	0.000	-3.046
02335000 GA	0.567	-0.163	0.001	0.051	NA	NA	0.000	1.137
02336000 GA	0.696	0.094	0.005	0.054	NA	NA	0.000	-2.288
02336120 GA	0.833	0.084	0.527	0.021	0.857	0.004	0.928	0.035
02336240 GA	0.527	0.090	0.452	0.024	0.976	-0.002	0.366	0.463
02336300 GA	0.383	0.121	0.383	0.023	0.321	-0.015	0.696	-0.487
02336313 GA	0.125	0.144	0.416	0.016	0.508	-0.009	0.006	-3.422
02336360 GA	0.140	-0.211	0.452	-0.017	0.588	0.011	0.000	1.347
02336410 GA	0.157	-0.253	0.321	0.023	0.718	-0.006	0.000	1.411
02336526 GA	0.050	-0.222	0.928	-0.004	0.489	-0.011	0.050	-1.480
02336728 GA	0.012	-0.475	0.176	0.021	0.035	0.028	0.508	-0.283
03254520 KY	0.004	-4.134	0.452	-0.025	0.265	-0.038	0.292	2.342
03431083 TN	0.196	0.161	NA	NA	0.810	-0.004	0.527	0.442
03527220 TN	0.609	0.082	0.567	0.012	NA	NA	NA	NA
05054000 ND	0.176	-0.196	0.002	-0.014	0.630	-0.010	0.044	-9.137
05082500 ND	0.157	-0.710	0.028	-0.007	0.527	0.024	0.000	23.680

06818000 MO	0.009	-3.659	0.452	0.001	0.351	0.019	0.000	10.758
06894000 MO	0.000	-2.137	0.001	-0.062	0.003	-0.058	0.004	5.763
06934500 MO	0.058	-4.406	0.002	-0.009	0.104	0.069	0.000	24.072
07061270 MO	0.452	0.042	1.000	0.000	0.004	0.070	0.351	1.029
07143672 KS	0.176	-0.764	0.066	-0.004	0.076	-0.056	0.321	-9.985
07144100 KS	0.038	-1.138	0.157	-0.005	0.976	0.001	0.176	-7.519
071912213 OK	0.022	0.095	0.006	-0.038	0.470	-0.012	0.001	2.873
07191222 OK	0.044	0.124	0.140	-0.024	0.399	-0.021	0.000	2.943
07263296 AR	0.050	-0.277	0.156	-0.011	0.489	-0.032	0.904	0.028
08068500 TX	0.000	4.035	0.050	0.021	0.066	-0.042	0.015	-13.278
08070200 TX	0.000	4.641	0.033	0.011	0.321	-0.012	0.033	-1.884
08155500 TX	0.000	0.174	0.000	0.059	0.004	0.096	0.005	-2.849
08181500 TX	1.000	0.025	0.741	0.001	0.253	-0.022	0.489	-3.352
08317400 NM	0.076	0.515	0.012	-0.002	0.000	-0.102	1.000	0.049
09406000 UT	0.696	-1.533	0.696	0.000	0.110	0.017	0.140	3.980
10346000 CA	0.001	0.155	0.125	-0.010	NA	NA	NA	NA
11501000 OR	0.066	-0.228	1.000	0.000	NA	NA	NA	NA
11502500 OR	0.292	-0.036	0.489	-0.001	NA	NA	NA	NA
14206950 OR	0.001	-0.602	0.696	-0.006	0.015	-0.044	0.292	1.017
14207200 OR	0.024	-0.145	NA	NA	0.588	-0.010	0.001	4.312
14209710 OR	0.007	-0.081	NA	NA	0.000	-0.056	0.058	0.442
14210000 OR	0.044	-0.072	0.033	-0.056	0.000	-0.084	0.007	0.367
14211010 OR	0.763	0.010	0.176	-0.038	NA	NA	0.007	0.518
14211400 OR	0.044	-0.507	0.265	-0.004	NA	NA	NA	NA
14316460 OR	0.741	-0.008	NA	NA	0.000	-0.025	0.005	0.363
14317450 OR	0.086	-0.061	NA	NA	0.000	-0.063	0.000	0.543
453004122510301 OR	0.038	-0.162	NA	NA	0.015	-0.069	0.033	-1.467
453030122560101 OR	0.000	-0.676	NA	NA	0.001	-0.060	0.265	-1.330
453040123065201 OR	0.017	-0.231	NA	NA	0.003	-0.049	0.009	1.015

Table A 1-3. All results of simple linear regression for land use changes as independent variables and water quality parameters as dependent variables. Discharge – $ft^3s^{-1}mile^{-2}$, Dissolved Oxygen – mg/l, Specific Conductance - $\mu S\ cm^{-1}$ @ 25 Celsius, Turbidity - FNU

Dependent Variable	Independent Variable	Coefficient	p stat	R2
Discharge	Open water	8.91	0.16	0.08
Discharge	Developed	0	0.75	0.00
Discharge	Barren land	-14.58	0.23	0.06
Discharge	Forest	1.62	0.13	0.06
Discharge	Shrub/Grass land	-4.55	0.01	0.26
Discharge	Cultivated	4.88	0.03	0.16
Discharge	Wetland	-17.01	0.22	0.02
Discharge	Impervious	0.81	0.79	-0.04
Dissolved Oxygen	Open water	-16.2	0.58	-0.04
Dissolved Oxygen	Developed	0	0.90	-0.05
Dissolved Oxygen	Barren land	-13.77	0.84	-0.05
Dissolved Oxygen	Forest	0	0.39	-0.01
Dissolved Oxygen	Shrub/Grass land	-0.81	0.31	0.01
Dissolved Oxygen	Cultivated	-0.81	0.64	-0.04
Dissolved Oxygen	Wetland	4.05	0.28	0.01
Dissolved Oxygen	Impervious	0.81	0.72	-0.05
Specific Conductivity	Open water	-7009.8	0.00	0.25
Specific Conductivity	Developed	426.68	0.50	-0.02
Specific Conductivity	Barren land	-5341.95	0.19	0.03
Specific Conductivity	Forest	-10.53	0.78	-0.04
Specific Conductivity	Shrub/Grass land	17.01	0.64	-0.03
Specific Conductivity	Cultivated	-589.38	0.00	0.26
Specific Conductivity	Wetland	335.34	0.27	0.01
Specific Conductivity	Impervious	85.05	0.60	-0.03
Turbidity	Open water	-110.16	0.48	-0.02
Turbidity	Developed	-20.25	0.00	0.24
Turbidity	Barren land	400.95	0.66	-0.03
Turbidity	Forest	1.62	0.71	-0.03
Turbidity	Shrub/Grass land	0.81	0.89	-0.04
Turbidity	Cultivated	95.72	0.00	0.45
Turbidity	Wetland	69.64	0.14	0.04
Turbidity	Impervious	-56.21	0.00	0.23

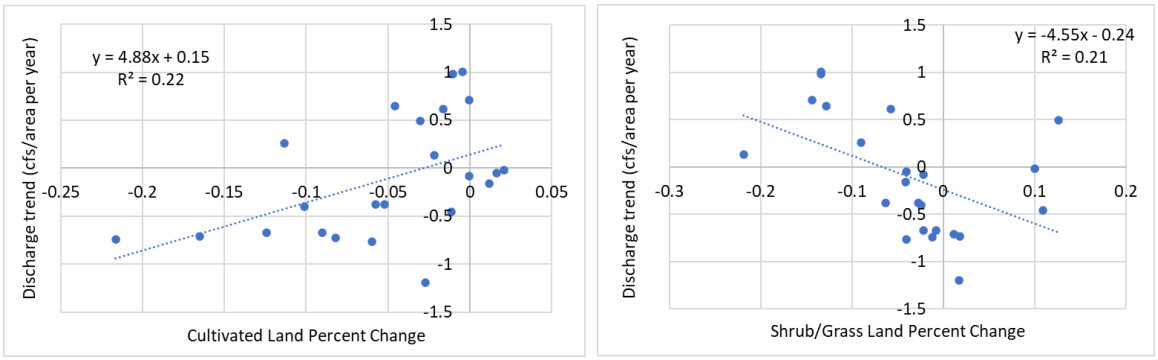

Figure A 1-3. Scatter plot and robust regression for Discharge trends as dependent variable and land use change as independent variable. Only trends with significance ($p < 0.05$) are shown.

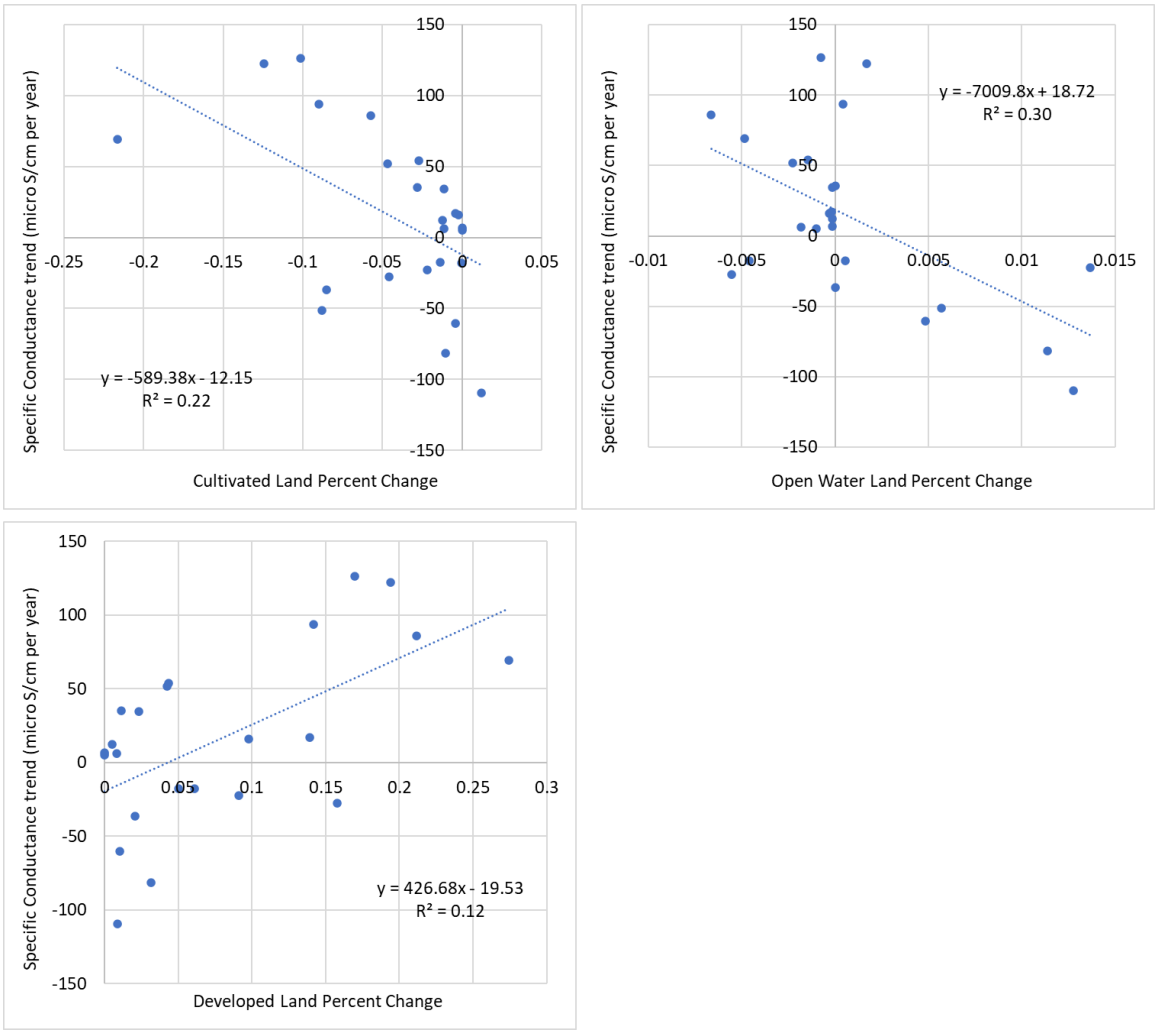

Figure A 1-4. Scatter plot and robust regression for Specific Conductance trends as dependent variable and land use change as independent variable. Only trends with significance ($p < 0.05$) are shown.

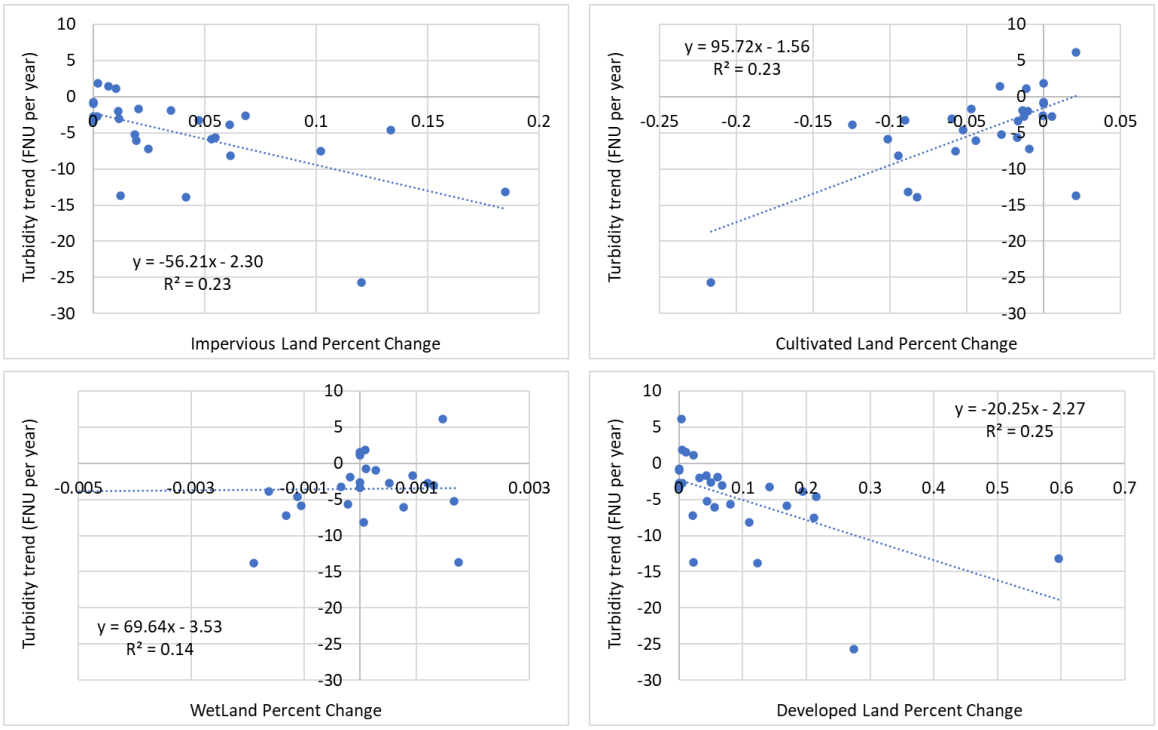

Figure A 1-5. Scatter plot and robust regression for Turbidity trends as dependent variable and land use change as independent variable. Only trends with significance ($p < 0.05$) are shown.

2. SUPPORTING DOCUMENTS FOR OBJECTIVE 2

Table A 2-1. Data used for analysis and their sources.

Data type	Source
TMDL data	https://www.epa.gov/waterdata/attains
Total stream lengths	https://www.epa.gov/waterdata/attains
EPA region	https://www.epa.gov/aboutepa/regional-and-geographic-offices
State land area	https://www.census.gov/en.html
Water area under state jurisdiction	https://www.census.gov/en.html
Average rainfall (1981 – 2010)	https://www.weather.gov/
Highest / Lowest elevation	https://www.usgs.gov/educational-resources/highest-and-lowest-elevations
Average slope of the topography	https://www.landfire.gov/slope.php
Population (2017)	https://www.census.gov/en.html
State gross domestic product (in BUSD)	https://www.census.gov/en.html
Percentage of population with no high school diploma (2017)	https://www.census.gov/en.html
Percentage of population with bachelor's degree or higher (2017)	https://www.census.gov/en.html
Per capita earnings (2017)	https://www.census.gov/en.html
Remote land percentage	https://www.ers.usda.gov/

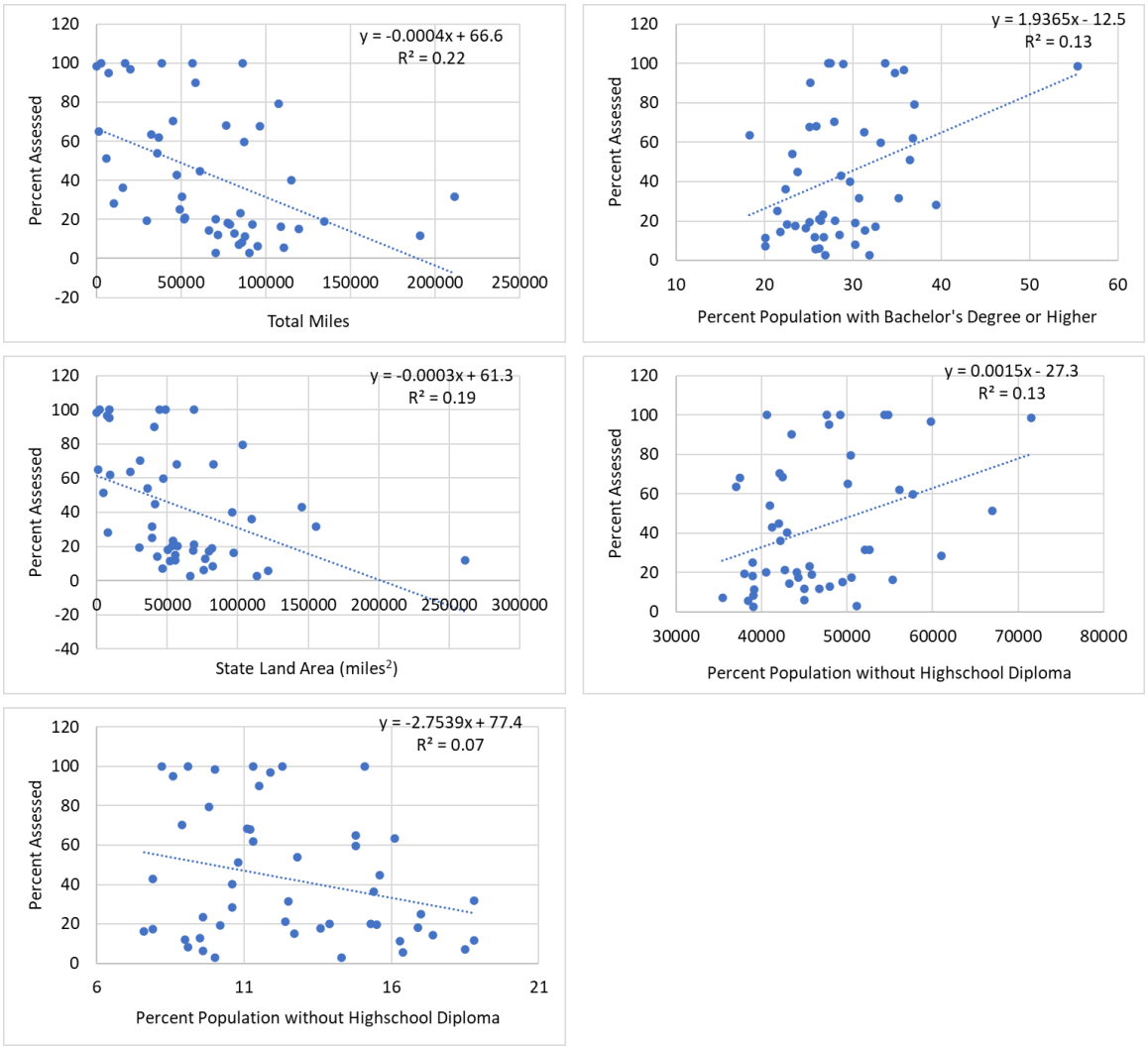

Figure A 2-1. Scatter plot and simple linear regression for Percent Assessments of rivers and streams as dependent variable and socioeconomic factors as independent variables. Only trends with significance ($p < 0.05$) are shown.

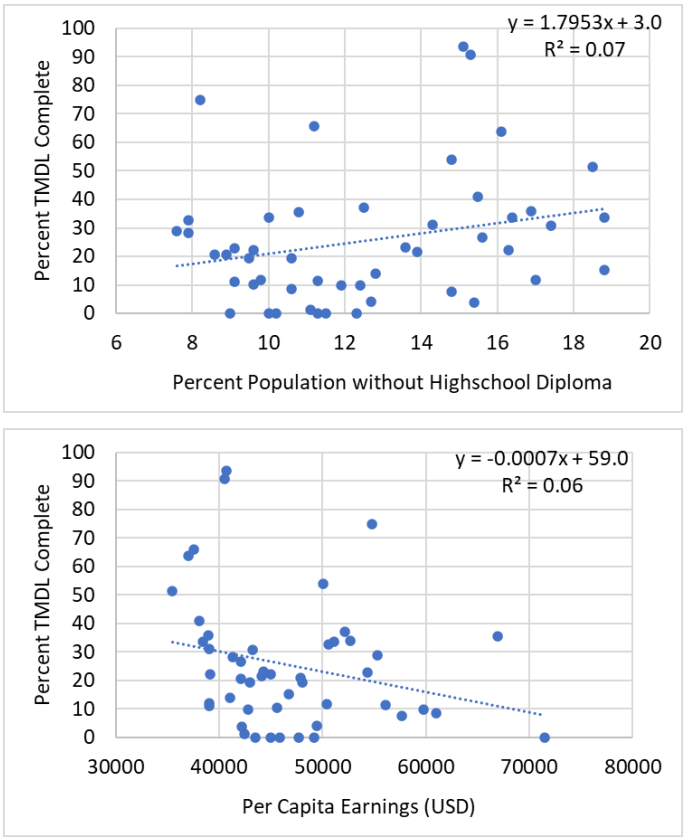

Figure A 2-2. Scatter plot and simple linear regression for Percent TMDL Completion of rivers and streams as dependent variable and socioeconomic factors as independent variables. Only trends with significance ($p < 0.05$) are shown.

3. SUPPORTING DOCUMENTS FOR OBJECTIVE 3

Table A 3-1. Volume data for each rain event. For each of the 21 rain events, the runoff volume, estimated by using rainfall (measured on site) and watershed data, and the outflow volumes measured on site for each GI practice monitored is tabulated.

			Permeable pavement		Bioswale 1		Bioswale 2	
Rain Event	Date	Event start time (HH:MM)	Runoff Volume (m^3)	Outlet volume (m^3)	Runoff Volume (m^3)	Outlet volume (m^3)	Runoff Volume (m^3)	Outlet volume (m^3)
1	6/29/2021	8:23	44.51	59.60	56.55	14.42	146.14	49.01
2	7/12/2021	14:32	7.41	0.17	8.66	1.51	13.42	1.20
3	7/14/2021	15:53	19.06	2.07	23.57	2.38	35.10	4.98
4	7/29/2021	0:53	5.41	1.07	6.15	1.09	10.67	0.83
5	8/6/2021	4:13	31.76	7.34	40.01	3.07	61.75	21.41
6	8/7/2021	19:42	174.53	118.60	225.72	120.35	523.21	267.19
7	8/9/2021	9:05	17.40	7.47	21.44	1.44	36.87	7.33
8	8/10/2021	19:32	9.21	0.98	10.95	1.23	16.86	1.49
9	8/11/2021	18:03	1.17	0.11	1.07	0.11	1.96	0.69
10	8/21/2021	5:36	8.10	1.49	9.53	0.77	15.11	1.37
11	8/24/2021	14:47	4.14	0.52	4.58	1.29	8.27	0.43
12	8/28/2021	14:51	19.81	6.40	24.55	2.31	40.59	9.47
13	9/7/2021	11:59	*	0.13	*	0.07	*	*
14	9/13/2021	3:38	*	10.47	*	7.39	*	*
15	9/21/2021	5:59	2.74	0.18	2.87	0.70	5.10	0.17
16	9/24/2021	20:47	4.27	0.45	4.73	0.79	7.90	0.18
17	10/3/2021	9:30	3.90	0.31	4.28	0.47	6.86	0.16
18	10/7/2021	11:07	18.76	2.71	23.18	1.58	34.46	1.24
19	10/11/2021	15:04	6.20	0.43	7.13	1.48	11.68	0.28
20	10/24/2021	16:16	53.11	9.36	67.72	2.48	97.99	9.87
21	10/28/2021	18:09	22.85	3.29	28.47	0.95	41.07	0.35

*gage not operational

Table A 3-2. Peak and event mean temperature for each runoff event. For each of the rain events and GIs, the observed peak temperatures and the summarized event mean temperatures for the effluents is tabulated.

			Peak Temperature (°C)			Event Mean Temperature (°C)		
Rain Event	**Date**	**Event start time (HH:MM)**	**Permeable Pavers**	**Bioswale 1**	**Bioswale 2**	**Permeable Pavers**	**Bioswale 1**	**Bioswale 2**
1	6/29/2021	8:23	28.29	24.09	21.88	25.65	20.93	21.39
2	7/12/2021	14:32	26.03	25.74	21.50	25.64	23.49	21.12
3	7/14/2021	15:53	28.99	26.52	22.74	26.19	21.88	21.78
4	7/29/2021	0:53	31.20	31.51	24.28	30.68	28.91	23.69
5	8/6/2021	4:13	31.10	28.79	25.54	30.70	23.99	24.79
6	8/7/2021	19:42	29.89	26.03	25.35	26.22	23.36	23.46
7	8/9/2021	9:05	27.60	24.48	24.19	30.70	23.40	23.67
8	8/10/2021	19:32	28.09	27.40	24.28	27.77	23.47	23.96
9	8/11/2021	18:03	27.99	27.40	24.28	27.83	24.40	24.13
10	8/21/2021	5:36	32.23	33.06	25.25	31.58	29.27	24.92
11	8/24/2021	14:47	30.80	31.82	24.96	30.43	29.69	24.79
12	8/28/2021	14:51	31.82	35.37	26.81	31.15	28.80	26.13
13	9/7/2021	11:59	28.69	27.30	*	27.16	26.43	*
14	9/13/2021	3:38	27.70	24.38	*	27.01	21.01	*
15	9/21/2021	5:59	26.91	26.71	22.74	26.71	24.65	22.47
16	9/24/2021	20:47	24.19	23.03	21.50	23.96	21.32	21.04
17	10/3/2021	9:30	25.15	24.77	21.21	25.06	23.60	21.06
18	10/7/2021	11:07	23.32	22.93	21.40	22.76	20.52	21.08
19	10/11/2021	15:04	22.93	22.17	21.02	22.78	21.23	20.84
20	10/24/2021	16:16	18.26	17.59	16.83	16.38	16.66	14.92
21	10/28/2021	18:09	16.45	16.73	15.68	16.01	15.93	14.87

4. LOW-COST ACTIVE CONTROLS TO IMPROVE VOLUME AND PEAK FLOW MITIGATION OF GREEN INFRASTRUCTURE

4.1. Introduction

Urban areas experience increased runoff due to a high amount of impervious surfaces combined with climate change that result in increasing intensity and frequency of stormwater runoff events. To address this challenge, municipalities are looking to green infrastructure as an adaptable and resilient stormwater management strategy that captures, treats, and infiltrates stormwater at the source. To that end, green infrastructure is becoming codified in many municipal stormwater programs as a requirement for new and redevelopments (City of Milwaukee, 2018). However, while green infrastructure is a prevalent approach to stormwater management, their hydrologic benefits have been difficult to quantify at the watershed scale (Bell et al., 2020; Jefferson et al., 2017; Miller et al., 2021) and models indicate that it may take significant implementation (e.g., > 20% coverage) at a high cost of time and resources before noticeable downstream impacts on hydrology are achieved (Avellaneda & Jefferson, 2020). Therefore, novel and adaptable approaches to stormwater management that can augment green infrastructure to improve performance could have significant benefits towards achieving downstream goals such as reduced peak flows, volumes, and combined sewer overflows.

An emerging technology that could address this concern is real-time control or active control of green infrastructure that uses sensors, actuators, and models to control the flow of water in stormwater systems. Real-time controls can vary from reactive controls, which use current and past information of the state of the system to make control decisions, to predictive controls, which additionally use predicted weather data to

determine how the system should react in the future. Real-time controls also include simple logistic localized controls, which are isolated from other infrastructure and are only controlled based on its own state, as well as centralized control systems, which control a network of controls using artificial intelligent algorithms to maximize overall system performance (Maiolo et al., 2020). While real-time controls have been used in industries such as waste water management (Xu et al., 2020), their application to stormwater and green infrastructure is an emerging field.

To that extent, a number of studies have demonstrated the benefits of active controls in green infrastructure such as bioretention, green roofs, and pervious pavement systems (Bryant & Wadzuk, 2017; Quigley & Brown, 2014). For example, a model of a real-time control on a green roof demonstrated an 157% increase in removed runoff volume (Bryant & Wadzuk, 2017) and modeled rain barrels with real-time control improved peak (35%) and volume (50%) reductions (Liang et al., 2019). Field applications of real-time control on a green roof and rain barrel system improved volume retention by 10% (Shetty et al., 2022). This range in volume reduction (10-157%) demonstrates the variability in performance of existing studies, which could be due to differences in control application, control logic, meteorological conditions, specific green infrastructure design specifications, geomorphological conditions, and green infrastructure type. This further highlights the need for research on real-time control applications in field studies. At a laboratory scale, column studies found that using controls to increase water retention time can improve the removal of nitrogen and ammonia while also capturing a greater volume (Persaud et al., 2022), as well as increase pathogen removal (Shen et al., 2020). Finally, at a watershed scale, modeling the

integration of grey and green infrastructure with real-time controls demonstrated robustness while being cost effective in controlling combined sewer overflows (CSOs) (Jean et al., 2021).

The studies cited demonstrate that active controls can improve green infrastructure performance to solve flooding, CSO, and water quality impairments in urban areas. However, a lack of adoption may be due to (1) a lack of field studies on the performance of real-time control of green infrastructure for meeting volume removal goals, and (2) the potential of prohibitive costs for removal goals. To that end, performance studies of real-time control of green infrastructure to date have largely been constrained to modeling scenarios that lack field validation. In addition, their application in different types of green infrastructure (e.g., permeable pavements and bioswales), with various groundwater conditions (e.g. low vs. high water tables), is underexplored. This is important for understanding the conditions and data inputs that are necessary for effectively implementing active controls in green infrastructure. In addition, even though active control of green infrastructure may have hydrologic benefits (e.g., peak flow and volume reductions), a significant limiting factor in the widescale adoption of active controls is its high cost. Many of these systems are designed as more complex controls systems, costing tens of thousands of dollars, and even the most optimistic estimates of active control of stormwater infrastructure in a mature market are $15,000 per control (Quigley and Brown, 2014). While such costs may be feasible for large green infrastructure practices such as a constructed wetland, they are prohibitive for widely adopted smaller green infrastructure practices such as green roofs, rain gardens, or pervious pavement.

To address these gaps, this study developed a low-cost power efficient active control system for green infrastructure to increase volume capture and infiltration and applied that system in three pilot green infrastructure practices. This study ***hypothesized*** that low-cost active controls could improve runoff capture and infiltration during storm events. This, in turn, would improve volume reduction of green infrastructure. To test this hypothesis, this study (1) developed low-cost active controls and tested them within a laboratory setting, (2) deployed and monitored three active controls on three green infrastructure practices in the Milwaukee area, and (3) applied the data in a model of green infrastructure that could identify the conditions under which active controls could produce the greatest benefit. The following sections contains the methods and results from the development and implementation of the active controls, as well as a discussion of the modeling results.

4.2. Study Objectives

The overarching goal of this study is to successfully implement a novel low-cost active control system for green infrastructure. The objectives to meet that goal are as follows:

(1) Develop a low-cost active control system for green infrastructure: An active control system was developed to control green infrastructure runoff during stormflow events. Components of the system design include decision algorithms for controlling flow rates, low-cost data collection hardware, actuated valves, rechargeable battery-power, and water-tight control box.

(2) Apply low-cost active control system in a green infrastructure practice and monitor performance: The low-cost active control system was deployed in three green infrastructure practices where its performance regarding volume mitigation was assessed.

(3) Model the conditions under which the developed active control system would be most appropriate for green infrastructure: Conditions to model include infiltration rates of the soil, blockage of the underdrain pipe, groundwater table levels, and extreme rainfall events.

4.3. Methods and Materials

4.3.1. Development of Real-Time Controls

A goal of the low-cost real-time controls was to reduce volumetric flow rate from green infrastructure. Therefore, reactive, localized controls were developed that used limited data inputs (water level only), as well as battery power to reduce infrastructure costs. To that end, the real-time controls were developed in the hydraulic engineering laboratory. Components of the control included (1) activated valves, (2) water level sensor (3) data collection and control hardware, (4) battery power, and (5) water-tight enclosure box. Figure A 4-1 below illustrates the valve set up within the hydraulics lab. These are butterfly valves with actuators that run on 24V DC power. In this study, valves were used from two manufacturers: Assured Automation NL series work gear actuator and COVNA electric PVC butterfly valve. The actuators are secured to a six-inch underdrain PVC pipe using an epoxy and supported using custom-built aluminum brackets. Inside of the valve is a Campbell stainless steel CS451 pressure transducer that collects water level measurements within the pipe. The valve and the pressure sensor are both connected to a Campbell CR1000X Measurement and Control Datalogger that

collects data from each device and is used to open and close the butterfly valve. Both the valve and the data logger are powered by batteries that are housed within a waterproof Pelican box (Figure A 4-2).

Figure A 4-1. Active control set-up in the laboratory. The figure on the left illustrates the activated valve connected to an underdrain and supported by aluminum legs; the picture in the center illustrates the testing apparatus of the activated valve in a hydraulic; the picture on the right illustrates the pressure transducer installed inside the 6-inch underdrain and shows the installation of the pressure transducer to measure water level within the underdrain and behind the butterfly valve.

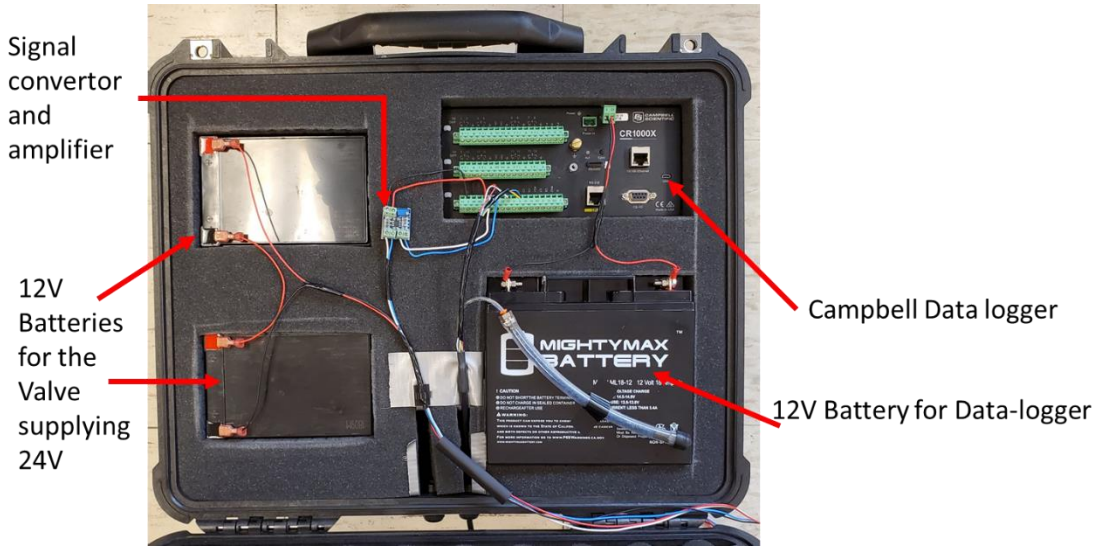

Figure A 4-2. Water-proof enclosure that houses the data collection and battery power components. These include 12V batteries in parallel to provide 24V power to the butterfly valve; a 12V batter for the measurement and control datalogger; a signal converter and amplifier; and finally, a measurement and control data logger.

Using this laboratory set-up, the components of the system were tested in the lab. To do so, the underdrain pipes (the underdrain pipe and the vertical pipe used to simulate the height of the infiltration trench) were connected to a hydraulic bench and simulated infiltration events into a green infrastructure system. In doing so, the communication and control components of the system were verified to ensure that the valve would work under expected hydraulic head conditions. The laboratory setup was also instrumental in developing and verifying the programmed algorithms to ensure they work as intended. Once the components were tested within the lab, three real-time controls were deployed into the field as discussed in the following section.

4.3.2. Site Descriptions

1. Green Alley

The first site selected is a green alley located in Wauwatosa, Wisconsin (Figure A 4-3). This green alley is composed of permeable pavers 13.6 ft across that stretch the length of the alley (415 ft). Beneath the pavers is an 8-inch base of crushed aggregate (angular ASTM No. 57), followed by a 24” subgrade crushed aggregate (angular ASTM No. 2) lined with an Ethylene Polypropylene Diene Monomer (EPDM) layer. A 6-inch perforated underdrain is located at the bottom of the trench within the crushed aggregate and runs the length of the alley and discharges into a junction box that is connected to the downstream stormwater system.

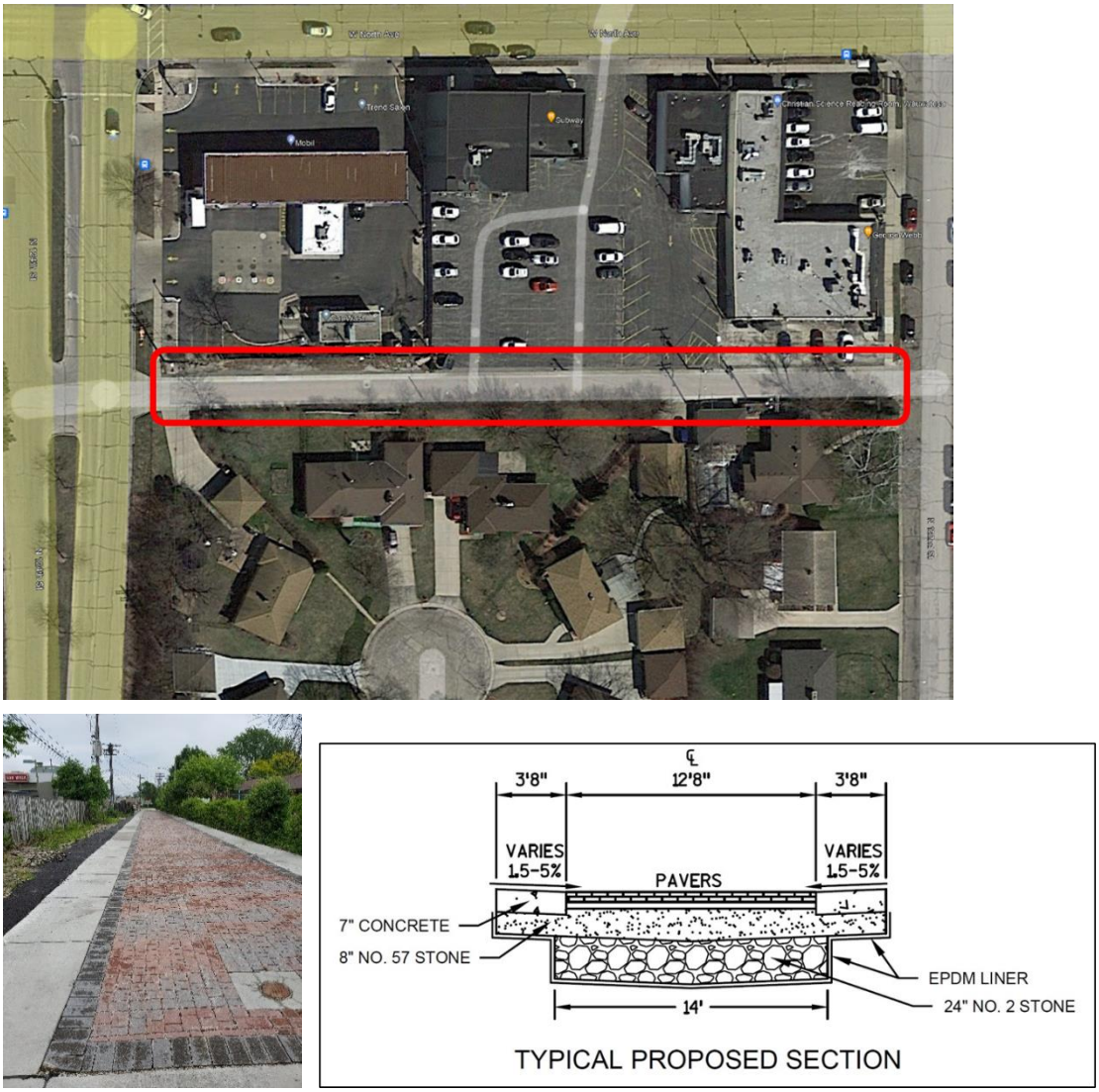

Figure A 4-3. Permeable pavers in a green alley in Wauwatosa, Wisconsin. The image on the top shows an arial image of the green alley location with the red square marking the alley; bottom left image shows the permeable pavement system at the site; the image on the right illustrates the design of the alley (source: City of Wauwatosa).

The real-time control system was attached to the underdrain of the green alley at the location of the junction box (Figure A 4-4). The system was connected to the underdrain using a flexible pipe coupling with worm clamps to ensure a watertight connection. The butterfly valve was further supported by adjustable metal legs that rested on footings on the bottom of the junction box. The box that housed the power and data

collection and control hardware was placed on a raised platform and connected to the butterfly valve. Water level was collected approximately 8 inches behind the valve using the pressure transducer. In addition, rainfall data was collected from a nearby MMSD rain gage (site WS1229).

Figure A 4-4. Active control installed at the underdrain of the green alley.

2. Bioswales

Two bioswales were selected for the real-time control systems. Both bioswales are located along Good Hope Road in Milwaukee between 60th and 76th streets (Figure A 4-5). These bioswales locations were provided by the City of Milwaukee and were selected based upon design criteria that included (1) a single source of inflow into the systems, (2) a single discharge location, and (3) an underdrain that is accessible (e.g., not located in a junction within the street) with clearance (> 12 inches) of the invert above the bottom of the junction to place the valve, and (4) a junction box big enough to house the data collection box without interfering with the hydraulics of the system. Over 20 sites were surveyed before finding the two selected sites that met these criteria.

Figure A 4-5. Locations of the bioswales (HellTy Bioswale at the entrance to Hellermann Tython headquarters; WI Club Bioswale at the entrance to Wisconsin Club county club).

The selected bioswales were constructed in 2019 and drain catchments that consist of roadway and grassed medians. The bioswales drain the roadway runoff through grade inlets in the curb that discharge into the bioswale through a rock swale. The bioswales were planted with a mix of switchgrass, purple coneflower, red hot daylily, diablo ninebark, and Zagreb coreopsis plantings. An example of the cross-section of the bioswales provided by the city of Milwaukee is illustrated in Figure A 4-6. These bioswales had a 2-inch layer of mulch above a 1.67-foot layer of engineered soil, and a 0.33-foot layer of 3/8 inch pea gravel. A 6-inch underdrain that runs the length of the bioswale was placed just below the engineered pea gravel layer and discharged into an overflow junction with a 2 ft x 2 ft overflow grate. The underdrain was also connected to an 8-inch diameter overflow standpipe placed approximately 6 inches above the soil

surface. A 1-inch crushed stone layer of 2-foot deep is located underneath the underdrain for storage.

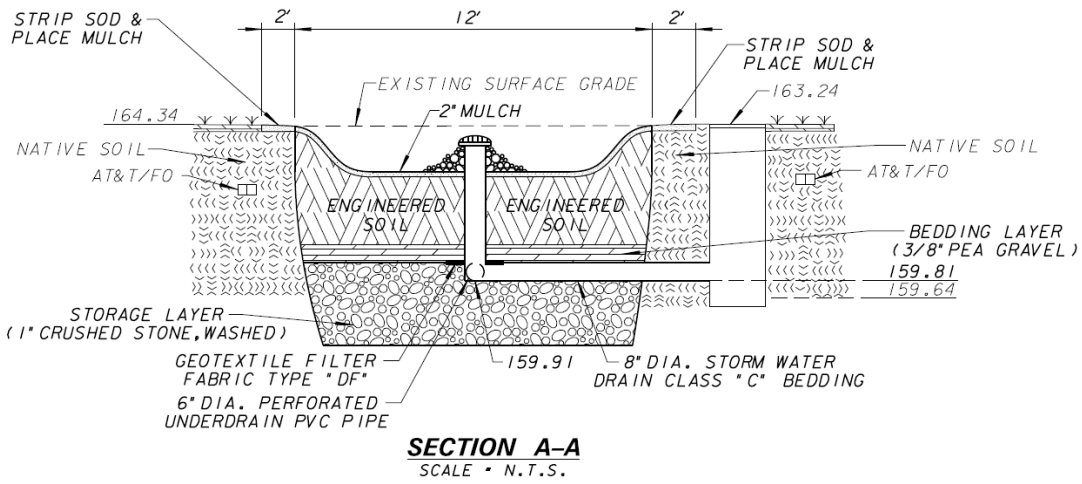

Figure A 4-6. Example of the cross section of the bioswales (source: City of Milwaukee).

HellTy Bioswale drains an area of 1.04 acres and is 70 ft long. It has one inlet location on both the north and south of the bioswale that drain the respective segments of road. WI Club Bioswale is larger and drains an area of 1.85 acres and is 65 ft long. Unlike HellTy Bioswale, it has two inlet locations on both the north and south of the bioswale that drain the respective segments of road. Figure A 4-7 illustrates pictures of the two bioswales.

Figure A 4-7. The image on the left shows the HellTy bioswale with the overflow grate open and the active control visible; the image on the right shows the real-time control attached to the underdrain of the HellTy bioswale.

4.3.3. Control Algorithms

1. Level Control Algorithm

The primary goal of the real-time controls was to reduce the volume of stormwater exiting the underdrains without overtopping the green infrastructure systems or extending the drawdown time beyond a maximum limit. To do so, a simple control rule was developed that was based upon the water level in the system (Figure A 4-8). This control algorithm is based upon (1) retaining water in the green infrastructure practice for 48 hours and then releasing to meet the drawdown time requirements and (2) releasing stored water if it reaches a maximum threshold to prevent bypass of water into the overflow grate and in doing so maximize treatment volume. This algorithm reads the water level at 5-minute intervals. If the water level (WL) is below a specific water level threshold set by the user (e.g., invert of underdrain pipe, level of the known groundwater table, etc.) it is assumed that there is no stormwater infiltration into the trench and defaults to a closed valve position. However, if the water level reading exceeds the set minimum threshold, then it is assumed that infiltration into the system has begun and the

next step in the logic begins. First, the system determines if it has been over 48 hours since the stormwater infiltration began. If it has, then the system opens to meet the draw-down requirements (this is illustrated as 48 hours but may range from 48-72 hours depending upon the regulatory authority). If it has not been longer than the set time threshold, then it checks for a second condition: has the water level reached a height at or above the maximum threshold (set as 2ft in the diagram). If not, it remains closed; if so, it opens to prevent bypass of the green infrastructure and maximize the volume that is treated.

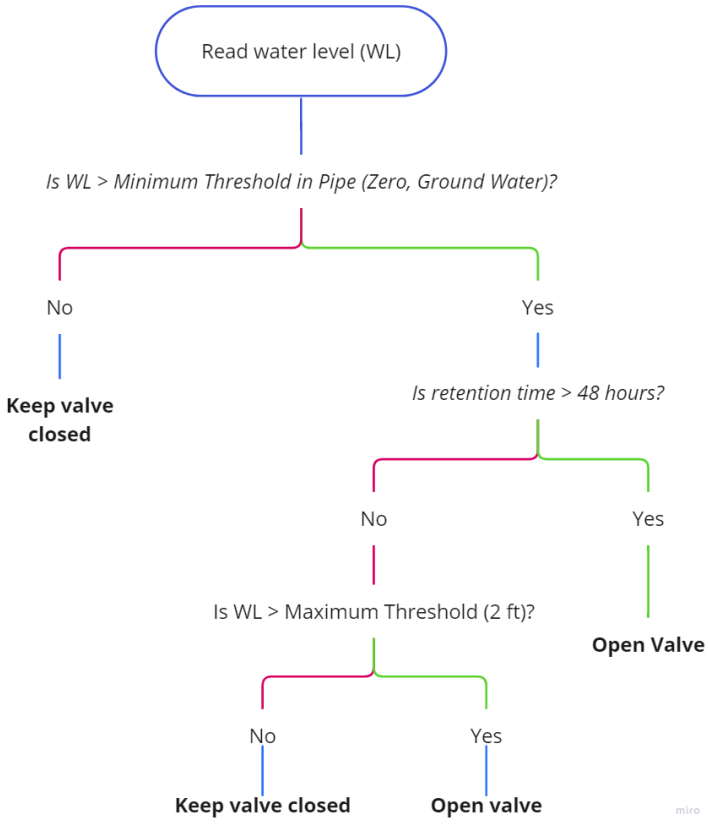

Figure A 4-8. Diagram of level-based control algorithm used for the active controls.

2. Gradient control algorithm

In some cases, high groundwater tables were observed at the site. Without prior knowledge of the groundwater level, which changes over time, it is difficult to determine when a runoff event begins simply based upon a minimum water level threshold. Therefore, in the following algorithm, the rate at which the water level changed was used as a determination of when runoff begins, negating the need to know where the groundwater level table is. This is illustrated in Figure A 4-9, where the event start is initiated using the rate of change in the water level reading. If the water level in the pipe increases at or greater than a set rate for 15 minutes, a runoff event is initiated. In addition, a threshold water level set at the surface may not be necessary in all cases, as excess water can either pond (as in the case of bioretention) or may reach the storm sewer system through an overflow grate. Therefore, this algorithm allows ponding for a period of 48 hours before emptying if the ponding is still occurring.

Compared to the level-based algorithm, this enables green infrastructure practices designed with ponding depths to take greater advantage of the ponding volume and therefore infiltrate a greater volume during runoff events. The downside of this is, in the case of an overflow, there would be untreated surface runoff that would directly flow into the sewer system. However, it has been shown that the first flush carries most of the pollutants, especially in smaller watersheds (Hathaway & Hunt, 2011; Lee et al., 2002); therefore, this algorithm ensures treatment of the first flush of pollutants, while also maximizing volume retention.

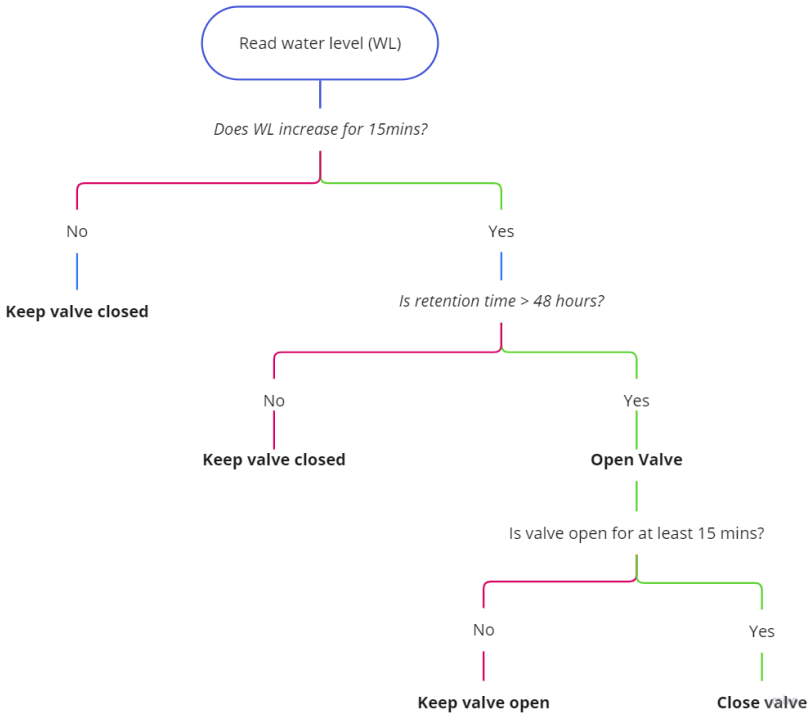

Figure A 4-9. Diagram of gradient-based control algorithm used for the active controls.

3. Gradient plus level control algorithm

The above two algorithms were tested in the field and based upon their field outcomes two more algorithms were developed and tested using the developed computer model (discussed in section 2.6). The level-based control algorithm was effective at retaining flow and maximizing infiltration; however, due to the logic, it frequently opened and closed during high runoff events when the maximum threshold was consistently exceeded. Therefore, to reduce wear and tear on the valve, a timer was integrated into the logic to keep the valve open for 15 mins (user adjustable) in order to drain down a larger portion of the runoff. This was combined with the gradient control logic that initiates storm runoff based upon a rate of change and enables the system to

effectively handle fluctuations in groundwater tables that are above the invert of the underdrain (Figure A 4-10).

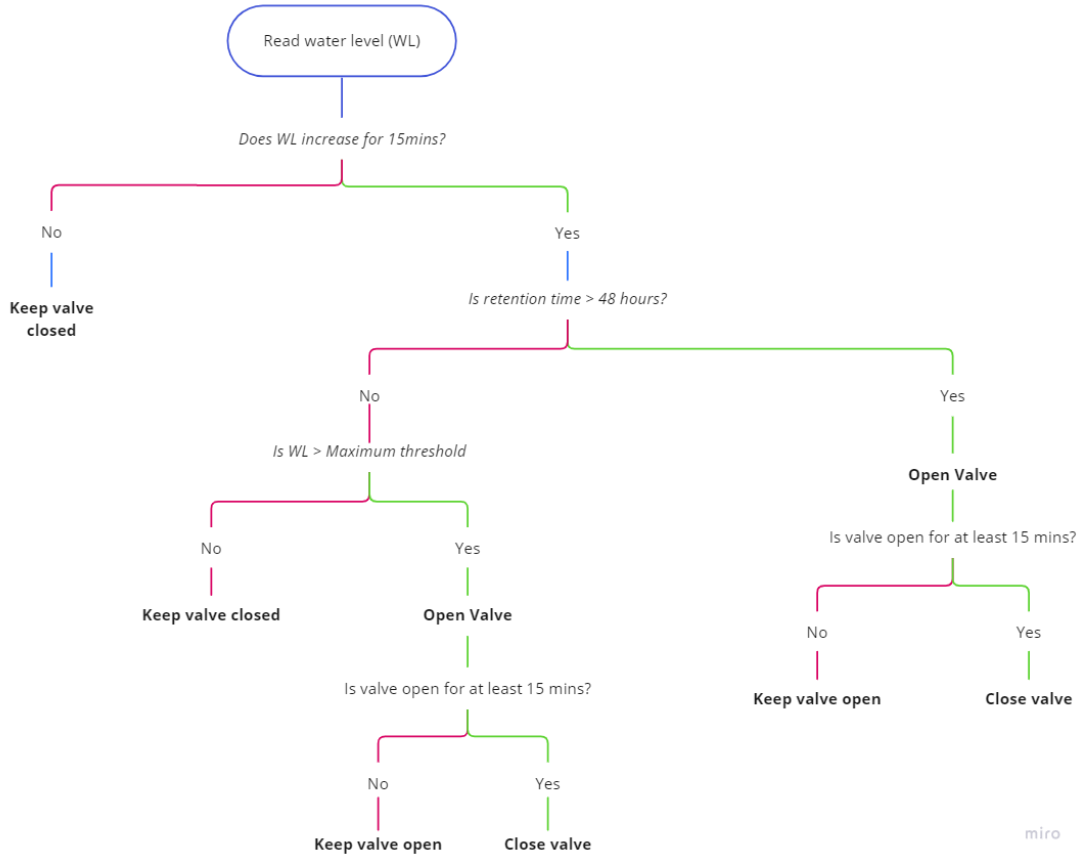

Figure A 4-10. Diagram of gradient / level-based control algorithm used for modeling.

4. Complex control algorithm

As mentioned previously, by removing a maximum water level threshold in the gradient control algorithm, infiltration is maximized but at the cost of risk to overflow. However, because the first flush (beginning of the runoff event) contains a higher concentration of pollutants, overflow that occurs at the end of the storm may not release a comparative amount of pollution downstream. Similarly, there is a risk to keeping runoff retained in a green infrastructure system for too long. If a green infrastructure practice is

fully saturated and a new runoff event begins, then that runoff, including the first flush of the new event, will be routed to an overflow pipe or grate without treatment. Therefore, a new algorithm was developed to try to reduce the risk of overflow during back-to-back events.

To account for this risk, a new complex algorithm based on the gradient control algorithm, was developed that adds an additional step in the logic which empties the green infrastructure practice based upon two criteria: (1) a declining water level gradient and (2) the level of the water table within the green infrastructure practice (Figure A 4-11). In this additional step, during the retention period, the gradient of the water level change is checked and if the water level (1) decreases for 8 hours (time adjustable by user) at a predetermined rate and (2) is above 50% maximum height of the trench, then the valve is opened for 15 minutes. The height limitation is used to disregard smaller runoff events and maximize volume capture through its lifetime.

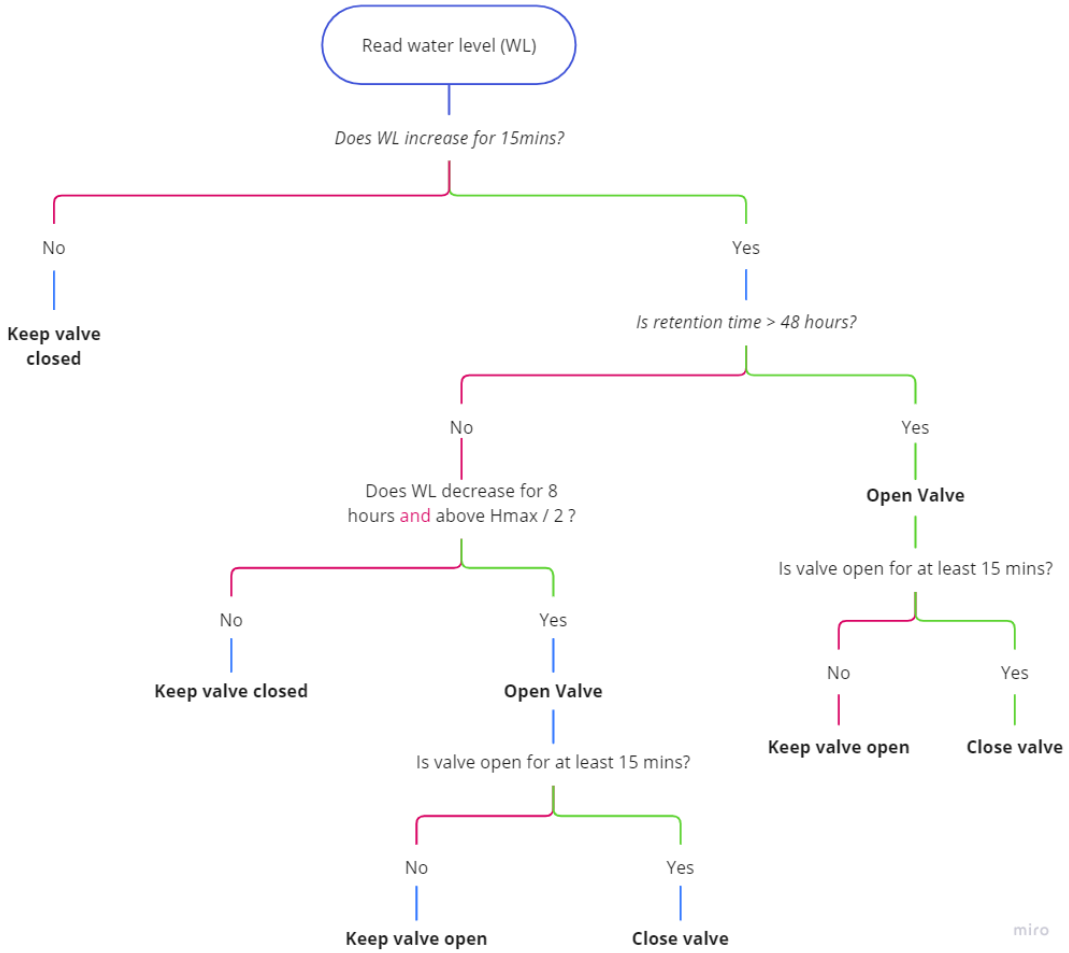

Figure A 4-11. Diagram of complex control algorithm used for modeling.

4.3.4. Estimating Water Balance

The influent volume into the green alley was estimated using rainfall data from WS1229 rain gage located approximately 1.3 miles from the site. The influent volume into the bioswales was estimated using rainfall data provided by MMSD for rain gages WS1207 and WS 1209 located approximately 1.8 and 2.7 miles from the site. Using this rainfall data, along with the drainage areas and runoff coefficients of the respective catchments, the rational method was applied to estimate input flow rates for storm events using the following equation:

$$Q = ciA \quad \text{Equation 1}$$

where Q is the flow rate in ft3/s, c is the runoff coefficient derived from land cover, i is the rainfall intensity, and A is the area in acres.

The effluent volume from the underdrain pipes were estimated using the water level within the pipe and two different hydraulic equations depending on the valve action. Unique to real-time controls are the opening condition, where full pipe flow exists for a brief period of time. Therefore, at the moment of valve opening (the first 5 minutes), the volume leaving the system was equivalent to the water volume inside the pipe. When the pipe empties, the effluent was estimated based upon the estimated water level in the green alley and the flow rate into the perforations of the pipe. The following empirical relationship was generated using observed data from 11 events:

$$Q_{in} = 0.0138\ (h - h_p)^{0.5} * A_p \quad \text{Equation 2}$$

where Q_{in} is the infiltrative flow into the pipe, h is the groundwater level height in the green infrastructure practice, h_p is the height of the water in the pipe, and A_p is the cross-sectional area of the pipe.

4.3.5. Data analysis

To evaluate the volume removal of the real-time control systems, the measured influent and effluent volume were used to compute a volume ratio:

$$R_{volume} = \frac{V_{out}}{V_{in}} \quad \text{Equation 3}$$

where R_{volume} is the ratio of the total volume of outflow (V_{out}) to the volume of inflow (V_{in}) (Davis, 2008). In doing so, this provides a quantifiable metric that can be used to understand the degree to which real-time controls on green infrastructure affected the volume removal of green infrastructure.

In addition, the rate at which water rises in the green infrastructure practice (i.e., infiltration – exfiltration during the rising limb of the water level) was evaluated, as well as the drawdown rate (i.e., infiltration – exfiltration during receding limb of the water level) while the real-time controls remained closed. This information provides us with an understanding of how the structure adheres to the design requirements while an active control system is in place. The rising rate of the water level in the green infrastructure is computed as:

$$R = \frac{(h_{peak} - h_{begin})}{(\Delta t)} \quad \text{Equation 4}$$

where R is the is the rising rate of the water level in inches/hour, h_{begin} is the water level height in the green infrastructure before runoff begins (i.e., groundwater level or invert of the underdrain), h_{peak} is the peak water level height in the green infrastructure in inches, and Δt is the time between h_{begin} and h_{peak}. Similarly, the drawdown rate is computed as:

$$D = \frac{(h_{peak} - h_{base})}{(\Delta t)} \quad \text{Equation 5}$$

where D is the is the drawdown rate in inches/hour, h_{peak} is the peak water level height in the green infrastructure in inches, h_{base} is the water level height in the green infrastructure when it returns to base levels (i.e., groundwater level or invert of the underdrain) and Δt is the time between h_{peak} and h_{base}.

4.3.6. Modeling

A third objective of the project was to model the real-time control systems using the data collected to evaluate the performance of the controls under simulated conditions. Doing so can simulate alternative site conditions (infiltration rates, pipe blockage, etc.)

and storm conditions (e.g., return period) to determine the conditions under which real-time controls for green infrastructure might be most appropriate. To do so, a water balance model was developed for the green alley using python code as illustrated in Figure A 4-12.

- Qin = Inflow to the trench
- Qout = Outflow from the under-drain
- Qspill = Overflow from the structure
- Qp = Flow into the pipe through perforations
- QL = Infiltration/exfiltration of storm water through soil
- E = Evaporation
- h = Height of water table from the bottom of the trench
- hmax = Maximum height of water table in trench
- hs = Maximum water table level allowed to retain (level control algorithm)
- hmin = Distance from bottom of trench to invert of underdrain
- hGW = Groundwater height from bottom of the trench
- GW = Groundwater level

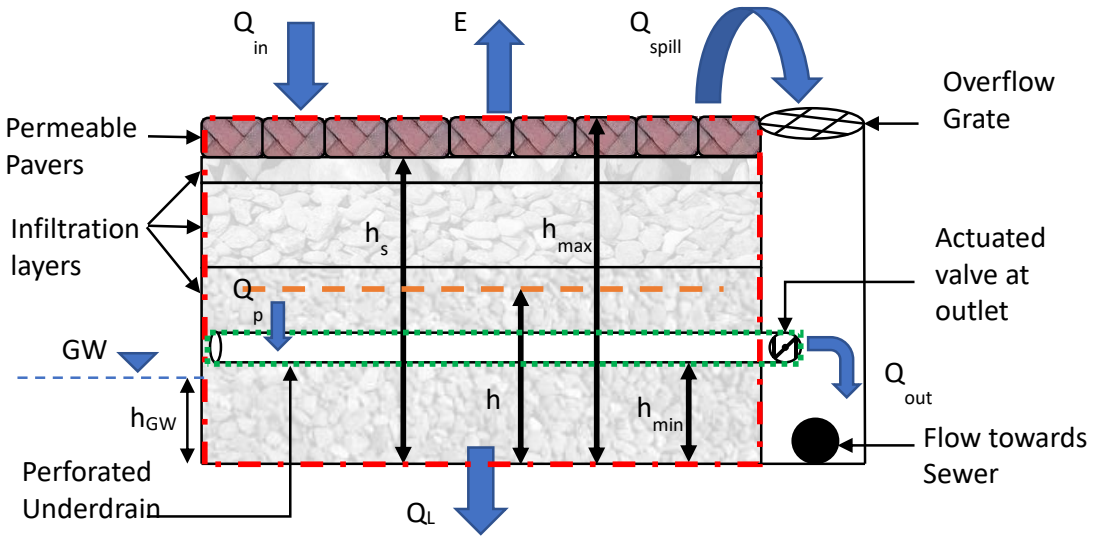

Figure A 4-12. Schematic of the water balance in the green alley.

To simplify the system, it is divided into two boundaries, the red (the trench without the underdrain) and the green (the underdrain). The variable hs is used as a constant parameter to control the valves operation while hmax is considered the upper bound where all water above it flows instantaneously to the sewer system through the overflow grate. The governing mass balance equation for the red boundaries are as follows:

$$\frac{dV(h,t)}{dt} = Q_{in}(t) - Q_p(h) - Q_{spill}(h,t) - Q_L(h,t) \quad \text{Equation 6}$$

Furthermore, Equation 6 can be written as a combination of Equations 7-11:

$$\frac{dV(h,t)}{dt} = \left(\frac{dh}{dt}\right) \times A_s \quad \text{Equation 7}$$

$$Q_{in}(t) = \frac{A_w p}{A_s \rho}\left(C_l \times A_l\% + C_{pl} \times A_{pl}\% + A_{pp}\%\right)\left(1 - C_{pp}\right) \quad \text{Equation 8}$$

where Q_{in} is the stormwater inflow into the trench, A_w is watershed area, A_s is surface of the green alley, p is the precipitation, ρ is the porosity of the trench media, $C_{l,pl,l}$ are the runoff coefficients, and $A_{l,pl,pp}$ are the areas with different runoff coefficients. The outflow from the green infrastructure trench to the underdrain as a function of the water height within the trench is modified from Equation 2 and given below:

$$Q_p = Cd \times L \times A_{p,total} \times B_1 \times (2g(h - h_p))^{0.5} \quad \text{Equation 9}$$

where, Cd is the discharge coefficient of perforations, L is the slope adjusted length of the pipe at each time step, Ap,total is the total area of perforations per 1m of pipe length, B1 is the clogging factor of perforations, g is the gravitational acceleration, h is the water height in the trench, and hp is the water height inside the underdrain. Groundwater infiltration / exfiltration was modelled using the equation below:

$$Q_L(h,t) = K \times A_T \times B_2 \times (2g(h - h_{gw}))^{0.5} \quad \text{Equation 10}$$

where K is the hydraulic conductivity of soil, AT is the effective bottom area of the trench, and B2 is the clogging factor of the geotextile. Finally, the overflow from the structure (Q_{spill}) if the water level is above the overflow invert is computed as:

$$Q_{spill}(h) = max[0, h - h_{max}] \quad \text{Equation 11}$$

where h_{max} is the maximum allowable water level before spillage occurs.

Finally, the mass balance of the green boundary can be written as:

$$\frac{dV(h,t)}{dt} = Q_p(h) - Q_{out}(h) \quad \text{Equation 12}$$

where,

$$Q_{out}(h) = \begin{pmatrix} Q_p + Volume\ in\ pipe & (at\ first\ time\ the\ valve\ opens) \\ Q_p & (if\ valve\ is\ still\ open) \end{pmatrix} \quad \text{Equation 13}$$

And Q_p is given by Equation 9.

Table A 4-1. Values of model coefficients.

Parameter	Value
Cd	0.6
K	$1.0E^{-6}$
B_1	0.75
B_2	1.0

Assumptions were made to simplify and properly model the system and are listed below.

1. All storm water reaching the pervious pavement is infiltrated into the trench, thus no bypass of surface runoff over the pavement is considered if there is infiltrative capacity within the trench itself (Cpp = 0).
2. For Equation 2, water height inside the trench is calculated considering the slope of the structure.

3. Evaporation compared to other factors is negligible and rainfall over the watershed flows into the structure without a time delay.
4. Due to the 1st assumption, Qspill occurs only when the trench has met its full capacity and the entire volume of the trench is fully saturated. Once it reaches full saturation, Qspill is calculated accordingly.
5. The water table surface inside the trench is assumed to have the same elevation throughout; therefore, the holding capacity is limited by the slope of the trench.
6. Pipe outflow is constrained by the area of the perforations in the underdrain, as well as the blockage or clogging factor (B1), which is considered to be 25% due to age of the structure.
7. For model simplicity, it is assumed that within the 5 min readout interval during which the valve is closed, water height inside the pipe fills up to 40% capacity, which matches the porosity of the trench media.

Given the assumptions above there are several limitations of the model to consider. For example, the water table surface inside the trench is assumed to have the same elevation throughout. However, in field conditions, soil water interactions may behave differently with varying infiltration locations, hydraulic conductivity, and storage capacity throughout. Additionally, the model uses a stepwise method to calculate overflow, underdrain infiltration, and ground exfiltration. Due to this, precedence is given to overflow over underdrain infiltration and underdrain infiltration over ground exfiltration. However, in real conditions these processes occur simultaneously; therefore, model overflow values could potentially be exaggerated while ground exfiltration is understated.

The overall model includes all the above equations to simulate the water balance through the system. This is further augmented with the control rules defined within the previous section to simulate the impact of real-time controls on the green infrastructure system. This was done at the green alley site using 5-minute rainfall data from a nearby MMSD gage.

4.4. Results

4.4.1. Green Alley: Time Series Analysis

The real-time control system was installed on the green alley in Wauwatosa, WI at the beginning of 2019. Figure A 4-13 shows an example of the rainfall depth, water level depth in the underdrain, and control (open or close), over a 1-month period (11/15/19 – 12/13/19). Over this time period, five rain events occurred. The valve is controlled using the level-based algorithm (as described in Figure A 4-9) and the orange lines on Figure A 4-13 show the times in which the valve is open, otherwise it is closed. The shaded area of orange represents the valve having been open for more than a 5-minute interval. An average groundwater table was computed using observed data and used as the pipe sill level later when the gradient-based algorithm was used.

In most cases, this site had a groundwater table that was above the invert of the underdrain pipe. This is illustrated in Figure A 4-13, where the level-based algorithm recognizes a water level above the invert as remaining stormflow that must be flushed. This causes the valve to open every two days since the algorithm utilizes a maximum of two days as the retention period. To overcome this shortcoming, the average groundwater table was computed using observed data and used as a lower threshold value in future algorithms in order to prevent this unnecessary opening and closing. This also ensures that non-stormwater flows from groundwater are retained and not emptied into the stormwater system.

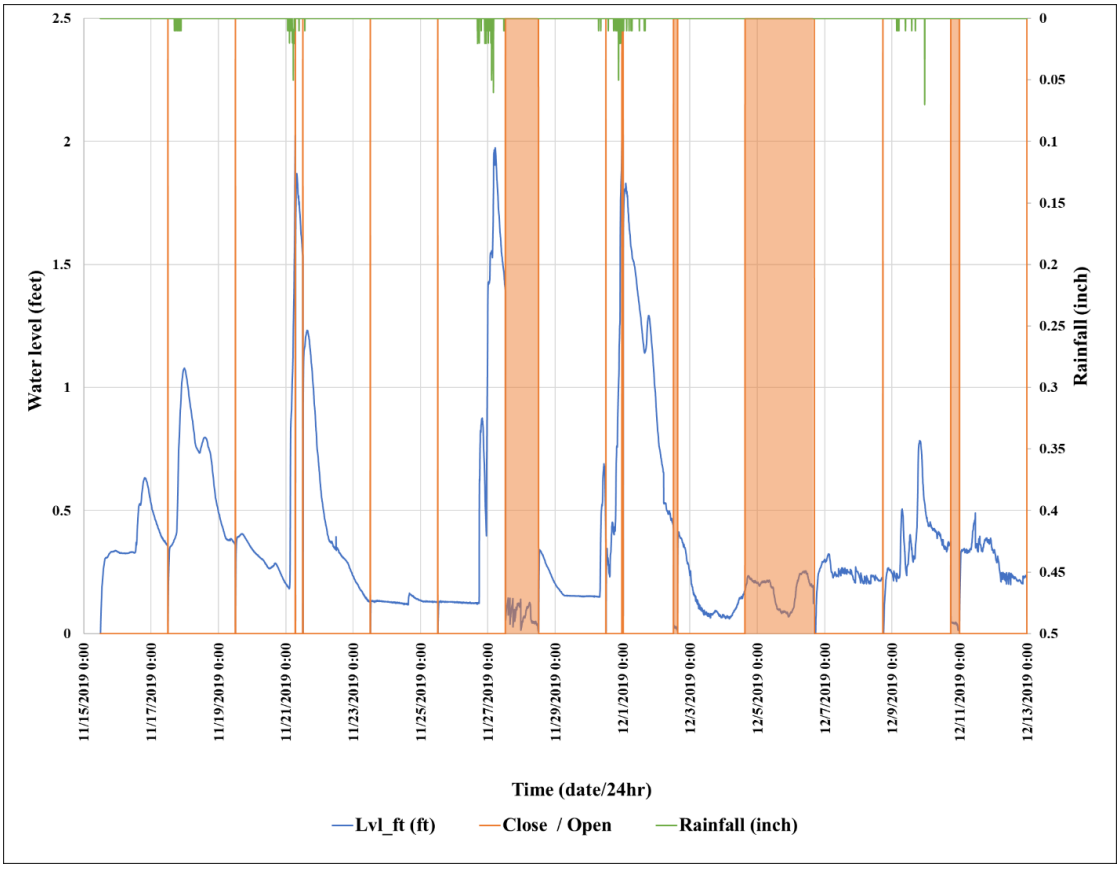

Figure A 4-13. 5-minute Time series data of Green Alley for the period of 11-15-2019 to 12-13-2019; Rainfall (green) in secondary axis and the corresponding water level measured (blue) in major axis; The valve opening is depicted by the orange line.

There are also instances in Figure A 4-13 in which the real-time controls opened due to an increased water level from stormwater runoff in order to prevent the system from overtopping. A closer inspection of this is highlighted in Figure A 4-14, which shows rainfall depth, water level depth in the underdrain, and control (open or close), at the green alley during a single event that transpired on 11/30/2019 to 12/01/2019. This event is an example of how the level-based algorithm works in the field. Valve openings are marked by the labels A, B, C, and D. The label A is a flush out event caused by two days of water retention due to the high groundwater level at this site as discussed previously. Shortly after the valve closes again, the water level quickly ascends above the

pipe invert level due to groundwater infiltration and therefore the retention timer starts again. The following retention flush-out occurs two days after A and is marked as D. Valve at D stays open for a longer period since the water level inside the pipe does not reach “zero” for 3 hours due to both faster groundwater infiltration and retained stormwater volume.

The labels B and C in Figure A 4-14 are valve openings that occur because the water level inside the trench reaches the 2 ft peak level (hs) set in the algorithm. When the water level reaches 2ft, the valve opens to release some of the retained water in order to prevent ponding on top of the green alley. A water volume equivalent to the volume of the underdrain is released swiftly and the hydraulic connection between the water inside the pipe and the trench is disconnected causing the water level to be read as near-zero. This low reading then causes the valve to then close after which hydraulic connectivity to the groundwater table is shortly restored and the system can read the level in the green alley.

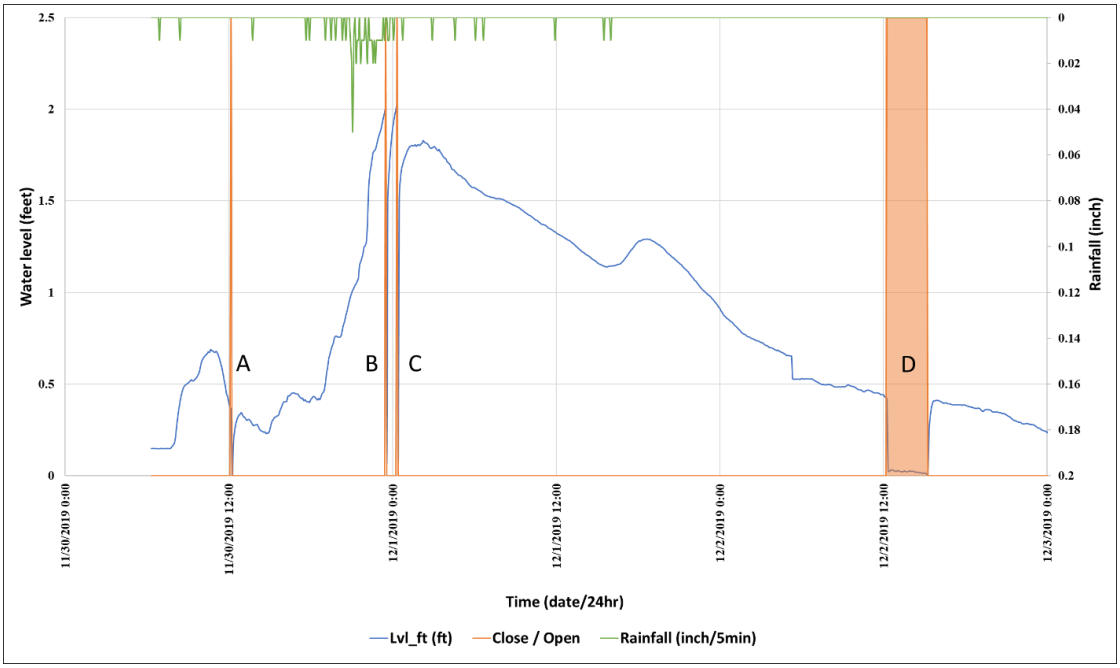

Figure A 4-14. 5-minute Time series data of Green Alley for a rain event which occurred during 11/30/2019 and 12/01/2019; A, B, C, and D are valve openings.

Another example of the algorithm functioning is provided in Figure A 4-15, which illustrates two rain events that occurred consecutively within 35 hours. During the rain event on the 22nd, the valve opens and closes five times during the peak of the event. This consistently releases a small volume of water to prevent ponding while also maximizing the volume retention of the system. In doing so, an estimated 85 ft3 was released during these valve openings. One day later, a second rain event occurred when only about two-thirds of the water inside the trench had exfiltrated or left the system. This resulted in a reduced volumetric holding capacity of the permeable pavement trench for the incoming event; however, the system was able to retain most of the volume while only opening once during the peak water level.

During the time that these events were captured, the drawdown time within the algorithm was set to 72 hours for each rain occurrence. Therefore, after 72 hours from the

first rain event, the valve was opened to flush out the system. However, this happened 5.7 hours after the second event, thereby flushing out water that would have been retained if not for back-to-back storms. The estimated pipe flow during this opening is 148 ft3. As a whole, the green alley with an active control system exfiltrates 96.9% of the influent volume across the two storms.

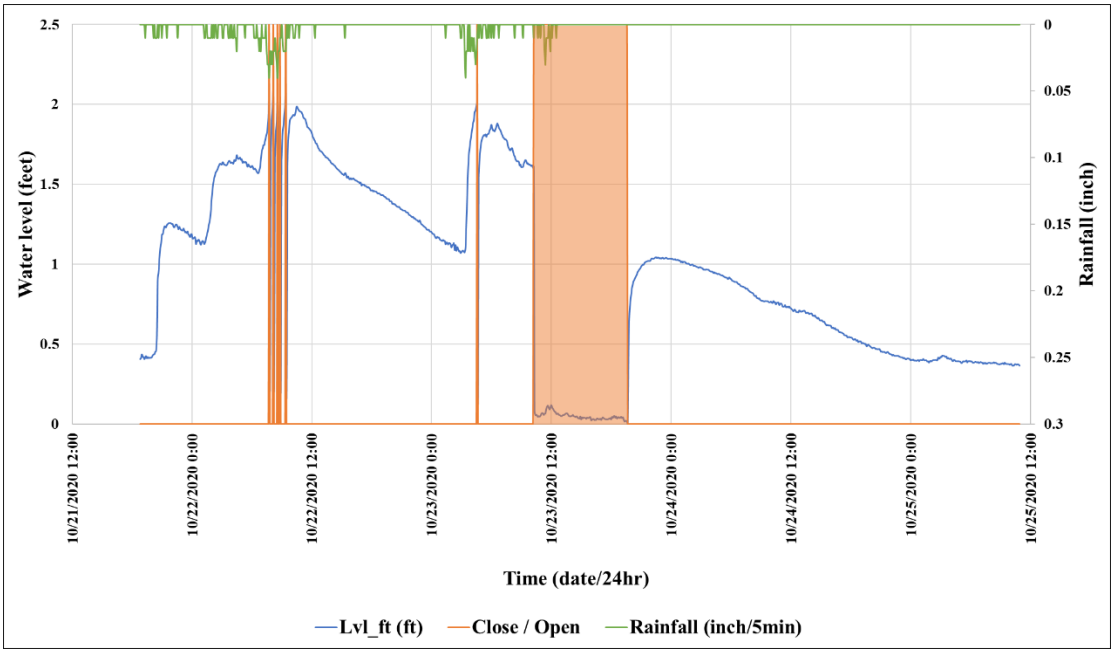

Figure A 4-15. 5-minute Time series data of Green Alley for the period of 10-21-2020 to 10-25-2020: Shows a few shortcomings of the level-based algorithm.

Not all rain events captured caused an opening of the real-time control valve once the groundwater level was known and accounted for. Figure A 4-16 shows observed data for the gradient-based algorithm (described in Figure A 4-9) for the period of 10-21-2020 to 10-25-2020. As illustrated, none of the events out of the 15 rain events observed triggered any of the thresholds set in the algorithm. This is largely due to the low-rainfall volume (0.02 – 0.32 inches) that occurred during these storm events and illustrates the way in which the valve can function as a plug that retains 100% of the volume of water

over a maximum time period, while allowing the system to drain. The influence of the rainfall depth on the volume retention of the system is further illustrated in Figure A 4-17. As illustrated, in general as the rainfall depth increases, the volume of water that is retained decreases due to the need to open the valve to prevent ponding.

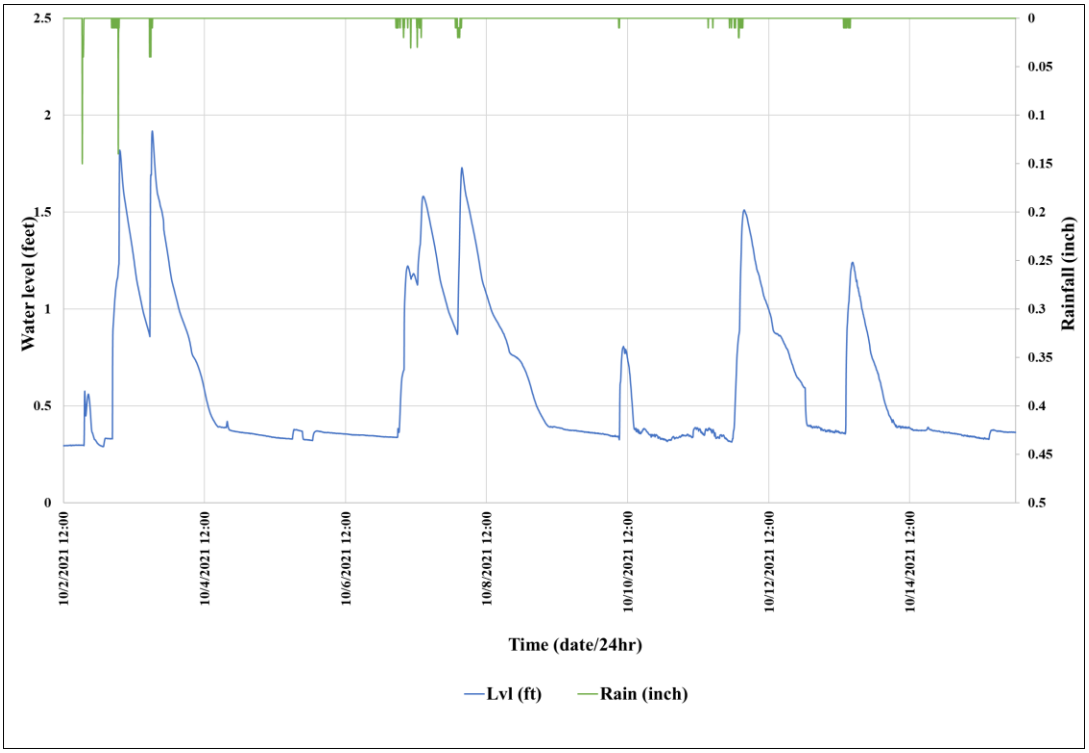

Figure A 4-16. 5-minute Time series data of Green Alley for the period of 10-21-2020 to 10-25-2020: Gradient-based algorithm.

4.4.2. Green Alley: Volume Reductions

To further evaluate if the real-time controls met the drawdown times required by regulations (48-72 hrs), the drawdown times were assessed across all storms. Figure A 4-18 shows the drawdown time for rain events as a function of rainfall depth. None of the observed rain events surpassed the WDNR technical standard requirement of drainage of the system within 72 hours. According to observed data and the regression developed, drawdown time increases as the rainfall depth increases. Although extreme rain events

were not observed during our observation periods, they were simulated within our model and are discussed later.

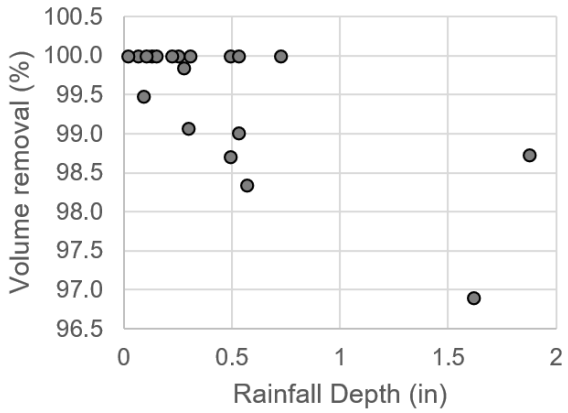

Figure A 4-17. The volume removed (%) as a function of the rainfall depth (in) for 20 captured runoff events.

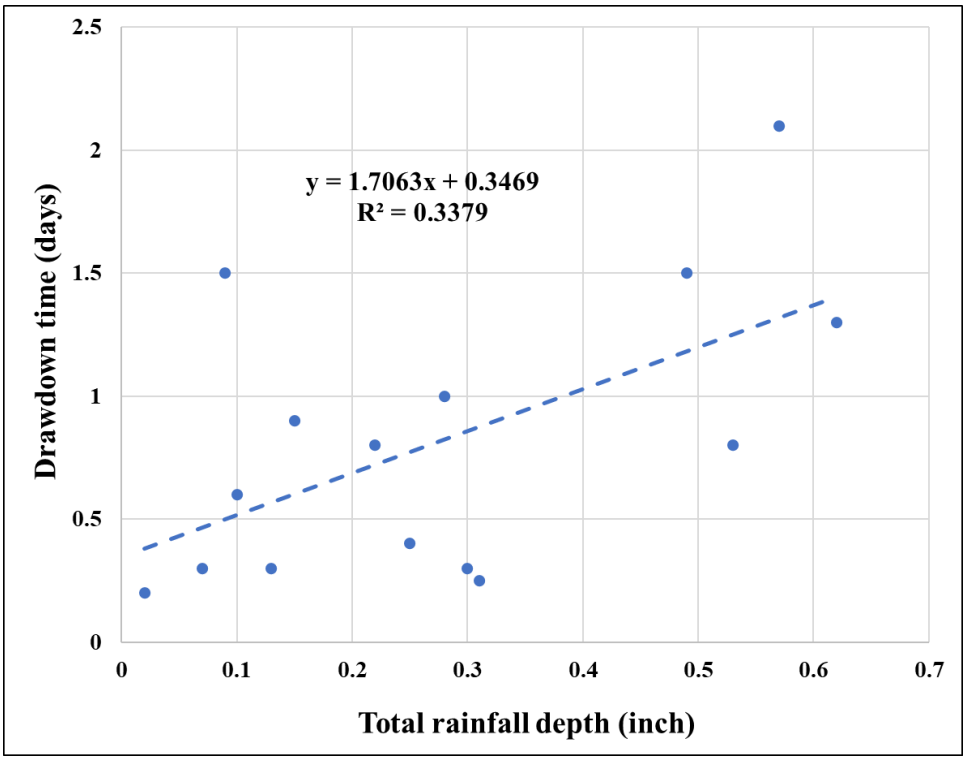

Figure A 4-18. Graph of drawdown time vs. total rainfall depth for the green alley site: Simple linear regression and the R2 value is shown within the graph.

The rising and drawdown rates of the green alley were evaluated as illustrated by their distributions in the boxplots in Figure A 4-19. The rising rate of the green ally trench (estimated from the water level in the system) is on average 8.5 times larger than the drawdown rate. This number is largely dominated by the infiltration into the system during the beginning of runoff when infiltration is larger than the exfiltration in the system. The WDNR standards require the infiltration rate of the porous pavement to be maintained at a minimum of 10 inches/hour and in a few rain events, the rising water level rates are higher than the specified limit suggesting that the porous pavement infiltrates as intended.

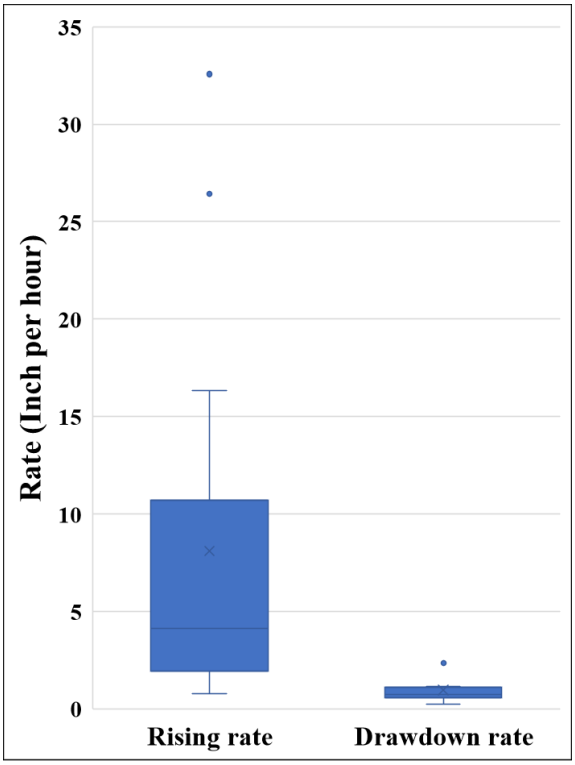

Figure A 4-19. Boxplot comparison of rising rate and the drawdown rate for the green alley site.

Table A 4-2 summarizes the data for all the events observed for the two different algorithms. This table demonstrates that the green infrastructure with a real-time control using both algorithms on average, exfiltrated more than 99% of the influent runoff. In both cases, this could be due to the retaining of volume when the valves are closed during the runoff events and the subsequent exfiltration after runoff while the valves remain closed. A direct comparison between the algorithms is challenging, however, because the average total runoff depths for each algorithm are different, and in no instances during the deployment of the gradient-based algorithm did the water level reach a threshold that required the system to open.

Table A 4-2. Average of each performance parameter used for the green ally site.

Parameter	**Level-based algorithm (n = 11)**	**Gradient-based algorithm (n = 9)**
Average total rainfall depth (inch)	0.6	0.3
Average influent volume (cf)	2761	1436
Average Drawdown time (days)	0.95	0.66
Average Drawdown rate (inch/hr)	0.85	1.11
Average rising rate (inch/hr)	7.43	9.08
Average effluent volume – Pipe (cf)	61	0
Average volume removed (%)	99.4	100

The results of this study demonstrate a greater volume reduction as compared to other studies that have evaluated the volumetric reduction of permeable pavements. Studies done by other researchers show volume removal rates of permeable pavements between 25% to 96% (W. Liu et al., 2020). In a previous study performed by this research team for MMSD at an adjacent green alley with similar hydrological and structural properties, it was found that the green alley removed 36% of influent flow. This value was found to be on the lower range of volume removal due to groundwater inputs

that also contributed volume to the underdrain during the runoff events. In the case of the green alley controlled in this study, groundwater was also found to be a factor. Therefore, the 99-100% volume removal on average demonstrates that the green alley with real-time controls is greater than the standard performance of uncontrolled permeable pavement systems with high groundwater tables.

4.4.3. Bioswales: Time Series

An example of the performance of the real-time control at a bioswale is illustrated in Figure A 4-20, which shows the rainfall data, water level inside the swale, and the valve (open/close) for the period of 8/6/2021 to 8/11/2021 at the WI Club bioswale utilizing the gradient-based algorithm. Three rain events occurred during this time and due to the high rate of drawdown, the thresholds to open the valve are never reached and therefore the valve never opens. In all three events, the exfiltration rates into the subsurface are high enough to reduce 100% of the influent flow. Furthermore, due to the storage capacity below the underdrain, only six rain events out of 15 observed displayed a water level increase above the underdrain invert level. This demonstrates the significant volumetric exfiltration capacity of the bioswale; however, it is unclear how these would perform during extreme events.

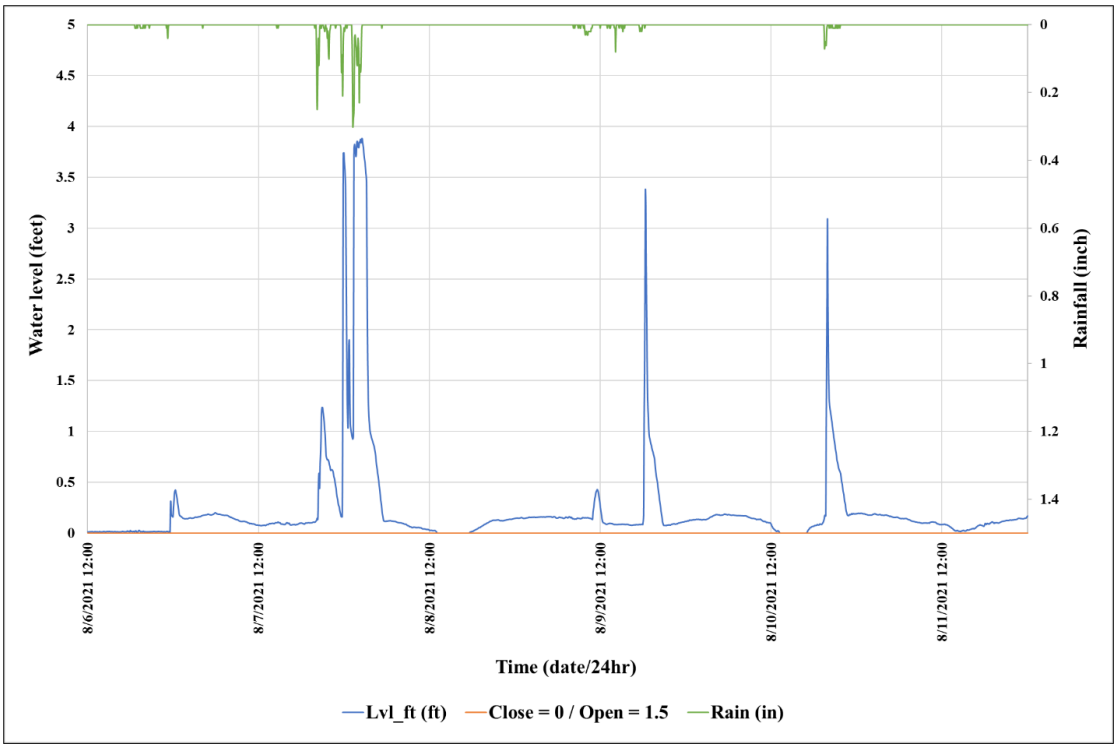

Figure A 4-20. 5-minute time series data of WI Club Bioswale for the period of 8-6-2021 to 8-11-2021.

The rain event that occurred on 8/7/2021 – 8/8/2021 is an event of a magnitude of 3.72 inches that occurred over a period of 12 hours. This is closely equivalent to the 10-year, 24-hour rain event (3.78 inch), according to National Oceanic and Atmospheric Administration (NOAA) data. The maximum water level above the pipe invert during this rain event was 3.88 feet, and the water level stayed above 3.8 ft for a duration of 30 mins. This height is above the overflow level (3.16 ft) that is designed to handle the 10-year storm, but below the maximum water level height in the bioretention (3.92ft). Therefore, this rain event, which is close in magnitude to the 10-year storm, appears to perform as designed, even with the valve completely closed during the event and, therefore, no underdrain flow.

4.4.4. Bioswales: Volume Reductions

Drawdown times for each observed event were quantified to evaluate how well the bioretention exfiltrates the stored volume of rainwater. As shown in Figure A 4-21, all six events receded in less than 0.14 days (3.5 hours). The outlier is the rain event with a 3.72-inch rain depth which was discussed in the previous paragraph.

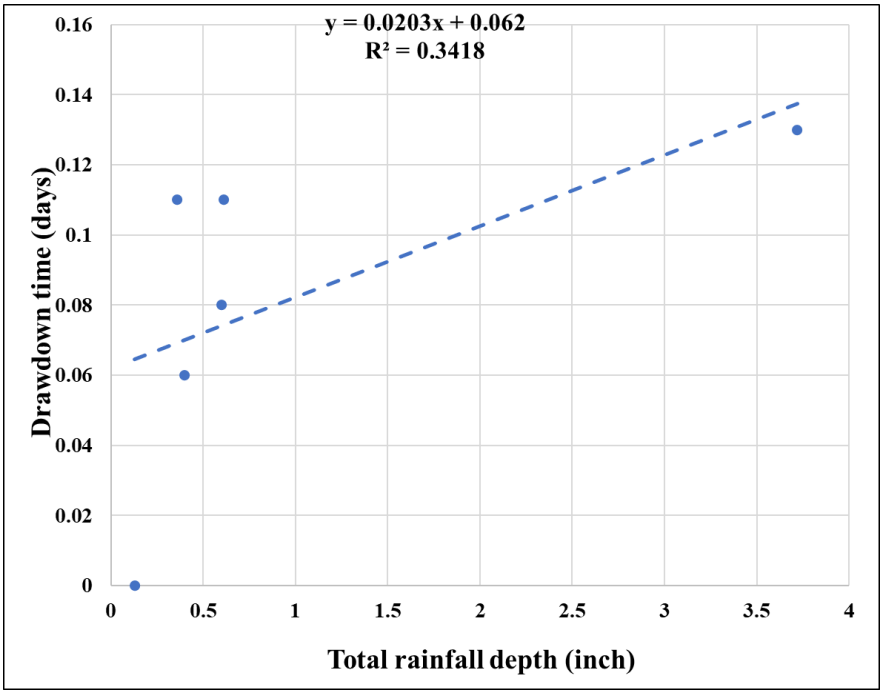

Figure A 4-21. Graph of drawdown time Vs. Total rainfall depth for the WI Club Bioswale site: Simple linear regression and the R2 value is shown within the graph.

The rising rates at the WI Club bioswale site are on average 15 times higher than that of the green alley, while the drawdown rates are 14 times higher. Figure A 4-22 shows the distribution of the rising and drawdown rates at the WI Club bioswale site. Similar to the green ally, the rising rates at the bioswale is 8.9 times higher than the drawdown rate. Compared to the green alley, the bioswales are newly built, which could increase infiltration rates as, with time, pore spaces within the structure get clogged with

incoming pollutants and due to settling of the soil media. However, they also have native vegetation that slows the infiltration rate compared to permeable pavers, and unlike the green alley, there is no groundwater interference reducing exfiltration rates at these sites.

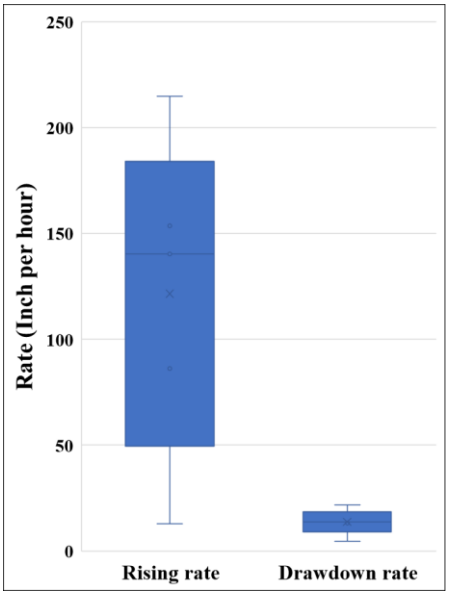

Figure A 4-22. Boxplot comparison of rising rate and the drawdown rate for the WI Club bioswale.

Table A 4-3 summarizes the data for the six rain events observed for the WI Club bioswale. Although the HellTy bioswale received the same rain events as the WI Club bioswale, due to its small watershed and similar design dimensions, no measurable water level was observed above the underdrain invert. This is due to a larger surface area to drainage area ratio of the bioswale, WI Club ratio is 0.011 while HellTy ratio is 0.017 (HellTy is 1.5 time that of WI Club), which has provided more than enough storage volume underneath the underdrain for the ten observed rain events during the period of August 2021 to November 2021.

Table A 4-3. Average of each performance parameter used for the WI Club bioswale site.

Parameter	Gradient-based algorithm (6 events out of 15)
Average total rainfall depth (inch)	0.97
Average rain volume (cf)	6512
Average influent volume - theoretical (cf)	4930
Average Drawdown rate (inch/hr)	13.72
Average rising rate (inch/hr)	121.46
Average Drawdown time (days)	0.08
Average effluent volume – Pipe (cf)	0
Average % release	0

4.4.5. Modeling

A model was developed for the green alley site to simulate the real-time control of green infrastructure. Field data collected over the study period was used to calibrate and validate the model. The model was applied to assess the performance of the four control algorithms mentioned in Section 2.3: level-based control, gradient-based control, gradient/level-based control algorithm, and the complex algorithm. These algorithms were applied to three years of continuous 5-min rainfall data, and were evaluated against each other, as well as a no-control scenario and a scenario where the underdrain was completely plugged. The models were also used to evaluate how the system responds to extreme rainfall events based on return periods. Finally, they were applied to evaluate the conditions under which the developed active control system would be most appropriate for green infrastructure, including infiltration rates of the surrounding soil, blockage of the underdrain, and groundwater table levels.

Model calibration to observed data:

A comparison of field and modeled data is provided in Figure A 4-23. Both the field (bottom graphic) and model (top graphic) systems were controlled using the level-control algorithm with a height threshold limit of 2 feet. As illustrated, the peaks and openings generally follow a similar trend. A notable difference is that the field data has openings every 48 hours due to issues with a high groundwater table initiating a false runoff event. While there are several methods to compare field and modeled data, such as the Nash Sutcliffe coefficient, root mean square error, and others (Moriasi et al., 2015), an application of these statistical tests is difficult with a system that opens and closes, thus changing the temporal nature of the hydraulics. Therefore, visual calibration was performed by attempting to match the peak water height (Table A 4-4), rather than applying statistical methods that assume uniformity in hydraulic conditions.

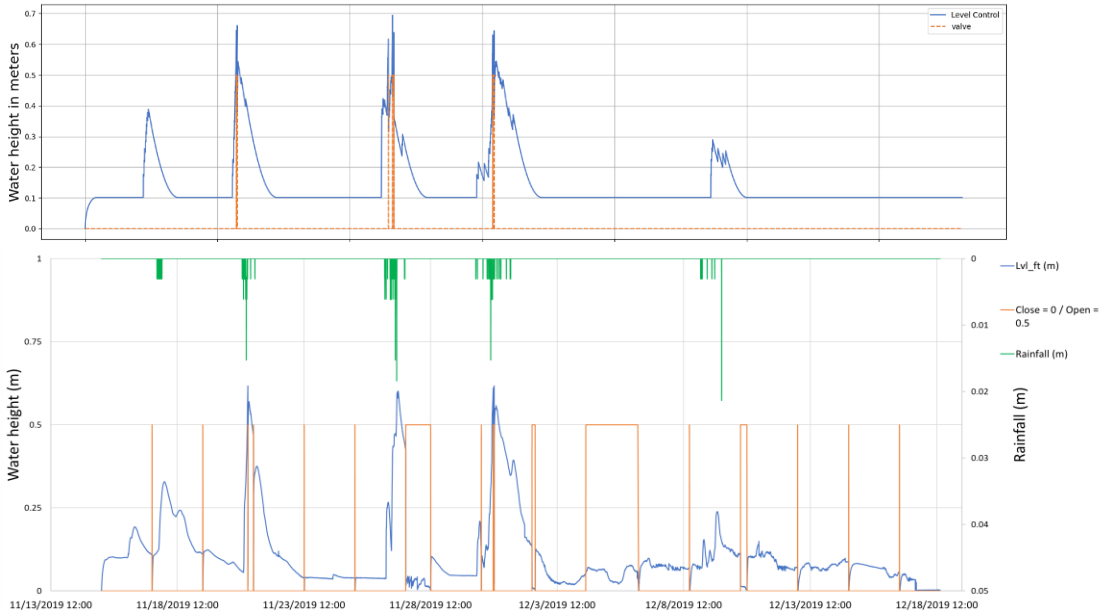

Figure A 4-23. Comparison of field and modeled data.

Table A 4-4. Difference between modeled and observed peaks.

Date	Modeled Peak (m)	Observed peak (m)	Percent difference
11/18/19	0.39	0.32	21.8
11/20/19	0.66	0.61	8.2
11/27/19	0.69	0.60	15.0
11/30/19	0.64	0.62	3.2
12/10/19	0.29	0.24	20.8

Performance of alternative control algorithms

An initial comparison of the performance of the control algorithms was applied to a 3-month dataset and the results are illustrated in Figure A 4-24 and A 4-25. As illustrated, there were five precipitation events that occurred over the course of the 3-month period. Modeled results demonstrate a quick response in the no-control scenario due to observed high infiltration rates and exfiltration through the underdrain, as well as a time of concentration equal to the 5-mintue time step of the model, that resulted in runoff instantaneously routed to the trench. The control algorithms are shown with a dashed black line that indicates if the valve is open (0.5) or closed (0). The level control and gradient/level perform similarly in that each of these control algorithms open the valve based upon a maximum threshold to reduce ponding or the risk of overflow. For example, during the third event that occurred near day 12, the level control opened three times while the gradient/level control opened two times to reduce overflow. The difference in the number of openings is due to the timer used in the gradient/level control that keeps the valve open for 15 minutes rather than closing it in one time step (5 min). Conversely, the gradient control and complex control do not have a maximum threshold and therefore neither of them open during the peak of the event, but only after a retention period has

passed (gradient control) or there is a descending water level for 8 hours (complex control).

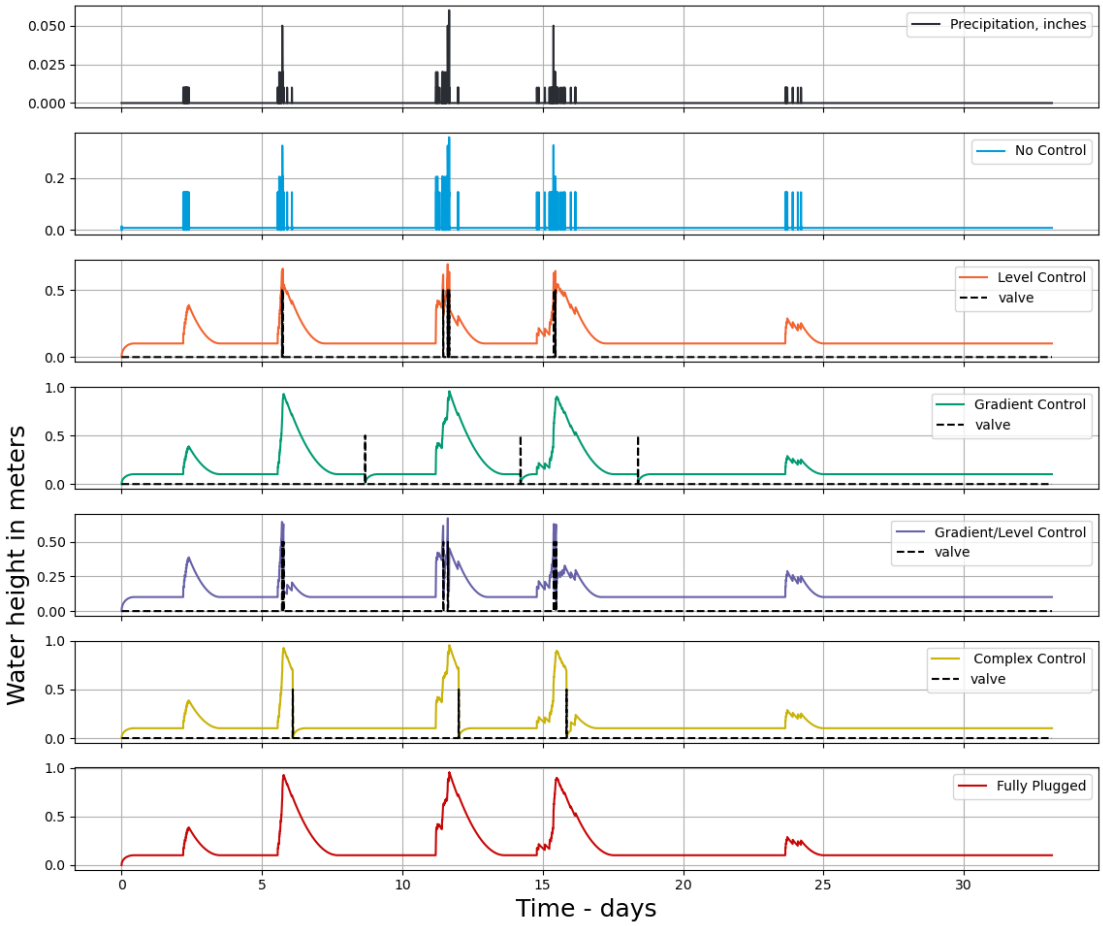

Figure A 4-24. Comparison of the behavior of algorithms for a month of data – Trench Water level.

Figure A 4-25 shows the exfiltration of water into the groundwater table. In this simulation, the groundwater table is set 4-inches above the underdrain invert as observed at the site. Therefore, in the no control conditions, there is constant groundwater infiltration into the trench that ultimately gets released to the sewer system. This is evident by the -41.22 m^3 exfiltration volume shown in the no control graph. Conversely,

the fully plugged scenario infiltrates 243 m^3 of runoff, demonstrating that the more the valve is closed, the more exfiltration is promoted.

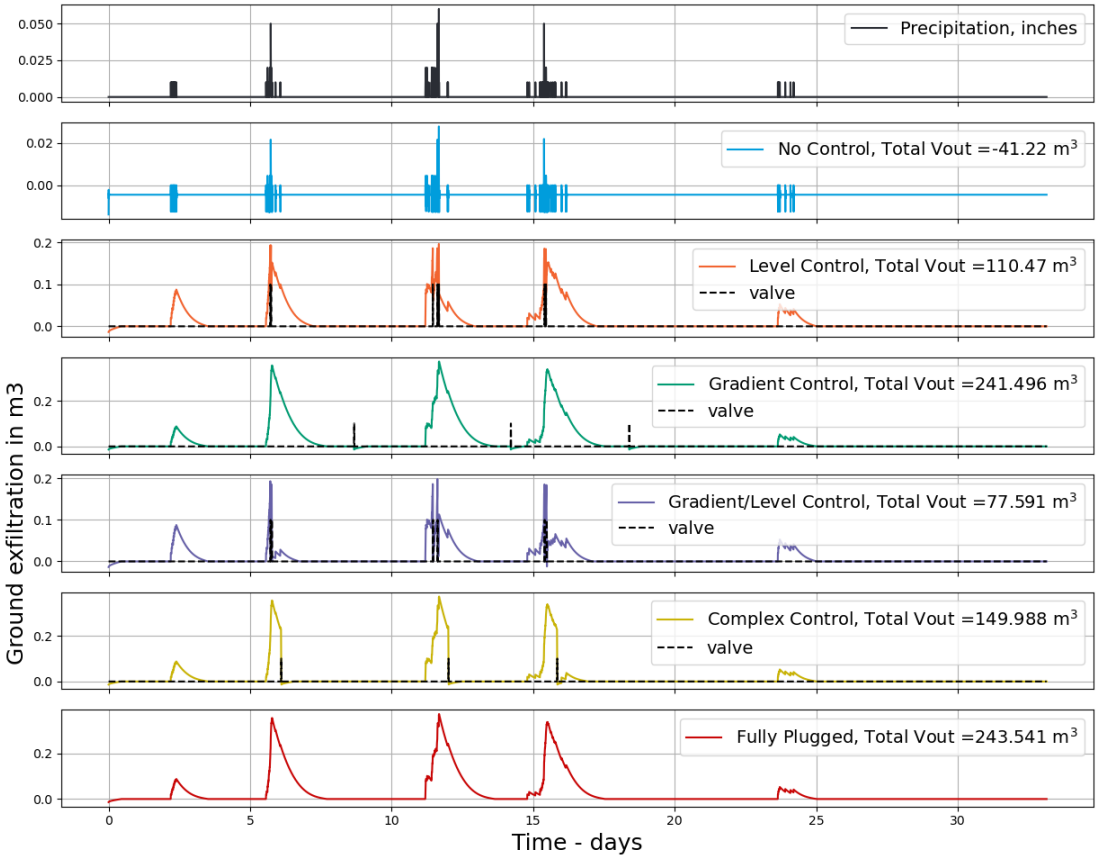

Figure A 4-25. Comparison of the behavior of algorithms for a month of data – Groundwater exfiltration.

To further evaluate the performance of the control algorithms, their performance was simulated over a 3-year period for the observed site conditions (i.e., groundwater table at + 4 inches) and the results are illustrated in Figure A 4-26. As illustrated, the no control scenario has by far the largest volume through the underdrain, only 16 m^3 of overflow, and negative groundwater exfiltration. This is because at the site the groundwater table was observed to be consistently above the invert of the underdrain,

thereby contributing groundwater volume into the system. In all cases, a real-time control improves the amount of water that is exfiltrated, suggesting that regardless of the control rule, when high groundwater tables are present, real-time controls can improve the exfiltration and prevent groundwater from entering into the stormwater system. Furthermore, in comparison to a fully plugged scenario, the level control and gradient/level control reduce the volume of untreated water that overflow, thereby improving the water quality benefits.

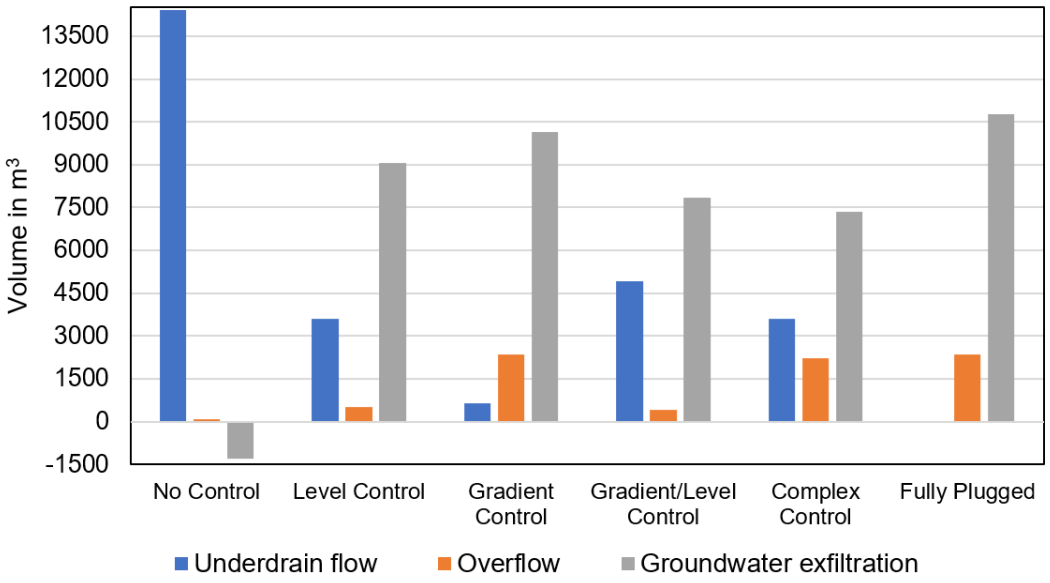

Figure A 4-26. Three-year performance of each algorithm compared to no control scenario.

As mentioned, a primary goal is increasing exfiltration; however, in doing so, a tradeoff exists between reducing the volume of treated water that is sent through the underdrain and the volume of untreated water that is overflow – representing two potentially competing objectives. Figure A 4-27 illustrates the comparative performance of the different algorithms. As illustrated in Figure A 4-27a, at the extreme ends are the

no-control algorithm which has very little overflow but a large underdrain volume (14,415 m^3), and the fully plugged scenario which has zero underdrain volume, but a larger overflow volume (2,355 m^3). The two algorithms that reduce both underdrain and overflow volumes – as evidenced by their location in the bottom left corner of Figure A 4-27a – are the level control and the level/gradient control. These two algorithms, while not having the greatest exfiltration as compared to the gradient control, do have a relatively smaller overflow volume (Figure A 4-27b). Therefore, if seeking both objectives, a control rule or algorithm that opens when a maximum water level is reached may be preferrable.

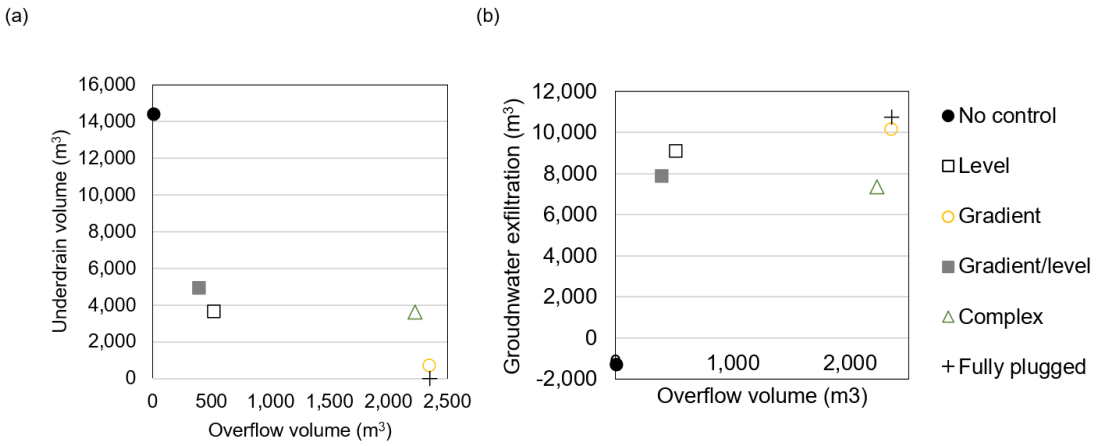

Figure A 4-27. Relationship between overflow volume and underdrain volume (a) and the overflow volume and groundwater exfiltration (b) for the different control algorithms over a 3-year period.

Design storms

In addition to the observed 3-year rainfall data, design storms (1-500 yr) were simulated to evaluate the impact that real-time controls would have during extreme events. The results of this analysis are in Figure A 4-28, which illustrates the performance in terms of overflow, groundwater exfiltration, and underdrain flow for all of the control

algorithms. As illustrated, overflow increases within increasing storm intensity in all cases, but is most pronounced for the gradient and complex controls, which have an equal amount of overflow as a fully plugged system. This is also evident in Figure A 4-28c, where there is little to no flow out of the underdrain of these systems. This is because neither of these controls (gradient and complex) try to prevent overflow, but only seek to maximize infiltration while also ensuring that a draw-down period is met. On the other hand, the level and gradient/level controls do attempt to prevent overflow by opening when a maximum water level is reached in the trench. In the scenario without a control, overflow occurs after the 10-year design storm events and is comparatively low to the other control systems; however, the no control algorithm releases the most volume through the underdrain while promoting little to no exfiltration.

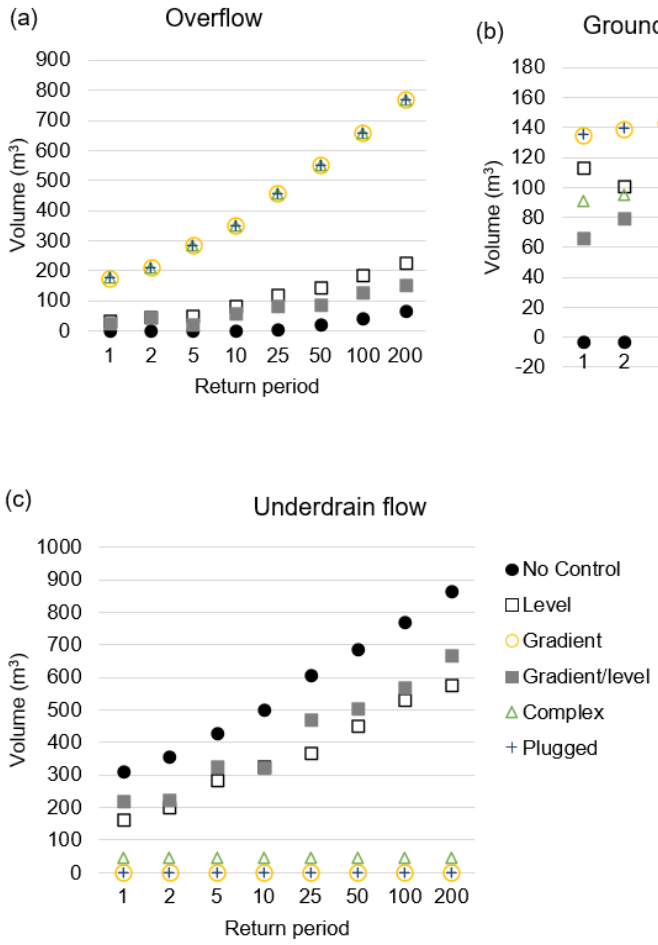

Figure A 4-28. Model performance of different algorithms for standard design storms (1-200 yr) in regards to the overflow (a), groundwater exfiltration (b), and the underdrain flow (c).

Sensitivity analysis

The model was also used to analyze the performance of the algorithms with varying site conditions, including hydraulic conductivity of the soils, blockage of perforations in the underdrain, and static groundwater levels. The groundwater level for the hydraulic conductivity and blockage evaluation was set 1m below the invert of the underdrain to represent a more general site condition without a high groundwater table.

The impact on the model under soil types with varying hydraulic conductivity is illustrated in Figure A 4-29. The three soil types tested represent are compacted clay (K =

1.0E-13), silty sand (K = 1.0E-6), and uniform sand/gravel (K = 1.0E-1). As would be expected, exfiltration increases when hydraulic conductivity increases, and all algorithms promote exfiltration to a similar degree (Figure A 4-29c). The difference in exfiltration is high between that of compacted clay and that of silty sand and uniform gravel, the latter two of which are within 71-86% of each other. In addition, for all algorithms, the underdrain and overflow reduce as the hydraulic conductivity of the soil increases. However, there is a noted difference in the performance between the algorithms themselves that mirrors their performance in the previous 3-year analysis in that the level and gradient/level controls have a higher underdrain flow and lower overflow due to their maximum water level thresholds.

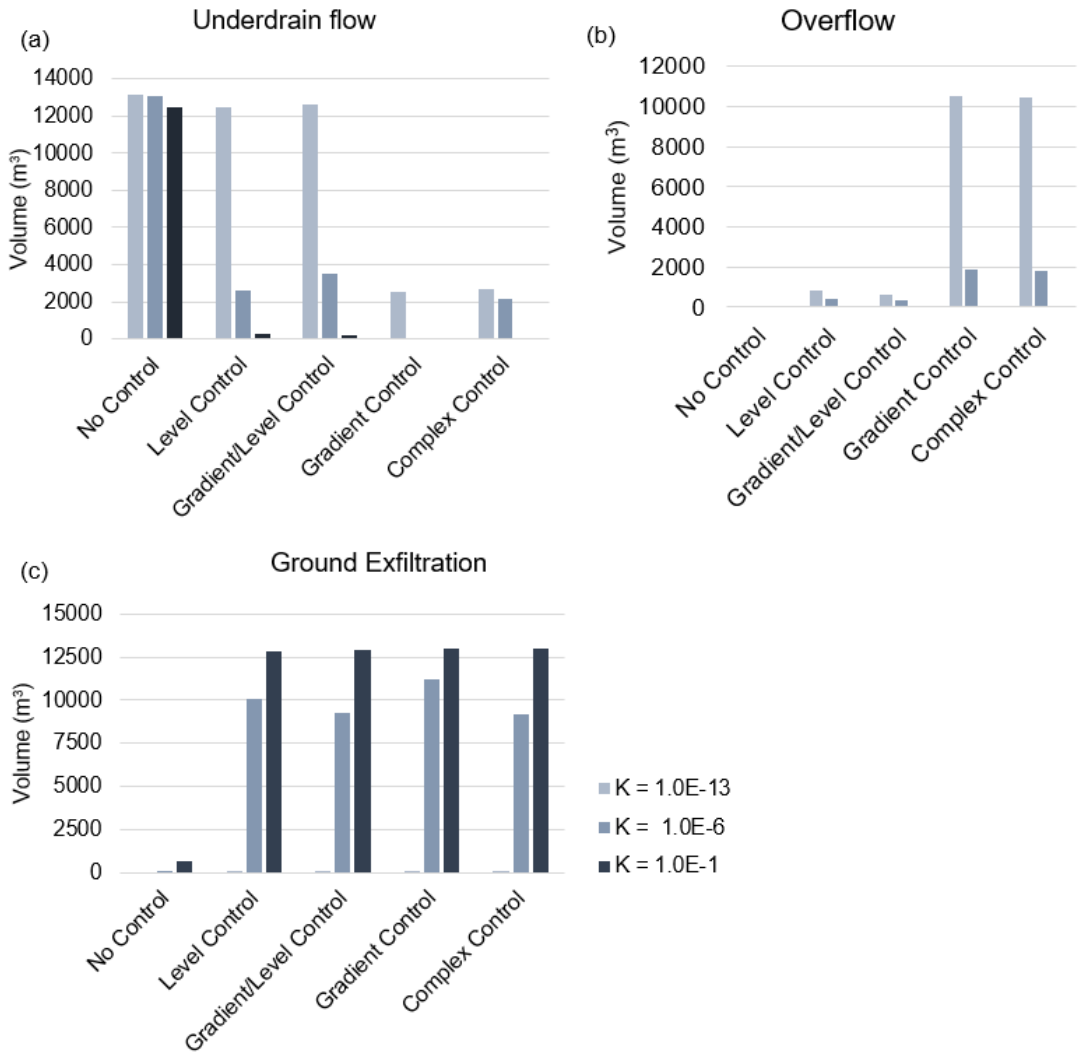

Figure A 4-29. Performance of the algorithms as soil type changes.

The model performance when the blockage of the underdrain is varied is illustrated in Figure A 4-30, where B of 0 represents fully blocked perforations and B of 1 represents no blockage. As illustrated in Figure A 4-30a, as the blockage in the underdrain perforations decreases (i.e., as B increases), the volume through the underdrain increases. Figure A 4-30b represents the overflow, and as illustrated there is no impact on the gradient control because the system is plugged during peak events and therefore overflow is unaffected by the flow rate through the underdrain perforations.

However, as blockages increase, so does the overflow that occurs for the level and level/gradient controls. Therefore, as the perforations of an underdrain get blocked overtime, this may be a concern for the performance of these algorithms in reducing overflows.

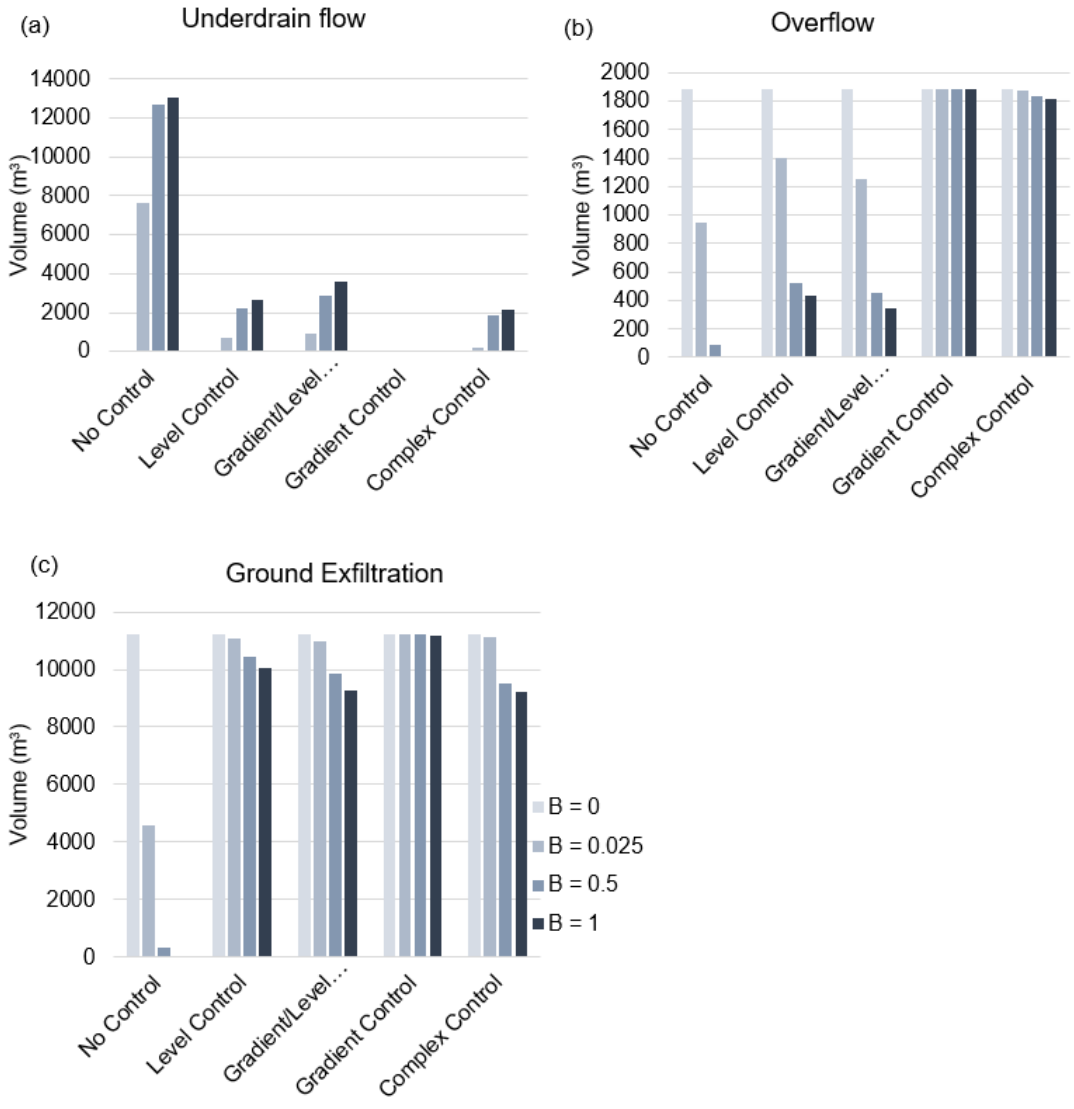

Figure A 4-30. Performance of the algorithms as blockage of perforations changes.

The impact of groundwater levels on the model is illustrated in Figure A 4-31, which shows the performance of the algorithms based on three different groundwater levels: 3 m below the invert level (-3 m), at the invert (0 m), and 0.5 m above the invert of the underdrain. In the case of no control, the groundwater table above the invert level infiltrates water into the trench and ultimately adds a considerable volume (>14,000 m3) into the sewer system (Figure A 4-31c). However, when the groundwater table is above the invert, all real-time control algorithms have a cumulative volume reduction through exfiltration. As evident in Figures A 4-31a and A 4-31b, as the groundwater table increases, both overflow and underdrain volumes also increase across all algorithms. This indicates that despite an ability to significantly reduce groundwater infiltration into the stormwater system through the underdrain, the higher the water table the lower the performance of the system with real-time controls.

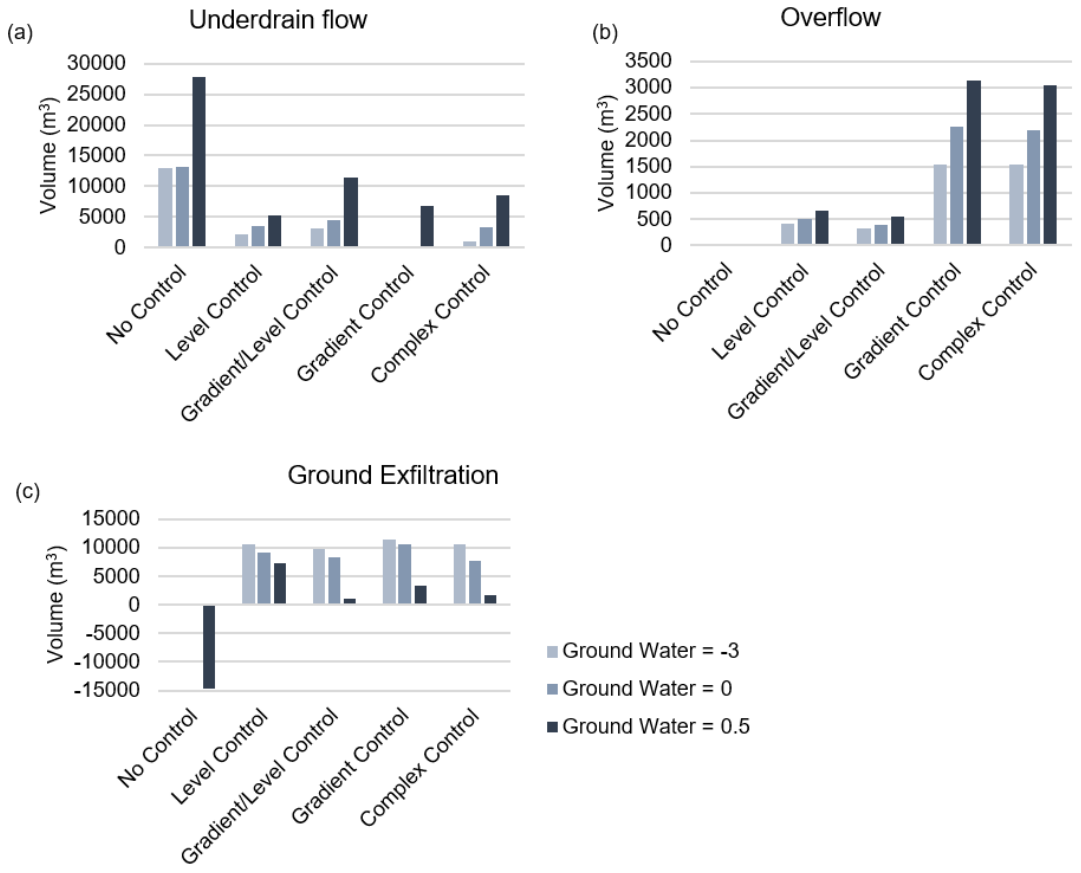

Figure A 4-31. Performance of the algorithms as groundwater table changes.

4.5. Costs of Real-Time Control Systems

One of the objectives of the study was to develop a low-cost active control system to control flow through small scale urban green infrastructure. To this end, an active control system was built for a maximum budget of $5,000. Table A 4-5 breaks down the major components required to build the system. Two options are given in which Setup 1 is a relatively expensive option that utilizes top of the line hardware and computing components, while Setup 2 looks for cost savings through cheaper manufacturers.

The actuator and valve used in Setup 1 is bought from an American supplier (Assured Motors), while the other is from a Chinese supplier (CONVA). While there is a

drastic price difference, throughout the deployment of the system, the authors noticed no difference in the function and the quality of the two valves. The Assured Motors valve was installed at the green alley and one of the bioswales, while the valve produced by CONVA was installed at one of the bioswales.

Campbell data loggers were used for their reliability in scientific instrumentation. In addition, Campbell and METER Group pressure transducers were used with no observed differences in their performance or maintenance needs. The Hydro 21 sensor from METER Group has the added advantage of having a temperature and a specific conductance sensor as well as the water level sensor while being competitively cheaper.

Table A 4-5. Cost breakdown of 2 options for the active control system.

Component	**Cost of Setup 1 ($)**	**Cost of Setup 2 ($)**
Valve + Actuator (Assured motors)	1500	-
Valve + Actuator (CONVA)	-	380
Data logger (CR300 Campbell)	900	900
Pressure transducer (CS451 Campbell)	790	-
Pressure transducer (Hydro 21 METER Group)	-	490
Signal convertor	10	10
Pelican Box	155	155
Two 12V 15AH rechargeable Lead-acid batteries	65	65
12V 18AH rechargeable Lead-acid batteries	40	40
Other material (e.g., steel legs, wires, etc.)	250	250
Total Cost	**3,410**	**2,290**

4.6. Discussion

In this project a real-time control system was developed to improve the volume removal of green infrastructure. Three real-time control systems were applied to green infrastructure (one green alley and two bioswales), and it was found that 97-100% of the

influent stormwater volume was removed on average across the storms that were monitored. The alley or bioswales were not monitored during uncontrolled conditions and the controlled valves were closed during most of the monitoring period; therefore, it is difficult to quantify the level of additional removal the real-time controls provided beyond the valve-closed condition. However, in this study, measured volume removal was greater than other monitoring studies that observed a range of 25% to 96% volume removal for permeable pavements (W. Liu et al., 2020) and an average of 61% volume removal for bioretention with underdrains (Poresky et al., 2011). Additionally, the green alley was modeled using python and three years of rainfall data to test the performance of additional algorithms, extreme rain events, and varying site conditions. The model results suggest that real-time control systems can be applied to balance the relative amounts of stormwater partitioned to underdrain flow, groundwater exfiltration, and overflow. This capability could be used to prevent untreated overflows or to maximize pollutant removal credits. To that end, the following conclusions can be made.

Green infrastructure with closed underdrain valves removed a large volume of runoff. As demonstrated by the summary of results above, the green infrastructure with real-time controls had a large removal of volume for both the green alleys (97%) and the bioswales (100%) during the observed time. The extent to which this is due to the real-time controls versus the infrastructure itself is not possible to determine with the data collected. However, modeling results indicate that controls do play a factor in controlling the pathways of effluent stormwater, i.e., underdrain, exfiltration, and overflow. In addition, compared to other monitoring studies, bioswales with underdrains have found an average of 56% removal for those with underdrains (14 studies) and 89% (100% for

75th percentile) for those without underdrains (six studies) (Poresky et al., 2012). Because the real-time controls effectively plugged the underdrain during these events and the observed high infiltration rate, these bioswales performed similar to high-performing bioswales without underdrains. The value proposition of the proposed system is in maximizing volume removal while preventing overtopping (if included as a constraint) and ensuring drawdown times are met. Under the right conditions (defined further in the following paragraphs), these could be useful as an option for improving volume removal, while reducing risk of prolonged saturation or drawdown times that are beyond those required by regulations (usually between 48 and 72 hours).

Groundwater table levels influence the type of control rules that should be used. The green alley exhibited high groundwater tables during the study period. In using a real-time control at the site, there were challenges in developing control algorithms that would function properly without prior knowledge of groundwater level in the system. This is because groundwater levels could fluctuate above the invert of the underdrain causing the system to recognize a runoff event when none was present. The rate of change in the water level reading, rather than a water level threshold, was applied to overcome this challenge; however, further application of this method may require an understanding of the site-specific groundwater table dynamics to accurately delineate between water level changes caused by groundwater movement versus runoff. Modeling results further indicated that real-time controls in situations with high water tables have the added benefit of reducing unforeseen groundwater infiltration into the stormwater network by holding back groundwater.

Exfiltration capacity of green infrastructure is an important consideration when implementing real-time controls. This study showed that for the bioswales, there was significant exfiltration of influent volumes across all storms. This is not unfounded as other studies have found that green infrastructure practices often have a greater than designed removal of runoff volume (Lewellyn et al., 2016). In this case, the real-time controls at the bioswales acted as a factor-of-safety for events in which the infiltrative capacity of the system were less than the runoff volume into the bioswales. However, over the course of the study period, no events were captured in which this was the case. This does not mean that these controls are not appropriate in these locations, but that their value is primarily in ensuring near 100% removal while preventing overflow and standing water during extreme events, such as design storms. This was further supported by the sensitivity analysis of the hydraulic conductivity, which demonstrated limited overflow and underdrain flow for soils with high infiltration capacity.

Performance objectives of the green infrastructure should inform the type of control algorithm used. Modeling results indicated a range in the performance of the algorithms based upon the control rules that were implemented. For example, there was a higher overflow volume for algorithms that sought to only increase exfiltration versus those that sought to also prevent the trench from exceeding a maximum threshold. While the former resulted in a greater exfiltration into the ground, they also resulted in a greater volume of untreated stormwater in the overflow. This may meet volumetric goals, but if water quality is a concern, then the algorithms that prevent overtopping by allowing treated stormwater to leave through the underdrain may be preferred.

Real-time controls may not provide the most value in all cases. In locations in which exfiltration was high, the real-time controls did not need to open to prevent overflows or to decrease drawdown rates to meet minimum drawdown times. Therefore, a cheaper alternative could be to simply plug the underdrain. In fact, similar approaches, such as a constricted underdrain orifice or a plug, have been promoted as an option in other stormwater BMP guidance manuals and studies (Maine DEP, 2012). For example, in Philadelphia green infrastructure has been implemented with endcaps on the underdrain to promote complete infiltration (Ballestero, 2020; PWD, 2020). In these cases, performance is observed and if the systems do not drain adequately between events, then a hole is drilled into the end cap. Alternative approaches could include modified valves that open under specified pressures related to the level of water in a system. Such an approach could be a cost-effective means of obtaining more volume removal. However, it would not be able to adapt to field conditions rapidly in the way a real-time control system can. This was demonstrated by the modeling results (e.g., Figure A 4-27) where the fully plugged system has a larger volume of overflow than many of the real-time control algorithms that are able to open during periods of high runoff events and release treated underdrain flow, as opposed to untreated overflow.

Limitations of real-time controls should be considered. Limitations to the proposed real-time controls systems include the need to replace battery power and necessary field conditions for installation. In this study, with the provided capacity of batteries, the systems were able to continuously run for an average of five weeks before needing to be recharged; however, power requirements may change based on the opening frequency of the valve and the frequency of data collection. In our case, the frequency of

data collection was set conservatively at five minutes, but this could be extended to improve battery life. Alternative power sources could include solar or grid connections; however, these may increase costs and would be dependent upon site conditions. In addition, the real-time control valve requires an accessible junction where the underdrain meets the stormwater system. This is not always the case as some underdrains are directly connected to a stormwater pipe, and therefore, there is no space to place a control valve. Others that do meet at a junction could be inaccessible due to the junctions location in the middle of the street, deep within a manhole, or at a low invert elevation (e.g., a few inches from the bottom of the junction) that prevents the installation of real-time control, which in our case requires 12 inches of clearance or more to install. If these types of systems are desired, the placement of the underdrain connection in an accessible location with space for a valve would be a primary design consideration. Finally, while the valves were able to function throughout the study, even after continued deployment through the winter, there may be components of the system that need to be maintained during the lifetime of the system.

Hardware for real-time controls of green infrastructure are not cost-prohibitive. Cost savings were found through controls based solely upon water level that eliminate the need for extensive monitoring equipment and communications hardware, as well as low-power sensors and actuators that eliminate the need for connections to grid or solar power. Such a system could add significant value to green infrastructure practices, which already have a high cost per gallon of detention and treatment compared to gray infrastructure (Environment Water Federation, 2015). To this end, low-cost, power-efficient active control of green infrastructure has the potential to enhance adoption of

active control technology. Not included within the cost estimates may be other significant costs such as overhead, engineering design, and maintenance and operations.

4.7. Conclusion

This section presents the outcomes from implementing three real-time control systems on three different green infrastructure practices (one green alley and two bioswales) and modeling of various conditions at the green alley location. Results demonstrate that green infrastructure with real-time controls removed a significant amount of volume during runoff events (97-100%). However, the controlled valves were closed during most of the monitoring period and, therefore, this effect cannot be attributed to the real-time controls and may be the result of simply plugging the underdrain. While plugging of the underdrain may maximize volume removal without compromising drawdown requirements in many cases, model results suggest that real-time controls may have the added benefit of reducing the amount of untreated water that is overflowed. Further research would be needed to study and demonstrate this potential benefit of real-time controls. Realization of the proposed technology could directly advance and support improved stormwater management, through improved volume mitigation of green infrastructure practices.